frontiers | Research Topics

Development, metabolism, senescence and mechanotransduction of bone

Edited by
Airong Qian, Cory J. Xian, Lifang Hu and Changqi Zhu

Published in
Frontiers in Cell and Developmental Biology

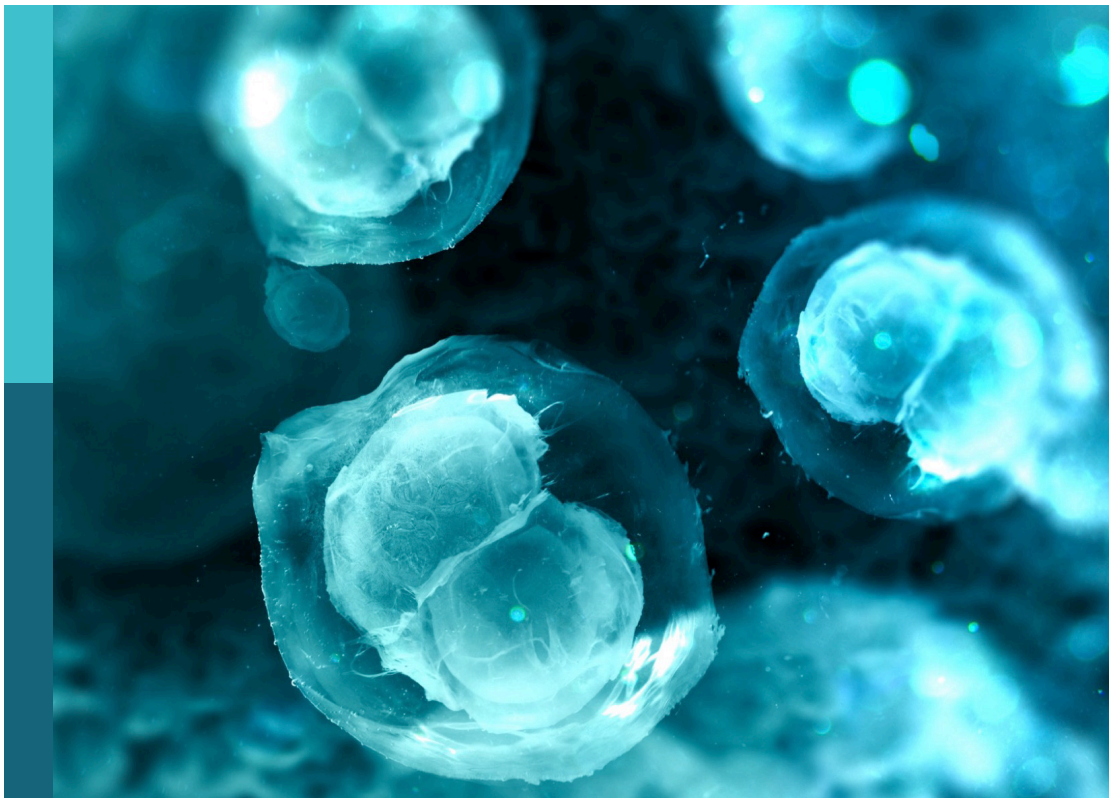

ISSN 1664-8714
ISBN 978-2-83251-120-6
DOI 10.3389/978-2-83251-120-6

About Frontiers

Frontiers is more than just an open access publisher of scholarly articles: it is a pioneering approach to the world of academia, radically improving the way scholarly research is managed. The grand vision of Frontiers is a world where all people have an equal opportunity to seek, share and generate knowledge. Frontiers provides immediate and permanent online open access to all its publications, but this alone is not enough to realize our grand goals.

Frontiers journal series

The Frontiers journal series is a multi-tier and interdisciplinary set of open-access, online journals, promising a paradigm shift from the current review, selection and dissemination processes in academic publishing. All Frontiers journals are driven by researchers for researchers; therefore, they constitute a service to the scholarly community. At the same time, the *Frontiers journal series* operates on a revolutionary invention, the tiered publishing system, initially addressing specific communities of scholars, and gradually climbing up to broader public understanding, thus serving the interests of the lay society, too.

Dedication to quality

Each Frontiers article is a landmark of the highest quality, thanks to genuinely collaborative interactions between authors and review editors, who include some of the world's best academicians. Research must be certified by peers before entering a stream of knowledge that may eventually reach the public - and shape society; therefore, Frontiers only applies the most rigorous and unbiased reviews. Frontiers revolutionizes research publishing by freely delivering the most outstanding research, evaluated with no bias from both the academic and social point of view. By applying the most advanced information technologies, Frontiers is catapulting scholarly publishing into a new generation.

What are Frontiers Research Topics?

Frontiers Research Topics are very popular trademarks of the *Frontiers journals series*: they are collections of at least ten articles, all centered on a particular subject. With their unique mix of varied contributions from Original Research to Review Articles, Frontiers Research Topics unify the most influential researchers, the latest key findings and historical advances in a hot research area.

Find out more on how to host your own Frontiers Research Topic or contribute to one as an author by contacting the Frontiers editorial office: frontiersin.org/about/contact

Development, metabolism, senescence and mechanotransduction of bone

Topic editors

Airong Qian — Northwestern Polytechnical University, China
Cory J. Xian — University of South Australia, Australia
Lifang Hu — Northwestern Polytechnical University, China
Changqi Zhu — Ferris State University, United States

Citation

Qian, A., Xian, C. J., Hu, L., Zhu, C., eds. (2023). *Development, metabolism, senescence and mechanotransduction of bone*. Lausanne: Frontiers Media SA. doi: 10.3389/978-2-83251-120-6

The authors declare that the research was conducted in the absence of any commercial or financial relationships that could be construed as a potential conflict of interest.

Table of contents

frontiers | Frontiers in Cell and Developmental Biology

TYPE Editorial
PUBLISHED 08 December 2022
DOI 10.3389/fcell.2022.1103581

OPEN ACCESS

EDITED AND REVIEWED BY
Andrew B. Goryachev,
University of Edinburgh,
United Kingdom

*CORRESPONDENCE
Lifang Hu,
hulifang@nwpu.edu.cn
Changqi Zhu,
ChangqiZhu@ferris.edu
Cory J. Xian,
cory.xian@unisa.edu.au
Airong Qian,
qianair@nwpu.edu.cn

SPECIALTY SECTION
This article was submitted to Morphogenesis and Patterning, a section of the journal Frontiers in Cell and Developmental Biology

RECEIVED 20 November 2022
ACCEPTED 28 November 2022
PUBLISHED 08 December 2022

CITATION
Patil S, Hu L, Zhu C, Xian CJ and Qian A (2022), Editorial: Development, metabolism, senescence and mechanotransduction of bone. *Front. Cell Dev. Biol.* 10:1103581. doi: 10.3389/fcell.2022.1103581

Editorial: Development, metabolism, senescence and mechanotransduction of bone

Suryaji Patil[1], Lifang Hu[1]*, Changqi Zhu[2]*, Cory J. Xian[3]* and Airong Qian[1]*

[1]Lab for Bone Metabolism, Xi'an Key Laboratory of Special Medicine and Health Engineering, Key Lab for Space Biosciences and Biotechnology, Research Center for Special Medicine and Health Systems Engineering, NPU-UAB Joint Laboratory for Bone Metabolism, School of Life Sciences, Northwestern Polytechnical University, Xi'an, Shaanxi, China, [2]Ferris State University, Big Rapids, MI, United States, [3]Clinical and Health Sciences, University of South Australia, Adelaide, SA, Australia

KEYWORDS

bone development, bone meta, bone mechanotransduction, bone senescence, bone disease

Editorial on the Research Topic
Development, metabolism, senescence and mechanotransduction of bone

Bone is an integral part of the musculoskeletal system, providing physical scaffolding as well as an attachment surface for tendons and ligaments to link muscles and bones. Importantly, it is the site of hematopoiesis, which is responsible for the rejuvenation of blood and immune cell populations essential for healthy physiology (Salhotra et al., 2020). The extraordinary ability of bone to repair and restore itself throughout life is tightly regulated by the coordinated processes of bone formation/mineralization and bone resorption, which are mediated by two of the most important bone cells, osteoblasts and osteoclasts, respectively. The anabolic and catabolic pathways of these cells, such as BMP-Smad, Wnt/β-catenin, Notch, and Hedgehog, determine and influence their ability to repair bone. Thus, any change in these pathways can disrupt bone homeostasis and lead to bone disorders such as osteoporosis (Suzuki et al., 2020). As a result, it is critical to investigate the expression of molecules in diseased conditions of bone in order to understand their role, which may open up new avenues for therapeutic development. Shin et al. Used knockout mice to demonstrate the importance of TLE4 in bone homeostasis. *Tle4* deficiency may impair not only hematopoiesis but also skeleton calcification *via* osteoblast function and differentiation by downregulating alkaline phosphatase (ALP), runt-related transcription factor 2 (Runx2), and osteocalcin expression.

The bone is an endocrine and mechanosensing organ in addition to its regular functions. Mechanical stimuli induce the bone to express and release "osteokines," such as osteocalcin, sclerostin, Dickkopf-related protein 1 (Dkk1), and fibroblast growth factor, which have an effect on other tissues (Gerosa and Lombardi, 2021). Its

ability to sense sensory cues and forces, particularly mechanical stimulation, influences its development and facilitates adaptation to changing environments (Liang et al., 2021). Osteocytes are the most abundant endocrine bone cells that regulate bone remodeling through calcium and phosphate metabolism as well as mechanical stimulation. When exposed to mechanical stress, their ability to recognize mechanical stimuli directly and indirectly allows them to promote bone adaptation and formation *via* the mechanotransduction process in individual cells, between neighboring cells, and their microenvironments *via* cell junctions (Qin et al., 2020). One of such gap junctions, connexin 43 (Cx43), has been shown to play an important role in bone formation in response to mechanical loading. Researchers discovered impaired anabolic responses in transgenic mouse models that expressed dominant-negative Cx43 in osteocytes, as well as increased endosteal osteoclast activity (Zhao et al., 2022).

Hua et al. discovered that Cx43 regulates the transition of osteoblast to osteocyte. Its deletion can postpone the transition while increasing osteoclastogenesis *via* the receptor activator of nuclear factor kappa-B ligand (RANKL)/osteoprotegerin (OPG). Aside from genetic changes, there is growing evidence that epigenetic changes such as DNA methylation, post-translational modifications, and non-coding RNA expression in cells can influence gene expression and bone metabolism (Yang et al., 2020). Huang et al. Have comprehensively reviewed one such modification, m^6A methylation in bone marrow mesenchymal stem cells (BMSC), osteoblasts, and osteoclasts. Their work summarizes the effects of m^6A modification on cell proliferation, differentiation, and apoptosis in these cells and osteoporosis and suggests that m6A modification could be a new target for osteoporosis treatment.

While many available therapeutics are promising in terms of bone regeneration, their long-term application is frequently limited due to adverse side effects. According to Gong et al., recombinant human globular adiponectin (ADPN) could be used to repair bone fractures. The study's findings indicated that ADPN administration could promote bone formation by increasing osteogenic differentiation and proliferation of BMSCs *via* the AdipoR1 receptor. Importantly, it may reduce the number of osteoclasts *via* the OPG/RANKL pathway and promote bone fracture healing. Traditional Chinese medicines and their derivatives have played important roles in a variety of diseases due to their lower side effects (Huang et al.). Yan et al. discovered that by activating the BMP2/Smad/Runx/Osterix signaling pathway,β -ecdysterone, a steroidal phytohormone with the same chemical structure as estrogen, can improve bone regeneration in a bone injury mouse model. However, key component groups and the mechanisms of action of the constituents present in such medicines remain a mystery. Liu et al. Described a novel bioinformatics model that was used to identify the components and mechanisms of Gushukang Granules (GSK), Xianling Gubao Capsules (XLGB), and Er-xian Decoction (EXD). The model identified key components as quercetin, isoliquiritigenin, rutaecarpine, isofraxidin, and secoisolariciresinol, with a possible mechanism targeting osteoclast differentiation, calcium signaling pathways, MAPK signaling pathways, and the PI3K-Akt signaling pathway.

The articles in this Research Topic present and discuss broader aspects of bone physiology, ranging from elucidating the roles of various molecules and forces on bone cell development and differentiation, to investigating various molecules as potential therapeutics, to elucidating the effect of bone on other tissues, to identifying and proposing novel molecules as targets for bone disorders. These articles provide the basis for future experimental works and even for clinical applications.

Author contributions

All authors listed have made a substantial, direct, and intellectual contribution to the work, and approved it for publication.

Funding

This study was supported by the National Natural Science Foundation of China (No. 82072106, 31570940, 32000924, 32101055).

Conflict of interest

The authors declare that the research was conducted in the absence of any commercial or financial relationships that could be construed as a potential conflict of interest.

Publisher's note

References

Gerosa, L., and Lombardi, G. (2021). Bone-to-Brain: A round trip in the adaptation to mechanical stimuli. *Front. Physiol.* 12, 623893. doi:10.3389/fphys.2021.623893

Huang, K., Zhang, P., Zhang, Z., Youn, J. Y., Wang, C., Zhang, H., et al. (2021). Traditional Chinese Medicine (TCM) in the treatment of COVID-19 and other viral infections: Efficacies and mechanisms. *Pharmacol. Ther.* 225, 107843. doi:10.1016/j.pharmthera.2021.107843

Liang, W., Wu, X., Dong, Y., Chen, X., Zhou, P., and Xu, F. (2021). Mechanical stimuli-mediated modulation of bone cell function-implications for bone remodeling and angiogenesis. *Cell Tissue Res.* 386 (3), 445–454. doi:10.1007/s00441-021-03532-6

Qin, L., Liu, W., Cao, H., and Xiao, G. (2020). Molecular mechanosensors in osteocytes. *Bone Res.* 8, 23. doi:10.1038/s41413-020-0099-y

Salhotra, A., Shah, H. N., Levi, B., and Longaker, M. T. (2020). Mechanisms of bone development and repair. *Nat. Rev. Mol. Cell Biol.* 21 (11), 696–711. doi:10.1038/s41580-020-00279-w

Suzuki, A., Minamide, M., Iwaya, C., Ogata, K., and Iwata, J. (2020). Role of metabolism in bone development and homeostasis. *Int. J. Mol. Sci.* 21 (23), 8992. doi:10.3390/ijms21238992

Yang, Y., Yujiao, W., Fang, W., Linhui, Y., Ziqi, G., Zhichen, W., et al. (2020). The roles of miRNA, lncRNA and circRNA in the development of osteoporosis. *Biol. Res.* 53 (1), 40. doi:10.1186/s40659-020-00309-z

Zhao, D., Riquelme, M. A., Guda, T., Tu, C., Xu, H., Gu, S., et al. (2022). Connexin hemichannels with prostaglandin release in anabolic function of bone to mechanical loading. *Elife* 11, e74365. doi:10.7554/eLife.74365

frontiers in Cell and Developmental Biology

ORIGINAL RESEARCH
published: 06 August 2021
doi: 10.3389/fcell.2021.671029

TLE4 Is a Critical Mediator of Osteoblast and Runx2-Dependent Bone Development

*Thomas H. Shin[1,2], Evangelos Theodorou[1], Carl Holland[1], Rae'e Yamin[1], Cathleen L. Raggio[3], Philip F. Giampietro[4] and David A. Sweetser[1]**

[1] Department of Pediatrics, Center of Genomic Medicine, Divisions of Pediatric Hematology/Oncology and Medical Genetics, Massachusetts General Hospital, Harvard Medical School, Boston, MA, United States, [2] Department of Molecular and Translational Medicine, Boston University School of Medicine, Boston, MA, United States, [3] Department of Pediatric Orthopedics, Hospital for Special Surgery, New York, NY, United States, [4] Department of Pediatrics, University of Illinois, Chicago, IL, United States

Healthy bone homeostasis hinges upon a delicate balance and regulation of multiple processes that contribute to bone development and metabolism. While examining hematopoietic regulation by *Tle4*, we have uncovered a previously unappreciated role of *Tle4* on bone calcification using a novel *Tle4* null mouse model. Given the significance of osteoblasts in both hematopoiesis and bone development, this study investigated how loss of *Tle4* affects osteoblast function. We used dynamic bone formation parameters and microCT to characterize the adverse effects of *Tle4* loss on bone development. We further demonstrated loss of *Tle4* impacts expression of several key osteoblastogenic genes, including *Runx2*, *Oc*, and *Ap*, pointing toward a potential novel mechanism for *Tle4*-dependent regulation of mammalian bone development in collaboration with the RUNX family members.

Keywords: *Tle4*, osteoblast, *Runx2*, bone mineralization, Tle4-Runx axis, bone calcification

OPEN ACCESS

Edited by:
Cesare Indiveri, University of Calabria, Italy

Reviewed by:
Bram van der Eerden, Erasmus Medical Center, Netherlands
Dian Widya Damaiyanti, Universitas Hang Tuah, Indonesia

****Correspondence:***
David A. Sweetser
dsweetser@mgh.harvard.edu

Specialty section:
This article was submitted to Cellular Biochemistry, a section of the journal Frontiers in Cell and Developmental Biology

Received: *22 February 2021*
Accepted: *14 July 2021*
Published: *06 August 2021*

Citation:
Shin TH, Theodorou E, Holland C, Yamin R, Raggio CL, Giampietro PF and Sweetser DA (2021) TLE4 Is a Critical Mediator of Osteoblast and Runx2-Dependent Bone Development. Front. Cell Dev. Biol. 9:671029. doi: 10.3389/fcell.2021.671029

INTRODUCTION

Normal bone development is a dynamic process that depends on the balance between bone formation and bone resorption. These two processes are largely mediated by osteoblasts and osteoclasts, respectively. An imbalance of these two forces results in various bone pathologies, including osteopetrosis and osteoporosis (Cohen, 2006; Kaul et al., 2015). Osteoblasts are derived from mesenchymal cells that are triggered by Wnt signaling toward osteoblastic differentiation (Hill et al., 2005; Houschyar et al., 2019). Various factors, including Wnt, BMP signaling, and *Runx2*, have been found to play roles, not only in normal osteoblast function, but also maturation and viability (Cohen, 2006; Kozhemyakina et al., 2015). *Runx2* and *Osterix* regulate the differentiation of mesenchymal stem cells (MSCs) to osteoblastic lineages (Asada and Katayama, 2014). The loss of *Runx2*, a known interaction partner of *Tle* co-repressors, results in the absence of bone formation thought to be secondary to aberrant osteoblast differentiation in mice (Choi et al., 2001). Additionally, previous studies have shown that *Runx2* expression induces osteoblastic differentiation of mouse stromal cells (Baniwal et al., 2012). Runx2 augments mesenchymal lineage proliferation while also assisting the commitment to osteoblasts by regulating a series of signaling pathways that include Wnt, FGF and PTH, as well as *Dlx5* (Komori, 2019). Moreover, *Runx2* enhances the expression of bone matrix protein genes including

Col1a1, Spp1, Ibsp, Bglap2 and *Fin1* (Komori, 2019). *Smad* and p38 *MAPK* signaling pathways regulate *Runx2* promoting osteoblast and chondrocyte differentiation (Wu et al., 2016). Other key regulators of osteoblast differentiation include osteoproteregin, osterix, and alkaline phosphatase, and osteopontin. These factors are expressed at different stages of osteoblast differentiation and regulate osteoblast precursor fate decisions, bone metabolism, and osteoclast induction (Cohen, 2006).

The Groucho/TLE family of proteins are intimately involved in the regulation of various signaling pathways critical to cell fate and development, including receptor tyrosine kinase/Ras/MAPK, Notch, and Wnt signaling (Zhang and Dressler, 2013; Chodaparambil et al., 2014). The Groucho/TLE family have been extensively studied as corepressors of various binding partners, including the RUNX/AML family through the C-terminal VWRPY Groucho recruitment motif (Levanon et al., 1998; Chen and Courey, 2000). In leukemia, we have shown *t*(8;21) leukemic cell viability and growth are sensitive to TLE4 levels and that loss of the TLE homolog in zebrafish, Gro3, cooperates with AML1-ETO to create a myeloid leukemia phenotype (AML) (Dayyani et al., 2008). Having identified the tumor suppressor role of *TLE4* in myeloid leukemias, we generated a novel *Tle4* knockout mouse model to better understand its role in mammalian development (Sweetser et al., 2005; Dayyani et al., 2008; Wheat et al., 2014). In addition to various hematopoietic abnormalities, we unexpectedly found a severe bone development defect in these mice leading to severe runting and decreased bone mineralization (Wheat et al., 2014). Similar dual functions have been described for other regulators of bone development that also can function as tumor suppressor genes including FoxO members and ARF which drives bone remodeling and osteosarcoma development in mice through both p53 independent and dependent mechanisms (Rauch et al., 2010; Le et al., 2018; Ma et al., 2018; Schmitt-Ney, 2020).

Hematopoiesis and normal bone development are intimately connected (Bianco, 2011; Despars and St-Pierre, 2011). In concert with other resident bone tissue cells, osteoblasts create and protect a hospitable hematopoietic stem cell (HSC) microenvironment (Cohen, 2006; Yin and Li, 2006). Co-cultures of MSCs with various leukemic cell lines increase osteoblastic markers such as *Runx2, Osx, Opn* (Le et al., 2018). Initial studies of hematopoiesis in the bone marrow found many HSCs in close proximity to the inner bone endosteal area, which has triggered much inquiry into the specific relevance of osteoblasts in HSC maintenance and niche (Yin and Li, 2006; Garcia-Garcia et al., 2015). Osteoblasts communicate with HSCs through direct receptor-ligand interactions (e.g., Ang1/Tie2 and TPO/MPL), to support HSC adhesion and residence in the niche, including interactions between N-cadherin/β-catenin, and osteopontin/$\beta_1$integrin (Yin and Li, 2006; Le et al., 2018). In addition, osteoblasts secrete factors including G-CSF, hepatocyte growth factor and osteopontin that regulate the pool size of the $CD34^+$ progenitor population (Le et al., 2018). Osteoblasts regulate HSC migration in and outside of the bone marrow through CXCL12/CXCR4 and VCAM-1/VLA-4 (Le et al., 2018). The constitutive activation of β-catenin in osteoblasts and resultant expression of the Notch ligand Jagged-1 activates Notch signaling in HSC leading to the development of AML. This underscores the importance of normal regulation of mediators of osteoblast differentiation on normal hematopoiesis (Kode et al., 2014). *Dicer1* or *Ptpn11* deficient osteoprogenitor cells in mice display myelodysplastic syndrome and secondary acute myeloid leukemias, as well as juvenile myelomonocytic leukemia-like myeloproliferative neoplasms, respectively (Le et al., 2018). This is further demonstrated by studies that found HSC populations increased in parallel with expansion of osteoblasts due to parathyroid hormone treatment in mice (Calvi et al., 2003), while PTH activation enhances the migration of long-term repopulating HSCs (Even et al., 2021). Moreover, a previous study targeted ablation of osteoblasts in mice found that the loss of osteoblasts significantly reduced HSC and hematopoietic progenitor populations (Visnjic et al., 2004). Furthermore, animals deficient in Sca marker present bone abnormalities (Aguila and Rowe, 2005). Thus, osteoblast function intimately connects bone formation and hematopoiesis. Specifically Car/$LepR^+$ CXCL12 expressing cells create a niche for HSCs cells while simultaneously give rise to osteoblasts (Galan-Diez and Kousteni, 2018). The similarity of *Tle4* null mice to *Runx2* null mice suggested the loss of *Tle4* might either impair the function or the expression of *Runx2*. To better characterize the nature of the defect in bone development and maintenance in *Tle4* null mice we have used *Tle4* null and conditional *Tle4* knockout mice and performed assays of osteoblast function and development in bone stromal cultures and mesenchymal bone marrow cell lines.

MATERIALS AND METHODS

Generation of *Tle4* Null and Conditional *Tle4* Knockout Mice

For these experiments we used *Tle4* null (T4KO) and *Tle4* conditional knockout mice generated in our laboratory as previously described (Wheat et al., 2014). Briefly, conditional mice were constructed by targeting LoxP sites to flank exon 2 of *Tle4 via* homologous recombination using the 129S6/SvEvTac ES cell line (T4F). To generate T4KO, resultant mice were crossed with β-actin:Cre mice (gift of Dr. Susan Dymecki) to delete exon 2 in all tissues. Heterozygote mice were backcrossed to C57BL/6 background for over six generations and interbred to generate *Tle4* null mice. For conditional knockout of *Tle4*, homozygous T4F mice containing *Mx1*-Cre (T4F cre) were used. Excision of *Tle4* exon 2 was induced with three intraperitoneal injections of 15 mg/kg polyinosinic-polycytidylic acid (pIpC; Sigma) separated by 48 h. pIpC treatment induces interferon-γ signaling with activation of Cre expression and subsequent Cre recombinase excision of exon 2 of *Tle4.* This is predicted to cause a frameshift resulting in a premature stop codon and non-functional truncated *Tle4* protein (Wheat et al., 2014). Demonstration of T4F knockout efficiency by pIpC was performed by PCR using primers mT4WTvFlpR 5′- GGAGACTTGGAAAACGCTGA-3′, mT4PcreF 5′- CAAAGGGCCCCAGAATCTT-3′and mT4PcreR 5′- CGACCGACTTGTAGCCATTT-3′. Mice were housed in

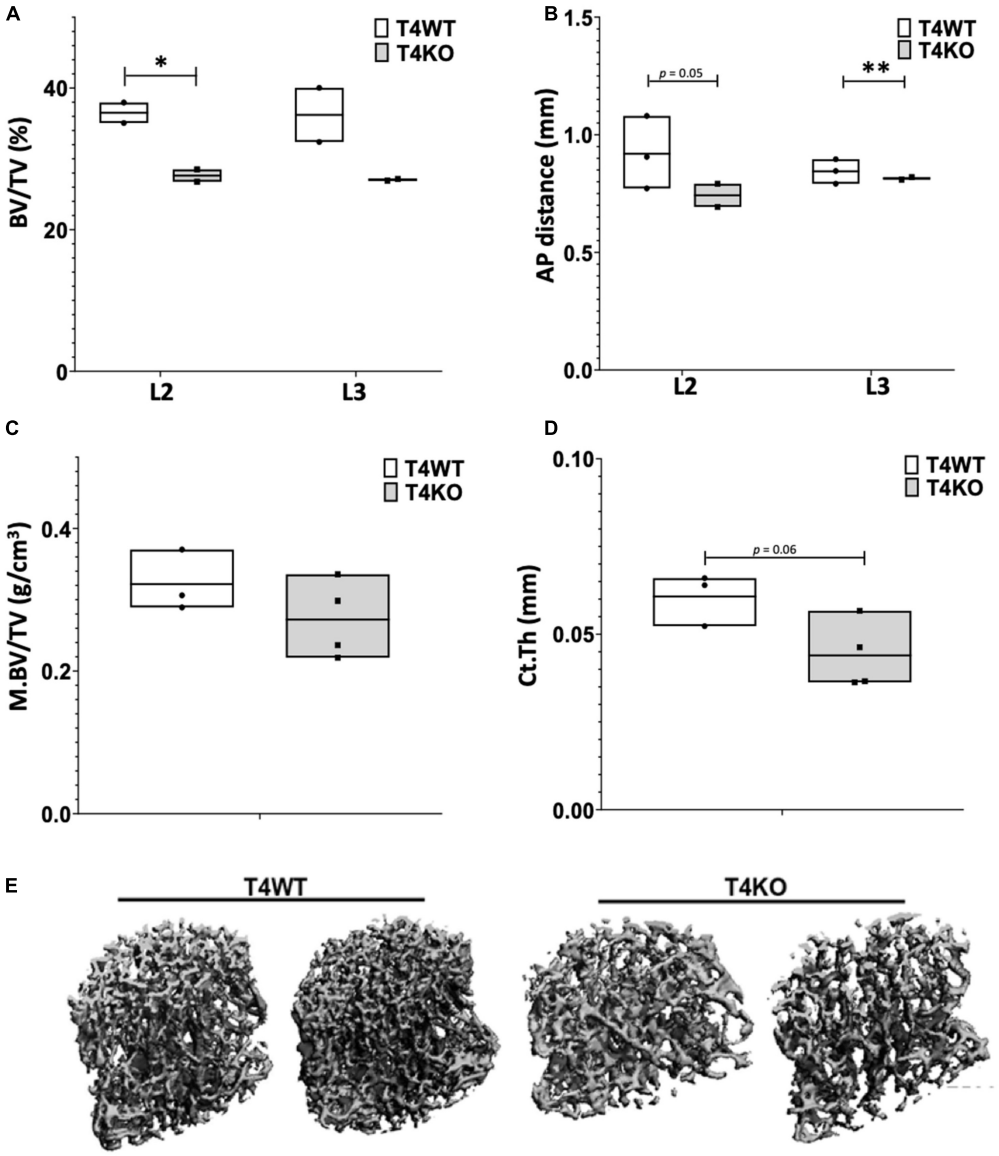

FIGURE 1 | T4KO mice exhibit deficiencies in bone formation. MicroCT measurements of **(A)** BV/TV and **(B)** AP distance in L2 and L3 vertebrae of T4KO and T4WT littermates demonstrate decreased bone density and spinal canal diameters (n = 2 biologic duplicates per arm; *$p < 0.05$, **$p < 0.01$, Student t-test). Femurs collected from 9-day old T4KO and T4WT littermates were analyzed for **(C)** medullary bone density and **(D)** cortical thickness. Both measurements show decreased trend in T4KO vs. T4WT mice (n = 3–4 mice per arm, technical duplicates). **(E)** MicroCT image reconstructions of trabecular bone in L3 vertebrae of 3-to-4 weeks old T4WT and T4KO mice, illustrating decreased bone density and trabecular bone formation in *Tle4* null mice (n = 2 biologic duplicates per arm).

a specific pathogen-free environment with a 12-h light/dark cycle, 30–70% relative humidity and approximately 70°F ambient temperature, in groups not surpassing four adult animals. Mice had *ad libitum* access to tap water and standard rodent chow (Prolab® RMH 3500, Scotts Distributing, Hudson, NH, United States). For analysis mice were euthanized by inhalation of 100% CO2. This study was carried out in strict accordance with recommendations in the Guide for the Care and Use of Laboratory Animals of the National Institutes of Health and approved by the Massachusetts General Hospital Institutional Animal Care and Use Committee.

Cell Culture, shRNA Construction, and Lentiviral Infection

ST2D cells (Generous gift of Dr. Baruch Frenkel) were generated by stably transforming mouse mesenchymal ST2 cells derived from bone marrow with a doxycycline-inducible *Runx2* expression vector (Baniwal et al., 2012). ST2D cells were cultured in RPMI-1640 (Lonza, Walkersville, MD, United States) supplemented with 10% FBS (Sigma-Aldrich, St. Louis, MO, United States) and 1% penicillin/streptomycin (Invitrogen, United States). Cells were maintained at 37°C and 5% CO_2. When indicated, cells were also cultured with 350 ng/mL

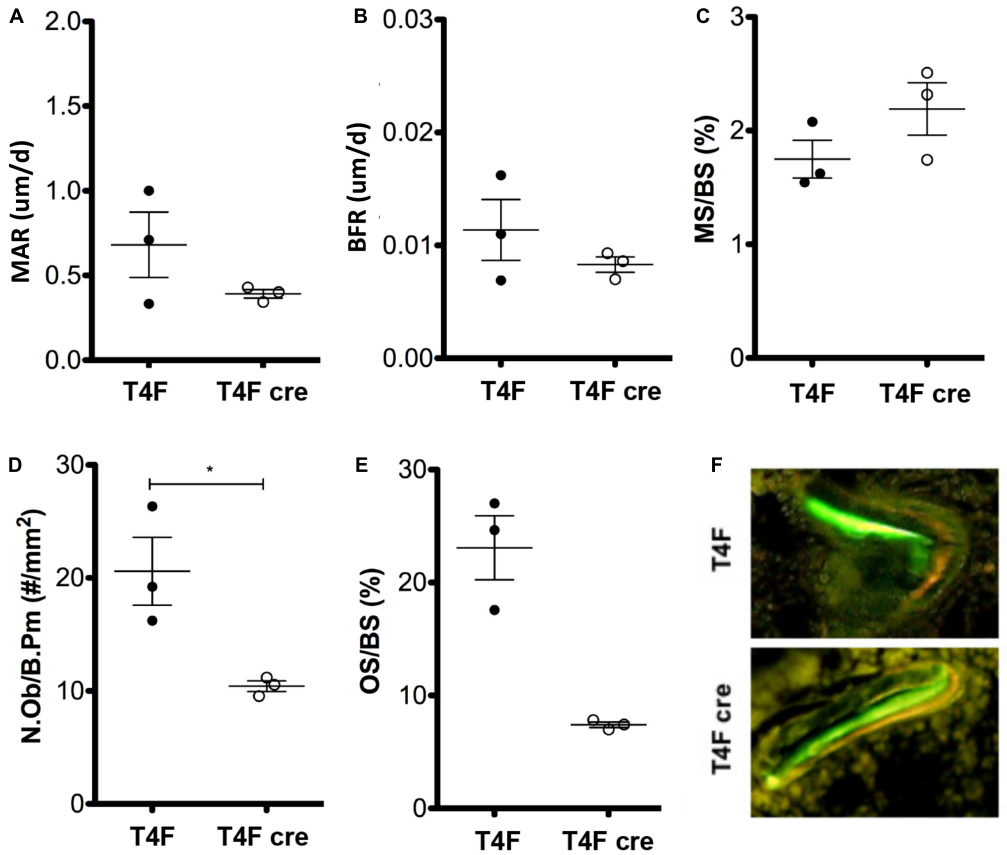

FIGURE 2 | MAR assay and trichrome staining results indicate contrasting effects of *Tle4* loss on bone formation and calcification. T4F cre mice of 8-to-9 days old have decreased **(A)** MAR and **(B)** BFR rates, measurements of average bone calcification per osteoblast and total bone formation, respectively, while having similar **(C)** ratio of mineralizing to bone surface ratios. **(D)** T4F cre mice also had less N.Ob/B.Pm values, an estimate of the number of osteoblasts per area of bone surface. **(E)** Trichrome staining reveals T4F cre mice have significantly reduced osteoid compared to T4F controls ($n = 3$ mice per arm; $^*p < 0.05$, Student *t*-test). **(F)** Representative image demonstrating decreased bone formation in T4F cre mice vs. T4F mice *via* MAR double-stain of calcein and demeclocycline.

doxycycline (Sigma-Aldrich, United States) or DMSO (Sigma-Aldrich, United States). Non-targeting control (scr) and Tle4-specific shRNA constructs were developed using the lentiviral vector FUGW and delivered to cells *via* lentiviral delivery as previously described (Dayyani et al., 2008). The Tle4 shRNA (shTle4) used has the following target sequence: AGTGATGACAACTTGGTGG and a control scrambled shRNA (scr) CAGTCGCCATTAGTTCCAC. Infected cells were identified by GFP fluorescence detected using FACS LSRII or GFP-selected *via* cell sorting with FACS Aria (BD, United States).

Generation of Stromal Cultures

Stromal cultures were generated from bones of 1-week old T4WT or T4KO littermates as previously described (Mukherjee et al., 2008; Wheat et al., 2014). After harvesting femur and humeri, whole bones were crushed and plated on tissue culture plates with MEMα (Invitrogen, United States) supplemented with 20% FBS and 1% Penicillin/Streptomycin (Invitrogen, United States). After 3 days, non-adherent cells were removed and media was changed to osteogenic media containing 100 μM β-glycerophosphate, 2.84 μM ascorbic acid, and 10 nM dexamethasone. After 1 week in osteogenic media, stromal cultures were either lysed with Trizol (Invitrogen, United States) for RNA or stained for alkaline phosphatase activity (Sigma).

In osteoblast function experiments, ST2D cells were treated with *Tle4*-specific (T4KD) or scramble control shRNA (SCR) *via* lentiviral expression. One week after spinoculation, GFP + ST2D cells were selected using FACS Aria (BD, United States) and cultured in 6-well plates. Upon reaching confluence, ST2D cells were cultured in osteogenic media, with or without 350 ng/mL doxycycline. After 2 days, ST2D cultures were lysed with Trizol (Invitrogen, United States) for RNA. In a separate experiment RNA was harvested from ST2D cells cultured after stimulation with 350 ng/mL doxycycline at 24, 48, and 72 h.

Expression Analysis *via* qRT-PCR

RNA was harvested from whole bone lysate, stromal cultures, or ST2D cell culture using Trizol (Invitrogen, United States). Expression levels of select differentially expressed genes and others of interest were performed *via* qRT-PCR as previously described (Wheat et al., 2014). Briefly, the RNA was reversed transcribed using the M-MLV Reverse transcriptase kit

(Invitrogen, United States), followed by the quantitative analysis using either SYBR Green system (Bio-Rad, United States) or predesigned TaqMan Gene Expression Assay (Applied Biosystems, United States). Primer sequences for SYBR Green assays are listed in **Supplementary Table 1**. Tle4 expression was assayed using the TaqMan Gene Expression Assay (Tle4: Mm01196934). The expression levels of genes of interest were normalized to the expression levels of the 18S housekeeping gene.

Mineral Apposition Rate Assay

For mineral apposition assay, 2-month old T4F and T4F cre littermates were irradiated with two doses of 450cGy and subsequently transplanted with 1×10^4 Lineage- c-Kit + Sca-1 + (LKS) cells from 2-month old wild-type C57BL/6 mice *via* tail vein injection. These transplanted wild-type LKS cells were isolated using a FACS Aria (BD, United States). Eight weeks after transplant, *Tle4* excision was induced by three pIpC (Sigma) intraperitoneal injections at a dose of 15 mg/kg every 48 h. Four weeks after *Tle4* excision, recipient mice were pulsed with 20 mg/kg calcein (Sigma- Aldrich, United States) *via* intraperitoneal injection. After 1 week, recipients were given 30 mg/kg demeclocycline (Sigma- Aldrich, United States) *via* intraperitoneal injection. Femurs were harvested 3 days after demeclocycline injection and fixed in 70% ethanol. Femurs were processed for resin embedding for mineral apposition rate analysis and for immunohistochemistry staining of Runx2 (PA5-86506, ThermoFisher Scientific, Waltham, MA, United States), Oc (MBS2003553, MyBiosource, San Diego, CA, United States) and β-catenin (ab6302, Abcam, Cambridge, United Kingdom) (Bouxsein et al., 2010).

MicroCT Bone Analysis

Microcomputed tomographic analysis (microCT) was performed on a subset of lumbar vertebrae. The femora were scanned at a resolution of 6 μm using a Scanco-35 microCT (Scanco United States, Inc., Southeastern, PA, United States). Each scan included a phantom containing air, saline and a bone reference material (1.18 g/cm3) for conversion of Houndsfield units to mineral density in g/cm3. Reconstruction of the individual projections to computed tomography volume data was performed using instrument software. Specimen-specific thresholds were determined by first selecting a volume of interest, generating the attenuation histogram, and determining the threshold that segments mineralized tissue from background. Properties determined included medullary bone mineral density (BMD), cortical bone thickness, AP distance, vertebral pedicle length, and trabecular bone volume fraction (trabecular bone volume to total volume ratio, BV/TV) (Bouxsein et al., 2010).

Statistics

Analyses used student's unpaired *t*-test with Graphpad Prism for comparing two genotypes (Graph-pad Software, La Jolla, CA, United States). Data are presented as floating bars showing the minimum to maximum values or scatter plots, and values of $p < 0.05$ are considered statistically significant.

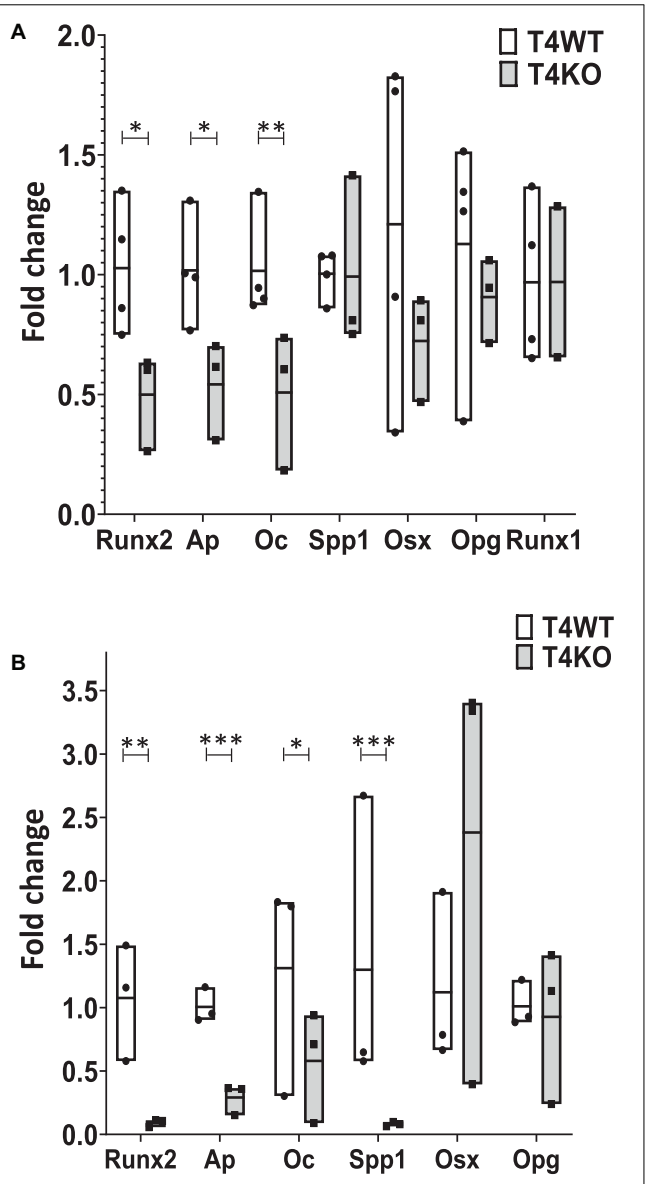

FIGURE 3 | Loss of *Tle4* affects expression of osteoblast function and differentiation regulators. **(A)** qRT-PCR using RNA from 1-week old T4WT and T4KO flushed whole bone lysate shows T4KO has decreased expression of *Ap, Runx2, and Oc* ($n = 6$ biologic replicates, technical triplicates; $^*p < 0.05$, $^{**}p < 0.01$, Student *t*-test). **(B)** Stromal cultures from T4WT and T4KO were lysed for qRT-PCR analysis, which shows significantly reduced levels of *Runx2*, *Ap*, *Oc*, and *Spp1* expression in T4KO compared to T4WT ($n = 3$ biologic replicates per arm, technical triplicates; $^*p < 0.05$, $^{**}p < 0.01$, $^{***}p < 0.001$, and Student *t*-test).

RESULTS

Loss of *Tle4* Leads to Defective Bone Development

To assess bone formation in *Tle4* null mice, we performed microCT analysis of lumbar vertebrae of 3-day old T4KO and wild-type (T4WT) littermates. T4KO mice exhibit decreased

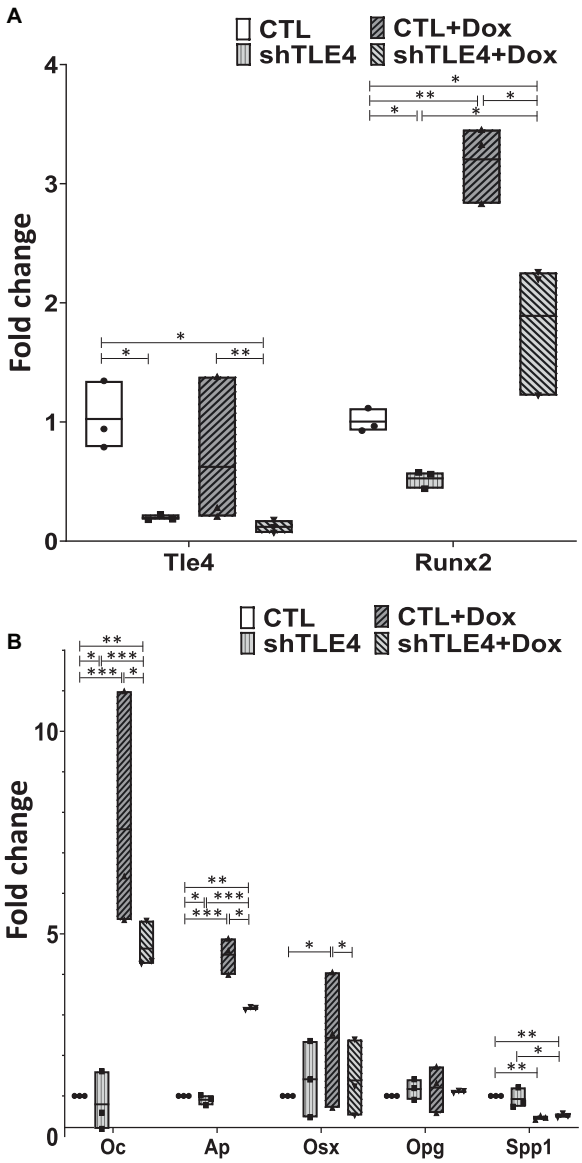

FIGURE 4 | *Tle4* knockdown in ST2D mouse mesenchymal cells demonstrates similarities in aberrant expression of osteoblast regulator genes seen in osteoblast cultures derived from T4KO mice. **(A)** qRT-PCR using RNA harvested from *Tle4* knockdown (shTle4) and control (CTL) ST2D cells using scrambled shRNA confirm effective *Tle4* knockdown and *Runx2* induction after 48 hr of doxycycline induction which remains decreased compared to the scramble controls. **(B)** qRT-PCR experiments show expression of *Ap* and *Oc* are significantly reduced in *Tle4* knockdown ST2D cells compared to control. Doxycycline-induced expression of *Runx2* significantly increases expression of these genes compared to DMSO control, remaining however, in lower levels compared to scramble ($n = 3$ biologic replicates per arm, technical triplicates; $^{*}p < 0.05$, $^{**}p < 0.01$, $^{***}p < 0.001$, and Student *t*-test).

trabecular bone volume fraction (BV/TV) and AP distance measurements compared to T4WT counterparts, suggesting loss of *Tle4* is associated with decreased bone density and vertebral pedicle length (**Figures 1A,B**). Additionally, femurs of 8 to 9-day-old T4KO and T4WT littermates were harvested for microCT analysis of medullary and cortical bone (**Figures 1C,D**). This analysis showed T4KO mice have reduced medullary bone density (M.BV/TV) and cortical bone thickness (Ct.Th). Moreover, microCT image reconstructions of trabecular bone in L3 vertebrae of 3 to 4-week old T4KO and T4WT littermates further illustrate decreased bone calcification and increased trabecular space in T4KO vertebrae compared to those of T4WT (**Figure 1E**). This is consistent with previous findings that loss of *Tle4* is associated with deficits in vertebral and long bone formation.

Dynamic Bone Formation and Osteoblast Deficiencies in Conditional *Tle4* Knockout Mouse

To further characterize the effects of *Tle4* loss on bone development, we pursued a dynamic double-label mineral apposition rate (Calvi et al., 2003) assay using mice that have *loxP* target sites flanking exon 2 of *Tle4* with or without Cre recombinase driven by the *Mx1* promoter (T4F cre and T4F, respectively). In order to isolate the effects of *Tle4* loss to bone marrow mesenchymal cells we replaced the bone marrow hematopoietic cells with wild type cells by bone marrow transplantation prior to knockout of Tle4 by pIpC in these Mx1-Cre expressing mice. The high degree of knockout efficiency of exon 2 of Tle4 in these conditional T4F-cre mice was demonstrated in harvested bone marrow of similarly pIpC treated T4F-cre compared to T4F mice lacking Mx1-cre (**Supplementary Figure 1**). The MAR assay revealed T4F cre mice have multiple lower dynamic parameters of bone formation (**Figures 2A–F**). While ratios of mineralizing to bone surface areas (MS/BS) were similar, MAR and bone formation rates (BFR) were lower in T4F cre mice compared to their control T4F counterparts (**Figures 2A–C**). Additionally, T4F cre mice had lower numbers of osteoblasts per given bone perimeter area (**Figure 2D**). Combined with lower osteoid to bone surface area ratios (**Figure 2E**), these results point toward an association between decreased bone formation and conditional loss of *Tle4* in adult mice.

Bone Defects Due to Tle4 Loss May Be Mediated Through Dysregulation of Canonical Regulators of Bone Development

Given the defective bone and bone marrow phenotype seen in T4KO mice, we hypothesized that loss of *Tle4* may affect osteoblast function and development. To assess this, we first harvested RNA from flushed whole bone lysates of 1-week-old T4KO and T4WT littermates. Expression analysis, using qPCR, revealed T4KO bone had significantly lower levels of *Ap*, *Runx2*, and *Oc* expression (**Figure 3A**). *Ap* is often used as a proxy for osteoblast function while *Runx2* and *Oc* have previously been connected to osteoblast maturation and bone anabolic regulation (Jang et al., 2012). To minimize bone cell heterogeneity, crushed 1-week-old T4KO and T4WT femurs were cultured in osteogenic media to generate osteoblast stromal cultures. T4KO stromal cultures demonstrated significant decreases in osteoblast genes,

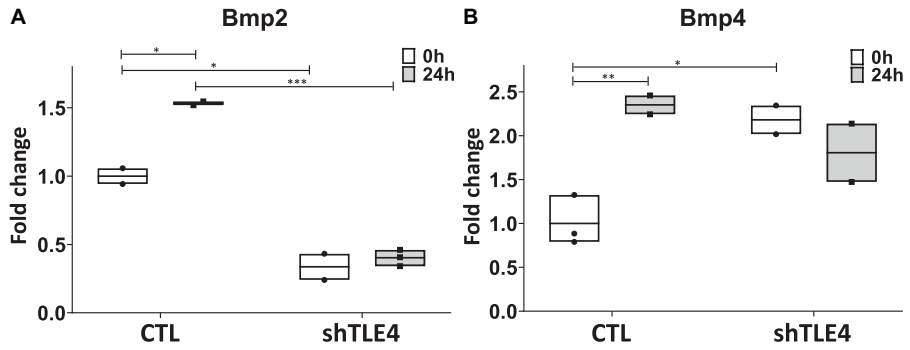

FIGURE 5 | *Tle4* knockdown in ST2D cells cause aberrant levels of *Bmp2* and *Bmp4* expression in response to *Runx2* expression. **(A)** Twenty-four hours after *Runx2* induction, upregulation of Bmp2 in control (CTL) cells. Knockdown of *Tle4* represses Bmp2 expression and blocks upregulation with Runx2 induction. **(B)** Induction of *Runx2* also leads to an upregulation of *Bmp4* in control cells. This upregulation is not seen in the presence of *Tle4* knockdown ($n = 3$ biologic replicates per arm, technical triplicates; $^{*}p < 0.05$, $^{**}p < 0.01$, $^{***}p < 0.001$, and Student *t*-test).

including *Runx2*, *Ap*, *Oc*, and *Spp1* (**Figure 3B**). Moreover, alkaline phosphatase staining qualitatively showed a trend toward decreased alkaline phosphatase activity in T4KO stromal cells (**Supplementary Figure 2**).

Our T4KO results revealed that absence of *Tle4* was associated with significant reductions of *Runx2*, suggesting T4KO-associated bone abnormalities might be due to decreased *Runx2* expression. To further elucidate the time course of Tle4-mediated effects on bone development factors through the Runx axis and considering the recent data on the Runx1 involvement in bone development (Tang et al., 2020), we assessed the expression levels of Runx1 in the 1-week-old T4KO and T4WT littermates, and found that the absence of Tle4 does not affect the expression levels of *Runx1* (**Figure 3A**) suggesting the calcification defects in Tle4 KO mice are more likely explained by Runx2 inhibition.

To better understand the mechanisms underlying Tle4 effect on bone development and the interplay with Runx2, we turn to an *in vitro* system using mouse mesenchymal ST2 cells stably transformed with a doxycycline-inducible *Runx2* vector (ST2D) (Dayyani et al., 2008; Baniwal et al., 2012). In these ST2D cells the addition of doxycycline leads to an induction of *Runx2* expression (**Figure 4A**). In this system we evaluated the effects of knocking down Tle4 expression *via* lentiviral delivery of *Tle4*-specific shRNA. Expression analysis using qPCR demonstrated over 80% reduction in *Tle4* message *via* shRNA in both doxycycline and DMSO cultures and showed that ectopic expression of *Runx2* in the absence of Tle4 shRNA did not significantly affect *Tle4* expression levels (**Figure 4A**). In this system we demonstrated *Tle4* knockdown reduced endogenous *Runx2* expression levels by approximately 50% in ST2D cells cultured in control DMSO media. This result correlated nicely with that found *in vivo*. The addition of doxycycline significantly increased *Runx2* expression levels. *Tle4* knockdown *via* shRNA was not able to prevent this increase driven from a lentiviral promoter, though the increase was blunted, likely reflecting repression of *Runx2* from the endogenous promoter. Induction of *Runx2* by doxycycline resulted in a significant increase in the expression of *Oc, Ap,* and *Osx* after 48 h, and this increase was significantly decreased in *Tle4* knockdown arms (**Figure 4B**). To further understand the relationship between *Tle4* and *Runx2*, we queried expression levels of *Bmp2* and *Bmp4*, given their previously described roles as regulators of *Runx2* and normal skeletal development (Bandyopadhyay et al., 2006; Krishnan et al., 2006). We demonstrated that loss of *Tle4* caused a significant reduction of *Bmp2* expression at baseline and prevented upregulation in response to Runx2 induction. Interestingly, levels of *Bmp4* were increased with *Tle4* knockdown, but the upregulation seen with Runx2 expression was blocked (**Figure 5**).

Extended time-course experiments demonstrate that *Tle4* knockdown creates an initial surge of Runx2 expression by 24 h of knockdown compared to control, followed by decreased *Runx2* levels at 48 and 72 h; consistent with the above observations (**Figure 6**). However, we found decreased expression levels of *Runx2*-mediated regulators of bone, including *Alp* and *Osx* at 24 h. This suggests the loss of Tle4 blunted the ability of Runx2 to upregulate Osx and Alp expression at early time points. By 72 h after *Tle4* knockdown, the differential expression of these genes is lost, suggesting a time-delay of *Alp* and *Osx* induction due to *Tle4* knockdown. These experiments support a role of Tle4 in regulating Runx2 and, subsequently, its target genes canonically associated with osteoblast differentiation and function.

Immunohistochemistry using femurs from mice used in MAR assay revealed decreased amounts of Runx2 and Osteocalcin in T4F cre mice compared to control (**Figure 7**). In T4F mice, Runx2 positivity can be seen in numerous osteoid-lining cells, suggestive of Runx2-positive periosteal osteoblasts. The frequency and localization of these Runx2-positive cells dramatically drops in T4F cre mice. Similarly, osteocalcin positivity in cortical bone seen in T4F mice is not evident in the conditional *Tle4* knockout mice. In addition to *Runx2*, β-catenin-mediated Wnt signaling has also been previously described as an important mediator of bone development and osteoblast differentiation (Hill et al., 2005; Cohen, 2006; Rodda and McMahon, 2006; Kook et al., 2015). Given previous reports implicating *Tle4* as a negative regulator of Wnt signaling, we queried β-catenin levels *via* immunohistochemistry in bones of the T4F and T4F

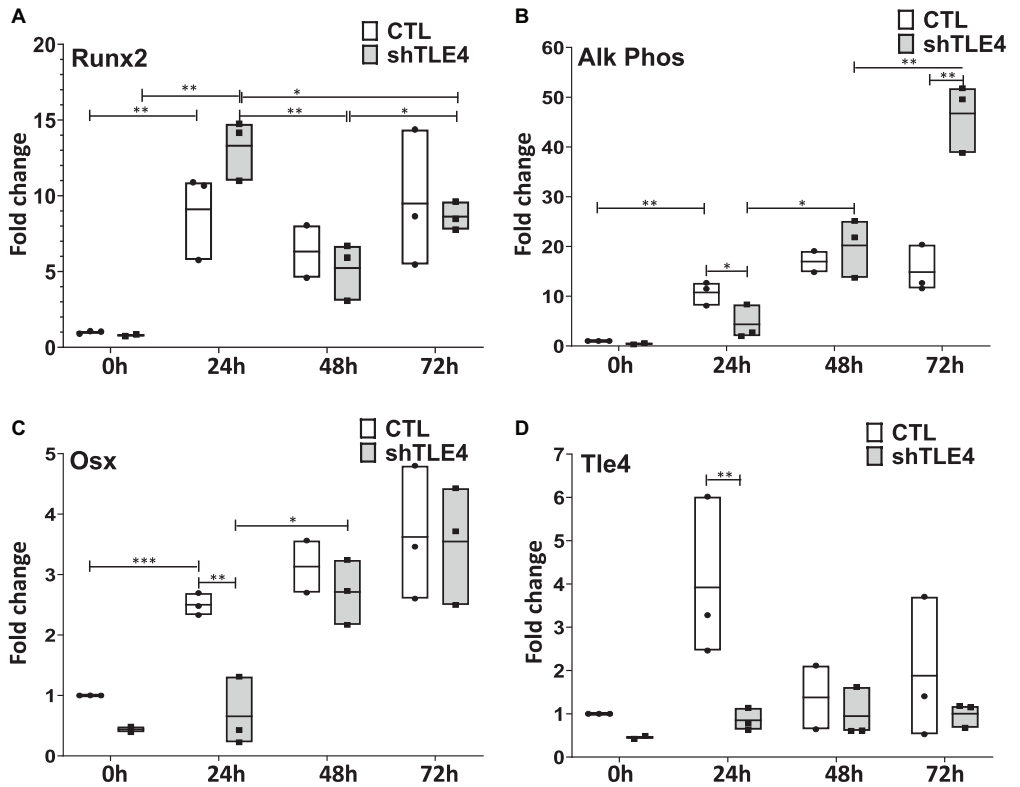

FIGURE 6 | Time-course gene expression study demonstrates altered expression of *Runx2* and its bone-related targets due to *Tle4* knockdown (shTLE4) compared with control cells (CTL) in ST2D cells at 0, 24, 48, and 72 h. **(A)** ST2D cells that contain a doxycycline inducible Runx2 gene demonstrated maximal Runx2 induction after 24 h. **(B)** This is associated with an upregulation of alkaline phosphatase that was slightly delayed with Tle4 knockdown. **(C)** Tle4 knockdown also slows the induction of the osteoblast-specific transcription factor Osterix (Osx). **(D)** The knockdown of Tle4 achieved with a Tle4 specific shRNA was demonstrated at the different time points in this experiment. (0—knockdown to 37%, 24 h to 22%, 48 h to 69%, 72 h to 53%) (n = 3 biologic replicates per arm, technical triplicates; $^{*}p < 0.05$, $^{**}p < 0.01$, $^{***}p < 0.001$, and Student t-test).

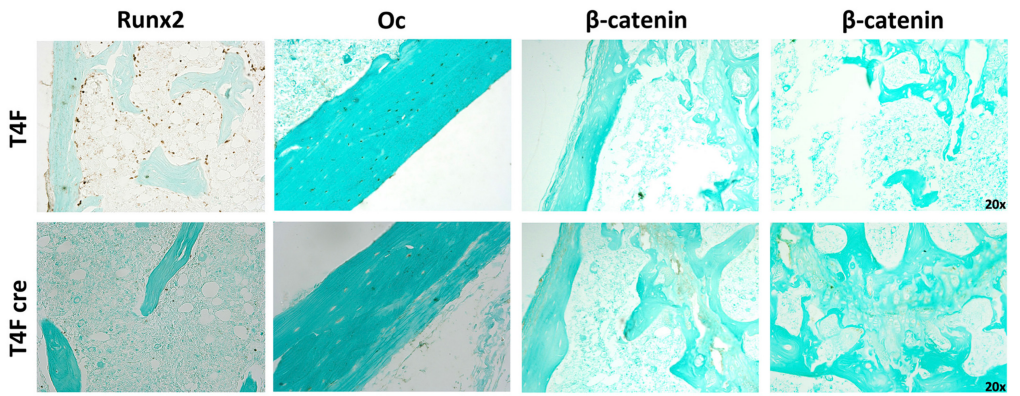

FIGURE 7 | T4F cre mice have significantly reduced levels of key regulators of bone development and osteoblast function. Immunohistochemistry assay using femurs harvested from T4F cre mice of 8-to-9 days old in MAR assay reveals decrease in Runx2 and Oc levels and increased β-catenin signals in the epiphyseal and cortical areas compared to T4F control counterparts (n = 3 mice per arm, representative images).

cre mice used in the above MAR assay as an exploratory objective. T4F cre femurs showed increased β-catenin signals in the epiphyseal and cortical areas. While T4F cre and T4KO mice display bone calcification and osteoblast function defects, loss of *Tle4* in bone leads to increased β-catenin levels, which is consistent with previous reports implicating *Tle4* as a repressor of Wnt signaling. However, using the above-described ST2D system, we were not able to find a *Tle4* knockdown-dependent

change in expression of canonical *Wnt* target gene expression (data not shown).

DISCUSSION

The Groucho/TLE family of proteins has been extensively studied in Drosophila where it has been termed a master regulatory gene in development *via* its interaction with a number of important signaling pathways including Notch and Wnt and also can be recruited by transcription factors members of Hex, Runx, Nkx, Lef1/Tcf, Pax, Six and c-myc (Jennings and Ish-Horowicz, 2008; Agarwal et al., 2015). Our understanding of the roles of this protein family in vertebrate development is limited. The novel *Tle4* null mouse provides valuable insight into the previously unappreciated roles of *Tle4* in mammalian vertebrates regarding bone maturation, medullary hematopoiesis and HSPC maintenance. One of the striking abnormalities in the T4KO mice is a decreased calcification of the skeleton (Wheat et al., 2014). This impaired ossification is apparent in both membranous and endochondral bones by birth. The above phenotypes are more intense and progressive in an age-dependent manner in T4KO mice than in *Grg5* null mice lacking a truncated member of the Groucho/TLE family (Wheat et al., 2014). Our earlier characterization of Tle4 KO mice suggested *Tle4* also affects osteoclast function as demonstrated by an increase in osteoclasts by tartrate-resistance acid phosphatase (TRAP) staining (Wheat et al., 2014). In the current study microCT and MAR assay measurements indicate loss of Tle4 impaired bone formation, calcification, and osteoid production. The lethality of *Tle4* null mice and the effects in hematopoietic cells and observed degradation of the bone marrow niche made it technically challenging to isolate the effect on osteoblasts in germline knockout mice. Conditional *Tle4* mice transplanted with normal bone marrow hematopoietic cells served as a proxy for osteoblast-specific effects of *Tle4* loss. Mx1-cre system has been demonstrated as one of the most commonly "deleter strain" in experimental hematology (Velasco-Hernandez et al., 2016). Previous work by Park et al. (2012) have demonstrated the contributory role of *Mx1*-expressing bone mesenchymal cells toward the generation of new osteoblasts responsible for new bone formation, supporting the use of the *Mx1*-Cre model in our experiments to examine the role of *Tle4* loss in osteoblast function (Park et al., 2012). The concordance of observations seen in these models and studies strongly suggest that *Tle4* may affect osteoblasts and other periosteal cells that are responsible for bone production and maintenance.

In the context of our previous work identifying hematopoietic defects in *Tle4* null mice, we have attempted to determine whether the bone abnormalities due to *Tle4* loss can be attributable to dysfunctional osteoblasts. We had shown Tle4 loss significantly impairs LSK differentiation into granulocyte, monocyte, macrophage progenitors and LSK self-renewal and adversely affects the integrity of bone marrow niche and stroma (Wheat et al., 2014). Osteoblasts are known to play a critical role in maintaining the bone marrow niche (Calvi et al., 2003; Asada et al., 2013; Fulzele et al., 2013; Even et al., 2021). In this current work qRT-PCR analysis using T4KO mouse samples from flushed whole bones and cultured stromal cells revealed significantly decreased expression of various transcription factors and regulators responsible for osteoblast function and differentiation, including *Ap* and *Oc*—both frequently used proxies for describing osteoblast function. Interestingly, osteocalcin is one of the main components of ground substance that, together with Type 1 collagen, constitute the bone matrix (Hill et al., 2005; Asada et al., 2013; Fulzele et al., 2013). *Osx* demonstrates a multifunctional role on osteoblast differentiation, growth and homeostasis, since its deletion in several time points postnatally in growing and adult bones causes defects in maturation, morphology and function of osteocytes (Zhou et al., 2010; Liu et al., 2020). Decreased *Oc* expression may lend insight into a physiologic basis for the *Tle4* knockout-induced bone phenotype.

Wnt signaling has been described as a central mediator of bone formation (Hill et al., 2005; Cohen, 2006; Rodda and McMahon, 2006; Kook et al., 2015). Surprisingly, we observed defective bone formation and calcification in T4KO mice, in which Wnt signaling is expected to be activated especially given higher levels of β-catenin signal as determined by immunohistochemistry (Kronenberg, 2003; Chodaparambil et al., 2014). However, previous studies have shown that there is an intimate relationship between the timing of Wnt signaling and normal osteoblast differentiation; and thus, constitutive or increased Wnt signaling at an inappropriate stage of osteoblast development may be detrimental to normal bone growth (Rodda and McMahon, 2006; Janeway and Walkley, 2010). Alternatively, the detrimental effects of *Tle4* loss on Runx2 activity might outweigh the effects of Wnt activation on osteoblast differentiation and calcification. Our results do not preclude the possibility that loss of *Tle4* is responsible for the bone defects through other mechanisms and the potential effects of paracrine hormonal or *Tle4* levels in other non-*Mx1*-expressing compartments.

The ST2D system provided insight into potential molecular mechanisms that may explain our findings, including not only Wnt signaling but also dysregulation of Bmp signaling and consequently *Runx2* expression. Previous studies have demonstrated loss of function of *Bmp2* and *Bmp4* impair bone condensation and skeletal development (Bandyopadhyay et al., 2006; Krishnan et al., 2006; Wu et al., 2016). There is an interplay between BMP and RUNX2 in regulating osteoblast differentiation (Lowery and Rosen, 2018). BMP signaling is required for transcriptional activity of Runx2 and Runx2 enhances the sensitivity of cells to BMPs (Phimphilai et al., 2006).

Our experiments indicate there is a decrease in *Runx2* expression in T4KO bone, T4KO stromal cells, and in ST2D cells with *Tle4* knockdown in a time dependent manner. Previous studies have shown that TLE proteins are capable of interacting with Runx2, a critical regulator of bone development and maturation (McLarren et al., 2000; Choi et al., 2001; Kaul et al., 2015). The RUNX protein family is known to form co-repressor complexes with TLE proteins (Javed et al., 2000). Thus, the TLE proteins might affect both *Runx2* expression as well as the activity of the Runx2 protein. The TLE effect on *Runx2* expression could reflect interference of Runx2 transcriptional

autoregulation (Drissi et al., 2000). In our studies, even if the experiments do not distinguish whether the blunting in the expression of these osteoblast genes with *Tle4* knockdown is due to decreased *Runx2* expression or decreased function of the Runx2 protein in the absence of Tle4, the differential expression levels of *Runx2*-mediated regulators of bone development are most likely a downstream effect consequent of the decreased endogenous *Runx2* expression after *Tle4* knockdown. *Runx2* null mice demonstrate bone phenotypes similar, but more severe than our T4KO mouse: expiring at birth and completely missing skeletal and bone development, owing to defective osteoblast maturation (Komori et al., 1997; Otto et al., 1997; Okura et al., 2014). Previous studies have shown the importance of *Runx2* in normal bone development, as *Runx2* null mice lack bone ossification and osteoblast differentiation (Cohen, 2006). The similarity of *Tle4* null mice to *Runx2* null mice suggested the loss of *Tle4* might either impair the function or the expression of *Runx2*. The less severe effect observed with *Tle4* knockout could reflect complementary effects from the expression of other *Tle* family members along with Runx2 residual expression which thus induce the osteoblastic genes expression later during bone development in the Tle4 loss background, in contrast to the early in time severe effects of Tle4 loss in bone development. Additional studies are required to further characterize the interaction and potential regulatory role of *Tle4* on *Runx2* expression levels and function as it may relate to the defective bone development in the absence of Tle4. While direct functional interactions between RUNX and TLE have been described (Westendorf, 2006) and a possibility of the requirement of such a direct active interaction in the early osteoblastic development is suggested in our time dependent experiments, additional experiments may reveal further insight into whether TLE exerts a direct regulatory effect on RUNX transcription, stability or targets.

DATA AVAILABILITY STATEMENT

The original contributions presented in the study are included in the article/**Supplementary Material**, further inquiries can be directed to the corresponding author/s.

ETHICS STATEMENT

The animal study was reviewed and approved by Guide for the Care and Use of Laboratory Animals of the National Institutes of Health and approved by the Massachusetts General Hospital Institutional Animal Care and Use Committee.

AUTHOR CONTRIBUTIONS

DS, TS, and ET: study conception and design, writing manuscript, and study supervision. TS, ET, CH, RY, CR, and PG: study conduct and data acquisition. TS, ET, CR, PG, and DS: methodology development and data analysis and interpretation. ET and DS: revising manuscript. All authors contributed to the article and approved the submitted version.

FUNDING

This work was supported in part by the National Institutes of Health Grant R01 CA115772 (DS), Swim Across America (TS and DS), The Hill Family Fund for the Diagnosis and Management of Rare and Undiagnosed Diseases at Mass General (DS and ET), the Eunice Kennedy Shriver National Institute of Child Health and Human Development of the National Institutes of Health under Award Number R03HD099516 (PG), and The Malika Ray, Asok K. Ray, M.D., FRCS/(Edin) Initiative for Child Health Research (PG).

ACKNOWLEDGMENTS

The authors would like to thank Baruch Frenkel and Jiali Yu for generous gift of ST2D cells and scientific discourse. We would also like to thank Nicolas Severe, Janaina Da Silva, and Marie Demay for guidance with mineral apposition rate assay and bone histology. We would also further like to thank Meredith Weglarz, Amy Galvin, and Maris Handley for assistance with flow cytometry and cell sorting. The authors would also like to thank Joanna Yeh, Yiyun Zhang, Matthew Jones, George Murphy, and Bob Varelas for their guidance, comments, and discourse. The authors gratefully acknowledge the support of the Malika Ray, Asok K. Ray, FRCS/(Edin) Initiative for Child Health.

SUPPLEMENTARY MATERIAL

The Supplementary Material for this article can be found online at: https://www.frontiersin.org/articles/10.3389/fcell.2021.671029/full#supplementary-material

REFERENCES

Agarwal, M., Kumar, P., and Mathew, S. J. (2015). The Grpucho/Transducin-like enhacer of split protein family in animal development. *IUBMB Life* 71: 1824.

Aguila, H., and Rowe, D. (2005). Skeletal development, bone remodeling, and hematopoiesis. *Immunol. Rev.* 208, 7–18. doi: 10.1111/j.0105-2896.2005.00333.x

Asada, N., and Katayama, Y. (2014). Regulation of helatopoiesis in endosteal microenvironments. *Int. J. Hematol.* 99, 679–684. doi: 10.1007/s12185-014-1583-1

Asada, N., Katayama, Y., Sato, M., Minagawa, K., Wakahashi, K., Kawano, H., et al. (2013). Matrix-embedded osteocytes regulate mobilization of hematopoietic stem/progenitor cells. *Cell Stem Cell* 12, 737–747. doi: 10.1016/j.stem.2013.05.001

Bandyopadhyay, A., Tsuji, K., Cox, K., Harfe, B. D., Rosen, V., and Tabin, C. J. (2006). Genetic analysis of the roles of BMP2, BMP4, and BMP7 in limb patterning and skeletogenesis. *PLoS Genet.* 2:e216. doi: 10.1371/journal.pgen.0020216

Baniwal, S. K., Shah, P. K., Shi, Y., Haduong, J. H., Declerck, Y. A., Gabet, Y., et al. (2012). Runx2 promotes both osteoblastogenesis and novel osteoclastogenic signals in ST2 mesenchymal progenitor

cells. *Osteoporos. Int.* 23, 1399–1413. doi: 10.1007/s00198-011-1728-5

Bianco, P. (2011). Bone and hematopoietic niche: atale of two stem cells. *Blood* 117, 5281–5288. doi: 10.1182/blood-2011-01-315069

Bouxsein, M. L., Boyd, S. K., Christiansen, B. A., Guldberg, R. E., Jepsen, K. J., and Muüller, R. (2010). Guidelines for assessment of bone microstructure in rodents using micro-computed tomography. *J. Bone Miner. Res.* 25, 1468–1486. doi: 10.1002/jbmr.141

Calvi, L., Adams, G., Weibrecht, K., Weber, J. M., Olson, D. P., Knight, M. C., et al. (2003). Osteoblastic cells regulate the haematopoietic stem cell niche. *Nature* 425, 841–845. doi: 10.1038/nature02040

Chen, Q., and Courey, A. (2000). Groucho/TLE family proteins and transcriptional repression. *Genes Chromosomes Cancer* 249, 1–16. doi: 10.1016/s0378-1119(00)00161-x

Chodaparambil, J. V., Pate, K. T., Hepler, M. R., Tsai, B. P., Muthurajan, U. M., Luger, K., et al. (2014). Molecular functions of the TLE tetramerization domain in Wnt target gene repression. *EMBO J.* 33, 719–731. doi: 10.1002/embj.201387188

Choi, J. Y., Pratap, J., Javed, A., Zaidi, S. K., Xing, L., Balint, E., et al. (2001). Subnuclear targeting of Runx/Cbfa/AML factors is essential for tissue-specific differentiation during embryonic development. *Proc. Natl. Acad. Sci. U.S.A.* 98, 8650–8655. doi: 10.1073/pnas.151236498

Cohen, M. M. Jr. (2006). The new bone biology: pathologic, molecular, and clinical correlates. *Am. J. Med. Genet. A* 140, 2646–2706. doi: 10.1002/ajmg.a.31368

Dayyani, F., Wang, J., Yeh, J. R., Ahn, E. Y., Tobey, E., Zhang, D. E., et al. (2008). Loss of TLE1 and TLE4 from the del(9q) commonly deleted region in AML cooperates with AML1-ETO to affect myeloid cell proliferation and survival. *Blood* 111, 4338–4347. doi: 10.1182/blood-2007-07-103291

Despars, G., and St-Pierre, Y. (2011). Bidirectional interactions between bone metabolism and hematopoiesis. *Exp. Hematol.* 39, 809–816. doi: 10.1016/j.exphem.2011.04.008

Drissi, H., Luc, Q., Shakoori, R., Chuva De Sousa Lopes, S., Choi, J. Y., Terry, A., et al. (2000). Transcriptional autoregulation of the bone related CBFA1/RUNX2 gene. *J. Cell. Physiol.* 184, 341–350. doi: 10.1002/1097-4652(200009)184:3<341::aid-jcp8>3.0.co;2-z

Even, J., Yi, L., Chang, C. K., and Rossi, F. M. V. (2021). The parathyroid hormone-dependent activation of osteoblasts enhances hematopoietic stem cell migration and reduces their engraftment abilities. *bioRxiv* [Preprint]. doi: 10.1101/2021.03.04.433901

Fulzele, K., Krause, D. S., Panaroni, C., Saini, V., Barry, K. J., Liu, X., et al. (2013). Myelopoiesis is regulated by osteocytes through Gsalpha-dependent signaling. *Blood* 121, 930–939. doi: 10.1182/blood-2012-06-437160

Galan-Diez, M., and Kousteni, S. (2018). A bone marrow niche-derived molecular switch between oestogenesis and hematopoiesis. *Genes Dev.* 32, 324–326. doi: 10.1101/gad.314013.118

Garcia-Garcia, A., de Castillejo, C. L., and Mendez-Ferrer, S. (2015). BMSCs and hematopoiesis. *Immunol. Lett.* 168, 129–135. doi: 10.1016/j.imlet.2015.06.020

Hill, T. P., Später, D., Taketo, M. M., Birchmeier, W., and Hartmann, C. (2005). Canonical Wnt/beta-catenin signaling prevents osteoblasts from differentiating into chondrocytes. *Dev. Cell* 8, 727–738. doi: 10.1016/j.devcel.2005.02.013

Houschyar, K. S., Tapking, C., Borelli, M. R., Popp, D., Duscher, D., Maan, Z. N., et al. (2019). Wnt pathway in bone repair and regeneration-what do we know so far. *Front. Cell Dev. Biol.* 6:170. doi: 10.3389/fcell.2018.00170

Janeway, K. A., and Walkley, C. R. (2010). Modeling human osteosarcoma in the mouse: from bedside to bench. *Bone* 47, 859–865. doi: 10.1016/j.bone.2010.07.028

Jang, W. G., Kim, E. J., Kim, D. K., Ryoo, H. M., Lee, K. B., Kim, S. H., et al. (2012). BMP2 protein regulates osteocalcin expression via Runx2-mediated Atf6 gene transcription. *J. Biol. Chem.* 287, 905–915. doi: 10.1074/jbc.m111.253187

Javed, A., Guo, B., Hiebert, S., Choi, J. Y., Green, J., Zhao, S. C., et al. (2000). Groucho/TLE/R-esp proteins associate with the nuclear matrix and repress RUNX (CBFa/AML/PEBP2a) dependent activation of tissue-specific gene transcription. *J. Cell Sci.* 113, 2221–2231. doi: 10.1242/jcs.113.12.2221

Jennings, B. H., and Ish-Horowicz, D. (2008). The Groucho/TLE/Grg family of transcriptional co-repressors. *Genome Biol.* 9:205. doi: 10.1186/gb-2008-9-1-205

Kaul, H., Hall, B. K., Newby, C., and Ventikos, Y. (2015). Synergistic activity of polarised osteoblasts inside condensations cause their differentiation. *Sci. Rep.* 5:11838. doi: 10.1038/srep11838

Kode, A., Manavalan, J. S., Mosialou, I., Bhagat, G., Rathinam, C. V., Luo, N., et al. (2014). Leukaemogenesis induced by an activating beta-catenin mutation in osteoblasts. *Nature* 506, 240–244. doi: 10.1038/nature12883

Komori, T. (2019). Regulation of proliferation, differentiation and functions of osteoblasts by Runx2. *Int. J. Mol. Sci.* 20:1694. doi: 10.3390/ijms20071694

Komori, T., Yagi, H., Nomura, S., Yamaguchi, A., Sasaki, K., Deguchi, K., et al. (1997). Targeted disruption of Cbfa1 results in a complete lack of bone formationowing to maturational arrest od osteoblasts. *Cell* 89, 755–764. doi: 10.1016/s0092-8674(00)80258-5

Kook, S. H., Heo, J. S., and Lee, J. C. (2015). Crucial roles of canonical Runx2-dependent pathway on Wnt1-induced osteoblastic differentiation of human periodontal ligament fibroblasts. *Mol. Cell. Biochem.* 402, 213–223. doi: 10.1007/s11010-015-2329-y

Kozhemyakina, E., Lassar, A., and Zelzer, E. (2015). A pathway to bone: signaling molecules and transcription factors involved in chondrocyte development and maturation. *Development* 142, 817–831. doi: 10.1242/dev.105536

Krishnan, V., Bryant, H. U., and Macdougald, O. A. (2006). Regulation of bone mass by Wnt signaling. *J. Clin. Invest.* 116, 1202–1209. doi: 10.1172/jci28551

Kronenberg, H. (2003). Developmental regulation of the growth plate. *Nature* 423, 332–335. doi: 10.1038/nature01657

Le, P. M., Andreeff, M., and Battula, V. L. (2018). Osteogenic niche in the regulation of normal hematopoiesis and leukemogenesis. *Haematologica* 103, 1945–1955. doi: 10.3324/haematol.2018.197004

Levanon, D., Goldstein, R., Bernstein, Y., Tang, H., Goldenberg, D., Stifani, S., et al. (1998). Transcriptional repression by AML1 and FEF-1 is mediated by the TLE/Groucho corepressors. *Proc. Natl. Acad. Sci. U.S.A.* 95, 11590–11595. doi: 10.1073/pnas.95.20.11590

Liu, Q., Li, M., Wang, S., Xiao, Z., Xiong, Y., and Wang, G. (2020). Recent advances of osterix transcription factor in osteoblast differentiation and bone formation. *Front. Cell Dev. Biol.* 8:601224. doi: 10.3389/fcell.2020.601224

Lowery, J., and Rosen, V. (2018). The BMP pathway and its inhibitor in the skeleton. *Physiol. Rev.* 98, 2431–2452. doi: 10.1152/physrev.00028.2017

Ma, X., Liu, Y., Liu, Y., Alexandrov, L. B., Edmonson, M. N., Gawad, C., et al. (2018). Pan-cancer genome and transcriptome analyses of 1,699 paediatric leukaemias and solid tumours. *Nature* 555, 371–376. doi: 10.1038/nature25795

McLarren, K., Lo, R., Grbavec, D., Thirunavukkarasu, K., Karsenty, G., and Stifani, S. (2000). The mammalian basic helix loop helix protein HES-1 binds to and modulates the transactivating function of the Runt-related factor Cbfa1. *J. Biol. Chem.* 275, 530–538. doi: 10.1074/jbc.275.1.530

Mukherjee, S., Raje, N., Schoonmaker, J. A., Liu, J. C., Hideshima, T., Wein, M. N., et al. (2008). Pharmacologic targeting of a stem/progenitor population *in vivo* is associated with enhanced bone regeneration in mice. *J. Clin. Invest.* 118, 491–504.

Okura, H., Sato, S., Kishikawa, S., Kaneto, S., Nakashima, T., Yoshiba, N., et al. (2014). Runx2-I isoform contributes to fetal bone formation even in the absence of specific N-terminal amino acids. *PLoS One* 9:e108294. doi: 10.1371/journal.pone.0108294

Otto, F., Thornell, A., Crompton, T., Denzel, A., Gilmour, K. C., Rosewell, I. R., et al. (1997). Cbfa1, a candidate gene for cleidocranial dysplasia syndrome, is essential for osteoblast differentiation and bone development. *Cell Stem Cell* 89, 765–771. doi: 10.1016/s0092-8674(00)80259-7

Park, D., Spencer, J. A., Koh, B. I., Kobayashi, T., Fujisaki, J., Clemens, T. L., et al. (2012). Endogenous bone marrow MSCs are dynamic, fate-restricted participants in bone maintenance and regeneration. *Cell Stem Cell* 10, 259–272. doi: 10.1016/j.stem.2012.02.003

Phimphilai, M., Zhao, Z., Boules, H., Roca, H., and Franceschi, R. T. (2006). BMP signaling is required for RUNX2-dependent induction of the osteoblast phenotype. *J. Bone Miner. Res.* 21, 637–646. doi: 10.1359/jbmr.060109

Rauch, D. A., Hurchla, M. A., Harding, J. C., Deng, H., Shea, L. K., Eagleton, M. C., et al. (2010). The ARF tumor suppressor regulates bone remodeling and osteosarcoma development in mice. *PLoS One* 5:e15755. doi: 10.1371/journal.pone.0015755

Rodda, S. J., and McMahon, A. P. (2006). Distinct roles for Hedgehog and canonical Wnt signaling in specification, differentiation and maintenance of osteoblast progenitors. *Development* 133, 3231–3244. doi: 10.1242/dev.02480

Schmitt-Ney, M. (2020). The FOXO's advantages of being a family: considerations on function and evolution. *Cells* 9:787. doi: 10.3390/cells9030787

Sweetser, D. A., Peniket, A. J., Haaland, C., Blomberg, A. A., Zhang, Y., Zaidi, S. T., et al. (2005). Delineation of the minimal commonly deleted segment and identification of candidate tumor-suppressor genes in del(9q) acute myeloid leukemia. *Genes Chromosomes Cancer* 44, 279–291. doi: 10.1002/gcc.20236

Tang, J., Xie, J., Chen, W., Tang, C., Wu, J., Wang, Y., et al. (2020). Runt-related transcription factor 1 is required for murine osteoblast differentiation and bone formation. *J. Biol. Chem.* 295, 11669–11681. doi: 10.1074/jbc.ra119.007896

Velasco-Hernandez, T., Sawen, P., Bryder, D., and Cammenga, J. (2016). Potential pitfalls of the Mx1-cre system: implications for experimental modeling of normal and malignant hematopoiesis. *Stem Cell Rep.* 7, 11–18. doi: 10.1016/j.stemcr.2016.06.002

Visnjic, D., Kalajzic, Z., Rowe, D. W., Katavic, V., Lorenzo, J., and Aguila, H. L. (2004). Hematopoiesis is severely altered in mice with an induced osteoblast deficiency. *Blood* 103, 3258–3264. doi: 10.1182/blood-2003-11-4011

Westendorf, J. J. (2006). Transcriptional co-repressors of Runx2. *J. Cell. Biochem.* 98, 54–64. doi: 10.1002/jcb.20805

Wheat, J. C., Krause, D. S., Shin, T. H., Chen, X., Wang, J., Ding, D., et al. (2014). The corepressor Tle4 is a novel regulator of murine hematopoiesis and bone development. *PLoS One* 9:e105557. doi: 10.1371/journal.pone.0105557

Wu, M., Chen, G., and Li, Y. P. (2016). TGF-β and BMP signaling in osteoblast, skeletal development, and bone formation, homeostasis and disease. *Bone Res.* 4:16009.

Yin, T., and Li, L. (2006). The stem cell niches in bone. *J. Clin. Invest.* 116, 1195–1201.

Zhang, P., and Dressler, G. R. (2013). The Groucho protein Grg4 suppresses Smad7 to activate BMP signaling. *Biochem. Biophys. Res. Commun.* 440, 454–459. doi: 10.1016/j.bbrc.2013.09.128

Zhou, X., Zhang, Z., Feng, J. Q., Dusevich, V. M., Sinha, K., Zhang, H., et al. (2010). Multiple functions of Osterix are required for bone growth and homeostasis in postnatal mice. *Proc. Natl. Acad. Sci. U.S.A.* 107, 12919–12924. doi: 10.1073/pnas.0912855107

Conflict of Interest: The authors declare that the research was conducted in the absence of any commercial or financial relationships that could be construed as a potential conflict of interest.

Publisher's Note: All claims expressed in this article are solely those of the authors and do not necessarily represent those of their affiliated organizations, or those of the publisher, the editors and the reviewers. Any product that may be evaluated in this article, or claim that may be made by its manufacturer, is not guaranteed or endorsed by the publisher.

frontiers in Cell and Developmental Biology

ORIGINAL RESEARCH
published: 01 November 2021
doi: 10.3389/fcell.2021.762335

Paracrine Effects of Recombinant Human Adiponectin Promote Bone Regeneration

*Yanping Gong[1], Yang Wang[1], Yiqing Zhang[2,3], Liangchen Wang[1], Lijuan Wan[1], Yuan Zu[1], Chunlin Li[1], Xin Wang[4] and Zhong-Kai Cui[2,3,5]**

[1] Department of Endocrinology, The Second Medical Center, National Clinical Research Center for Geriatric Disease, The Chinese People's Liberation Army General Hospital, Beijing, China, [2] Department of Cell Biology, School of Basic Medical Sciences, Southern Medical University, Guangzhou, China, [3] Guangdong Provincial Key Laboratory of Bone and Joint Degeneration Diseases, The Third Affiliated Hospital, Southern Medical University, Guangzhou, China, [4] Institute of Orthopedics, The First Medical Center, The People's Liberation Army General Hospital, Beijing, China, [5] Bioland Laboratory, Guangzhou, China

Bone regeneration is a delicate physiological process. Non-union and delayed fracture healing remains a great challenge in clinical practice nowadays. Bone and fat hold a close relationship to remain balanced through hormones and cytokines. Adiponectin is a well-known protein to maintain the hemostasis, which may be an interesting target for fracture healing. Herein, we provided a facile and efficient method to obtain high-purity and high-yield recombinant human adiponectin (ADPN). The biocompatibility and the pharmaceutical behaviors were evaluated in Sprague–Dawley rats. The paracrine effects of adiponectin on bone fracture healing were investigated with a rat tibia fracture model *via* intrabone injection. Significantly accelerated bone healing was observed in the medulla injection group, indicating the paracrine effects of adiponectin could be potentially utilized for clinical treatments. The underlying mechanism was primarily assessed, and the expression of osteogenic markers, including bone morphogenic protein 2, alkaline phosphatase, and osteocalcin, along with adiponectin receptor 1 (AdipoR1), was markedly increased at the fracture site. The increased bone healing of ADPN treatment may result from both enhanced osteogenic proliferation as well as differentiation. Cell experiments confirmed that the expression of osteogenesis markers increased significantly in ADPN treatment groups, while it decreased when the expression of AdipoR1 was knocked down by siRNA. Our study provided a feasible and efficacious way for bone fracture treatment with local administration of ADPN, which could be rapidly translated into the clinics.

Keywords: adiponectin, bone formation, paracrine effect, AdipoR1, medulla injection

OPEN ACCESS

Edited by:
Lifang Hu,
Northwestern Polytechnical University, China

Reviewed by:
Zheng-Jie Li,
Chengdu University of Traditional Chinese Medicine, China
Xiaojing He,
Huazhong University of Science and Technology, China

****Correspondence:***
Zhong-Kai Cui
zhongkaicui@smu.edu.cn

Specialty section:
This article was submitted to Morphogenesis and Patterning, a section of the journal Frontiers in Cell and Developmental Biology

Received: *21 August 2021*
Accepted: *27 September 2021*
Published: *01 November 2021*

Citation:
Gong Y, Wang Y, Zhang Y, Wang L, Wan L, Zu Y, Li C, Wang X and Cui Z-K (2021) Paracrine Effects of Recombinant Human Adiponectin Promote Bone Regeneration. Front. Cell Dev. Biol. 9:762335. doi: 10.3389/fcell.2021.762335

INTRODUCTION

Bone regeneration is a delicate and complex physiological process (Clarke, 2008). Bone defects resulted from traumatic injury, tumor resection, and degenerative diseases are challenging problems in clinics (Burge et al., 2007). The gold standard in clinical practice is an autologous bone graft (Einhorn and Gerstenfeld, 2015). Unfortunately, the limited sources, the injury of the donor

site and perioperative complications significantly restrict the employment of this approach (Baqain et al., 2009). Bone morphogenic protein 2 (BMP-2) is considered the most efficacious cytokine for bone repair and has been extensively studied for the treatment of various bone fractures and bone defects (Glassman et al., 2008; Long, 2011). However, supraphysiological dosage is necessary in clinical practice, causing undesirable side effects, including hollow bone formation, life-threatening tissue edema, and cancer (Cahill et al., 2009; Barbour et al., 2011; Skovrlj et al., 2015). In addition, the high cost for BMP-2 becomes a heavy financial burden for the health system. Therefore, developing alternative strategies are imperative for bone regeneration.

The close relationship between bone and fat formation was well acknowledged in the literature (Gimble et al., 2006). The bone marrow mesenchymal stem cells may take different pathways during their lifetime, to differentiate and transdifferentiate in response to changes in the microenvironment to bone or fat (Chen et al., 2016). The inverse relationship between bone and fat implied that agents inducing adipogenesis inhibited osteoblast differentiation and *vice versa* (Naot et al., 2017). These results coincided with classic pathological and epidemiological phenomena of increased marrow adiposity with aging and bone loss.

Human adiponectin is a 30-kDa adipose-derived secreted protein containing 244 amino acid residues, with an N-terminal signal sequence, a hypervariable region, a collagenous domain, and a globular domain (Scherer et al., 1995). Since it was first discovered in 1995, efforts have been devoted to unraveling the biological activities of adiponectin. Metabolic regulation and maintenance of whole-body energy homeostasis are recognized as the main physiological role of adiponectin (Wang and Scherer, 2016; China et al., 2018). Anti-inflammatory and antiapoptotic effects were demonstrated as major physiological activities of adiponectin as well (Ohashi et al., 2010). Adiponectin binds to two seven-transmembrane domain receptors, AdipoR1 and AdipoR2. Interestingly, unlike the well-known G-protein-coupled receptors, the N-terminus is located inside the cell, whereas the C-terminus faces outward for both AdipoR1 and AdipoR2. AdipoR1 was found abundant in skeletal muscle and the liver *via* ubiquitous expression, while AdipoR2 was isolated mostly from the liver (Kang et al., 2009). T-cadherin, highly expressed in endothelial and smooth muscle cells, was identified as a third adiponectin receptor (Matsuda et al., 2015).

In light of the inverse relationship between serum adiponectin levels and fat mass, the inverse relationship between bone marrow fat and bone mass inspired researchers to focus on the effects of adiponectin on bone regeneration. *In vitro*, adiponectin was reported to increase the mRNA expression of alkaline phosphatase (ALP) in preosteoblasts and promote the mineralization of the bone matrix (Williams et al., 2009; Naot et al., 2017). Furthermore, in a mouse model, the elevated adiponectin in the bloodstream significantly increased the volume of cancellous bone (China et al., 2017). Interestingly, an inverse correlation was demonstrated in clinical studies between serum adiponectin concentrations and bone mineral density (BMD) (Napoli et al., 2010). AdipoR1 and AdipoR2 were found to be expressed in primary human osteoblasts and in bone marrow macrophages, which could be the possible reasons for adiponectin playing a significant role in bone regeneration (Berner et al., 2004; Wu et al., 2019). Contradictory results in the literature were demonstrated as well; therefore, more evidence is needed to further clarify the physiological role of adiponectin in bone biology.

Although the endocrine effects of the secreted protein adiponectin from adipose tissue into the circulation account for the energy homeostasis, its local paracrine effects may play a pivotal role in bone regeneration (Martinez-Huenchullan et al., 2020). Here, we recombined human globular adiponectin (ADPN) and further characterized the pharmacokinetic behaviors and toxicity through medulla injection. A rat tibia fracture model was exploited to evaluate the capability of ADPN for bone repair. In addition, we attempted to unravel the underlying mechanism of adiponectin promoting bone regeneration.

MATERIALS AND METHODS

Materials

Glutamine synthetase (GS), methionine sulfoximine (MSX), Chinese hamster ovary K1 (CHO-K1) cells, Dulbecco's modified Eagle's medium (DMEM), fetal bovine serum (FBS), penicillin/streptomycin (P/S), insulin, and pentobarbital sodium were supplied by Sigma-Aldrich (St. Louis, MO, United States). Biotin-conjugated monoclonal antibodies for ELISA were purchased, including osteoprotegerin (OPG) ab255723, ADPN ab108784 (Abcam, Cambridge, United Kingdom). Antibodies for Western blot were GAPDH ab8245, AdipoR1 ab70362, BMP-2 ab14933 (Abcam, Cambridge, United Kingdom), and ALP sc-271431 and Osteocalcin (OCN) sc-376726 (Santa Cruz, CA, United States). Antibodies used for immunofluorescent staining were BMP-2 ab6285 (Abcam, Cambridge, United Kingdom); ALP sc-271431, OCN sc-390877 (Santa Cruz, CA, United States); and AdipoR1 BM4566 (Boster Bio, CA, United States).

Methods

Evaluation of Pharmacokinetics and Toxicity

All animal experiments were performed in accordance with the guidelines of the Ethics Committee of the Chinese People's Liberation Army General Hospital, Beijing, China. Sprague–Dawley male rats (n = 15, 8 weeks old) were randomly divided into three groups, which were treated with 0, 1, and 2 mg/kg of recombinant ADPN in PBS *via* medulla injection (G1, G2, and G3, respectively). Blood samples were collected in 1% heparin tubes *via* fundus vein plexus at predetermined time points. The supernatant was obtained by centrifugation at 3,000 rpm for 10 min, and ADPN concentration in serum was assessed with the ELISA kit (m1061301-3, Mlbio, Shanghai, China), following the protocol of the manufacturer. An automated enzymatic procedure (Cobas E601, Roche, Basel, Switzerland) was employed for blood biochemistry evaluation. Sysmex XE22100 automatic blood analyzer was used for blood routine examination. Organs including hearts, livers, spleens, lungs, kidneys, brains, and

pancreases were harvested at the end time point. After weighing, all the organs were fixed in 4% paraformaldehyde, embedded in paraffin, and sectioned at the thickness of 5 μm. H&E staining (G1120, Solarbio, Beijing, China) was carried out for all the sections to evaluate the toxicity.

Tibia Fracture Model

Sprague–Dawley male rats (8 weeks old) were anesthetized with 3 ml/kg of 3% pentobarbital sodium *via* intraperitoneal injection. A scalpel blade (#15) was used to open the knee joint. A 20-gaged syringe was inserted into the medulla of the tibia for drug injection. A Kirshner needle (1 mm) was inserted into the distal tibia at a penetration depth of about 22 ± 2 mm. The excess proximal needle was cut off with a bone cutter. Three-point forceps were fixed to the left leg. The forceps were closed until a crack was heard, and the resistance of the forceps suddenly dropped. After surgery, all animals were allowed to recover on a warm sheet and then transferred to the vivarium for postoperative care. In preparation for the operative treatment, all animals received analgesia with subcutaneous injections of buprenorphine at a concentration of 0.1 mg/kg for 3 days. To prevent potential infection, all animals received 80,000 U of penicillin *via* intramuscular injection for 3 days.

Microcomputerized Tomography Scanning

Animals were imaged, at weeks 2, 4, and 6, using a high-resolution microcomputerized tomography (μCT) (Quantum GX μCT System, PerkinElmer, Waltham, MA, United States) with 90 kV, 80 μA, and 4.5-μm resolution. Visualization and reconstruction of the data were obtained using the Quantum GX μCT Workstation imaging software (PerkinElmer, Waltham, MA, United States). The volume of interest was defined manually as follows: The cortex area was defined as the region enclosed by the callus and cortical boundaries in tomograms. The trabecular area was an irregular and anatomic region of interest drawn manually, a few voxels away from endocortical surface to medullary space. The cortical pad area (CT. Ar) and cortical pad thickness (CT. Th), BMD, bone volume density (BV/TV, %) and mean thickness of the trabecular (Tb. Th), trabecular number (Tb. N, mm^{-1}), trabecular separation (Tb. Sp), structure model index (SMI), and bone density of connection (Conn. D, mm^{-1}) were derived using the Analyze software (AnalyzeDirect, KS, United States).

Mechanical Evaluation

Six weeks post surgery, rats were euthanized, and tibias were harvested and undergone three-point flexural mechanical testing on the biomechanics machine (MTS 858, MTS, United States). An axial force of 5 N was preloaded to the bone, and constant linear propulsion (5 mm min^{-1}) was applied to a lever arm attached to one of the pivoted axes to provide a uniform movement.

Histological Evaluation

The harvested tibias were fixed in 4% paraformaldehyde for 48 h, followed by decalcification in 10% EDTA solution under gentle shaking for 4 weeks. The EDTA solution was changed every 2 days. Decalcified samples were embedded in paraffin and cut into 5-μm-thick sections. The tissue sections were deparaffinized and stained with H&E.

Masson trichrome staining (G1340, Solarbio, Beijing, China) was also performed to detect new bone formation. The blue color, indicative of new or mature bone, was observed using an Olympus U-RFL-T microscope. Additional sections underwent immunohistochemical analysis. The deparaffinized sections were processed with citric acid for antigen retrieval and thereafter incubated with the primary antibody BMP-2 (1:400 dilution), AdipoR1 (1:400 dilution), ALP (1:200 dilution), and OCN (1:200 dilution) and were detected by the HRP/DAB kit (Beyotime, Beijing, China). The sections were further counterstained with Mayer's hematoxylin (Beyotime, Beijing, China).

Protein Quantification

The expression of ALP, BMP-2, OCN, and AdipoR1 were examined with Western blot, and the normalized values of the blots were quantified with imageJ. OPG in the serum was quantified with ELISA.

Callus tissue (approximately 5 mm) around each bone fracture position was collected, weighed, and transferred into 1.5-ml Eppendorf tubes. RIPA buffer (6 μl/mg) and 0.174 mg/ml of PMSF (benzyl sulfonyl fluoride, pyrolysis liquid with PMSF, 100:1 v/v) were added into each tube. Proteins were extracted, and Bio-Rad Dc protein assay (Bio-Rad, Hercules, CA) was carried out to determine the protein concentration for further Western blot experiments.

Knockdown of AdipoR1 by siRNA

BMSCs (P3) were inoculated in 12-well plates at a cell density of 1×10^4 cells/well. AdipoR1 siRNA (0.8 μg) was diluted with 50 μl of DMEM, and 2 μl of Lipofectamine 2000 (SolarBio China, Beijing, YZ-11668) was diluted with 50 μl of DMEM, and incubated for 5 min at room temperature. The transfection reagent and AdipoR1 siRNA diluent were mixed, and the complex was added to the well plate and incubated for 24 h. The transfection was performed on the first and fourth day, respectively.

Immunofluorescent Images of Bone Marrow Mesenchymal Stem Cells

BMSCs (P3) were inoculated in 12-well plates at a cell density of 1×10^4 cells/well. ADPN (10 μg/ml) and the control group without drugs were added accordingly. The medium was replaced every other day for 7 days. The wells were rinsed with PBS three times. Four percent neutral paraformaldehyde was added. Fifteen minutes later, 0.1% Triton X-100 was applied to lysate the cells for 15 min. Five percent goat serum was used for blocking. Drops of primary antibodies were added (the same antibodies as in animal experiments) with dilution concentrations of 1:100 and incubated overnight in a wet box in a refrigerator at 4°C. Secondary antibody (antibody dilution: 1:200, ZSGB-Bio, China Beijing, Alexa Fluor® 488, ZF-0512, Alexa Fluor® 594 ZF-0513) was added, and the nuclei were stained with DAPI.

Statistical Analysis

Data were presented as mean ± standard deviation. Multiple comparisons were assessed using the one-way or two-way

analysis of variance (ANOVA). The analysis of variances followed by the *Tukey's hoc* test was employed in this work, and $p < 0.05$ was considered statistically significant.

RESULTS

Amplification and Identification of Human Globular Adiponectin

Natural human adiponectin fragment (∼748 bp) was successfully amplified from cDNA sequence after optimizing codons. The size of adiponectin-Fc-GS fragment was around ∼1,434 bp. Two-way sequencing results confirmed that the sequence of inserted gene was identical to human globular adiponectin gene. After screening and purification, the recombinant human ADPN protein migrated at around 60 kDa by SDS-PAGE electrophoresis. ELISA was carried out to quantify the collected protein, and the yield was 20 μg/ml. The obtained ADPN was stored in glass vials after lyophilization. Details are described in **Supplementary Figure 1**.

Pharmacokinetics of Adiponectin Based on Medulla Injection

The pharmacokinetic profiles of ADPN after medulla injection were plotted (**Figure 1**), and the calculated pharmacokinetic parameters are listed in **Table 1**. For G3 and G2, T_{max}, the time to reach the maximum concentration (C_{max}), was 8 and 4.8 h, and C_{max} was 4.9 ± 0.8 and 1.7 ± 0.3 μg/ml, respectively. The area under the curve (AUC) showed that ADPN exposure was significantly higher in G3 than that in G2 ($p < 0.01$). No significant difference was observed with the half-life of ADPN in the plasma between the two groups. The pharmacokinetic results indicated that most of ADPN could remain in the bone marrow *via* medulla injection.

Toxicity of Adiponectin Based on Medulla Injection

All rats showed distinct difficulty in motion with their left legs right after surgery. Such symptom was alleviated a few hours later, yet four rats in each group still exhibited mild confined activity. All rats could move freely 24 h post surgery, with no abnormalities in the hair, canthus secretion, anus, genital, feces, behaviors, eating, drinking, etc., Organs, including hearts, livers, spleens, lungs, kidneys, pancreases, and brains, were harvested and weighed. Compared with controls, rats receiving ADPN presented significantly heavier spleens and pancreases (**Figure 2A**). H&E staining for all harvested organs was carried out to further examine the histomorphological variations (**Figure 2B**). No obvious changes were observed in all the organs among the three groups, indicating no direct toxicity of ADPN.

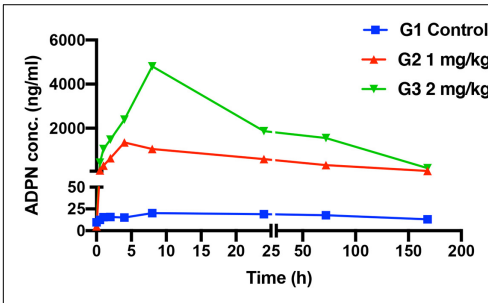

FIGURE 1 | The serum concentrations of adiponectin (ADPN) based on medulla injections, $n = 5$.

TABLE 1 | Pharmacokinetic parameters for adiponectin (ADPN) in SD rats.

Parameters	Unit	Medulla injection	
		1 mg/kg	2 mg/kg
Ke	h^{-1}	0.02 ± 0.01	0.02 ± 0.01
$T_{1/2}$	H	50.98 ± 22.51	54.24 ± 24.79
T_{max}	H	4.80 ± 1.79*	8.00 ± 0.00
C_{max}	$\mu g \cdot L^{-1}$	1,693.64 ± 302.30*	4,869.57 ± 825.30
AUC_{0-t}	$h \cdot \mu g \cdot L^{-1}$	3,158.48 ± 1,812.61**	79,483.18 ± 63,165.40
AUC_{0-8}	$h \cdot \mu g \cdot L^{-1}$	48,520.51 ± 89,123.65**	88,637.29 ± 68,594.26
Vd	$L \cdot kg^{-1}$	1,103.49 ± 596.23	532.71 ± 161.80
MRT	h	45.72 ± 5.56*	50.39 ± 5.20

*$p < 0.05$, **$p < 0.01$, G2 vs. G3.

Hematology and serum biochemistry tests were carried out to further evaluate the biocompatibility of ADPN *in vivo*. RBC (red blood cell), HGB (hemoglobin), MCHC (mean corpuscular hemoglobin concentration), and HCT (hematocrit) in the ADPN treatment groups (G2 and G3) were significantly increased at day 42 compared with that in the control group postinjection. In contrast, eosinophilic granulocytes, lymphocytes, and leukocytes showed no remarkable alteration (**Figure 2C**). Hepatorenal function, blood glucose, triglyceride, high-density lipoprotein, and uric acid levels demonstrated no obvious changes for the investigated period (**Supplementary Figure 2**).

Rat bone marrow mesenchymal stem cells (BMSCs) were isolated and treated with different concentrations of ADPN (0, 1, 5, 10, 30 μg/ml) *in vitro*. CCK-8 assay was employed to plot the cell viability profiles with time progression. Enhanced proliferation was observed among all the treatment groups up to 48 h. Non-toxicity was present in all the groups for 72 h (**Supplementary Figure 3**).

Osteogenic Ability of Adiponectin in Rat Tibia Fracture Model

In vivo high-resolution μCT was employed to evaluate the status of bone healing. ADPN treatment significantly improved callus formation after fracture. The three-dimensional μCT reconstruction analyses were carried out 6 weeks after surgery. The images delineated the recovery progress of tibial continuity gradually with time. With no treatment in the control group, the tibia healed 6 weeks postsurgery. The administration of ADPN *via* medulla injection remarkably shortened the recovery time. Especially, the higher dosage of ADPN (2 mg/kg) in G3 accelerated the healing within 3 weeks. For G2, 1 mg/kg of ADPN was administrated, and comparable healing was observed at week

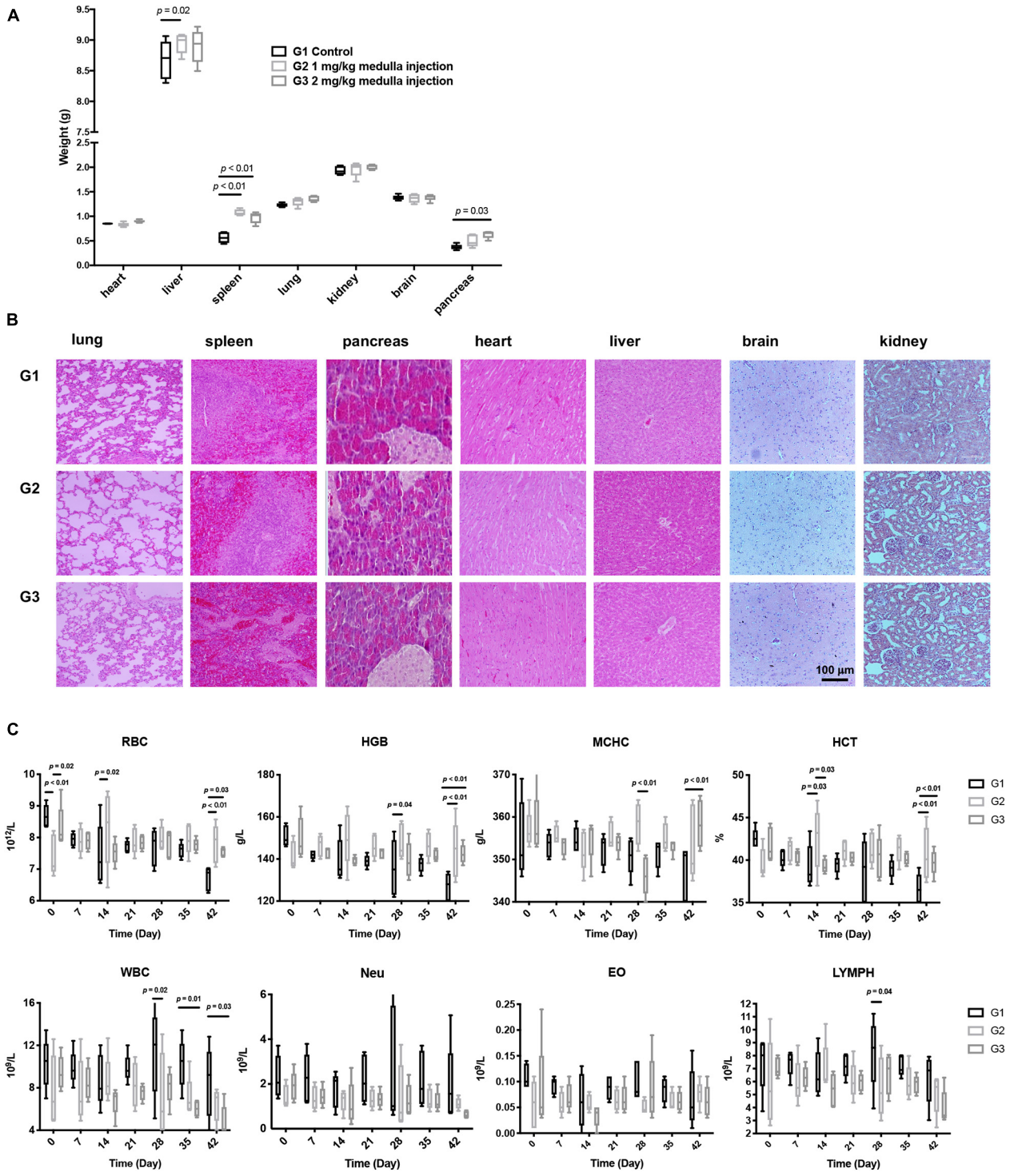

FIGURE 2 | Toxicological experiments of ADPN based on local medulla injection. **(A)** The weight of various organs. **(B)** H&E staining images of various organs, scale bar = 100 μm. **(C)** The changes of red blood cell (RBC), hemoglobin (HGB), mean corpuscular hemoglobin concentration (MCHC), hematocrit (HCT), eosinophilic granulocyte, lymphocyte, and leukocyte levels after ADPN administration among the G1, G2, and G3 groups, $n = 5$.

4. Interestingly, as observation continued in G3 for 6 weeks, heterotrophic hyperplasia was observed in the μCT scans of some rats, even to the extent of the non-fractured fibula (**Figure 3A**).

Trabecular bone morphometric indices, including the bone volume fraction (BV/TV, %), trabecular number (Tb. N., mm^{-1}), trabecular thickness (Tb. Th., μm^{-1}), trabecular separation (Tb.

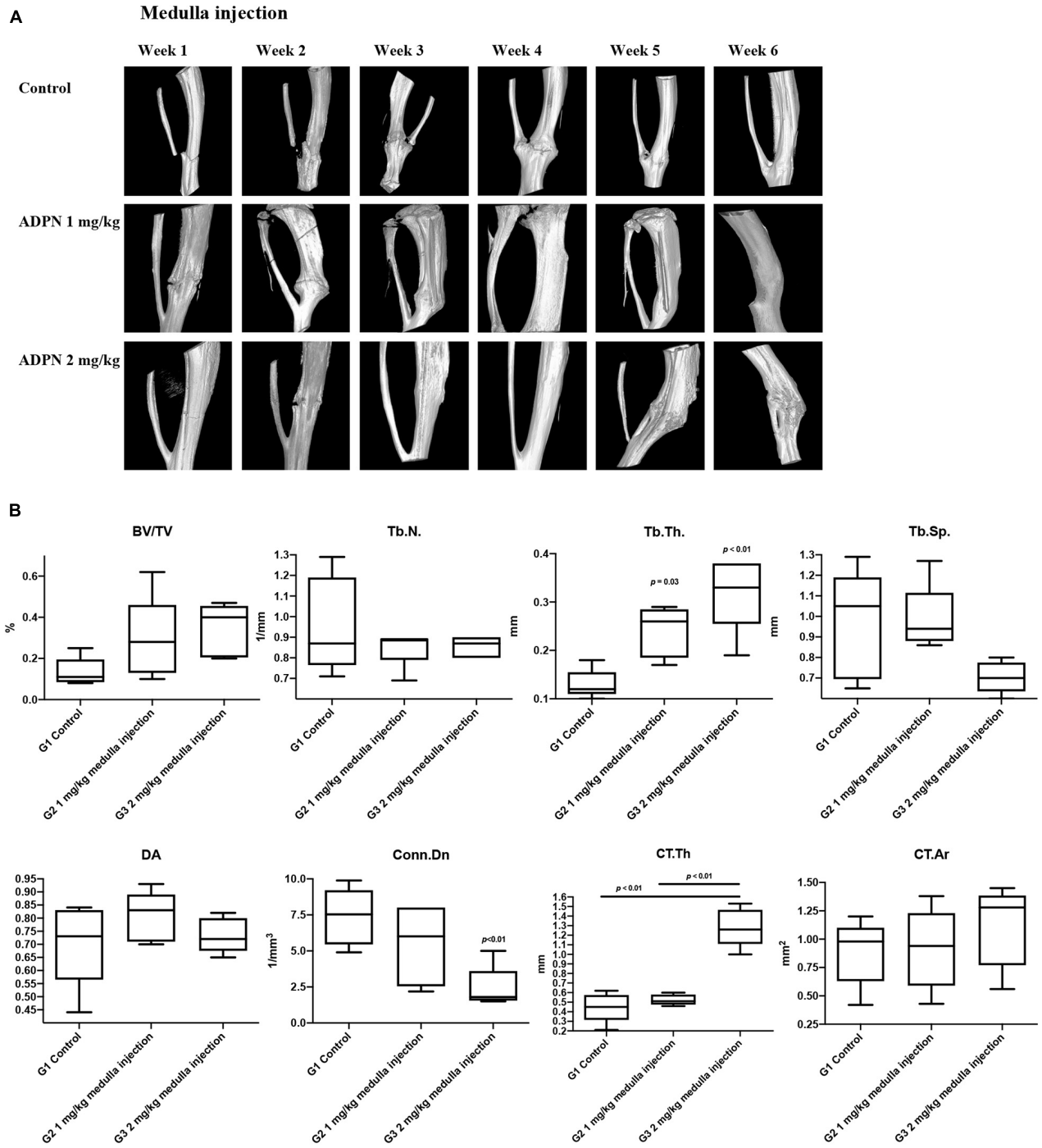

FIGURE 3 | Local medulla injection of ADPN accelerated fracture healing and significantly influenced bone microarchitecture. **(A)** The three-dimensional μCT reconstruction of rat tibia from week 1 to 6. **(B)** Bone morphometric indices extracted from microcomputerized tomography (μCT) at week 6, $n = 6$.

Sp., μm^{-1}), degree of anisotropy (DA), and connectivity density (Conn. Dn., mm^{-3}) were extracted from the μCT images to evaluate the trabecular bone microarchitecture. The Tb. Th rose to 0.24 and 0.32 mm^{-1} for G2 and G3, respectively, considerably higher compared with that of the control group (0.13 mm^{-1}). However, significant decrease in Conn. Dn. was observed for G3 to 2.42 from 7.47 mm^{-3} in the control group. Comparable values were derived for other extracted indices (**Figure 3B**).

Cortical bone morphometric indices, including cortical bone area (Ct. Ar., mm^2) and average cortical thickness (Ct. Th., mm), were derived to assess the cortical bone microarchitecture. The Ct. Th. was markedly increased to 1.28 mm for G3, while

comparable values of 0.45 and 0.52 were obtained for G1 and G2. Hyperplasia was obvious in G3, even extended to the fibula, which may contribute to the elevated Ct. Th. value.

The quality of new bone was further evaluated by histological evaluation with hematoxylin and eosin (H&E), and Masson trichrome staining (MS) (**Figure 4**). Immature and non-calcified calluses occupied an obvious larger area in the ADPN-treated groups, compared with the control group with time progression. The thickness of internal and external callus, and the quantitative values were plotted. Twelve directions evenly distributed from the center of the ring to the edge on each section were selected to measure the thickness. At week 6, the space between calluses increased in the control group, and abnormal hyperplasia was found in the 2 mg/kg ADPN group. Bone cortex became

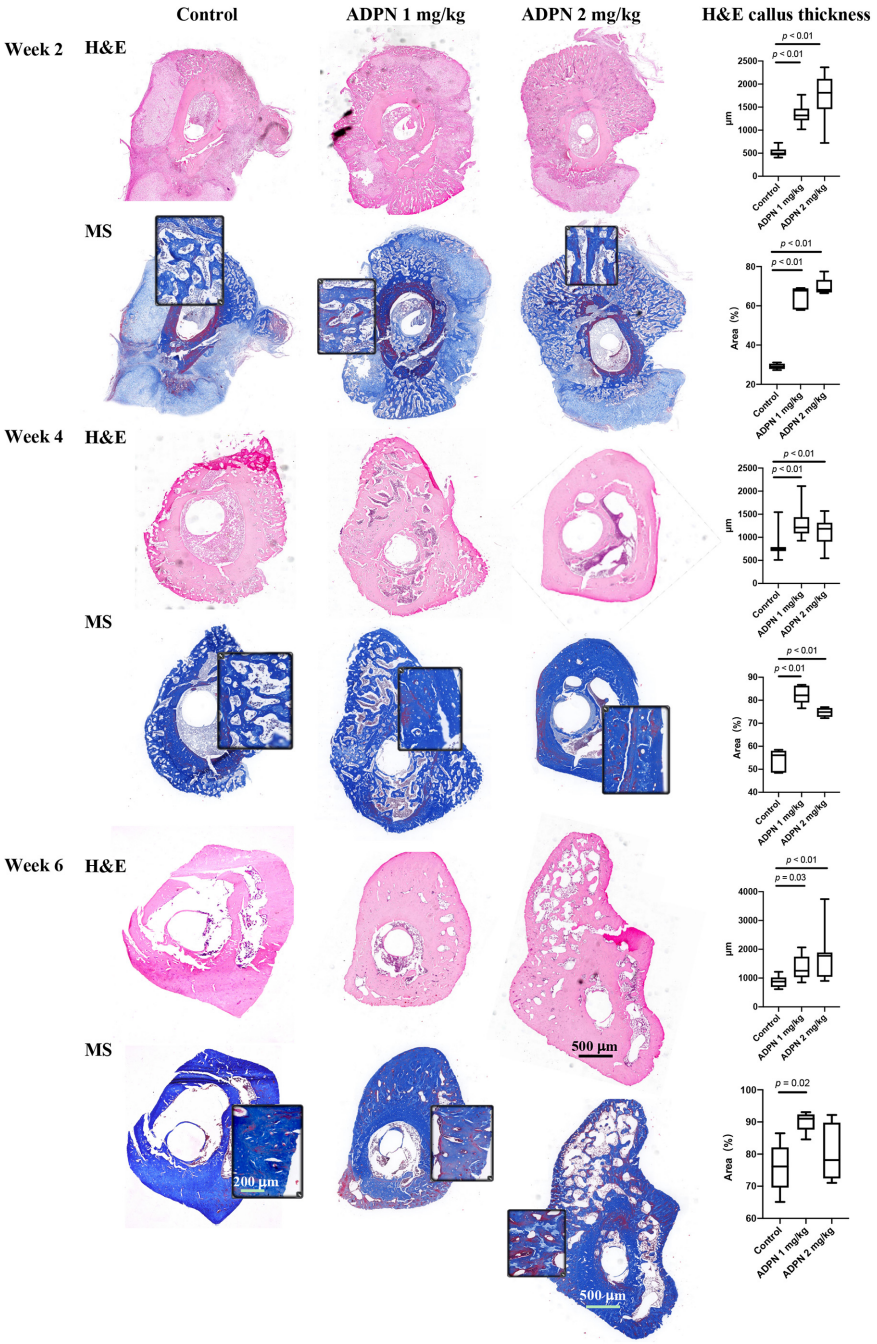

FIGURE 4 | Histology evaluation of bone regeneration. The hematoxylin and eosin (H&E) and Masson trichrome staining (MS) images of rat tibia transverse sections at weeks 2, 4, and 6 (n = 5), scale bar = 500 μm and scale bar = 200 μm in the magnified images. The ADPN treatment groups showed thicker cortical bone and bone calluses. The callus thickness and the blue-stained area, indicative of new bone formation, were quantified and plotted.

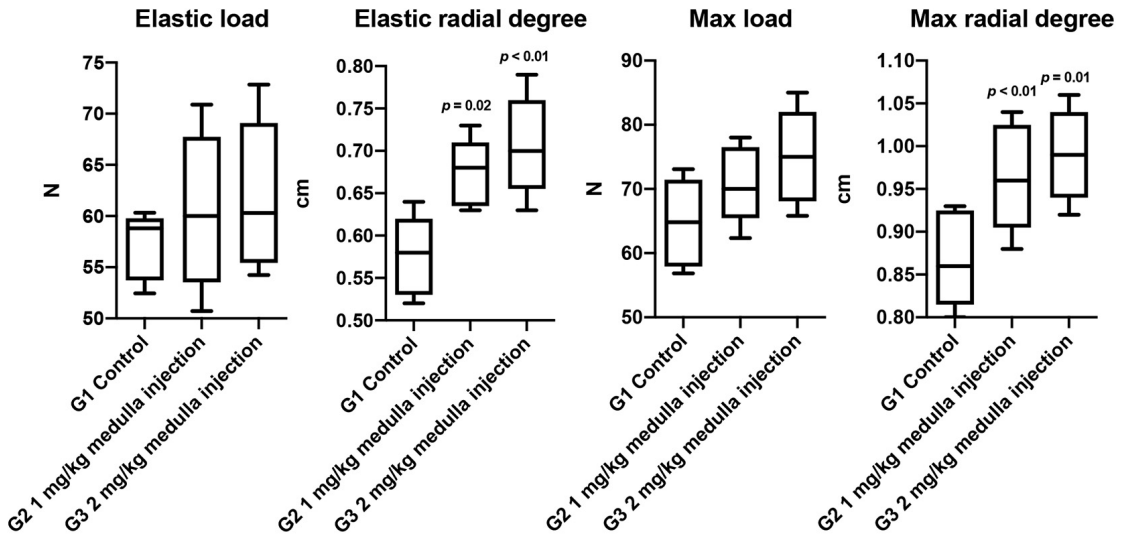

FIGURE 5 | The biomechanical properties of rat tibia at week 6, $n = 6$.

thicker, and relatively large gaps existed between multilayer immature bone calluses.

The blue-stained area in Masson's trichrome staining was measured to evaluate the changes in bone regeneration. At week 2, hematoma and granulation tissue were mainly found in the treatment group, with little bone formation. The quality of bone tissue in the ADPN treatment group was better than that in the control group; however, no significant difference was observed between groups. At week 4, the hematoma was almost absorbed, and the callus became smaller with the regeneration of bone tissue. The quality of bone tissue in the treatment group was significantly better than that in the control group. At week 6, abnormal bone formation was found in the ADPN 2 mg/kg group. The MS section showed less blue staining, probably due to the formation of heterotopic hyperplasia. The quality of the new generated bone with ADPN 1 mg/kg treatment on week 6 was satisfactory with the blue stain area > 90%.

The biomechanical properties of the regenerated bone, including elastic load, elastic radial degree, max load, and max radial degree, were evaluated (**Figure 5**). Significant improvements were observed in structural biomechanics of the healed tibia in the ADPN-treated groups, as well as in the elastic radial degree, maximal radial degree, and maximum load, especially in the ADPN 2 mg/kg group.

Potential Mechanism of Adiponectin Promoting Fracture Healing

Osteoprotegerin (OPG) in the serum was considerably elevated after administration of ADPN. OPG is a well-known decoy receptor for RANKL, and OPG can inhibit RANK–RANKL interactions, resulting in suppressing osteoclastogenesis and bone resorption. The expression of OPG peaked at week 4 in both treatment groups. OPG level was significantly higher in the ADPN-treated groups than that in the control group (**Figure 6A**).

Western blot analysis showed that the maximum level of the early osteogenic marker ALP appeared at week 2 post surgery in both treatment groups, and its expression decreased with time progression. The BMP-2 and late osteogenic marker OCN were peaked at week 4 for the ADPN 1 mg/kg group. The ADPN 1 mg/kg treatment group exhibited significantly higher expressions of all three osteogenic markers, ALP, BMP-2, and OCN, than that of the ADPN 2 mg/kg at the three investigated time points (**Figure 6B**). The ADPN receptor AdipoR1 was also quantified with high expression in both the treatment groups at week 2 and markedly lower values at weeks 4 and 6 for the G3 than that of G2. Immunofluorescent staining images demonstrated that AdipoR1, ALP, BMP-2, and OCN were highly expressed during fracture healing following ADPN treatment (**Figure 6C**).

Rat BMSCs were treated with 10 μg/ml of ADPN and the AdipoR1 siRNA + 10 μg/ml of ADPN to evaluate the effects on osteogenesis. The addition of ADPN significantly elevated the expression of AdipoR1 as shown with the intensified red color in the image (**Figure 7**). After transfecting the AdipoR1 siRNA, the expression of AdipoR1 was remarkably knocked down. The osteogenic markers ALP, BMP-2, and OCN were significantly increased with the treatment of ADPN, while when knocking down of AdipoR1 with siRNA, the expression of those osteogenic markers declined concomitantly.

DISCUSSION

Bone regeneration and bone fracture healing remain great challenges in daily clinical practice. Alternative therapies are being developed, including the FDA-approved BMP-2 and BMP-7 treatments (Jo et al., 2015), to overcome the adverse effects of autologous bone transplantation. Unfortunately, supraphysiological dosage, short half-life

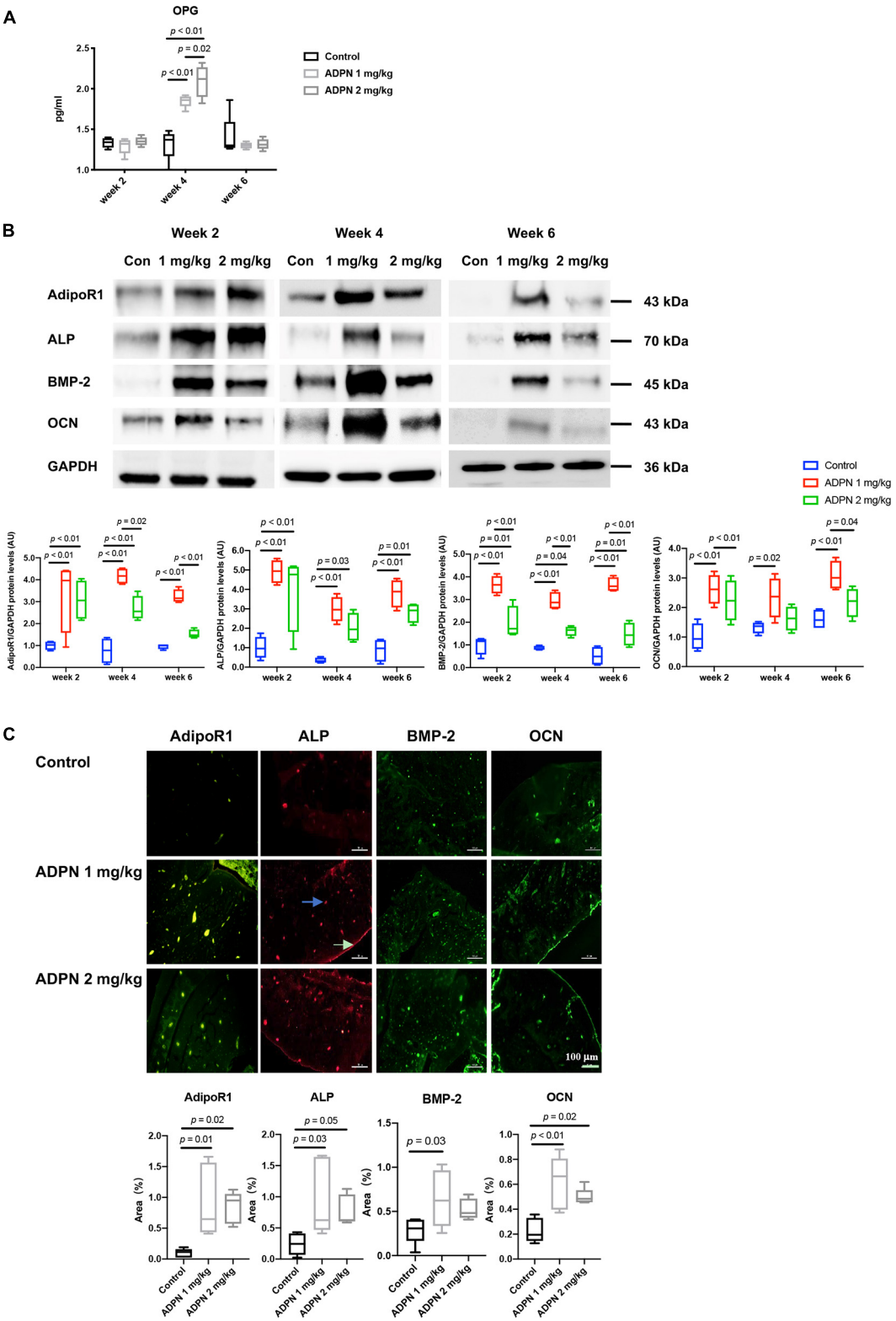

FIGURE 6 | Mechanisms for local medulla injection of ADPN promoting bone healing. **(A)** Serum Osteoprotegerin (OPG) levels at weeks 2, 4, and 6. **(B)** WB analysis of alkaline phosphatase (ALP), bone morphogenic protein 2 (BMP-2), osteocalcin (OCN), and adiponectin receptor 1 (AdipoR1) expressions with corresponding quantification, **(C)** Immunofluorescent staining of ALP, OCN, BMP-2, and AdipoR1 in G2 (ADPN 1 mg/kg) and G3 (ADPN 2 mg/kg), and the corresponding quantification, $n = 5$. The white arrow indicates the periosteum, and the blue arrow indicates the lacuna, scale bar = 100 μm.

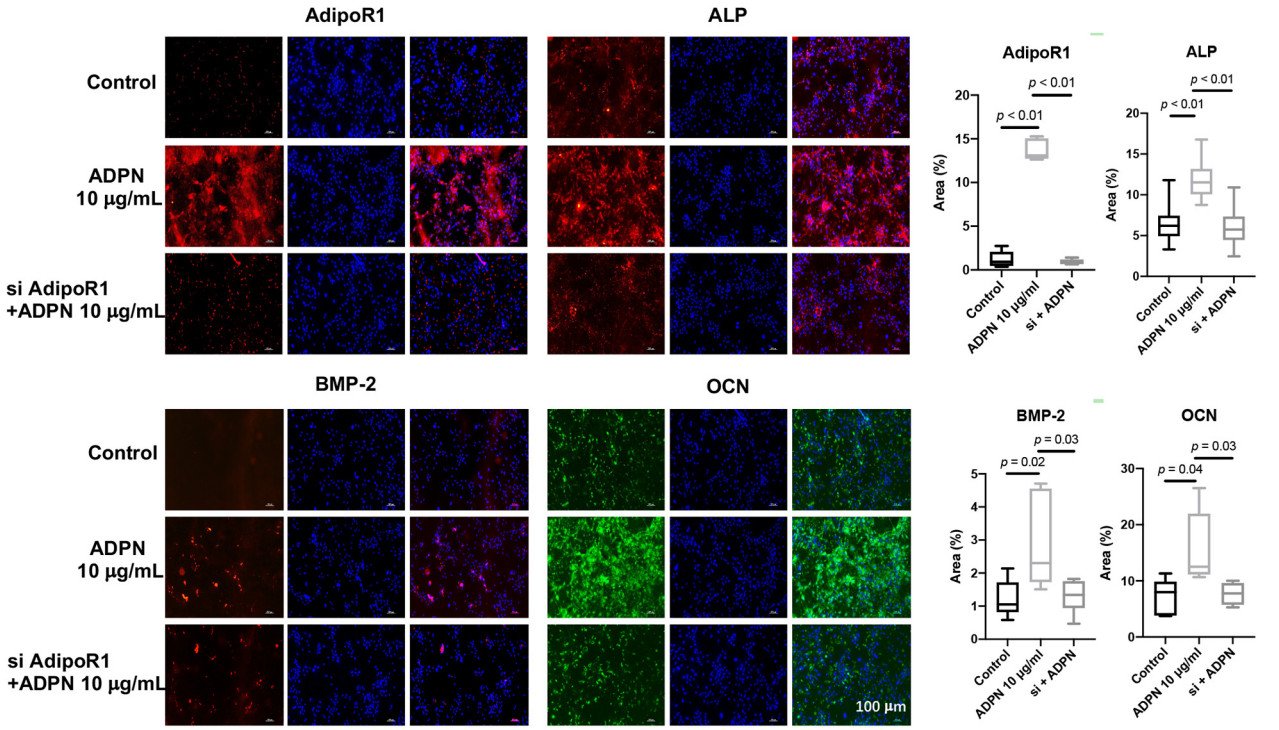

FIGURE 7 | The immunofluorescent staining of ALP, OCN, BMP-2, and AdipoR1 on BMSCs with ADPN 10 μg/ml and AdipoR1 siRNA + ADPN 10 μg/ml, and the corresponding quantification, scale bar = 100 μm.

time, and extremely high cost significantly limit the applicability of these protein therapies.

Adiponectin, a protein hormone produced primarily in adipose tissue, is secreted into the bloodstream and is very abundant in plasma (5–10 mg/L), accounting for approximately 0.01% of all plasma proteins, compared with many other hormones (Nien et al., 2007). In the last 20 years, the physiological functions of adiponectin in whole-body energy homeostasis have been well documented, particularly the connections with obesity, diabetes mellitus, and atherosclerosis (Li et al., 2009; Yamauchi and Kadowaki, 2013). An interesting finding was the inverse relationship between adiponectin levels and fat mass, which distinguished adiponectin from other adipokines, such as leptin (Yadav et al., 2013). Fat and bone tissues can crosstalk with each other through hormones and cytokines to maintain their balance. In 2004, adiponectin and its receptors, AdipoR1 and AdipoR2, were reported to be present in human osteoblasts (Berner et al., 2004). In addition, the supplementation of culture medium with adiponectin enhanced cell proliferation of mice (Kanazawa et al., 2007). Thereafter, more attention has been garnered on the activity of adiponectin in bone. Numerous studies *in vitro*, *in vivo*, and in clinical settings were carried out to clarify the role of adiponectin in bone physiology (Williams et al., 2009). Adiponectin enhances osteoblast proliferation and differentiation concurrently with the inhibition of osteoclastogenesis *in vitro* (Yang et al., 2019); however, an inverse relationship between serum adiponectin concentrations and BMD was dominantly demonstrated in clinical studies (Richards et al., 2007). The most inconsistent results reported in the literature were obtained from different animal models. The variations are most likely due to the different forms of intercellular signaling, including paracrine effects of adiponectin produced in bone marrow adipocytes, endocrine effects of adiponectin released from white adipose tissue into the bloodstream, and second-order effects from the balance of whole-body energy (Naot et al., 2017).

We particularly focused on the relationship between adiponectin and bone fracture repair in this study, to extend our understanding on the paracrine effects of ADPN through medulla injection. First of all, a facile and efficient approach was designed to obtain purified recombinant human adiponectin. The endogenous glutamine synthetase gene in CHO-K1 cells was selected to be knocked out with the CRISPR technique to speed up the screening process. High purity protein (20 μg/ml) was yielded with our more optimal preparation method. The lyophilized protein powder in glass vials was easy for storage and further usage. The pharmacokinetic behaviors of the derived adiponectin were further evaluated. The C_{max} reached a maximum after 8 h *via* medulla injection of ADPN. Longer retention in the bone marrow of ADPN was achieved with intrabone marrow injection, which could provide extended bioavailability. Local administration of ADPN remarkably promoting the growth of callus and bone healing was confirmed in the rat tibia fracture model. With longer duration of local action, ADPN induced hyperplasia, which extended to the non-fractured fibula, indicating, to some extent, the osteogenic

ability of local ADPN. This hyperplasia may result from the high dosage of local ADPN and the leakage of the local injection of ADPN to the fibula. This phenomenon warns that the proper dosage and duration of locally administrated ADPN are crucial factors for bone fracture treatment in practice. Biosafety and non-toxicity are of importance for every therapy. Hematology and serum biochemistry tests confirmed the biocompatibility of ADPN for medulla injection.

Local administration of ADPN promoting bone formation in our study mainly results from enhancing osteogenic differentiation. In BMSCs, the ADPN promoted osteogenic differentiation through its receptor AdipoR1 to increase the expression of osteogenic markers ALP, BMP-2, and OCN. In addition, the ADPN also presented the ability of enhancing proliferation up to 30 μg/ml *in vitro*. The addition of ADPN can increase the expression of AdipoR1 in BMSCs considerably, while knocking down of AdipoR1 with ADPN loses their osteogenic ability. Our observations coincide with the results reported in the literature that adiponectin could decrease the number of osteoclasts and improve bone healing *via* the OPG/RANKL pathway (Luo et al., 2006). A potential mechanism for bone regeneration promoted by recombinant human adiponectin was preliminary investigated; however, systemic signal transduction process should be thoroughly examined to unravel the underlying mechanism for the bioactivity of adiponectin in bone regeneration. Heterotopic ossification is the process by which bone tissue forms outside of the skeleton. Heterotopic hyperplasia was observed in the higher-dosage ADPN group in our study, which could have a certain extent of influence on the μCT data, however, it did not alter the conclusion of the ability to enhance osteogenesis and bone regeneration of ADPN. In our future experiment, this phenomenon of hyperplasia is planned to be further investigated.

CONCLUSION

In conclusion, we provided a facile method to obtain high-purity and high-yield ADPN for bone fracture treatment, which presented great biocompatibility as well as efficacy for improved bone healing *via* medulla injection. ADPN plays a potential significant role in stimulating the expression of ALP, BMP-2, and OCN at the fracture site through increasing the expression of its own receptor AdipoRl. A dosage of 1 mg/kg of ADPN was optimal to accelerate bone fracture healing in our experimental setting. Our findings demonstrated that local fracture treatment with ADPN could be a useful therapeutic option to shorten healing time and potentially be rapidly translated into the clinics.

DATA AVAILABILITY STATEMENT

The data that support the findings of this study are available from the corresponding author upon reasonable request.

ETHICS STATEMENT

The animal study was reviewed and approved by the Ethics Committee of the Chinese People's Liberation Army General Hospital, Beijing, China.

AUTHOR CONTRIBUTIONS

YG and Z-KC conceived the ideas for the experimental designs, analyzed the data, and wrote the manuscript. YG, YW, YQZ, LCW, LJW, and YAZ conducted all the experiments and helped with manuscript preparation. CL provided suggestions and revised the manuscript. All authors contributed to the article and approved the submitted version.

FUNDING

This work was supported by the grants from the Youth Training Program of Military Medical Science and Technology (20QNPY103), the National Natural Science Foundation of China (32070774), the Science and Technology Program of Guangzhou (202002030486), the Key Research and Development Program of Bioland Laboratory (2018GZR110104002), the Translational Medicine Projects of the Chinese People's Liberation Army General Hospital (2017TM-021), and the Military Logistics research projects of China (CWS13J054).

SUPPLEMENTARY MATERIAL

The Supplementary Material for this article can be found online at: https://www.frontiersin.org/articles/10.3389/fcell.2021.762335/full#supplementary-material

REFERENCES

Baqain, Z. H., Anabtawi, M., Abu Karaky, A., and Malkawi, Z. (2009). morbidity from anterior iliac crest bone harvesting for secondary alveolar bone grafting: an outcome assessment study. *J. Oral Maxillofac. Surg.* 67, 570–575. doi: 10.1016/j.joms.2008.09.023

Barbour, K. E., Zmuda, J. M., Boudreau, R., Strotmeyer, E. S., Horwitz, M. J., Evans, R. W., et al. (2011). Adipokines and the risk of fracture in older adults. *J. Bone Miner. Res.* 26, 1568–1576. doi: 10.1002/jbmr.361

Berner, H. S., Lyngstadaas, S. P., Spahr, A., Monjo, M., Thommesen, L., Drevon, C. A., et al. (2004). Adiponectin and its receptors are expressed in bone-forming cells. *Bone* 35, 842–849. doi: 10.1016/j.bone.2004.06.008

Burge, R., Dawson-Hughes, B., Solomon, D. H., Wong, J. B., King, A., and Tosteson, A. (2007). Incidence and economic burden of osteoporosis-related fractures in the United States, 2005-2025. *J. Bone Miner. Res.* 22, 465–475. doi: 10.1359/jbmr.061113

Cahill, K. S., Chi, J. H., Day, A., and Claus, E. B. (2009). Prevalence, complications, and hospital charges associated with use of bone-morphogenetic proteins in spinal fusion procedures. *JAMA* 302, 58–66. doi: 10.1001/jama.2009.956

Chen, Q., Shou, P., Zheng, C., Jiang, M., Cao, G., Yang, Q., et al. (2016). Fate decision of mesenchymal stem cells: adipocytes or osteoblasts? *Cell Death Differ.* 23, 1128–1139. doi: 10.1038/cdd.2015.168

China, S. P., Pal, S., Chattopadhyay, S., Porwal, K., Kushwaha, S., Bhattacharyya, S., et al. (2017). Globular adiponectin reverses osteo-sarcopenia and altered body

composition in ovariectomized rats. *Bone* 105, 75–86. doi: 10.1016/j.bone.2017.08.005

China, S. P., Sanyal, S., and Chattopadhyay, N. (2018). Adiponectin signaling and its role in bone metabolism. *Cytokine* 112, 116–131. doi: 10.1016/j.cyto.2018.06.012

Clarke, B. (2008). Normal bone anatomy and physiology. *Clin. J. Am. Soc. Nephrol.* 3, S131–S139. doi: 10.2215/CJN.04151206

Einhorn, T. A., and Gerstenfeld, L. C. (2015). Fracture healing: mechanisms and interventions. *Nat. Rev. Rheumatol.* 11, 45–54. doi: 10.1038/nrrheum.2014.164

Gimble, J. M., Zvonic, S., Floyd, Z. E., Kassem, M., and Nuttall, M. E. (2006). Playing with bone and fat. *J. Cell Biochem.* 98, 251–266. doi: 10.1002/jcb.20777

Glassman, S. D., Carreon, L. Y., Djurasovic, M., Campbell, M. J., Puno, R. M., Johnson, J. R., et al. (2008). RhBMP-2 versus iliac crest bone graft for lumbar spine fusion. *Spine* 33, 2843–2849. doi: 10.1097/BRS.0b013e318190705d

Jo, J. Y., Jeong, S. I., Shin, Y. M., Kang, S. S., Kim, S. E., Jeong, C. M., et al. (2015). Sequential delivery of BMP-2 and BMP-7 for bone regeneration using a heparinized collagen membrane. *Int. J. Oral Maxillofac. Surg.* 44, 921–928. doi: 10.1016/j.ijom.2015.02.015

Kanazawa, I., Yamaguchi, T., Yano, S., Yamauchi, M., Yamamoto, M., and Sugimoto, T. (2007). Adiponectin and AMP kinase activator stimulate proliferation, differentiation, and mineralization of osteoblastic MC3T3-E1 cells. *BMC Cell Biol.* 8:51. doi: 10.1186/1471-2121-8-51

Kang, K. H., Higashino, A., Kim, H. S., Lee, Y. T., and Kageyama, T. (2009). Molecular cloning, gene expression, and tissue distribution of adiponectin and its receptors in the Japanese monkey, *Macaca fuscata*. *J. Med. Primatol.* 38, 77–85. doi: 10.1111/j.1600-0684.2008.00298.x

Li, S. S., Shin, H. J., Ding, E. L., and van Dam, R. M. (2009). Adiponectin levels and risk of type 2 diabetes a systematic review and meta-analysis. *JAMA* 302, 179–188. doi: 10.1001/jama.2009.976

Long, F. (2011). Building strong bones: molecular regulation of the osteoblast lineage. *Nat. Rev. Mol. Cell Biol.* 13, 27–38. doi: 10.1038/nrm3254

Luo, X. H., Guo, L. J., Xie, H., Yuan, L. Q., Wu, X. P., Zhou, H. D., et al. (2006). Adiponectin stimulates RANKL and inhibits OPG expression in human osteoblasts through the MAPK signaling pathway. *J Bone Miner Res.* 21, 1648–1656. doi: 10.1359/jbmr.060707

Martinez-Huenchullan, S. F., Tam, C. S., Ban, L. A., Ehrenfeld-Slater, P., McLennan, S. V., and Twigg, S. M. (2020). Skeletal muscle adiponectin induction in obesity and exercise. *Metabolism* 102:154008. doi: 10.1016/j.metabol.2019.154008

Matsuda, K., Fujishima, Y., Maeda, N., Mori, T., Hirata, A., Sekimoto, R., et al. (2015). Positive feedback regulation between adiponectin and T-cadherin impacts adiponectin levels in tissue and plasma of male mice. *Endocrinology* 156, 934–946. doi: 10.1210/en.2014-1618

Naot, D., Musson, D. S., and Cornish, J. (2017). The activity of adiponectin in bone. *Calcif. Tissue Int.* 100, 486–499. doi: 10.1007/s00223-016-0216-5

Napoli, N., Pedone, C., Pozzilli, P., Lauretani, F., Ferrucci, L., and Incalzi, R. A. (2010). Adiponectin and bone mass density: the InCHIANTI study. *Bone* 47, 1001–1005. doi: 10.1016/j.bone.2010.08.010

Nien, J. K., Mazaki-Tovi, S., Romero, R., Erez, O., Kusanovic, J. P., Gotsch, F., et al. (2007). Plasma adiponectin concentrations in non-pregnant, normal and overweight pregnant women. *J. Perinat. Med.* 35, 522–531. doi: 10.1515/JPM.2007.123

Ohashi, K., Parker, J. L., Ouchi, N., Higuchi, A., Vita, J. A., Gokce, N., et al. (2010). Adiponectin promotes macrophage polarization toward an anti-inflammatory phenotype. *J. Biol. Chem.* 285, 6153–6160. doi: 10.1074/jbc.M109.088708

Richards, J. B., Valdes, A. M., Burling, K., Perks, U. C., and Spector, T. D. (2007). Serum adiponectin and bone mineral density in women. *J. Clin. Endocrinol. Metab.* 92, 1517–1523. doi: 10.1210/jc.2006-2097

Scherer, P. E., Williams, S., Fogliano, M., Baldini, G., and Lodish, H. F. (1995). A novel serum protein similar to C1q, produced exclusively in adipocytes. *J. Biol. Chem.* 270, 26746–26749. doi: 10.1074/jbc.270.45.26746

Skovrlj, B., Koehler, S. M., Anderson, P. A., Qureshi, S. A., Hecht, A. C., Iatridis, J. C., et al. (2015). Association between BMP-2 and carcinogenicity. *Spine* 40, 1862–1871. doi: 10.1097/BRS.0000000000001126

Wang, Z. V., and Scherer, P. E. (2016). Adiponectin, the past two decades. *J. Mol. Cell Biol.* 8, 93–100. doi: 10.1093/jmcb/mjw011

Williams, G. A., Wang, Y., Callon, K. E., Watson, M., Lin, J. M., Lam, J. B., et al. (2009). In vitro and in vivo effects of adiponectin on bone. *Endocrinology* 150, 3603–3610. doi: 10.1210/en.2008-1639

Wu, X., Huang, L., and Liu, J. (2019). Effects of adiponectin on osteoclastogenesis from mouse bone marrow-derived monocytes. *Exp. Ther. Med.* 17, 1228–1233. doi: 10.3892/etm.2018.7069

Yadav, A., Kataria, M. A., Saini, V., and Yadav, A. (2013). Role of leptin and adiponectin in insulin resistance. *Clin. Chim. Acta* 417, 80–84. doi: 10.1016/j.cca.2012.12.007

Yamauchi, T., and Kadowaki, T. (2013). Adiponectin receptor as a key player in healthy longevity and obesity-related diseases. *Cell Metab.* 17, 185–196. doi: 10.1016/j.cmet.2013.01.001

Yang, J., Park, O. J., Kim, J., Han, S., Yang, Y., Yun, C. H., et al. (2019). Adiponectin deficiency triggers bone loss by up-regulation of osteoclastogenesis and down-regulation of osteoblastogenesis. *Front. Endocrinol.* 10:815. doi: 10.3389/fendo.2019.00815

Conflict of Interest: The authors declare that the research was conducted in the absence of any commercial or financial relationships that could be construed as a potential conflict of interest.

Publisher's Note: All claims expressed in this article are solely those of the authors and do not necessarily represent those of their affiliated organizations, or those of the publisher, the editors and the reviewers. Any product that may be evaluated in this article, or claim that may be made by its manufacturer, is not guaranteed or endorsed by the publisher.

frontiers in Cell and Developmental Biology

REVIEW
published: 24 November 2021
doi: 10.3389/fcell.2021.778015

Endocrine Regulation of Extra-skeletal Organs by Bone-derived Secreted Protein and the effect of Mechanical Stimulation

Yuxiang Du[1†], Lingli Zhang[2†], Zhikun Wang[1], Xuan Zhao[1] and Jun Zou[1]*

[1]School of Kinesiology, Shanghai University of Sport, Shanghai, China, [2]School of Physical Education and Sports Science, South China Normal University, Guangzhou, China

Bone serves as the support for body and provide attachment points for the muscles. The musculoskeletal system is the basis for the human body to complete exercise. Studies believe that bone is not only the basis for constructing structures, but also participates in the regulation of organs outside bone. The realization of this function is closely related to the protein secreted by bone. Whether bone can realize their positions in the human body is also related to their secretion. Bone-derived proteins provide a medium for the targeted regulation of bones on organs, making the role of bone in human body more profound and concrete. Mechanical stimulation effects the extra-skeletal organs by causing quantitative changes in bone-derived factors. When bone receives mechanical stimulation, the nichle of bone responds, and the secretion of various factors changes. However, whether the proteins secreted by bone can interfere with disease requires more research. In this review article, we will first introduce the important reasons and significance of the in-depth study on bone-derived secretory proteins, and summarize the locations, structures and functions of these proteins. These functions will not only focus on the bone metabolism process, but also be reflected in the cross-organ regulation. We specifically explain the role of typical bone-derived secretory factors such as osteocalcin (OCN), osteopontin (OPN), sclerostin (SOST) and fibroblast growth factor 23 (FGF23) in different organs and metabolic processes, then establishing the relationship between them and diseases. Finally, we will discuss whether exercise or mechanical stimulation can have a definite effect on bone-derived secretory factors. Understanding their important role in cross-organ regulation is of great significance for the treatment of diseases, especially for the elderly people with more than one basic disease.

Keywords: bone, secreted protein, cross-organ regulation, endocrine regulation, exercise prescription, mechanical stimulation

OPEN ACCESS

Edited by:
Airong Qian,
Northwestern Polytechnical University, China

Reviewed by:
Yun Shen,
Shanghai Jiao Tong University, China
Tadahiro Iimura,
Hokkaido University, Japan

***Correspondence:**
Jun Zou
junzou@sus.edu.cn

[†]These authors have contributed equally to this work

Specialty section:
This article was submitted to Morphogenesis and Patterning, a section of the journal Frontiers in Cell and Developmental Biology

Received: *16 September 2021*
Accepted: *03 November 2021*
Published: *24 November 2021*

Citation:
Du Y, Zhang L, Wang Z, Zhao X and Zou J (2021) Endocrine Regulation of Extra-skeletal Organs by Bone-derived Secreted Protein and the effect of Mechanical Stimulation. Front. Cell Dev. Biol. 9:778015. doi: 10.3389/fcell.2021.778015

INTRODUCTION

The bones form the outline of the body, provide attachment points for muscle and serve as a support for the body physically. But bone is not generally considered an endocrine gland. The definition of endocrine gland is that it must be highly vascularized to form a system and directly secrete hormones into the blood so as to affect distant targets. According to this definition, the osteocyte lacunar

contains bone fluid of bone cells release factors which can be found in circulation. It has the role of supporting and remodeling, also keep closely with the balance and maintenance of multiple trace elements in the human body. In adult bones, osteoblasts may account for approximately 5% of bone cells. Compared with 1% of osteoclasts, 90–95% are bone cells. Osteoblasts can release factors such as osteocalcin. In addition, bone cells can produce circulating factors such as FGF23 and SOST. With the gradual deepening of research, study showed that bone has the function of secreting protein factors, and believe that bone is an important endocrine organ (Brunetti et al., 2017; DeLuccia et al., 2019; Gomarasca et al., 2020). In recent years, it was found that bones are the largest secretory organs in the whole body, and secretory factors affect organs outside the bones through bone-derived factors including FGF23, prostaglandin E2 (PGE2), transforming growth factor-β (TGF-β), OCN and SOST. The structure and function of bone-derived secreted protein can be divided into two parts according to their positions. Intraosseous one can regulate the balance between bone formation and resorption. In addition to changes happened in its own bone microstructure and bone mass, the changes of its secretion factors will inevitably affect the external organs. Once they turn into extraosseous one, the function will be affecting extra-skeletal organs. These organs involve in the nervous system, glucose and lipid metabolism, blood cardiovascular system, muscles, thyroid and so on. The effect is of great difference.

The motor system includes bones, bone connections and skeletal muscles. Under the innervation of the nerve, the muscle contracts and pull the bone to which it is attached. Bone will respond when it receiving mechanical stimulation (or exercise) by changing its bone secretion. What we can determine till now is that mechanical stimulation (or exercise) will have an effect on bone-derived secreted proteins, and this impact will continuous exist for a short term. Mechanically sensitive cells can perceive mechanical stimuli through receptors on the envelope, such as primary ciliary complexes, integrins, and Ca^{2+} channels. For bone cells, the lacuno-canalicular network (LCN) can be used to quickly transmit signals. When the mechanical stimulus changes, the system responds quickly, generating fluid shear force on the surrounding cells. This change can affect the up-regulation of SOST and RANKL. The complex tensile and compressive stresses generated by mechanical stimulation can reduce the expression of SOST in bone cells and promote the process of bone formation and mineralization. For osteoclasts, the application of mechanical load stimulation can inhibit osteoclast differentiation, and the formation of osteoclasts is promoted after the stimulation is removed. Mechanical stimulation signals can induce osteoprotegerin (OPG) and inhibit RANKL to reduce osteoclast differentiation. Mechanical stimulation can change the bone niche, thereby changing the secretion of bone-derived proteins.

The protein factors secreted by bones not only participate in the metabolic process of the bone itself, but also communicate and regulate information with various organs to jointly achieve and maintain balances in the human body. From this point of view, bone-derived secretory factors should not only be protein factors involved in bone metabolism. These factors are important mediators for bones to regulate extra-skeletal organs. These proteins will specifically act on different target organs, depending on the distribution of their receptors. Not all bone-derived secreted proteins have the same properties.

This article analyzes the structures and source characteristics of common bone-derived secreted proteins to understand their basics of biology. Summarize their regulatory effects in extra-skeletal organs and their manifestations in diseases. For brain and neural network, OPN and OCN can have different effects on Alzheimer's Disease (AD) patients. A variety of bone-derived secretory proteins can play a role in glucose and lipid metabolism, the target organs include liver, kidney, pancreas and so on. In the cardiovascular system, SOST, OPN and FGF23 can affect the state of blood vessels and change the impact of blood on the vessel wall. In the musculoskeletal system, these proteins can regulate inflammatory factors, cardiomyocytes and chondrocytes through specific pathways. Because bone-derived proteins can act on thyroid, they mainly interfere with thyroid bone diseases and hormone regulations. Mechanical stimulation has a regulatory effect on bone-derived proteins, but whether this effect can be used to treat diseases through specific intervention remains to be studied.

THE LOCATION, STRUCTURE AND FUNCTION OF BONE-DERIVED SECRETED PROTEIN

Bone is now considered to be an endocrine organ. Bone cells have the ability to secrete and release protein factors. But there are still some differences among the factors, for example, the secretory cells. Some proteins are secreted by specific cells, while others can be derived from multiple cells. Therefore, the differences also exist in their structures and functions. Typical proteins secreted by specific cells include SOST secreted by osteocytes, FGF23 secreted by osteocytes and osteoblasts, OCN secreted by osteoblasts. At the same time, the proteins secreted and expressed by a variety of cells include OPN, PGE2 and TGF-β.

Proteins Secreted by Specific Cells

Sclerostin

SOST is a glycoprotein secreted by mature bone cells. It is an inhibitor of Wnt signaling and bone morphogenetic protein (BMP), which can negatively regulate bone formation. For development and maintenance of bone, it plays an important role (Wang et al., 2018). The molecular weight of SOST is about 22kD. It is a secreted glycoprotein with cystine knot structure, including a signal sequence for secretion and two putative glycosylation sites. The cystine knot is a finger-like structure formed by two pairs of (Vázquez-Sánchez et al., 2021) twisted anti-parallel β chains. After SOST is secreted, it will anchor on the low-density lipoprotein receptor-related protein-4 (LRP4) receptor of the osteoblast membrane, so that SOST can be retained in the bone cavity. When SOST binds to the receptor LRP5/6 of osteoblasts, it will inhibit the downstream cascade of Wnt/β-catenin signaling in the cell through competitive binding (Xiong and O'Brien, 2012). SOST can do effect on inhibiting bone formation and negatively regulating Wnt/β-catenin signaling pathway.

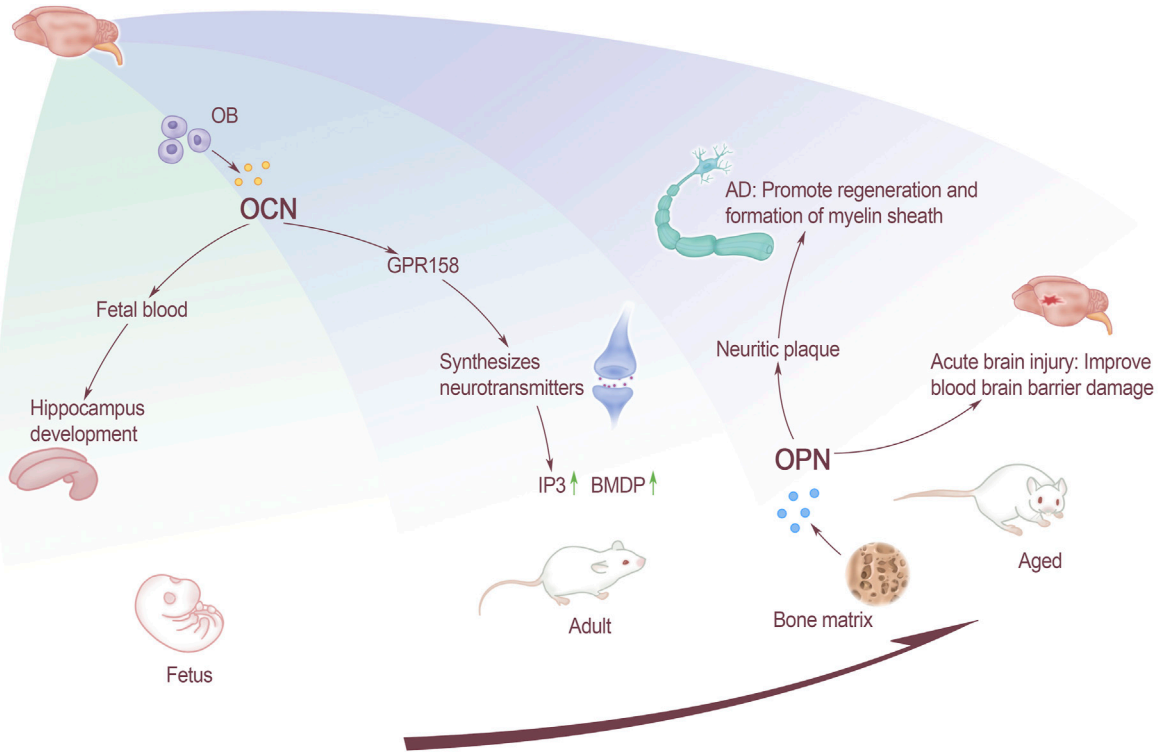

FIGURE 1 | The effect of bone-derived factors on brain at all stages. OCN affects the development of fetal hippocampus through fetal blood, and the GPR158 receptors that acted on adults affects the synthesis of neurotransmitters. For elderly, OPN affects inflammatory plaques and promotes the remyelination and formation of AD patients. Improve the function of the blood-brain barrier in patients with acute brain injury.

Fibroblast Growth Factor 23

FGF23 is a hormone-like protein secreted by osteoblasts and osteocytes. It is a bone-derived factor that regulates the mineralization of extracellular matrix and a systemic hormone that participates in mineral metabolism. The length of FGF23 is more than 8.5 kb. The FGF23 gene is located on chromosome 12 for human and chromosome 6 for mouse, contains 3 exons (Goetz and Mohammadi, 2013). Hormone-like FGF23 has a poor affinity with heparan sulfate. It can be secreted from cells and diffuse into blood, circulating to target cells in distant organs (Asada et al., 2009). The co-receptor α-Klotho is on the surface of target cells for FGF23. The interaction between FGF23 and α-Klotho depends on the carboxyl end of FGF23 (Urakawa et al., 2006). The expression of FGF23 is regulated by many factors, such as 1,25 Dihydroxyvitamin D. It can promote the expression of FGF23 by activating VDR. At the same time, FGF23 can also inhibit the production of 1,25 dihydroxyvitamin D (Yu et al., 2005).

Osteocalcin

OCN is a non-collagenous acid glycoprotein which is synthesized and secreted by osteoblasts in bones (Gallop et al., 1980). It is a kind of calcium-binding protein that depends on vitamin K and is the main component of bone matrix. The relative molecular mass of osteocalcin is about 6kD. It has three γ-carboxyglutamate fragments at three positions of the peptide chain, 17, 21, and 24, which has a high affinity for calcium ions. The gene structure of OCN for both human and rat contains 4 exons and 3 introns (Hauschka et al., 1975). OCN is composed of an unstructured N-terminal, C-terminal hydrophobic core and 3 alpha helices (Zoch et al., 2016). Through γ-glutamyl carboxylase (GGCX) as catalysis, OCN will occur carboxylation reactions under acidic conditions. The difference in the completion of reactions will lead to different products. Undercarboxylated osteocalcin (ucOCN) is the active form of OCN. The protein structure of ucOCN after the removal of the propeptide contains 0–2 γ-carboxyglutamate residues. Carboxylated osteocalcin (cOCN) is inactive and mainly stored in bone to form the skeleton structure.

Proteins Secreted by a Variety of Cells

Osteopontin

OPN is a non-collagen protein secreted by bone cells, osteoblasts, osteoclasts and other cells. It belongs to small integrin-binding lIgand, n-linked glycoproteins (SIBLING) and is an important component for regulating the mineralization of extracellular matrix (De Fusco et al., 2017). The length of OPN is about 8 kb. The OPN coding gene is located on chromosome 4 for human and chromosome 5 for mouse (Bouleftour et al., 2019). It contains 7 exons and 6 introns. The C-terminal of OPN binds two heparin molecules and the CD44 variant, the N-terminal contains the binding region of the integrin receptor (Han et al., 2019). OPN is related to osteoblast mRNA of bone morphogenetic protein signaling pathways (BMPS) downstream, which can stimulate the proliferation and

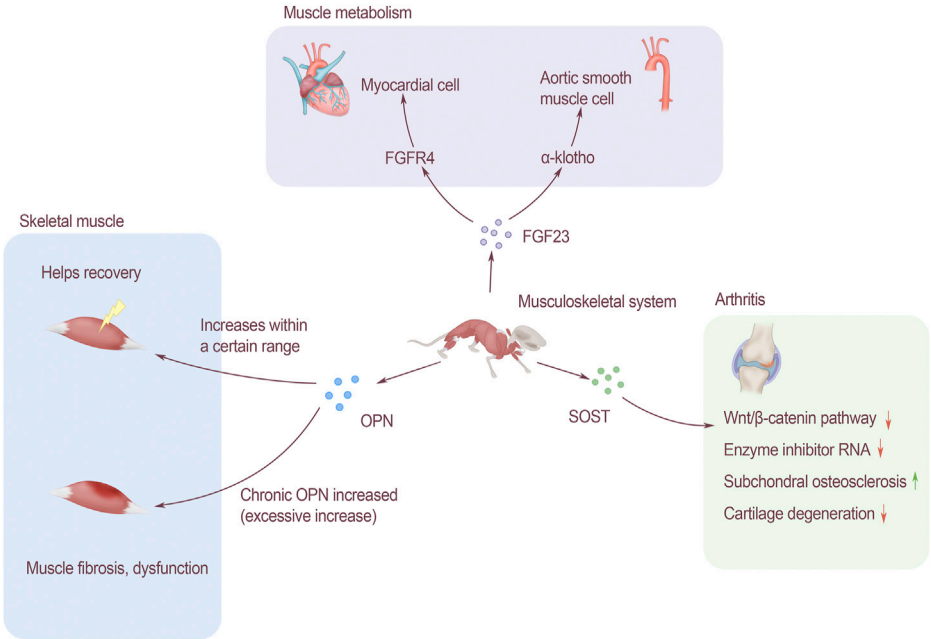

FIGURE 2 | The effect of bone-derived factors on modules of musculoskeletal system. FGF23 affects muscle metabolism. It is associated with cardiomyocytes through FGFR4 and acts on α-Klotho to change aortic smooth muscle. OPN affects skeletal muscles, and the increase in a certain range after injury will help recovery, but long-term increase of OPN will lead to muscle fibrosis and affect muscle function. SOST affects arthritis through the Wnt/β-catenin signaling pathway, which can inhibit the activity of enzyme inhibitor RNA, promote subchondral bone sclerosis, and inhibit cartilage degradation.

calcification of osteoblasts. It is also a pro-inflammatory cytokine that can regulate migration and communication of immune cells, also response to brain injury. It plays an important role in many kinds of neuroinflammatory diseases (Sun et al., 2013).

Prostaglandin E2

PGE2 is one of the diverse prostaglandins (Narumiya et al., 1999), which composed of 378 amino acids. The relative molecular mass of PGE2 is about 43. It is one of the metabolites of arachidonic acid (Wang and Dubois, 2010). The synthesis and catabolism of PGE2 require the participation of multiple enzymes. PGE2 is a hormone-like chemical messenger, which is rapidly oxidized in the body. With an extremely short half-life, it only plays a role in the vicinity of synthetic cells after being released (Tai et al., 2002). By binding to its receptors, it activates and transduces the corresponding signaling pathways in the cells to achieve biological functions. After PGE2 binds to the E-type prostaglandin receptor, which is a G protein-coupled receptor. It will stimulate a variety of downstream signaling pathways (Hatae et al., 2002). Among which the most classic signaling pathway is Wnt/β-catenin. PGE2 can promote regeneration by improving the stability of β-catenin to increase the activity of the pathway (Zhu et al., 2017). This is different from the negative regulation effect of SOST.

Transforming Growth Factor-β

TGF-β is a polypeptide signaling molecule, the superfamily of which includes more than 40 structurally related factors. TGF-β has a wide range of regulatory effects on cell functions, including regulating growth and maintaining the balance of the internal environment (Ismaeel et al., 2019). It can stimulate fibroblasts to synthesize collagen and fibronectin, promoting their deposition in the extracellular matrix. It has a strong chemotactic effect on inflammatory cells and fibroblasts, which can enhance local inflammation. In addition, it also has the function of enhancing the synthesis of denervated skeletal muscle myogenic stem cells and increasing the secretion of extracellular matrix. This process will promote the fibrosis of denervated skeletal muscle. According to research investigations, there are currently known that TGF-β has at least 6 isomers. Mammalian TGF-β mainly includes TGF-β1, TGF-β2, and TGF-β3 subtypes. The three genes of human are respectively located on chromosomes 19q3, 1q41 and 14q24 (Baugé et al., 2014). The nucleotide sequence of each subtype is highly homologous. All exist in the form of homodimers, containing 7 exons. These three TGF-β subtypes are expressed in chondrocytes.

CROSS-ORGAN REGULATION OF BONE-DERIVED SECRETED PROTEIN

Brain and Neural Network

Osteocalcin Affects Cognitive Ability by Binding to Receptors in the Brain

The function of OCN is diversified. It can be divided into two parts: internal and external bones. OCN can indicate the efficiency of bone turnover and take part in the formation of skeletal structure (Vlot et al., 2018). Carboxylated osteocalcin (cOCN) can locate and adsorb hydroxyapatite, which is the basis for maintaining normal bone mineralization. OCN is only

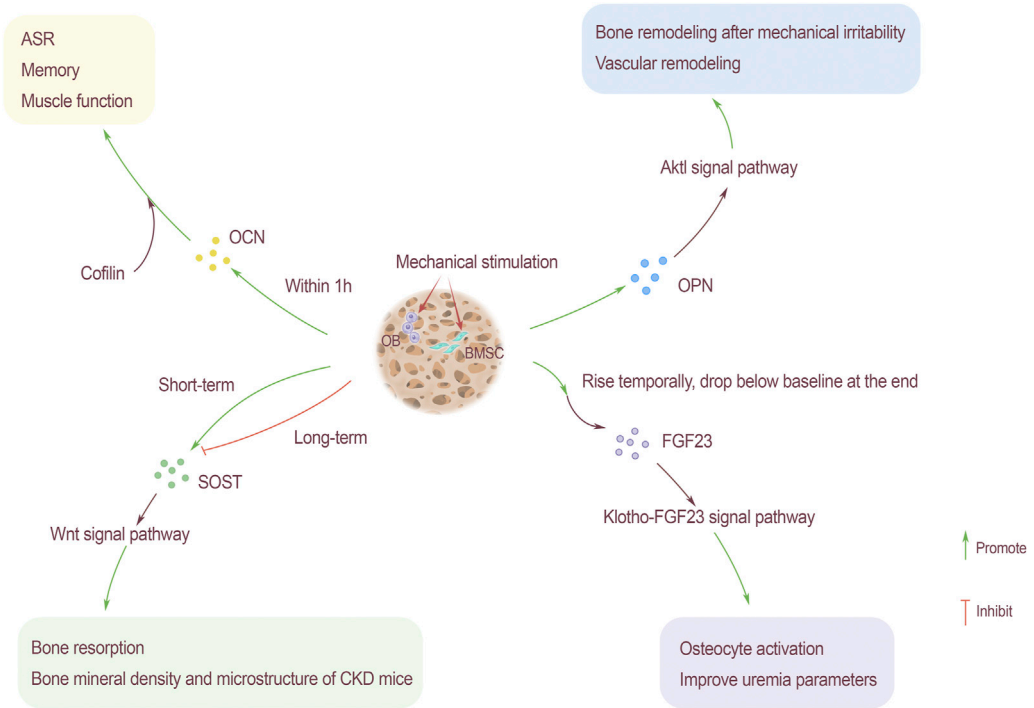

FIGURE 3 | Mechanical stimulation as an influencing factor of bone-derived factors. OCN rises within 1 hour after mechanical stimulation, and through the participation of actin binding protein cofilin, it promotes ASR, memory and muscle function. Mechanical stimulation also promotes the content of OPN, the Akt1 signaling pathway can promote bone remodeling caused by mechanical stress and hypertension-related vascular remodeling. The relationship between SOST content and mechanical stimulation is that SOST rises sharply after short-term mechanical stimulation and then drops below the baseline level. Long-term stimulation slows down the increase of SOST, which has an inhibitory effect. SOST promotes bone resorption and improves the bone density and microstructure of CKD rats through the Wnt signaling pathway. FGF23 rises briefly after receiving mechanical stimulation, and then drops to the baseline level slowly. Through Klotho-FGF23 signaling pathway, the activation of bone cells is enhanced and parameters of uremia will be improved.

synthesized and secreted by mature osteoblasts and osteocytes, then expressed under the control of Runx2/Cfa1 transcription factor. Therefore, its content in serum can indicate bone turnover efficiency and osteoblast activity. As one of the biochemical indicators that specifically reflect bone formation, it can be used for the diagnosis of bone-related diseases. It can also used to check bone condition and observe the effect of intervention treatment. It also has the characteristics of hormones. The active ucOCN can regulate extraosseous organs.

Patients with AD are more likely to get osteoporosis than normal people (Rousseaud et al., 2016). OCN is present in the blood of the fetus during the pre-embryonic period when the fetus undergoes skeletal development. The OCN content of pregnant mice has an effect on the normal development of the fetus' brain, and the benign effect can help the hippocampus development. Knockout of the mother mouse OCN will lead to apoptosis of some fetal nerve cells, and even affect the learning and memory-like behaviors of adult offspring. OCN can cross the blood-brain barrier and bind to G protein-coupled receptor 158 (GPR158) on neurons in the brainstem, midbrain, and hippocampus. GPR158 has been clearly confirmed to be an OCN receptor in brain (Kosmidis et al., 2018), which binds in the CA3 area (Lee et al., 2007), promotes inositol triphosphate (IP3) and brain-derived neurotrophic factor (BDNF) accumulation. G protein-coupled receptor Class C Group 6 Member A (GPRC6A) does not express OCN signals in brain, but OCN can affect cognitive performance through the expression of other receptors (Obri et al., 2018). Therefore, OCN uses a variety of receptors to achieve its functions and play an important role of regulatory in the central nervous system. Although OCN works in conjunction with neurons in the dorsal brainstem and the median sulcus, GPR158 is not expressed in this area. Therefore, it is speculated that OCN may also have a third receptor. This speculation supports the previous view that multiple receptors work (**Figure 1**).

In the process of aging, improving bone health can do good effect on cognitive function. Exercise can have a positive impact on mind, such as preventing AD and so on. Whether the change of OCN can correct AD caused by aging needs further research to know. As a new part of endocrine organs, more and more researches have focused on the influence of OCN on brain, including the regulation pathways of the nervous system, the effect on memory formation and so on.

The influence of OCN on the nervous system can throughout body's life. From the fetal period through the maternal blood affecting fetal brain development, to affect the neurotransmitter synthesis in adulthood, and then participating in the process of cognitive dysfunction and even cause AD. As a research hotspot

of endocrine organs, the researches of bones are focusing on the effects of OCN on the brain. These include the regulation of brain development, pathways of nervous system, memory formation, and intervention in neurological diseases. However, OCN, especially ucOCN, as an important intervention method for the diagnosis and treatment of neurological diseases needs to be further improved.

Osteopontin Promotes Macrophage Migration and Pro-inflammatory Cytokine Production

OPN can inhibit the pathology of various brain diseases through neuroprotection and promotion of repair (Rentsendorj et al., 2018). Not only plays an important role in the extracellular matrix of the central nervous system (CNS), but is also a key factor for matrix remodeling and cell repairing after CNS injury. In addition, OPN plays a key role in traumatic brain injury, stroke, ischemia and neurodegenerative diseases, such as AD and other diseases. The expression of OPN in the brain is low under normal circumstances. It is mainly expressed in the olfactory bulb, cerebellum and brainstem neurons, and the expression in the pons and medulla is higher than that in the midbrain. But it is significantly up-regulated in the case of injury or inflammation (Zhou et al., 2020), such as acute brain injury. Activating the P42/44 MAPK and PI3/Akt pathway can lead to the synthesis of a new protein in the cell, and the PI3/Akt pathway plays a key role in cell apoptosis, blood-brain barrier destruction, neurogenesis and angiogenesis. After acute brain injury, endogenous OPN can improve the damage of the blood-brain barrier through different mechanisms.

Sun found through the rat model of intravascular perforation that OPN is associated with brain injury. The increase of endogenous OPN and autophagy-related proteins suggests that OPN may regulate the autophagy-apoptosis interaction by activating the function of autophagy to reduce early brain damage and inhibit neuronal apoptosis (Condomitti et al., 2018). In the case of cerebral hemorrhage, the expression of OPN will rise. This causes microglia and macrophages to be activated accordingly. By inducing the migration and proliferation of neuroblasts and promoting nerve regeneration, it accelerates the recovery of brain function (Yan et al., 2009). In the case of cerebral hemorrhage, the expression of OPN will increase and it will cause the activation of microglia and macrophages to induce neuroblasts to migrate and proliferate, which will accelerate the recovery of brain function (Yan et al., 2009).

AD is the most common neurodegenerative disease today. Its mainly pathological features are the accumulation of β-amyloid peptide (Aβ) and neurofibrillary tangles, which ultimately manifests as severe cognitive dysfunction. Studies have found that inflammation is closely related to Aβ precipitation. OPN is a molecule involved in the recruitment and activation of macrophages, and may contribute to the repair promotion process in the brain. Previous studies have suggested that without OPN, the migration of macrophages and the production of pro-inflammatory cytokines will be impaired. OPN can promote the formation and regeneration of myelin (Carecchio and Comi, 2011), it may play a role in the remodeling process related to abnormal neuron re-entry into the cell cycle in the brain of AD patients. OPN in brain tissues of AD rats are mostly concentrated on inflammatory plaques, and their expression increases. The staining intensity of OPN in the hippocampus is positively correlated with age and Aβ precipitation. It is suggested that the increase in OPN expression may be a manifestation of accelerated neurodegeneration and pathological changes (Wung et al., 2007; Liao et al., 2019). The occurrence of AD will cause a large number of neurons in the brain tissue to loss. Through cell culture *in vitro*, OPN was found to promote the formation and regeneration of myelin sheath (Le Guenno et al., 1990). It is speculated that OPN may play a role in the remodeling process associated with abnormal neuronal re-entry into the cell cycle in the brain of AD patients. However, current research shows that OPN's effect on neurodegenerative diseases seems to be a double-edged sword, and there may be two different effects. On the one hand, OPN can act as a neuroprotective agent by up-regulating the formation of myelin sheath and remyelin sheath. On the other hand, OPN may play a role in accelerating the disease by triggering neuronal toxicity and apoptosis (Sun et al., 2013) (**Figure 1**).

Glucose and Lipid Metabolism

Osteocalcin Maintains the Body's Glucose Homeostasis and Reduces Fat Accumulation

The lackness of OCN may lead to decreases in the number of islet β cells, insulin content and an increase in blood glucose. As an OCN receptor, GPRC6A can mediate its corresponding functions in the endocrine system, including regulating and maintaining glucose homeostasis. For example, the loss of GPRC6A receptor will cause glucose intolerance (Lee et al., 2007). Increasing OCN can promote the proliferation of islet β-cells and insulin secretion, also enhance insulin sensitivity. Decreasing or even lack of OCN will cause pancreatic islets to shrink, decrease t islet β-cells and insulin.

Regarding the interaction between osteoblasts and insulin, studies have proposed the mechanism of "skeleton-pancreas feedback loop". When insulin content rises, it can directly stimulate osteoblasts and promote their differentiation, increasing OCN content. If the insulin content decreases, it will reduce the number of osteoblasts, resulting in decreased OCN activity, affecting the process of bone formation and bone turnover. Insulin acting on the corresponding receptors in osteoblasts can also inhibit OPG expression and increase osteoclast activity. Create an acidic environment in the matrix for the conversion of OCN to active ucOCN. The liver is the central organ of energy metabolism, and the concentration of commonly used indicators of liver damage is negatively correlated with the level of OCN. OCN can be used as an independent indicator to judge the degree of ballooning of non-alcoholic steatohepatitis.

OCN can also reduce non-alcoholic steatohepatitis by decreasing the expression of pro-inflammatory factors and pro-fibrotic genes. It can improve liver cell steatosis, degeneration and fibrosis caused by ballooning (Chamouni et al., 2015). Due to abnormal bile secretion, patients with

primary biliary cirrhosis will reduce OCN secreted by osteoblasts (Gupte et al., 2014). OCN can play a key role in the formation and activation of GPRC6A receptors in adipocytes. When ucOCN binds to the GPRC6A receptor in adipose tissue, it participates in energy metabolism. It changes liver fat and triglyceride levels, too. By increasing energy consumption and promoting metabolism, ultimately make weight loss achieved (Condomitti et al., 2018). OCN secreted by bones acts on adipose tissue, promotes the secretion of Leptin (LEP) and adiponectin (APN) from adipose tissue.

OCN regulates glucose and lipid metabolism through LEP, so that bones are believed to affect fat metabolism by controlling appetite. The interaction between OCN and APN is closely related to insulin sensitivity, obesity and serum triglyceride levels. First of all, OCN can send a feeding saturation signal to the hypothalamus of the feeding center through the interaction of LEP and serotonin to suppress appetite, reducing fat intake and affecting glucose and lipid metabolism. Secondly, OCN reduces body fat content by inducing the expression of APN in adipocytes. Esp−/− mice will not develop into obesity or diabetes. Overexpression of APN can enhance insulin sensitivity. Therefore, increasing the expression of APN can improve insulin sensitivity, promote fat metabolism, reduce the levels of free fatty acids and triglycerides in the body, and ultimately reduce body weight. Changes in the content of adipokines will in turn affect the OCN content. On the one hand, LEP binds to receptors in the hypothalamus and brainstem through the blood-brain barrier, and sends a signal to prevent the synthesis of serotonin. By inhibiting the release of serotonin from the midnuclear suture, it reduces sympathetic nerve activity. This leads to increased bone resorption and inhibition of bone formation, which in turn affects the content of active OCN. On the other hand, APN can bind to Adiponectin receptor protein 1 (AdipoR1) and activate intracellular signaling pathways. The increase of APN content enhences the expression of APN on the surface of osteoclast precursor cells, which affects the differentiation and maturation of osteoclast, in turn affects OCN content.

Sclerostin Provides Reference for the Diagnosis of Liver and Kidney Disease

Wnt signaling may have a potential role in chronic kidney disease (CKD). Chronic kidney disease-mineral bone disorder (CKD-MBD) is an abnormal mineral metabolism caused by chronic kidney disease. This disease is characterized by renal dystrophy, calcification of blood vessels and soft tissues. As the glomerular filtration rate (GFR) decreases, the concentration of SOST increases. In patients with end-stage renal disease (ESRD), the circulating level of SOST can reach 2–4 times that of the normal population. Kidney transplantation is the choice for patients with CKD in the end-stage disease. Studies have found that elevated serum SOST levels are an independent risk factor for death in kidney transplant patients (Zeng et al., 2018). The serum SOST level of CKD patients is higher than that of the general population, and it gradually increases as the level of renal function deteriorates. Decreased renal function and the occurrence of osteoporosis in the elderly may be related to the increase in SOST. SOST was detected in the proximal tubular cells, indicating that SOST is actively reabsorbed from urine. Increased renal excretion of SOST in CKD patients may be due to increased SOST production and decreased tubular reabsorption. However, whether the inhibition of SOST can prevent the bone loss or vascular calcification of CKD remains to be further studied. The detection of serum SOST can be used as a biomarker of bone metabolism disorders in patients with end-stage renal disease (Maré et al., 2019). There is a negative correlation between serum SOST and PTH in patients with end-stage renal disease, and PTH can be used as a regulation of serum SOST. SOST level can provide a reference for the severity of nephritis and other diseases, elevated serum SOST is a risk factor for kidney disease (Wakolbinger et al., 2020).

Osteoporosis is a common complication in patients with chronic hepatitis. About 75% of patients with chronic liver disease will suffer from osteoporosis. The disease affects the patient's quality of life and increases the patient's risk of fracture. Cirrhosis is the end-stage manifestation of chronic liver disease, and the SOST level of patients is higher than that of healthy people. SOST is negatively correlated with serum albumin, which is a marker of liver dysfunction. Moderate or severe liver dysfunction will affect the level of serum SOST. Alcoholism is an important inducing factor of osteoporosis, 35.9% of patients with alcoholic liver disease have changes in bone metabolism and structure. Patients with alcoholic liver disease have lower SOST levels, which may be caused by alcohol promoting bone cell apoptosis. The main site of increased SOST in patients with primary biliary cirrhosis (PBC) is the bile duct (Ehnert et al., 2019), and the level of SOST in serum is related to the decrease of BMD. Regulating SOST levels through blood circulation will affect bone metabolism, which will help improve osteoporosis in patients with liver cirrhosis. The serum SOST level of patients with early PBC showed a downward trend with time. In the later stage of liver disease, bile acids gradually accumulate, and bilirubin reduces the mitochondrial activity of bone cells. SOST in the serum of the bile nodules will affect the proliferation ability of bone cells. The bile and serum of patients with macula will reduce the survival and mineralization ability of bone cells, and the increase of SOST will affect bone cells in the process of bile formation (Guañabens et al., 2016).

Prostaglandin E2 Promotes DNA Synthesis in Liver Cells and Affects Fat Production

PGE2 is involved in the regulation of fat metabolism (Yan et al., 2009) and has the function of promoting regeneration of liver tissues (Stock et al., 2001). Prostaglandin E synthases (PGESs) and corresponding receptors are highly expressed in white fat, they are closely related to the occurrence of liver diseases. PGESs includes the following three types, microsomal prostaglandin E synthase (mPGES)-1, mPGES-2 and cytosolicprostaglandin E synthase (cPGES) (Miyoshi et al., 2017). These PGESs directly participate in the synthesis of PGE2 and affect liver diseases such as NAFLD, NASH, DILI and liver cancer. PGE2 has influence on fat with the participation of the receptor EP4. EP4 is a G protein-coupled receptor with 7-pass transmembrane structure, which

mainly distributed in white fat (Hara et al., 2010). Activation of the EP4 receptor will inhibit the differentiation of adipocytes (Madden and Morrison, 2004), and lipid breakdown can be promoted by the lack of this receptor (Inazumi et al., 2011).

PGE2 has the effect of promoting DNA synthesis in liver cells, the effect is related to the concentration of PGE2. The increase of PGE2 is synchronized with the increase of cAMP in hepatocytes. PGE2 can change the stability of β-catenin through the phosphorylation process mediated by cAMP/PKA signaling pathway. By regulating the activity of the Wnt signaling pathway, liver regeneration is promoted. Inhibition of PGE2 synthesis will block Wnt-induced liver regeneration. The binding pathway of PGE2 and EP4 receptor can protect liver function, the use of EP4 selective agonist will reduce the degree of liver ischemic damage.

Osteopontin Affects Kidney Stones and Changes the Cycle of Cancer Cells

In the kidneys of healthy adults, OPN is mainly expressed in the thick ascending branches of the ring of Henle. In recent years, OPN has been reported in the study of kidney stones, kidney cancer and other related kidney diseases (Xie et al., 2001). The expression is regulated by many factors, such as parathyroid hormone, calcium, phosphorus, tumor necrosis factor α (TNF-α), transforming growth factor β1 (TGF-β1), epithelial growth factor and so on.

In kidney stone disease, OPN not only plays a key role in regulating the nucleation, growth and aggregation of calcium oxalate (CaOx), but also affects the adhesion of CaOx to renal epithelial cells, participating in the reservation of kidney stone. The main component of kidney stones is CaOx crystals. OPN, as the main crystal regulator, is considered to be one of the most important macromolecules affecting mineralization and kidney stone formation (Tsuji et al., 2014). However, whether OPN plays a role in inhibiting or promoting the formation of stones is still a controversial issue. As the urine form of OPN, urinary calcin can induce the formation of calcium oxalate dihydrate (COD) by inhibiting the accumulation of calcium oxalate monohydrate (COM). This can reduce the growth and aggregation of CaOx, prevent the combination of crystals and renal epithelial cells, and ultimately protect the kidneys from the deposition of calcium oxalate crystals.

Kidney cancer is one of the most common cancers in the world. OPN plays a key role in the growth and invasion of renal cancer. On the one hand, it may inhibit the apoptosis of cancer cells, promote the growth of tumor cells. On the other hand, it may provide favorable conditions for tumor cell tissues to occurrence and metastasis by inducing urokinase-type plasminogen activator (UPA) (Ghorbani et al., 2015).

Fibroblast Growth Factor 23 Is Related to G-3-P and can Promote Renal Phosphate Excretion

As a bone-derived hormone-like protein, FGF23 also plays an important role in regulating metabolism of multiple organs. Among them, the most widely studied is the regulation of FGF23 on the kidneys. FGF23 reaches kidney after it is secreted, and stimulates the excretion of phosphate in the urine by inducing the endocytosis of sodium-phosphate cotransporters NPT2a and NPT2c on the root tip of the proximal tubule cells of the kidney (Kaleta, 2019).

Elevated FGF23 levels are an early progressive and common complication of chronic kidney disease (CKD). Elevated FGF23 in CKD patients can promote renal phosphate excretion and help delay the onset of hyperphosphatemia. But it can cause a large number of compensatory harms, including calcitriol deficiency, changes in calcium homeostasis, and secondary hyperparathyroidism (Gutierrez et al., 2005; Musgrove and Wolf, 2020). In addition, the high level of FGF23 in CKD patients can cause pathological left ventricular remodeling, atrial fibrillation and heart failure, the risk of infection and death will increase. In mice and CKD patients, FGF23 elevated inhibits the activation, adhesion and transepithelial migration of neutrophils. Thereby reducing the recruitment of neutrophils and host defense during inflammation (Rossaint et al., 2016). In acute kidney injury (AKI), the level of FGF23 will also increase immediately, which shows that certain factors are produced in the kidney to promote the production of FGF23.

Existing studies use proteomics and metabolomics to analysis proteins and metabolites related to arterial FGF23 levels which screened out from renal venous blood of patients undergoing cardiac catheterization. It was identified that renal vein glycerol-3-phosphate (G-3-P) has a significant correlation with FGF23 (Simic et al., 2020). Renal vein G-3-P has a significant correlation with FGF23 (Simic et al., 2020). G-3-P can affect related physiological phenotypes caused by changes of FGF23. Circulating G-3-P is locally converted to lysophosphatidic acid (LPA) in bone and bone marrow through G-3-P acyltransferase isoform 2 (GPAT2). LPA binds to LPA receptor 1 (LPAR1) on cells which secret FGF23 to stimulate the production of FGF23 (Simic et al., 2020). G-3-P is an intermediate metabolite in the process of glycolysis, lipogenesis and oxidative phosphorylation (Possik et al., 2017). But its function is not limited to this. It can regulate insulin secretion, the synthesis and storage of fat, and FGF23 production.

In CKD patients, iron deficiency and increased blood erythropoietin (EPO) levels can stimulate the expression of FGF23. In CKD patients and kidney transplant recipients, iron deficiency is an important determinant of total FGF23 levels, which has a significant impact on the progression and mortality of CKD (Eisenga et al., 2017; Eisenga et al., 2019).

Blood and Cardiovascular System

Sclerostin Affects Atherosclerosis by Inhibiting Angiotensin II

Atherosclerosis is a clinical manifestation of vascular aging, mainly due to abnormal proliferation of vascular smooth muscle (VSMC). SOST exists in the atherosclerotic tissue, the main function of it is to inhibit the Wnt pathway by binding to the transmembrane Wnt core receptors LRP-4,-5, and-6. SOST is expressed in the thoracic and abdominal aorta of an arterial-calcification mouse model, which is induced by the inhibition of angiotensin II (Ang II). This expression plays an important role in the pathogenesis of aneurysms and atherosclerosis (Krishna et al., 2017).

The up-regulation of SOST can down-regulate the expression of OPN and OPG in the mouse aorta. OPN can promote

inflammation and participate in the activation of arterial calcification in Ang II mice, increasing the activity of Matrix metalloproteinase-9 (MMP-9). The concentration of OPG is positively correlated with hemangioma, and it can promote the inflammatory response of vascular smooth muscle cells through cathelicidin S, Matrix metalloproteinase-2 (MMP-2) and MMP-9. SOST can inhibit the formation of aneurysms and atherosclerosis induced by Ang II, and regulating SOST can be used as a potential way to inhibit these diseases.

In patients with type 2 diabetes, the circulating SOST of those with atherosclerosis will increase. In male patients with atherosclerosis, the levels of serum sclerostin are positively correlated with aging, but this difference has not found in women (Morales-Santana et al., 2013). The high level of SOST is related to death caused by cardiovascular disease. Hyperglycemia, insulin resistance and other cardiovascular risk factors can cause vascular endothelial damage, which promotes vascular calcification. The increase of serum SOST in hemodialysis patients (Brandenburg et al., 2013) may be due to the increase of SOST produced by bone, it may also be caused by the decrease in renal clearance or the physiological adaptation of blood vessels as a result of increased calcification.

Osteopontin Is Involved in Vascular Calcification and Endothelial Hyperplasia

OPN mediates the process of cell adhesion, proliferation and migration, which is related to the pathophysiology of tumors. As one of the extracellular matrix (ECM), overexpression of OPN will promote cardiac fibrosis and participate in the remodeling process of the heart and blood vessels (Sawaki et al., 2018). In addition, it will also affect the formation of vascular calcification. The serum OPN level of patients with vascular calcification will be significantly increased, which is one of the signs of vascular calcification (Wolak, 2014). OPN affects the formation of atherosclerotic plaques in arteries, and elevated blood glucose levels will promote the expression of OPN in endothelial cells. Vascular remodeling refers to the thickening of the vessel wall and the increase of resistance in the vessel. OPN is associated with vascular remodeling and ventricular hypertrophy in hypertensive patients. After lowering blood pressure, the OPN level of patients decreases (Hou et al., 2014). Lack of OPN will inhibit the process of tissue remodeling, especially in the fibrosis process after myocardial infarction (Okamoto, 2007). In view of this fibrotic process, OPN is considered to be possible for treatment because it has the effect of promoting angiogenesis, wound healing and tissue regeneration (Abdelaziz Mohamed et al., 2019).

Fibroblast Growth Factor 23 Affects Nephropathy Secondary Cardiovascular Disease

FGF23 plays an important role in the regulation of vitamin D and blood phosphorus levels. Klotho, the receptor cofactor of FGF23, is very important in this metabolic regulation (Hu et al., 2010). Klotho deficiency is a biomarker of kidney disease, and it is also an important pathogenic factor for cardiovascular disease in chronic kidney disease such as myocardial fibrosis and vascular calcification (Sopjani et al., 2015). Increasing klotho levels can tireduce serum creatinine and urea nitrogen levels by indirectly regulating the homeostasis of phosphorus and calcium in the body. At the early stage of patients with chronic kidney disease, the decrease of Klotho level will cause a compensatory increase in FGF23. By inhibiting the reabsorption of phosphorus in the proximal renal tubules, it promotes urinary phosphorus excretion to maintain the balance of blood phosphorus metabolism. The compensatory increase of FGF23 can inhibit the level of $1,25\text{-}(OH)_2D_3$ and induce parathyroid glands to continuously secrete PTH. This change will stimulate the bones to release phosphorus into the blood, causing blood phosphorus to increase, and aggravating disorders of calcium and phosphorus metabolism. If phosphate continues to stimulate bone tissue to secrete FGF23, kidney klotho secretion will decrease, and the compensatoryly increased FGF23 will also lose its effective regulation of bone minerals. Lead to the imbalance of bone mineral metabolism and accelerate the process of vascular calcification in chronic renal failure (Lu and Hu, 2017).

Skeletal Muscle Movement System

Osteopontin Plays a Regulatory Role in Skeletal Muscle

OPN plays an important role in regulating the proliferation, differentiation and regeneration of skeletal muscle cells. Studies have shown that OPN is a key inflammatory cytokine of tissue remodeling[63]. Many types of inflammatory cells express OPN, including T cells, neutrophils and macrophages. The expression of OPN in normal muscles is relatively low, but when the muscles are injured, it will be approximately 120 times that of the baseline level within 12–24 h (Hoffman et al., 2013). OPN may support the rapid return of muscle function to normal in the early stage of injury (Uaesoontrachoon et al., 2013). Limited acute OPN overexpression is beneficial to damaged muscles, but chronic overexpression of OPN may lead to fibrosis and functional impairment of damaged muscles (Pagel et al., 2014). The expression of OPN is significantly increased in Duchenne muscular dystrophy (DMD) patients and muscular dystrophy (MDX) mice, suggesting that OPN is involved in muscle regeneration and ammoniation. It is currently known that OPN plays an important role in DMD and skeletal muscle injury, but its related functions and regulatory effects are still unclear (**Figure 2**).

The Role of Fibroblast Growth Factor 23 in Muscle Metabolism

Left ventricular hypertrophy (LVH) is a common pattern of cardiovascular damage among CKD patients, and 75% of them were founded LVH when they reached the end-stage of renal disease (Faul et al., 2011). The complex pathogenesis of LVH involves ventricular pressure and volume overload, and the bone-derived FGF23 plays an important role in it (Gutiérrez et al., 2009). FGF23 induces the hypertrophic growth of cardiomyocytes and the left ventricle of rodents through a mechanism directly dependent on FGFR, but does not depend on α-klotho receptors. In terms of molecular mechanism, FGF23 specifically activates FGFR4 on cardiomyocytes to activate phospholipase Cγ/calcineurin/nuclear factor of activated T

signaling (PLCγ/calcineurin/NFAT signaling). Soluble Klotho is a circulating form of FGF23 receptor, which can prevent the effect of FGF23 on cardiomyocytes by increasing the expression of PDE3A and PDE3B (Lindner et al., 2020). Klotho is expressed in human arterial and aortic smooth muscle cells. In CKD patients, chronic circulating stress factors including uremic serum, high calcium, TNF-α and other components can inhibit the expression of Klotho in vascular smooth muscle. Therefore, when α-Klotho is missing, it will cause smooth muscle cell calcification and loss of response to FGF23 through Runx2 and muscle cell-serum response factor pathways (Huang et al., 2020). FGF23 and Klotho play an important role in the pathogenesis of vascular calcification in CKD patients (**Figure 2**).

Sclerostin Regulates Arthritis Process

SOST gene can be expressed by chondrocytes, and changing the activity of SOST will have an impact on articular cartilage. In osteoarthritis, the SOST of chondrocytes increases locally, but decreases in the subchondral bone. SOST can inhibit Wnt/β-catenin signaling, and can also reduce the RNA levels of key matrix components and enzyme inhibitors. SOST can regulate the process of osteoarthritis of bone and cartilage. Promoting the sclerosis of subchondral bone, at the same time inhibiting cartilage degradation.

As the age increases, the number of cartilage cells in animals decreases, and the same as the expression of SOST (Thompson et al., 2016). There was no significant change in the expression of SOST in the bone tissue of patients with knee osteoarthritis. Normally aging articular cartilage will not be affected by changes in SOST levels (Roudier et al., 2013). It is speculated that SOST may have nothing to do with cartilage destruction in knee osteoarthritis, or there are other compensation molecules in the cartilage, so the effect of SOST inhibition is masked (**Figure 2**).

Thyroid and Related Hormones

Osteocalcin Affect Thyroid Bone Disease

The occurrence of thyroid bone disease is related to abnormal thyroid level (Cheng et al., 2021). Thyroid hormone has a non-genomic effect in osteoblasts of primary mouse (Asai et al., 2009). This effect can inhibit tyrosine kinase through thyroid hormone to stimulate OCN expression. Excessive or insufficient thyroid hormone can cause bone mineral loss, leading to the occurrence of osteoporosis. When the thyroid function of patients with hyperthyroidism returns to normal, the OCN level will significantly lower than that in the hyperthyroid stage (Ma et al., 2011).

Patients with abnormal levels of thyroid hormone have a chance of getting thyroid bone diseases. Among these diseases, osteoporosis is the most common. In the study of the relationship between OCN and thyroid, the treatment of osteoporosis may become the focus of research.

Regulation Between Fibroblast Growth Factor 23 and Parathyroid Hormone

PTH stimulates FGF23 serum levels indirectly by increasing the synthesis of 1,25-dihydroxyvitamin D. Loss of parathyroid glands in Gcm2 knockout mice led to a decrease in 1,25-dihydroxyvitamin D levels and FGF23 concentrations, and FGF23 levels will return to normal after 1,25-dihydroxyvitamin D injection (Liu et al., 2006). The parathyroid gland is one of the target organs of FGF23, mice that overexpressing FGF23 will get hyperparathyroidism (Bai et al., 2004). Recombination of FGF23 will increase the level of Klotho in the parathyroid glands. FGF23 activates the MAPK pathway of the parathyroid glands through the phosphorylation of ERK1/2 and increases the level of early growth response 1 (Erg1) mRNA. FGF23 can also inhibit secretion and gene expression of PTH(Ben-Dov et al., 2007).

THE EFFECT OF MECHANICAL STIMULATION ON BONE-DERIVED SECRETED PROTEIN

The circulating level of OCN will increase with exercise. The level of OCN increases in high-intensity intermittent exercise (Hiam et al., 2021). Changing regulation of glucose to mobilize bones, finally complete exercises. This change has nothing to do with gender. For adolescents, people who regularly participates in physical exercise show higher levels of OCN(Chahla et al., 2015). The increase of OCN level during exercise can promote acute stress response (ASR) (Berger et al., 2019), improve memory and enhance muscle function. For bone spine animals, ASR is related to the survivability in hostile environments such as the wild (**Figure 3**).

The homeostasis of bone is very important to the body's calcium and phosphorus balance. OPN is an important phosphorylated glycoprotein, the fluctuations of which play a key role in bone formation and bone resorption. To maintain bone homeostasis, moderate exercise and physical activity are vital factors. Knockout OPN gene can inhibit mechanical stress bone remodeling in mice. In obese people and adipose tissue of mouse, OPN is widely up-regulated. After exercise to lose weight, the level of OPN in serum appears to decrease. The reason may be the body vibration caused by exercise or physiological factors, rather than the loss of fat (Garfield et al., 2016) (**Figure 3**).

As one of the important bone-derived factors, the fluctuations of FGF23 are critical to the normal operation of the kidney, small intestine, cardiovascular and other organs. Over-distance walking will cause the serum FGF23 level to increase temporarily, but it will decrease by the end of the exercise, and return to baseline level soon after the game (Kerschan-Schindl et al., 2021). This transient high expression of FGF23 may be related to the short-term bone metabolism uncoupling signal, which is triggered by the endocrine system after excessive exercise. Osteocytes are the mechanical sensors of bone, the increase of FGF23 level may be related to the activation of bone cells induced by exercise. In addition, exercise also helps in the treatment of kidney-related diseases. Resistance training for patients with stage II chronic kidney disease can improve uremia parameters and the klothof-FGF23 signaling pathway, thereby alleviating the progression of the disease (Corrêa et al., 2021) (**Figure 3**).

SOST is mainly secreted by bone cells, which are the main cells responsible for mechanical signal transduction. Therefore, SOST is

regulated by mechanical stress, and exercise has a regulating effect on SOST. Under the stimulation of short-term exercise, the blood will release the synthesized SOST, which may be related to the physiological regulation of the kidneys. By reducing excretion, it increases the reabsorption of SOST by the renal tubules (Pickering et al., 2017). After endurance training, the concentration of serum SOST will increase, and the changes in SOST caused by exercise can be used as the basis for exercise metabolism monitoring (Jürimäe et al., 2021). The increase in serum SOST after exercise may be due to the release of SOST anchored in bone cells from bone cells into the blood, rather than the increase in SOST gene expression in a short period of time, and the increase in blood flow to bone caused by exercise (Kouvelioti et al., 2018). Exercise training slowed down the increase in serum SOST, the bone formation rate did not change but bone resorption was improved after intervention. Exercise can improve the density and microstructure of bone in CKD rats by inhibiting SOST, but it will not change the serum mineral content (Liao et al., 2019). After completing general short-term acute exercise, serum SOST increases acutely, and then decreases to normal levels or even lower. Long-term exercise makes the bones adapt to mechanical stress, the response of bone cells to exercise and serum SOST are both reduced. Long-term reduction of mechanical stress increases serum SOST, which is consistent with the regulation of bone metabolism by Wnt signaling pathway (**Figure 3**).

CONCLUSION

The existing research shows that the actuating scope of bone-derived secretory factors is not limited to bones. In fact, it displays more hormonal properties and can regulate organ activitivies through special receptors. It plays a role in multiple systems and is closely related to the body's metabolic process. According to different secreting cells, bone-derived factors can be divided into two categories, secreted by specific cells or multiple cells. Different bone-derived factors have differences in structures and locations, and these differences will affect their effects. Multiple bone-derived factors may simultaneously regulate the same organ or system. Organs and systems will also give feedbacks to the factors after receiving the signals, which further reflect the characteristics of their hormones. The effect of mechanical stimulation on bone will affect the secretion of bone-derived factors, and this effect will be reflected in the regulation of organs. Although it is not yet known that whether we could change the amount of bone-derived protein secretion by exerting mechanical stimulation to intervene in the treatment for dieases. However, the cross-organ regulation of bone-derived protein can provide theoretical bases for them.

AUTHOR CONTRIBUTIONS

JZ gave the brief introduction of this article. YD, LZ, ZW, and XZ were responsible for manuscript writing. LZ revised the manuscript. All authors approved the final version of this manuscript.

FUNDING

The work was supported by National Natural Science Foundation of China (81871835), China Postdoctoral Science Foundation funded project (2021T140224), and grants from Shanghai Frontiers Science Research Base of Exercise and Metabolic Health, Shanghai Key Laboratory of Human Sport Competence Development and Maintenance (Shanghai University of Sport) (No. 11DZ2261100).

ACKNOWLEDGMENTS

We appreciate the time and effort of the participants in this study.

REFERENCES

Abdelaziz Mohamed, I., Gadeau, A. P., Hasan, A., Abdulrahman, N., and Mraiche, F. (2019). Osteopontin: A Promising Therapeutic Target in Cardiac Fibrosis. *Cells* 8 (12). Epub 2019/12/11. doi:10.3390/cells8121558

Asada, M., Shinomiya, M., Suzuki, M., Honda, E., Sugimoto, R., Ikekita, M., et al. (2009). Glycosaminoglycan Affinity of the Complete Fibroblast Growth Factor Family. *Biochim. Biophys. Acta (Bba) - Gen. Subjects* 1790 (1), 40–48. Epub 2008/10/07. doi:10.1016/j.bbagen.2008.09.001

Asai, S., Cao, X., Yamauchi, M., Funahashi, K., Ishiguro, N., and Kambe, F. (2009). Thyroid Hormone Non-genomically Suppresses Src Thereby Stimulating Osteocalcin Expression in Primary Mouse Calvarial Osteoblasts. *Biochem. Biophysical Res. Commun.* 387 (1), 92–96. Epub 2009/07/01. doi:10.1016/j.bbrc.2009.06.131

Bai, X., Miao, D., Li, J., Goltzman, D., and Karaplis, A. C. (2004). Transgenic Mice Overexpressing Human Fibroblast Growth Factor 23 (R176Q) Delineate a Putative Role for Parathyroid Hormone in Renal Phosphate Wasting Disorders. *Endocrinology* 145 (11), 5269–5279. Epub 2004/07/31. doi:10.1210/en.2004-0233

Baugé, C., Girard, N., Lhuissier, E., Bazille, C., and Boumediene, K. (2014). Regulation and Role of TGFβ Signaling Pathway in Aging and Osteoarthritis Joints. *Aging Dis.* 5 (6), 394–405. Epub 2014/12/10. doi:10.14336/AD.2014.0500394

Ben-Dov, I. Z., Galitzer, H., Lavi-Moshayoff, V., Goetz, R., Kuro-o, M., Mohammadi, M., et al. (2007). The Parathyroid Is a Target Organ for FGF23 in Rats. *J. Clin. Invest.* 117 (12), 4003–4008. Epub 2007/11/10. doi:10.1172/JCI32409

Berger, J. M., Singh, P., Khrimian, L., Morgan, D. A., Chowdhury, S., Arteaga-Solis, E., et al. (2019). Mediation of the Acute Stress Response by the Skeleton. *Cell Metab.* 30 (5), 890–902. e8Epub 2019/09/17. doi:10.1016/j.cmet.2019.08.012

Bouleftour, W., Juignet, L., Verdière, L., Machuca-Gayet, I., Thomas, M., Laroche, N., et al. (2019). Deletion of OPN in BSP Knockout Mice Does Not Correct Bone Hypomineralization but Results in High Bone Turnover. *Bone.* 120, 411–422. Epub 2018/12/12. doi:10.1016/j.bone.2018.12.001

Brandenburg, V. M., Kramann, R., Koos, R., Krüger, T., Schurgers, L., Mühlenbruch, G., et al. (2013). Relationship between Sclerostin and Cardiovascular Calcification in Hemodialysis Patients: a Cross-Sectional Study. *BMC Nephrol.* 14, 219, 2013 . Epub 2013/10/12. doi:10.1186/1471-2369-14-219

Brunetti, G., D'Amelio, P., Wasniewska, M., Mori, G., and Faienza, M. F. (2017). Editorial: Bone: Endocrine Target and Organ. *Front. Endocrinol.* 8, 354, 2017 . Epub 2018/01/10. doi:10.3389/fendo.2017.00354

Carecchio, M., and Comi, C. (2011). The Role of Osteopontin in Neurodegenerative Diseases. *Jad* 25 (2), 179–185. Epub 2011/03/02. doi:10.3233/jad-2011-102151

Chahla, S. E., Frohnert, B. I., Thomas, W., Kelly, A. S., Nathan, B. M., and Polgreen, L. E. (2015). Higher Daily Physical Activity Is Associated with Higher

Osteocalcin Levels in Adolescents. *Prev. Med. Rep.* 2, 568–571. Epub 2015/08/04. doi:10.1016/j.pmedr.2015.06.017

Chamouni, A., Schreiweis, C., and Oury, F. (2015). Bone, Brain & beyond. *Rev. Endocr. Metab. Disord.* 16 (2), 99–113. Epub 2015/03/17. doi:10.1007/s11154-015-9312-5

Cheng, C.-W., Fang, W.-F., Tang, K.-T., and Lin, J.-D. (2021). Serum Interferon Levels Associated with the Disease Activity in Women with Overt Graves' Disease. *Cytokine.* 138, 155353, 2021 . Epub 2020/10/31. doi:10.1016/j.cyto.2020.155353

Condomitti, G., Wierda, K. D., Schroeder, A., Rubio, S. E., Vennekens, K. M., Orlandi, C., et al. (2018). An Input-specific Orphan Receptor GPR158-HSPG Interaction Organizes Hippocampal Mossy Fiber-CA3 Synapses. *Neuron* 100 (1), 201–215. Epub 2018/10/07. doi:10.1016/j.neuron.2018.08.038

Corrêa, H. L., Neves, R. V. P., Deus, L. A., Souza, M. K., Haro, A. S., Costa, F., et al. (2021). Blood Flow Restriction Training Blunts Chronic Kidney Disease Progression in Humans. *Med. Sci. Sports Exerc.* 53 (2), 249–257. Epub 2020/08/23. doi:10.1249/mss.0000000000002465

De Fusco, C., Messina, A., Monda, V., Viggiano, E., Moscatelli, F., Valenzano, A., et al. (2017). Osteopontin: Relation between Adipose Tissue and Bone Homeostasis. *Stem Cells Int* 2017, 4045238, 2017 . Epub 2017/02/15. doi:10.1155/2017/4045238

DeLuccia, R., Cheung, M., Ramadoss, R., Aljahdali, A., and Sukumar, D. (2019). The Endocrine Role of Bone in Cardiometabolic Health. *Curr. Nutr. Rep.* 8 (3), 281–294. Epub 2019/07/13. doi:10.1007/s13668-019-00286-0

Ehnert, S., Aspera-Werz, R. H., Ruoss, M., Dooley, S., Hengstler, J. G., Nadalin, S., et al. (2019). Hepatic Osteodystrophy-Molecular Mechanisms Proposed to Favor its Development. *Int. J. Mol. Sci.* 20 (10). Epub 2019/05/30. doi:10.3390/ijms20102555

Eisenga, M. F., De Jong, M. A., Van der Meer, P., Leaf, D. E., Huls, G., Nolte, I. M., et al. (2019). Iron Deficiency, Elevated Erythropoietin, Fibroblast Growth Factor 23, and Mortality in the General Population of the Netherlands: A Cohort Study. *Plos Med.* 16 (6), e1002818, 2019 . Epub 2019/06/07. doi:10.1371/journal.pmed.1002818

Eisenga, M. F., van Londen, M., Leaf, D. E., Nolte, I. M., Navis, G., Bakker, S. J. L., et al. (2017). C-terminal Fibroblast Growth Factor 23, Iron Deficiency, and Mortality in Renal Transplant Recipients. *Jasn* 28 (12), 3639–3646. Epub 2017/08/05. doi:10.1681/asn.2016121350

Faul, C., Amaral, A. P., Oskouei, B., Hu, M.-C., Sloan, A., Isakova, T., et al. (2011). FGF23 Induces Left Ventricular Hypertrophy. *J. Clin. Invest.* 121 (11), 4393–4408. Epub 2011/10/12. doi:10.1172/jci46122

Gallop, P. M., Lian, J. B., and Hauschka, P. V. (1980). Carboxylated Calcium-Binding Proteins and Vitamin K. *N. Engl. J. Med.* 302 (26), 1460–1466. Epub 1980/06/26. doi:10.1056/nejm198006263022608

Garfield, A. S., Davies, J. R., Burke, L. K., Furby, H. V., Wilkinson, L. S., Heisler, L. K., et al. (2016). Increased Alternate Splicing of Htr2c in a Mouse Model for Prader-Willi Syndrome Leads Disruption of 5HT2C Receptor Mediated Appetite. *Mol. Brain* 9 (1), 95, 2016 . Epub 2016/12/10. doi:10.1186/s13041-016-0277-4

Ghorbani, M., Teimourian, S., Farzad, R., and Namvar Asl, N. (2015). Apparent Histological Changes of Adipocytes after Treatment with CL 316,243, a SS-3-Adrenergic Receptor Agonist. *Dddt* 9, 669–676. Epub 2015/02/25. doi:10.2147/dddt.s73891

Goetz, R., and Mohammadi, M. (2013). Exploring Mechanisms of FGF Signalling through the Lens of Structural Biology. *Nat. Rev. Mol. Cell Biol.* 14 (3), 166–180. Epub 2013/02/14. doi:10.1038/nrm3528

Gomarasca, M., Banfi, G., and Lombardi, G. (2020). Myokines: The Endocrine Coupling of Skeletal Muscle and Bone. *Adv. Clin. Chem.* 94, 155–218. Epub 2020/01/19. doi:10.1016/bs.acc.2019.07.010

Guañabens, N., Ruiz-Gaspà, S., Gifre, L., Miquel, R., Peris, P., Monegal, A., et al. (2016). Sclerostin Expression in Bile Ducts of Patients with Chronic Cholestasis May Influence the Bone Disease in Primary Biliary Cirrhosis. *J. Bone Miner Res.* 31 (9), 1725–1733. Epub 2016/03/29. doi:10.1002/jbmr.2845

Gupte, A. A., Sabek, O. M., Fraga, D., Minze, L. J., Nishimoto, S. K., Liu, J. Z., et al. (2014). Osteocalcin Protects against Nonalcoholic Steatohepatitis in a Mouse Model of Metabolic Syndrome. *Endocrinology* 155 (12), 4697–4705. Epub 2014/10/04. doi:10.1210/en.2014-1430

Gutierrez, O., Isakova, T., Rhee, E., Shah, A., Holmes, J., Collerone, G., et al. (2005). Fibroblast Growth Factor-23 Mitigates Hyperphosphatemia but Accentuates Calcitriol Deficiency in Chronic Kidney Disease. *Jasn* 16 (7), 2205–2215. Epub 2005/05/27. doi:10.1681/asn.2005010052

Gutiérrez, O. M., Januzzi, J. L., Isakova, T., Laliberte, K., Smith, K., Collerone, G., et al. (2009). Fibroblast Growth Factor 23 and Left Ventricular Hypertrophy in Chronic Kidney Disease. *Circulation* 119 (19), 2545–2552. Epub 2009/05/06. doi:10.1161/CIRCULATIONAHA.108.844506

Han, X., Wang, W., He, J., Jiang, L., and Li, X. (2019). Osteopontin as a Biomarker for Osteosarcoma Therapy and Prognosis. *Oncol. Lett.* 17 (3), 2592–2598. Epub 2019/03/12. doi:10.3892/ol.2019.9905

Hara, S., Kamei, D., Sasaki, Y., Tanemoto, A., Nakatani, Y., and Murakami, M. (2010). Prostaglandin E Synthases: Understanding Their Pathophysiological Roles through Mouse Genetic Models. *Biochimie.* 92 (6), 651–659. Epub 2010/02/18. doi:10.1016/j.biochi.2010.02.007

Hatae, N., Sugimoto, Y., and Ichikawa, A. (2002). Prostaglandin Receptors: Advances in the Study of EP3 Receptor Signaling. *J. Biochem.* 131 (6), 781–784. Epub 2002/06/01. doi:10.1093/oxfordjournals.jbchem.a003165

Hauschka, P. V., Lian, J. B., and Gallop, P. M. (1975). Direct Identification of the Calcium-Binding Amino Acid, Gamma-Carboxyglutamate, in Mineralized Tissue. *Proc. Natl. Acad. Sci.* 72 (10), 3925–3929. Epub 1975/10/01. doi:10.1073/pnas.72.10.3925

Hiam, D., Landen, S., Jacques, M., Voisin, S., Alvarez-Romero, J., Byrnes, E., et al. (2021). Osteocalcin and its Forms Respond Similarly to Exercise in Males and Females. *Bone.* 144, 115818, 2021 . Epub 2020/12/19. doi:10.1016/j.bone.2020.115818

Hoffman, E. P., Gordish-Dressman, H., McLane, V. D., Devaney, J. M., Thompson, P. D., Visich, P., et al. (2013). Alterations in Osteopontin Modify Muscle Size in Females in Both Humans and Mice. *Med. Sci. Sports Exerc.* 45 (6), 1060–1068. Epub 2013/01/01. doi:10.1249/mss.0b013e31828093c1

Hou, X., Hu, Z., Huang, X., Chen, Y., He, X., Xu, H., et al. (2014). Serum Osteopontin, but Not OPN Gene Polymorphism, Is Associated with LVH in Essential Hypertensive Patients. *J. Mol. Med.* 92 (5), 487–495. Epub 2013/12/29. doi:10.1007/s00109-013-1099-9

Hu, M. C., Shi, M., Zhang, J., Pastor, J., Nakatani, T., Lanske, B., et al. (2010). Klotho: a Novel Phosphaturic Substance Acting as an Autocrine Enzyme in the Renal Proximal Tubule. *FASEB J.* 24 (9), 3438–3450. Epub 2010/05/15. doi:10.1096/fj.10-154765

Huang, C., Zhan, J.-F., Chen, Y.-X., Xu, C.-Y., and Chen, Y. (2020). LncRNA-SNHG29 Inhibits Vascular Smooth Muscle Cell Calcification by Downregulating miR-200b-3p to Activate the α-Klotho/FGFR1/FGF23 axis. *Cytokine* 136, 155243, 2020 . Epub 2020/08/21. doi:10.1016/j.cyto.2020.155243

Inazumi, T., Shirata, N., Morimoto, K., Takano, H., Segi-Nishida, E., and Sugimoto, Y. (2011). Prostaglandin E2-EP4 Signaling Suppresses Adipocyte Differentiation in Mouse Embryonic Fibroblasts via an Autocrine Mechanism. *J. Lipid Res.* 52 (8), 1500–1508. Epub 2011/06/08. doi:10.1194/jlr.m013615

Ismaeel, A., Kim, J. S., Kirk, J. S., Smith, R. S., Bohannon, W. T., and Koutakis, P. (2019). Role of Transforming Growth Factor-β in Skeletal Muscle Fibrosis: A Review. *Int. J. Mol. Sci.* 20 (10). Epub 2019/05/22. doi:10.3390/ijms20102446

Jürimäe, J., Purge, P., and Tillmann, V. (2021). Serum Sclerostin and Cytokine Responses to Prolonged Sculling Exercise in Highly-Trained Male Rowers. *J. Sports Sci.* 39 (5), 591–597. Epub 2020/11/03. doi:10.1080/02640414.2020.1837428

Kaleta, B. (2019). The Role of Osteopontin in Kidney Diseases. *Inflamm. Res.* 68 (2), 93–102. Epub 2018/11/21. doi:10.1007/s00011-018-1200-5

Kerschan-Schindl, K., Skenderi, K., Wahl-Figlash, K., Gelles, K., Föger-Samwald, U., Thalmann, M., et al. (2021). Increased Serum Levels of Fibroblast Growth Factor 23 after an Ultradistance Run. *J. Sci. Med. Sport* 24 (3), 297–300. Epub 2020/10/07. doi:10.1016/j.jsams.2020.09.010

Kosmidis, S., Polyzos, A., Harvey, L., Youssef, M., Denny, C. A., Dranovsky, A., et al. (2018). RbAp48 Protein Is a Critical Component of GPR158/OCN Signaling and Ameliorates Age-Related Memory Loss. *Cell Rep.* 25 (4), 959–973. e6Epub 2018/10/26. doi:10.1016/j.celrep.2018.09.077

Kouvelioti, R., Kurgan, N., Falk, B., Ward, W. E., Josse, A. R., and Klentrou, P. (2018). Response of Sclerostin and Bone Turnover Markers to High Intensity Interval Exercise in Young Women: Does Impact Matter? *Biomed. Res. Int.* 2018, 4864952, 2018 . Epub 2018/12/06. doi:10.1155/2018/4864952

Krishna, S. M., Seto, S.-W., Jose, R. J., Li, J., Morton, S. K., Biros, E., et al. (2017). Wnt Signaling Pathway Inhibitor Sclerostin Inhibits Angiotensin II-Induced

Aortic Aneurysm and Atherosclerosis. *Atvb* 37 (3), 553–566. Epub 2017/01/08. doi:10.1161/atvbaha.116.308723

Le Guenno, B., Seck, O., Lagarde, E., Enel, C., and Pison, G. (1990). Transmission of HIV-2 Virus in a Rural Area of Senegal. *Dakar Med.* 35 (2), 265–267. Epub 1990/01/01.

Lee, N. K., Sowa, H., Hinoi, E., Ferron, M., Ahn, J. D., Confavreux, C., et al. (2007). Endocrine Regulation of Energy Metabolism by the Skeleton. *Cell* 130 (3), 456–469. Epub 2007/08/19. doi:10.1016/j.cell.2007.05.047

Liao, H. W., Huang, T. H., Chang, Y. H., Liou, H. H., Chou, Y. H., Sue, Y. M., et al. (2019). Exercise Alleviates Osteoporosis in Rats with Mild Chronic Kidney Disease by Decreasing Sclerostin Production. *Int. J. Mol. Sci.* 20 (8), 1, 2019 . Epub 2019/04/28. doi:10.3390/ijms20082044

Lindner, M., Mehel, H., David, A., Leroy, C., Burtin, M., Friedlander, G., et al. (2020). Fibroblast Growth Factor 23 Decreases PDE4 Expression in Heart Increasing the Risk of Cardiac Arrhythmia; Klotho Opposes These Effects. *Basic Res. Cardiol.* 115 (5), 51, 2020 . Epub 2020/07/24. doi:10.1007/s00395-020-0810-6

Liu, S., Tang, W., Zhou, J., Stubbs, J. R., Luo, Q., Pi, M., et al. (2006). Fibroblast Growth Factor 23 Is a Counter-regulatory Phosphaturic Hormone for Vitamin D. *Jasn* 17 (5), 1305–1315. Epub 2006/04/07. doi:10.1681/asn.2005111185

Lu, X., and Hu, M. C. (2017). Klotho/FGF23 Axis in Chronic Kidney Disease and Cardiovascular Disease. *Kidney Dis.* 3 (1), 15–23. Epub 2017/08/09. doi:10.1159/000452880

Ma, R., Morshed, S., Latif, R., Zaidi, M., and Davies, T. F. (2011). The Influence of Thyroid-Stimulating Hormone and Thyroid-Stimulating Hormone Receptor Antibodies on Osteoclastogenesis. *Thyroid.* 21 (8), 897–906. Epub 2011/07/13. doi:10.1089/thy.2010.0457

Madden, C. J., and Morrison, S. F. (2004). Excitatory Amino Acid Receptors in the Dorsomedial Hypothalamus Mediate Prostaglandin-Evoked Thermogenesis in Brown Adipose Tissue. *Am. J. Physiology-Regulatory, Integr. Comp. Physiol.* 286 (2), R320–R325. Epub 2003/10/18. doi:10.1152/ajpregu.00515.2003

Maré, A., Verhulst, A., Cavalier, E., Delanaye, P., Behets, G. J., Meijers, B., et al. (2019). Clinical Inference of Serum and Bone Sclerostin Levels in Patients with End-Stage Kidney Disease. *J. Clin. Med.* 8 (12). Epub 2019/11/24. doi:10.3390/jcm8122027

Miyoshi, H., VanDussen, K. L., Malvin, N. P., Ryu, S. H., Wang, Y., Sonnek, N. M., et al. (2017). Prostaglandin E2 Promotes Intestinal Repair through an Adaptive Cellular Response of the Epithelium. *EMBO J.* 36 (1), 5–24. Epub 2016/11/01. doi:10.15252/embj.201694660

Morales-Santana, S., Garcia-Fontana, B., Garcia-Martin, A., Rozas-Moreno, P., Garcia-Salcedo, J. A., Reyes-Garcia, R., et al. (2013). Atherosclerotic Disease in Type 2 Diabetes Is Associated with an Increase in Sclerostin Levels. *Diabetes Care* 36 (6), 1667–1674. Epub 2013/01/05. doi:10.2337/dc12-1691

Musgrove, J., and Wolf, M. (2020). Regulation and Effects of FGF23 in Chronic Kidney Disease. *Annu. Rev. Physiol.* 82, 365–390. Epub 2019/11/20. doi:10.1146/annurev-physiol-021119-034650

Narumiya, S., Sugimoto, Y., and Ushikubi, F. (1999). Prostanoid Receptors: Structures, Properties, and Functions. *Physiol. Rev.* 79 (4), 1193–1226. Epub 1999/10/03. doi:10.1152/physrev.1999.79.4.1193

Obri, A., Khrimian, L., Karsenty, G., and Oury, F. (2018). Osteocalcin in the Brain: from Embryonic Development to Age-Related Decline in Cognition. *Nat. Rev. Endocrinol.* 14 (3), 174–182. Epub 2018/01/30. doi:10.1038/nrendo.2017.181

Okamoto, H. (2007). Osteopontin and Cardiovascular System. *Mol. Cell Biochem.* 300 (1-2), 1–7. Epub 2006/12/01. doi:10.1007/s11010-006-9368-3

Pagel, C. N., Wasgewatte Wijesinghe, D. K., Taghavi Esfandouni, N., and Mackie, E. J. (2014). Osteopontin, Inflammation and Myogenesis: Influencing Regeneration, Fibrosis and Size of Skeletal Muscle. *J. Cell Commun. Signal.* 8 (2), 95–103. Epub 2013/12/10. doi:10.1007/s12079-013-0217-3

Pickering, M.-E., Simon, M., Sornay-Rendu, E., Chikh, K., Carlier, M.-C., Raby, A.-L., et al. (2017). Serum Sclerostin Increases after Acute Physical Activity. *Calcif Tissue Int.* 101 (2), 170–173. Epub 2017/04/05. doi:10.1007/s00223-017-0272-5

Possik, E., Madiraju, S. R. M., and Prentki, M. (2017). Glycerol-3-phosphate phosphatase/PGP: Role in Intermediary Metabolism and Target for Cardiometabolic Diseases. *Biochimie.* 143, 18–28. Epub 2017/08/23. doi:10.1016/j.biochi.2017.08.001

Rentsendorj, A., Sheyn, J., Fuchs, D.-T., Daley, D., Salumbides, B. C., Schubloom, H. E., et al. (2018). A Novel Role for Osteopontin in Macrophage-Mediated Amyloid-β Clearance in Alzheimer's Models. *Brain Behav. Immun.* 67, 163–180. Epub 2017/09/02. doi:10.1016/j.bbi.2017.08.019

Rossaint, J., Oehmichen, J., Van Aken, H., Reuter, S., Pavenstädt, H. J., Meersch, M., et al. (2016). FGF23 Signaling Impairs Neutrophil Recruitment and Host Defense during CKD. *J. Clin. Invest.* 126 (3), 962–974. Epub 2016/02/16. doi:10.1172/jci83470

Roudier, M., Li, X., Niu, Q.-T., Pacheco, E., Pretorius, J. K., Graham, K., et al. (2013). Sclerostin Is Expressed in Articular Cartilage but Loss or Inhibition Does Not Affect Cartilage Remodeling during Aging or Following Mechanical Injury. *Arthritis Rheum.* 65 (3), 721–731. Epub 2012/12/13. doi:10.1002/art.37802

Rousseaud, A., Moriceau, S., Ramos-Brossier, M., and Oury, F. (2016). Bone-brain Crosstalk and Potential Associated Diseases. *Horm. Mol. Biol. Clin. Investig.* 28 (2), 69–83. Epub 2016/09/15. doi:10.1515/hmbci-2016-0030

Sawaki, D., Czibik, G., Pini, M., Ternacle, J., Suffee, N., Mercedes, R., et al. (2018). Visceral Adipose Tissue Drives Cardiac Aging through Modulation of Fibroblast Senescence by Osteopontin Production. *Circulation* 138 (8), 809–822. Epub 2018/03/04. doi:10.1161/circulationaha.117.031358

Simic, P., Kim, W., Zhou, W., Pierce, K. A., Chang, W., Sykes, D. B., et al. (2020). Glycerol-3-phosphate Is an FGF23 Regulator Derived from the Injured Kidney. *J. Clin. Invest.* 130 (3), 1513–1526. Epub 2020/02/18. doi:10.1172/jci131190

Sopjani, M., Rinnerthaler, M., Kruja, J., and Dermaku-Sopjani, M. (2015). Intracellular Signaling of the Aging Suppressor Protein Klotho. *Cmm* 15 (1), 27–37. Epub 2015/01/21. doi:10.2174/1566524015666150114111258

Stock, J. L., Shinjo, K., Burkhardt, J., Roach, M., Taniguchi, K., Ishikawa, T., et al. (2001). The Prostaglandin E2 EP1 Receptor Mediates Pain Perception and Regulates Blood Pressure. *J. Clin. Invest.* 107 (3), 325–331. Epub 2001/02/13. doi:10.1172/jci6749

Sun, Y., Yin, X. S., Guo, H., Han, R. K., He, R. D., and Chi, L. J. (2013). Elevated Osteopontin Levels in Mild Cognitive Impairment and Alzheimer's Disease. *Mediators Inflamm.* 2013, 615745, 2013 . Epub 2013/04/12. doi:10.1155/2013/615745

Tai, H.-H., Ensor, C. M., Tong, M., Zhou, H., and Yan, F. (2002). Prostaglandin Catabolizing Enzymes. *Prostaglandins & Other Lipid Mediators* 68-69, 483–493. Epub 2002/11/16. doi:10.1016/s0090-6980(02)00050-3

Thompson, M. L., Jimenez-Andrade, J. M., and Mantyh, P. W. (2016). Sclerostin Immunoreactivity Increases in Cortical Bone Osteocytes and Decreases in Articular Cartilage Chondrocytes in Aging Mice. *J. Histochem. Cytochem.* 64 (3), 179–189. Epub 2015/12/25. doi:10.1369/0022155415626499

Tsuji, H., Shimizu, N., Nozawa, M., Umekawa, T., Yoshimura, K., De Velasco, M. A., et al. (2014). Osteopontin Knockdown in the Kidneys of Hyperoxaluric Rats Leads to Reduction in Renal Calcium Oxalate crystal Deposition. *Urolithiasis.* 42 (3), 195–202. Epub 2014/03/13. doi:10.1007/s00240-014-0649-0

Uaesoontrachoon, K., Wasgewatte Wijesinghe, D. K., Mackie, E. J., and Pagel, C. N. (2013). Osteopontin Deficiency Delays Inflammatory Infiltration and the Onset of Muscle Regeneration in a Mouse Model of Muscle Injury. *Dis. Model. Mech.* 6 (1), 197–205. Epub 2012/08/25. doi:10.1242/dmm.009993

Urakawa, I., Yamazaki, Y., Shimada, T., Iijima, K., Hasegawa, H., Okawa, K., et al. (2006). Klotho Converts Canonical FGF Receptor into a Specific Receptor for FGF23. *Nature* 444 (7120), 770–774. Epub 2006/11/07. doi:10.1038/nature05315

Vázquez-Sánchez, S., Poveda, J., Navarro-García, J. A., González-Lafuente, L., Rodríguez-Sánchez, E., Ruilope, L. M., et al. (2021). An Overview of FGF-23 as a Novel Candidate Biomarker of Cardiovascular Risk. *Front. Physiol.* 12, 632260, 2021 . Epub 2021/03/27. doi:10.3389/fphys.2021.632260

Vlot, M. C., den Heijer, M., de Jongh, R. T., Vervloet, M. G., Lems, W. F., de Jonge, R., et al. (2018). Clinical Utility of Bone Markers in Various Diseases. *Bone.* 114, 215–225. Epub 2018/06/20. doi:10.1016/j.bone.2018.06.011

Wakolbinger, R., Muschitz, C., Wallwitz, J., Bodlaj, G., Feichtinger, X., Schanda, J. E., et al. (2020). Serum Levels of Sclerostin Reflect Altered Bone Microarchitecture in Patients with Hepatic Cirrhosis. *Wien Klin Wochenschr.* 132 (1-2), 19–26. Epub 2020/01/09. doi:10.1007/s00508-019-01595-8

Wang, D., and Dubois, R. N. (2010). Eicosanoids and Cancer. *Nat. Rev. Cancer* 10 (3), 181–193. Epub 2010/02/20. doi:10.1038/nrc2809

Wang, N., Xue, P., Wu, X., Ma, J., Wang, Y., and Li, Y. (2018). Role of Sclerostin and Dkk1 in Bone Remodeling in Type 2 Diabetic Patients. *Endocr. Res.* 43 (1), 29–38. Epub 2017/10/04. doi:10.1080/07435800.2017.1373662

Wolak, T. (2014). Osteopontin - a Multi-Modal Marker and Mediator in Atherosclerotic Vascular Disease. *Atherosclerosis* 236 (2), 327–337. Epub 2014/08/17. doi:10.1016/j.atherosclerosis.2014.07.004

Wung, J., Perry, G., Kowalski, A., R. Harris, P., Bishop, G., Trivedi, M., et al. (2007). Increased Expression of the Remodeling- and Tumorigenic-Associated Factor Osteopontin in Pyramidal Neurons of the Alzheimers Disease Brain. *Car* 4 (1), 67–72. Epub 2007/02/24. doi:10.2174/156720507779939869

Xie, Y., Sakatsume, M., Nishi, S., Narita, I., Arakawa, M., and Gejyo, F. (2001). Expression, Roles, Receptors, and Regulation of Osteopontin in the Kidney. *Kidney Int.* 60 (5), 1645–1657. Epub 2001/11/13. doi:10.1046/j.1523-1755.2001.00032.x

Xiong, J., and O'Brien, C. A. (2012). Osteocyte RANKL: New Insights into the Control of Bone Remodeling. *J. Bone Miner Res.* 27 (3), 499–505. Epub 2012/02/23. doi:10.1002/jbmr.1547

Yan, Y.-P., Lang, B. T., Vemuganti, R., and Dempsey, R. J. (2009). Osteopontin Is a Mediator of the Lateral Migration of Neuroblasts from the Subventricular Zone after Focal Cerebral Ischemia. *Neurochem. Int.* 55 (8), 826–832. Epub 2009/08/19. doi:10.1016/j.neuint.2009.08.007

Yu, X., Sabbagh, Y., Davis, S., Demay, M., and White, K. (2005). Genetic Dissection of Phosphate- and Vitamin D-Mediated Regulation of Circulating Fgf23 Concentrations. *Bone.* 36 (6), 971–977. Epub 2005/05/05. doi:10.1016/j.bone.2005.03.002

Zeng, C., Guo, C., Cai, J., Tang, C., and Dong, Z. (2018). Serum Sclerostin in Vascular Calcification and Clinical Outcome in Chronic Kidney Disease. *Diabetes Vasc. Dis. Res.* 15 (2), 99–105. Epub 2017/11/24. doi:10.1177/1479164117742316

Zhou, Y., Yao, Y., Shen, L., Zhang, J., Zhang, J. H., and Shao, A. (2020). Osteopontin as a Candidate of Therapeutic Application for the Acute Brain Injury. *J. Cell Mol Med.* 24 (16), 8918–8929. Epub 2020/07/14. doi:10.1111/jcmm.15641

Zhu, A. S., Li, A., Ratliff, T. S., Melsom, M., and Garza, L. A. (2017). After Skin Wounding, Noncoding dsRNA Coordinates Prostaglandins and Wnts to Promote Regeneration. *J. Invest. Dermatol.* 137 (7), 1562–1568. Epub 2017/04/11. doi:10.1016/j.jid.2017.03.023

Zoch, M. L., Clemens, T. L., and Riddle, R. C. (2016). New Insights into the Biology of Osteocalcin. *Bone.* 82, 42–49. Epub 2015/06/10. doi:10.1016/j.bone.2015.05.046

Conflict of Interest: The authors declare that the research was conducted in the absence of any commercial or financial relationships that could be construed as a potential conflict of interest.

Publisher's Note: All claims expressed in this article are solely those of the authors and do not necessarily represent those of their affiliated organizations, or those of the publisher, the editors and the reviewers. Any product that may be evaluated in this article, or claim that may be made by its manufacturer, is not guaranteed or endorsed by the publisher.

frontiers in Cell and Developmental Biology

MINI REVIEW
published: 21 December 2021
doi: 10.3389/fcell.2021.783322

m6A Methylation Regulates Osteoblastic Differentiation and Bone Remodeling

Mei Huang[1,2], Shaozhe Xu[2], Lifei Liu[1], Miao Zhang[1], Jianmin Guo[1], Yu Yuan[1,3], Jiake Xu[4], Xi Chen[2] and Jun Zou[1]**

[1]School of Kinesiology, Shanghai University of Sport, Shanghai, China, [2]School of Sports Science, Wenzhou Medical University, Wenzhou, China, [3]School of Physical Education and Sports Science, South China Normal University, Guangzhou, China, [4]School of Biomedical Sciences, University of Western Australia, Perth, WA, Australia

Osteoporosis is a prevalent bone disease of the aging population, which is characterized by a decrease in bone mass because of the imbalance of bone metabolism. Although the prevention and treatment of osteoporosis have been explored by different researchers, the mechanisms underlying osteoporosis are not clear exactly. N6 methyladenosine (m6A) is a methylated adenosine nucleotide, which functions through its interaction with the proteins called "writers," "readers" and "erasers." The epigenetic regulation of m6A has been demonstrated to affect mRNA processing, nuclear export, translation, and splicing. At the cellular level, m6A modification has been known to affect cell proliferation, differentiation, and apoptosis of bone-related cells, such as bone marrow mesenchymal stem cells (BMSC), osteoblasts, and osteoclasts by regulating the expression of ALP, Runx2, Osterix, VEGF, and other related genes. Furthermore, PTH/Pth1r, PI3K-Akt, Wnt/β-Catenin, and other signaling pathways, which play important roles in the regulation of bone homeostasis, are also regulated by m6A. Thus, m6A modification may provide a new approach for osteoporosis treatment. The key roles of m6A modification in the regulation of bone health and osteoporosis are reviewed here in this article.

Keywords: m6A methylation, bone remodeling, osteoporosis, bone marrow mesenchymal stem cells, signaling pathways

OPEN ACCESS

Edited by:
Changqi Zhu,
Ferris State University, United States

Reviewed by:
Neha Tiwari,
Johannes Gutenberg University Mainz, Germany
Sei Kuriyama,
Akita University, Japan

****Correspondence:***
Xi Chen
chenab004@126.com
Jun Zou
junzou@sus.edu.cn

Specialty section:
This article was submitted to Morphogenesis and Patterning, a section of the journal Frontiers in Cell and Developmental Biology

Received: *26 September 2021*
Accepted: *06 December 2021*
Published: *21 December 2021*

Citation:
Huang M, Xu S, Liu L, Zhang M, Guo J, Yuan Y, Xu J, Chen X and Zou J (2021) m6A Methylation Regulates Osteoblastic Differentiation and Bone Remodeling. Front. Cell Dev. Biol. 9:783322. doi: 10.3389/fcell.2021.783322

1 INTRODUCTION

Epigenetic modifications regulate gene expression and translation and affect cell development and differentiation (Kohli and Zhang, 2013). Epigenetic abnormalities can occur in different ways, including DNA, RNA, and histone modification (Litt et al., 2001; Akhavan-Niaki and Samadani, 2013; Xu et al., 2016; Roignant and Soller, 2017). RNA transmits DNA genetic information to proteins and participates in biological processes via RNA post-transcriptional modification. Previous studies have identified more than 150 types of RNA modifications (Helm and Motorin, 2017). Among them, N6-methyladenosine (m6A) modification is the most common gene modification in mammalian cells, occurring in the adenosine base at the nitrogen-6 position of mRNAs (Desrosiers et al., 1974; Wei et al., 1975). The core sequence of m6A is RRm^{6}ACH ([G/A/U] [G > A]m^6 AC [U > A > C]), which is located in the 3′ untranslated region (3′UTR) adjacent to the stop codon of mRNA (Dominissini et al., 2012; Meyer et al., 2012). Unlike other gene modifications, the modification of m6A is dynamically reversible and regulates the maturation, translation, and degradation of precursor mRNAs (Haussmann et al., 2016; Guo et al., 2017; Yu et al., 2018). m6A RNA

methylation participates in the development of diseases, as an increase in m6A promotes the expression of oncoproteins. Studies have revealed that the high prevalence of m6A can enhance the proliferation, invasion, and survival of cancer cells, including cancer cells of gastric, lung, breast, and liver (Zhang et al., 2016; Du et al., 2017; Cai et al., 2018; Chen et al., 2019; Lin et al., 2019).

Recent studies have shown that m6A methylation is involved in the development of bone-related diseases such as osteoporosis (Wu et al., 2018), osteoarthritis (Liu et al., 2019), and osteosarcoma (Miao et al., 2019; Wang et al., 2019). Osteoporosis is a bone metabolic disease with a reduction in bone mass and degradation of bone structure, which increases the risk of bone fracture (Felsenberg and Boonen, 2005). With the growth of the aging population worldwide, the prevalence of osteoporosis is increasing rapidly, and the number of patients is estimated to be more than 200 million at present (Tian et al., 2017; Shapiro et al., 2019). The patient's bones gradually become fragile and can easily fracture, which seriously affects people's life span and quality of life (Muftic et al., 2013; Shapiro et al., 2019). m6A RNA methylation plays a crucial role in regulating bone formation and resorption by influencing cytokines, hormones, and signaling pathways. This study reviews the influence of m6A on osteoporosis, particularly its relationship with bone homeostasis through multiple mechanisms.

2 BASIC INTRODUCTION OF M6A METHYLATION

m6A is one of the most prevalent internal modifications in eukaryotic messenger RNA. m6A regulates gene expression through affecting the translocation, exporting, translation, and decay of RNA (Huang et al., 2020). Thus, dynamic m6A modification is important for many physiological processes. The abundance and function of m6A are effected by the interaction of methyltransferases ("writers"), binding proteins ("readers"), and demethylases ("erasers") (Panneerdoss et al., 2018; Shi et al., 2019).

2.1 Writers

Writers transfer a methyl group to the N-6 position of adenosine. N-methyladenosine (mA) is mainly catalyzed by the m6A methyltransferase complex, which encompasses Wilms tumor 1-associated protein (WTAP), methyltransferase-like 3 (METTL3), and methyltransferase-like14 (METTL14) (Ping et al., 2014). METTL3 plays a major catalytic role in regulating alternative splicing of mRNAs (Ke et al., 2017; Xu et al., 2017; Feng et al., 2018), while METTL14 assists in RNA substrate binding (Wang et al., 2016). WTAP is required for the METTL3-MELLT14 complex to be located in nuclear speckles and catalyzes the activation of m6A methyltransferase *in vivo* (Ping et al., 2014).

Recently, an increasing number of other components of the methyltransferase complex has been found, such as KIAA1429 (VIRMA, vir-like m6A methyltransferase associated) (Schwartz et al., 2014), methyltransferase-like protein 16 (METTL16) (Warda et al., 2017), RNA binding motif protein 15 (RBM15), RBM15B (Patil et al., 2016), and zinc finger CCCH-type containing 13 (ZC3H13) (Wen et al., 2018). These proteins interact with the methyltransferase complex to regulate the stability of the complex and affect m6A methylation of mRNAs (Knuckles et al., 2018). However, comprehension of m6A methyltransferase is still exploratory, so it remains further research on these writers.

2.2 Readers

Readers modulate the stability and translation of m6A-modified RNAs (Wang et al., 2014; Wang et al., 2015). The most common type of m6A "reader" proteins is the YTH family, including YTHDF1, YTHDF2, YTHDF3, YTHDC1, and YTHDC2, which contain the unique YTH domain and directly bind to m6A to regulate downstream targets (Luo and Tong, 2014; Xu et al., 2014; Kasowitz et al., 2018). Among them, YTHDF3 mainly attenuated methylated mRNAs and then decreased translation through cooperation with YTHDF1 and YTHDF2. Thus, these three YTHDF proteins interact and coordinate to regulate methylated mRNAs (Shi et al., 2017). The second type of "reader" proteins are the heterogeneous nuclear ribonucleoprotein (HNRNP) family proteins (HNRNPA2B1, HNRNPC, HNRNP G), which regulate the maturation of RNA substrates in the nucleus (Alarcón et al., 2015; Liu et al., 2015). With more studies focusing on m6A methylation, other RNA-binding proteins (Readers) have been found, such as insulin-like growth factor 2 mRNA-binding proteins (IGF2BP) (Huang et al., 2018), leucine-rich pentatricopeptide repeat-containing (LRPPRC), and fragile X mental retardation 1 (FMR1) (Zhang et al., 2018). The potential number of readers is large and m6A modifications depend on readers to fulfill biological functions, which contains a broad research space.

2.3 Erasers

Demethylase ("erasers") can remove the methyl group of m6A off RNAs, indicating that the methylation of m6A is a dynamic process and is reversible. There are two common demethylases: fat mass and obesity-associated protein (FTO) and alkB homolog 5 (ALKBH5) (Jia et al., 2011; Zheng et al., 2013). FTO was first reported related to body mass and obesity in humans (Dina et al., 2007; Zhao et al., 2014). In 2011, Jia et al. (2011) found that FTO is partially located on nuclear speckles and that m6A in nuclear RNA is the physiological substrate of FTO. FTO removes m6A methylation in RNAs to affect physiological activities such as glycolysis (Qing et al., 2021) and adipogenesis (Wang et al., 2020a). FTO depletion induces a notable increase in the total m6A levels of polyadenylated RNAs. ALKBH5 also localizes to the nucleus and significantly impacts mRNA export and RNA metabolism through demethylation activity. Alkbh5-deficient male mice showed increased m6A mRNA expression, which impairs fertility through aberrant spermatogenesis and apoptosis (Zheng et al., 2013). At present, few proteins exhibit demethylation activity. The functions and mechanisms of additional m6A demethylases still need further mining.

3 REGULATION OF M6A METHYLATION ON BONE CELLS

Human bones undergo remodeling through bone formation and resorption, and the coordination between osteogenesis and osteoclastogenesis maintains bone health (Felsenberg and Boonen, 2005). Any disruption to this balance leads to bone-related diseases, including osteoporosis, which is mainly characterized by bone mass loss, reduction of bone strength, and increased risk of fractures (Bliuc et al., 2015; Onsensus Development, 2001). Several studies have shown that m6A methylation plays an essential role in regulating bone cells, including bone marrow mesenchymal stem cells (BMSCs) and osteoblasts (Wu et al., 2018; Yu et al., 2019a; Mi et al., 2020; Yan et al., 2020). Thus, m6A methylation may open a new approach for the prevention and treatment of osteoporosis.

3.1 Regulation of m6A Methylation on Bone Marrow Mesenchymal Stem Cells

BMSCs are multiple differentiation potential cells that can differentiate into osteoblasts, chondrocytes, and bone marrow adipocytes. BMSCs play an essential role in human skeletal health by balancing osteogenic and lipogenic differentiation (Kawai et al., 2009; Chen et al., 2016). The preferential differentiation of mesenchymal stem cells into adipocytes leads to an increase in bone marrow fat and a decrease in osteoblasts and osteocytes, resulting in bone mass loss and even the development of osteoporosis (Rosen et al., 2009; Scheller and Rosen, 2014).

As METTL3 plays a crucial role in catalyzing m6A methylation, previous studies have primarily focused on regulating METTL3-mediated m6A methylation on osteogenesis. Recently, Wu et al. (2018) demonstrated that conditional knockout of METTL3 in BMSCs increased bone loss, leading to impairment of bone formation and development of the pathological characteristics of osteoporosis in mice, indicating that downregulation of METTL3-mediated m6A methyltransferase in BMSCs induced osteoporosis. The findings further revealed that the dysregulation of m6A methyltransferase increased adipocyte differentiation and decreased osteoblast differentiation, resulting in a reduction in osteogenesis. Mechanistically, METTL3-mediated m6A methyltransferase targeted Pth1r (parathyroid hormone receptor-1) and reduced protein translation, impaired the function of PTH (parathyroid hormone)-Pth1r signaling, and dysregulated BMSC-derived osteoblasts (Wu et al., 2018). Tian et al. (2019) also discovered that downregulation of METTL3 decreased the early and later osteoblast differentiation in BMSCs, as both ALP activity and mineralized nodules were reduced, indicating that downregulation of METTL3-mediated m6A methyltransferase affects osteoblast differentiation in BMSCs. Research revealed that as the downstream target of m6A methyltransferase after the knockdown expression of METTL3, the expression of osteogenic-related genes such as Runx2 and Osterix was reduced (Tian et al., 2019). Furthermore, the reduction of Akt phosphorylation and downregulation of the PI3K-Akt signaling pathway also regulate METTL3-mediated m6A on bone formation (Marie, 2012; Tian et al., 2019). Consistently, the knockdown of METTL3 in BMSCs increased adipocyte differentiation. Yao et al. (2019) demonstrated that silencing METTL3 in porcine BMSCs decreased Janus kinase1 (JAK1) mRNA m6A modification levels and promoted adipogenesis through the JAK1/STAT5/C–EBPβ signaling pathway. These results demonstrated that the downregulation of METTL3 in BMSCs suppressed osteoblast differentiation and promoted adipocyte differentiation, leading to decreased bone formation and even the development of osteoporosis.

On the contrary, overexpression of METTL3 increased osteogenic differentiation and remedied BMSC dysfunction in ovariectomized mice by directly promoting the m6A methylation of Runx2 to maintain the stability of mRNA Runx2, leading to a high expression level of Runx2. In addition, m6A methylation of precursor miR-320 indirectly amplified the effect of METTL3 overexpression on osteogenesis through the downregulation of mature miR-320 in BMSCs. Furthermore, downregulation of mature miR-320 levels protected against METTL3 silence-induced bone loss *in vivo* (Yan et al., 2020).

In addition, m6A methylation affects bone formation through blood vessels. Previous studies have found that vascular endothelial growth factor (VEGF), including three homologous spliced variants, 120, 164, and 188, promote angiogenesis and osteogenesis (Breier et al., 1992; Wallner et al., 2015; Hu and Olsen, 2016; Tong et al., 2019). Tian et al. (2019) illustrated that knockdown of METTL3 reduced the expression of VEGFA (VEGFA-164 and VEGFA -188). Previous studies have shown that VEGFA-164 and VEGFA -188 promote the proliferation and differentiation of osteoblasts from BMSCs (Carmeliet et al., 1999), suggesting that METTL3 also regulates bone formation through m6A methylation of VEGF in BMSCs, followed by the mutual promotion of angiogenesis and osteogenesis in bone (Ramasamy et al., 2014).

Further research showed that METTL3 promoted the activation of m6A methylation of MYD88-RNA in menstrual blood-derived mesenchymal stem cells (MenSCs), which upregulates the osteogenesis inhibitor NF-κB and thus suppresses bone formation. Knockdown of METTL3 inhibited the degradation of IκBα and the S536 site phosphorylation of p65, thereby restraining NF-κB nuclear translocation and suppressing downstream transcription. More interestingly, ALKBH5 reversed these results by demethylase of MYD88-RNA (Yu et al., 2019a). A recent study showed that ALKBH5 affects osteogenesis by targeting BMP2 (Wang et al., 2020b) and TRAF4 (Cen et al., 2020). FTO also inhibits osteogenic differentiation of BMSCs through m6A demethylation (Zhang et al., 2020).

These studies indicate that METTL3-mediated m6A methylation could regulate bone formation at multiple levels and might provide new strategies for the treatment of osteoporosis. However, more studies are required to better understand the role of m6A methylation in regulating BMSCs and bone formation.

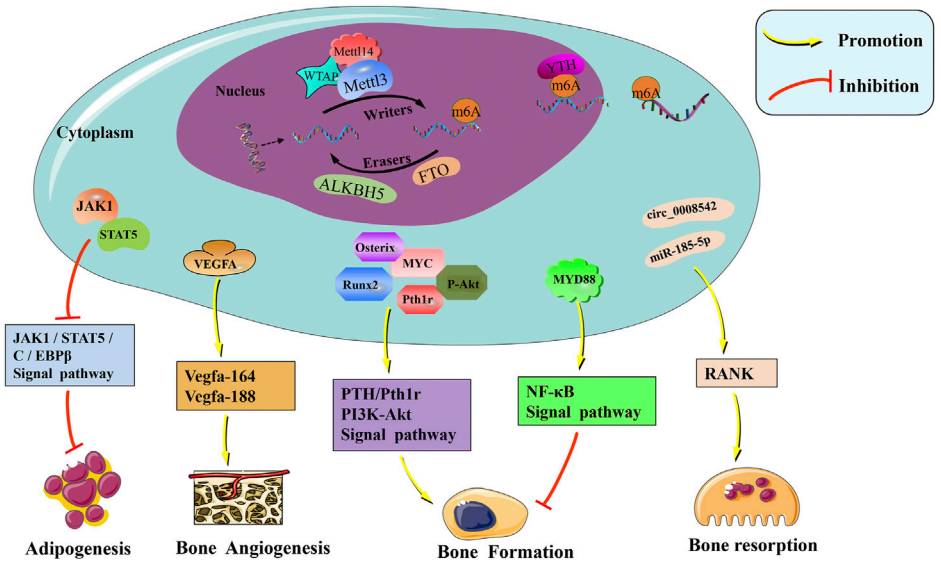

FIGURE 1 | The molecular mechanism and physiological regulation roles of m6A modification in bone. M6A is mainly catalyzed by the METTL3–METTL14–WTAP methyltransferase complex, and the demethylases ALKBH5 and FTO remove the methyl group of m6A off RNAs. Readers of the YTH domain family are effectors that recognize the m6A methylation code and convert it into signals. M6A modification regulates the expression of Runx2, Osterix, VEGF, RANK, and other related genes affecting bone metabolism. Furthermore, PTH/Pth1r, PI3K-Akt, NF-κB, and other signaling pathways were also mediated by m6A, which is important in the regulation of bone homeostasis.

3.2 Regulating m6A Methylation on Osteoblasts

Studies have also shown that m6A methylation regulates osteoblast differentiation. Mi et al. (2020) discovered that downregulation of METTL3 promoted the osteogenic process *in vitro* and *in vivo* by inhibiting the maturation of miR-7212-5p. Further studies showed that miR-7212-5p inhibited osteoblast differentiation of MC3T3-E1 cells by targeting FGFR3. These findings suggest that METTL3 inhibits osteogenic-related genes in MC3T3-E1 cells. It seemed that METTL3 had a dual role in osteogenic differentiation, especially in different cell lines. FTO, an important RNA demethylase, also plays an important role in modulating osteoblast differentiation. Shen et al. (2018) found that FTO was upregulated during aging or osteoporosis in humans and mice, which upregulated BMSC differentiation into adipocytes and downregulated osteoblasts. Interestingly, conditional knockout of FTO in osteoblasts inhibited the progression of osteopenia in ovariectomy (OVX) mice but not in sham-operated mice. Mechanistically, GDF11 (growth differentiation factor 11)-FTO-PPARγ (peroxisome proliferator-activated receptor-gamma) signaling inhibits the differentiation of osteoblasts and promotes osteoporosis in humans and mice. Similarly, Zhang et al. (2019) found that conditional knockout of FTO in osteoblasts showed no difference in bone volume in 12-week-old mice compared to wild-type mice. However, 30-week-old mice with FTO knockout in osteoblasts had lower bone volume than wild-type mice. This phenomenon may be explained by the different animal models used. Additionally, Wang et al. (2019) studied the m6A methylome of the transcriptome in osteosarcoma cells by chemotherapy, indicating that m6A methylation modification may potentially affect the totipotency of osteosarcoma cells (OSCs) through the Wnt and Notch signaling pathways. Miao et al. (2019) also found that METTL3-mediated m6A methylation in OSCs promoted m6A levels of lymphoid enhancer factor-1 (LEF1) and upregulates the Wnt/β-catenin signaling pathway, which plays a critical role in osteoblast differentiation and osteogenesis (Wang et al., 2017; Zheng et al., 2020). These findings illustrated that m6A methylation affected osteoblast differentiation in humans and mice.

3.3 Regulating m6A Methylation on Osteoclasts

The bone resorption mediated by osteoclasts is important in bone metabolism. A recent study revealed that m6A methylation plays a prominent role in osteoclast differentiation and bone resorption (Salzman, 2016). The RNA methylase METTL3 affected m6A levels through the 1956 bp in circ_0008542 (noncoding RNA with a closed circular structure) and promoted the initiation of osteoclast-induced bone absorption. Circ_0008542 upregulated the competitive binding of miRNA-185-5p and promoted the expression of the target gene RANK. Instead, RNA demethylase ALKBH5 downregulated the combination of circ_0008542 with miRNA-185-5p to rescue excessive bone resorption (Wang et al., 2021). In addition, several studies have shown that m6A has a regulatory effect on intracellular inflammatory factors such as interleukin-1β (IL-1β), IL-6, interferon-gamma (IFN-γ), and tumor necrosis factor-α (TNF-α), leading to bone loss through the bone immune system (Neurath and Finotto, 2011; Briot and

TABLE 1 | Multiple functions exerted by m6A RNA methylation in bone.

m6A component	m6A levels	Related targets	Biological function	Sample resources	Refs
Mettl3 knockout	Low	Pth1r ↓	Inhibit osteogenesis	BMSCs	Wu et al. (2018)
Mettl3 knockdown	Low	JAK1 ↑	Inhibit osteogenesis	BMSCs	Yao et al. (2019)
Mettl3 knockdown	Low	Vegfa-164 ↓ Vegfa-188 ↓	Inhibit osteogenesis	BMSCs	Tian et al. (2019)
Mettl3 knockdown	Low	MYD88 ↓	Promote osteogenesis	MenSCs	Yu et al. (2019)
Mettl3 knockdown	Low	miR-320 ↑ RUNX2 ↓	Inhibit osteogenesis	BMSCs	Yan et al. (2019)
Mettl3 knockdown	Low	miR-7212-5p ↓	Promote osteogenesis	MC3T3	Mi et al. (2020)
Mettl3 knockdown or ALKBH5 overexpression	Low	circ_0008542 ↓ RANK↓	Inhibit bone resorption	Osteoclast	Wang et al. (2021)
YTHDF2 knockdown	—	MAP2K4 ↑ MAP4K4 ↑	—	Raw264.7	Yu et al. (2019)
ALKBH5 knockdown	high	TRAF4 ↓	Inhibit osteogenesis	MSC	Cen et al. (2020)
ALKBH5 knockdown	high	BMP2 ↓ P-AKT ↓	Inhibit osteogenesis	OLF	Wang et al. (2020)
FTO knockdown	high	PPARγ ↓	Promote osteogenesis	BMSCs	Shen et al. (2018)
FTO knockdown	high	MYC ↑	Promote osteogenesis	BMSCs	Zhang et al. (2020)
FTO knockout	high	Hspa1a ↓	Inhibit osteogenesis	Osteoblast	Zhang et al. (2019)

Roux, 2015; van Bodegraven and Bravenboer, 2019). Estrogen deficiency also increases inflammatory cytokines (Tsangari et al., 2004), followed by the activation of osteoclasts, increased bone resorption, and osteoporosis (Chen et al., 2017). Liu et al. (2019) also found that during the process of IL-1 β-induced chondrocyte inflammation, the expression level of METTL3 mRNA increased in a dose-dependent manner. At the same time, knockdown of METTL3 reduced the mRNA expression level of inflammatory factors in chondrocytes, including IL-6, IL-8, IL-12, and TNF-α, suggesting that m6A mRNA methylation promotes inflammatory injury in chondrocytes. Another study found that the knockdown of "reader" protein YTHDF2 increased the expression of MAP4K4 and MAP2K4, then activated MAPK and NF-κB signaling pathways, upregulated osteoclasts differentiation, and enhanced LPS-induced stimulation in RAW 264.7 cells (Yu et al., 2019b). These results suggest that m6A mRNA methylation plays a critical role in regulating osteoclasts through inflammatory responses.

4 CONCLUSION AND PROSPECTS

In summary, m6A methylation regulated osteogenic differentiation and bone metabolism. But the function of m6A methylation maybe like a "double-edged sword," by which it can either promote or inhibit bone formation in different ways (**Figure 1**; **Table 1**). Undoubtedly, m6A regulation has provided novel insight into the molecular mechanism of bone metabolism.

However, the study of m6A modification on bone metabolism is still in its infancy. First, existing research on m6A in bone mainly focused on Writers; the mechanism of m6A Erasers and Readers in bone metabolism require further study. The methylation of m6A is a dynamic and reversible process, and how the Writers and Erasers coordinate and how the Readers play their role after recognizing RNA methylation needs further exploration. Second, osteoclast-mediated bone resorption is also an important part of bone metabolism, but there are few related studies. Moreover, although METTL3 targets Runx2, VEGF and different signaling pathways to promote osteogenic differentiation, it remains controversial whether METTL3 is a potential therapeutic target for osteoporosis, as METTL3 also activates osteoclasts and then increases bone resorption. Due to the complexity of regulating m6A methylation in bone metabolism, further studies are needed to explore its underlying mechanism.

AUTHOR CONTRIBUTIONS

XC and JZ designed this review and supervised the whole program; MZ and JG searched the articles and offered advice; XS and LL prepared the figures and the tables; MH and XC wrote the paper; JX revised the manuscript. All the authors reviewed and approved the manuscript.

FUNDING

The work is supported by funding from Wenzhou basic scientific research project (Grant No. Y20190019), the National Natural Science Foundation of China (Grant No. 81702235), Shanghai Frontiers Science Research Base of Exercise and Metabolic Health, and Shanghai Key Laboratory of Human Sport Competence Development and Maintenance (Shanghai University of sport) (Grant No. 11DZ2261100).

REFERENCES

Akhavan-Niaki, H., and Samadani, A. A. (2013). DNA Methylation and Cancer Development: Molecular Mechanism. *Cell Biochem Biophys* 67 (2), 501–513. doi:10.1007/s12013-013-9555-2

Alarcón, C. R., Goodarzi, H., Lee, H., Liu, X., Tavazoie, S., and Tavazoie, S. F. (2015). HNRNPA2B1 Is a Mediator of m6A-dependent Nuclear RNA Processing Events. *Cell* 162 (6), 1299–1308. doi:10.1016/j.cell.2015.08.011

Bliuc, D., Alarkawi, D., Nguyen, T. V., Eisman, J. A., and Center, J. R. (2015). Risk of Subsequent Fractures and Mortality in Elderly Women and Men with Fragility Fractures with and without Osteoporotic Bone Density: the Dubbo Osteoporosis Epidemiology Study. *J. Bone Miner Res.* 30 (4), 637–646. doi:10.1002/jbmr.2393

Breier, G., Albrecht, U., Sterrer, S., and Risau, W. (1992). Expression of Vascular Endothelial Growth Factor during Embryonic Angiogenesis and Endothelial Cell Differentiation. *Development* 114 (2), 521–532. doi:10.1242/dev.114.2.521

Briot, K., and Roux, C. (2015). Inflammation, Bone Loss and Fracture Risk in Spondyloarthritis: Figure 1. *RMD Open* 1 (1), e000052. doi:10.1136/rmdopen-2015-000052

Cai, X., Wang, X., Cao, C., Gao, Y., Zhang, S., Yang, Z., et al. (2018). HBXIP-elevated Methyltransferase METTL3 Promotes the Progression of Breast Cancer via Inhibiting Tumor Suppressor Let-7g. *Cancer Lett.* 415, 11–19. doi:10.1016/j.canlet.2017.11.018

Carmeliet, P., Ng, Y.-S., Nuyens, D., Theilmeier, G., Brusselmans, K., Cornelissen, I., et al. (1999). Impaired Myocardial Angiogenesis and Ischemic Cardiomyopathy in Mice Lacking the Vascular Endothelial Growth Factor Isoforms VEGF164 and VEGF188. *Nat. Med.* 5 (5), 495–502. doi:10.1038/8379

Cen, S., Li, J., Cai, Z., Pan, Y., Sun, Z., Li, Z., et al. (2020). TRAF4 Acts as a Fate Checkpoint to Regulate the Adipogenic Differentiation of MSCs by Activating PKM2. *EBioMedicine* 54, 102722. doi:10.1016/j.ebiom.2020.102722

Chen, Q., Shou, P., Zheng, C., Jiang, M., Cao, G., Yang, Q., et al. (2016). Fate Decision of Mesenchymal Stem Cells: Adipocytes or Osteoblasts? *Cell Death Differ* 23 (7), 1128–1139. doi:10.1038/cdd.2015.168

Chen, X., Zhi, X., Pan, P., Cui, J., Cao, L., Weng, W., et al. (2017). Matrine Prevents Bone Loss in Ovariectomized Mice by Inhibiting RANKL-induced Osteoclastogenesis. *FASEB j.* 31 (11), 4855–4865. doi:10.1096/fj.201700316R

Chen, Y., Peng, C., Chen, J., Chen, D., Yang, B., He, B., et al. (2019). WTAP Facilitates Progression of Hepatocellular Carcinoma via m6A-HuR-dependent Epigenetic Silencing of ETS1. *Mol. Cancer* 18 (1), 127. doi:10.1186/s12943-019-1053-8

Desrosiers, R., Friderici, K., and Rottman, F. (1974). Identification of Methylated Nucleosides in Messenger RNA from Novikoff Hepatoma Cells. *Proc. Natl. Acad. Sci.* 71 (10), 3971–3975. doi:10.1073/pnas.71.10.3971

Dina, C., Meyre, D., Gallina, S., Durand, E., Körner, A., Jacobson, P., et al. (2007). Variation in FTO Contributes to Childhood Obesity and Severe Adult Obesity. *Nat. Genet.* 39 (6), 724–726. doi:10.1038/ng2048

Dominissini, D., Moshitch-Moshkovitz, S., Schwartz, S., Salmon-Divon, M., Ungar, L., Osenberg, S., et al. (2012). Topology of the Human and Mouse m6A RNA Methylomes Revealed by m6A-Seq. *Nature* 485 (7397), 201–206. doi:10.1038/nature11112

Du, M., Zhang, Y., Mao, Y., Mou, J., Zhao, J., Xue, Q., et al. (2017). MiR-33a Suppresses Proliferation of NSCLC Cells via Targeting METTL3 mRNA. *Biochem. Biophysical Res. Commun.* 482 (4), 582–589. doi:10.1016/j.bbrc.2016.11.077

Felsenberg, D., and Boonen, S. (2005). The Bone Quality Framework: Determinants of Bone Strength and Their Interrelationships, and Implications for Osteoporosis Management. *Clin. Ther.* 27 (1), 1–11. doi:10.1016/j.clinthera.2004.12.020

Feng, Z., Li, Q., Meng, R., Yi, B., and Xu, Q. (2018). METTL 3 Regulates Alternative Splicing of MyD88 upon the Lipopolysaccharide-induced Inflammatory Response in Human Dental Pulp Cells. *J. Cel Mol Med* 22 (5), 2558–2568. doi:10.1111/jcmm.13491

Guo, M., Liu, X., Zheng, X., Huang, Y., and Chen, X. (2017). m6A RNA Modification Determines Cell Fate by Regulating mRNA DegradationA RNA Modification Determines Cell Fate by Regulating mRNA Degradation. *Cell Reprogramming* 19 (4), 225–231. doi:10.1089/cell.2016.0041

Haussmann, I. U., Bodi, Z., Sanchez-Moran, E., Mongan, N. P., Archer, N., Fray, R. G., et al. (2016). m6A Potentiates Sxl Alternative Pre-mRNA Splicing for Robust Drosophila Sex determinationA Potentiates Sxl Alternative Pre-mRNA Splicing for Robust Drosophila Sex Determination. *Nature* 540 (7632), 301–304. doi:10.1038/nature20577

Helm, M., and Motorin, Y. (2017). Detecting RNA Modifications in the Epitranscriptome: Predict and Validate. *Nat. Rev. Genet.* 18 (5), 275–291. doi:10.1038/nrg.2016.169

Hu, K., and Olsen, B. R. (2016). Osteoblast-derived VEGF Regulates Osteoblast Differentiation and Bone Formation during Bone Repair. *J. Clin. Invest.* 126 (2), 509–526. doi:10.1172/JCI82585

Huang, H., Weng, H., and Chen, J. (2020). m6A Modification in Coding and Non-coding RNAs: Roles and Therapeutic Implications in CancerA Modification in Coding and Non-coding RNAs: Roles and Therapeutic Implications in Cancer. *Cancer Cell* 37 (3), 270–288. doi:10.1016/j.ccell.2020.02.004

Huang, H., Weng, H., Sun, W., Qin, X., Shi, H., Wu, H., et al. (2018). Recognition of RNA N6-Methyladenosine by IGF2BP Proteins Enhances mRNA Stability and Translation. *Nat. Cel Biol* 20 (3), 285–295. doi:10.1038/s41556-018-0045-z

Jia, G., Fu, Y., Zhao, X., Dai, Q., Zheng, G., Yang, Y., et al. (2011). N6-methyladenosine in Nuclear RNA Is a Major Substrate of the Obesity-Associated FTO. *Nat. Chem. Biol.* 7 (12), 885–887. doi:10.1038/nchembio.687

Kasowitz, S. D., Ma, J., Anderson, S. J., Leu, N. A., Xu, Y., Gregory, B. D., et al. (2018). Nuclear m6A Reader YTHDC1 Regulates Alternative Polyadenylation and Splicing during Mouse Oocyte Development. *Plos Genet.* 14 (5), e1007412. doi:10.1371/journal.pgen.1007412

Kawai, M., Devlin, M. J., and Rosen, C. J. (2009). Fat Targets for Skeletal Health. *Nat. Rev. Rheumatol.* 5 (7), 365–372. doi:10.1038/nrrheum.2009.102

Ke, S., Pandya-Jones, A., Saito, Y., Fak, J. J., Vågbø, C. B., Geula, S., et al. (2017). m6A mRNA Modifications Are Deposited in Nascent Pre-mRNA and Are Not Required for Splicing but Do Specify Cytoplasmic turnoverA mRNA Modifications Are Deposited in Nascent Pre-mRNA and Are Not Required for Splicing but Do Specify Cytoplasmic Turnover. *Genes Dev.* 31 (10), 990–1006. doi:10.1101/gad.301036.117

Knuckles, P., Lence, T., Haussmann, I. U., Jacob, D., Kreim, N., Carl, S. H., et al. (2018). Zc3h13/Flacc Is Required for Adenosine Methylation by Bridging the mRNA-Binding Factor Rbm15/Spenito to the m6A Machinery Component Wtap/Fl(2)d. *Genes Dev.* 32 (5-6), 415–429. doi:10.1101/gad.309146.117

Kohli, R. M., and Zhang, Y. (2013). TET Enzymes, TDG and the Dynamics of DNA Demethylation. *Nature* 502 (7472), 472–479. doi:10.1038/nature12750

Lin, S., Liu, J., Jiang, W., Wang, P., Sun, C., Wang, X., et al. (2019). METTL3 Promotes the Proliferation and Mobility of Gastric Cancer Cells. *Open Med. (Wars)* 14, 25–31. doi:10.1515/med-2019-0005

Litt, M. D., Simpson, M., Gaszner, M., Allis, C. D., and Felsenfeld, G. (2001). Correlation between Histone Lysine Methylation and Developmental Changes at the Chicken β-Globin Locus. *Science* 293 (5539), 2453–2455. doi:10.1126/science.1064413

Liu, N., Dai, Q., Zheng, G., He, C., Parisien, M., and Pan, T. (2015). N6-methyladenosine-dependent RNA Structural Switches Regulate RNA-Protein Interactions. *Nature* 518 (7540), 560–564. doi:10.1038/nature14234

Liu, Q., Li, M., Jiang, L., Jiang, R., and Fu, B. (2019). METTL3 Promotes Experimental Osteoarthritis Development by Regulating Inflammatory Response and Apoptosis in Chondrocyte. *Biochem. Biophysical Res. Commun.* 516 (1), 22–27. doi:10.1016/j.bbrc.2019.05.168

Luo, S., and Tong, L. (2014). Molecular Basis for the Recognition of Methylated Adenines in RNA by the Eukaryotic YTH Domain. *Proc. Natl. Acad. Sci.* 111 (38), 13834–13839. doi:10.1073/pnas.1412742111

Marie, P. J. (2012). Signaling Pathways Affecting Skeletal Health. *Curr. Osteoporos. Rep.* 10 (3), 190–198. doi:10.1007/s11914-012-0109-0

Meyer, K. D., Saletore, Y., Zumbo, P., Elemento, O., Mason, C. E., and Jaffrey, S. R. (2012). Comprehensive Analysis of mRNA Methylation Reveals Enrichment in 3′ UTRs and Near Stop Codons. *Cell* 149 (7), 1635–1646. doi:10.1016/j.cell.2012.05.003

Mi, B., Xiong, Y., Yan, C., Chen, L., Xue, H., Panayi, A. C., et al. (2020). Methyltransferase-like 3-mediated N6-methyladenosine Modification of miR-7212-5p Drives Osteoblast Differentiation and Fracture Healing. *J. Cel Mol Med* 24 (11), 6385–6396. doi:10.1111/jcmm.15284

Miao, W., Chen, J., Jia, L., Ma, J., and Song, D. (2019). The m6A Methyltransferase METTL3 Promotes Osteosarcoma Progression by Regulating the m6A Level of

LEF1. *Biochem. Biophysical Res. Commun.* 516 (3), 719–725. doi:10.1016/j.bbrc.2019.06.128

Muftic, M., Selimovic, E., and Miladinovic, K. (2013). Osteoporosis - Comparative Study between Quantitative Ultrasound of Calcaneus and DXA. *Med. Arh* 67 (4), 289–291. doi:10.5455/medarh.2013.67.289-291

Neurath, M. F., and Finotto, S. (2011). IL-6 Signaling in Autoimmunity, Chronic Inflammation and Inflammation-Associated Cancer. *Cytokine Growth Factor. Rev.* 22 (2), 83–89. doi:10.1016/j.cytogfr.2011.02.003

NIH Consensus Development Panel on Osteoporosis Prevention, Diagnosis, and Therapy, March 7-29, 2000: Highlights of the Conference. *South. Med. J.* (2001) 94(6):569–573. doi:10.1001/jama.285.6.785

Panneerdoss, S., Eedunuri, V. K., Yadav, P., Timilsina, S., Rajamanickam, S., Viswanadhapalli, S., et al. (2018). Cross-talk Among Writers, Readers, and Erasers of M 6 A Regulates Cancer Growth and Progression. *Sci. Adv.* 4 (10), eaar8263. doi:10.1126/sciadv.aar8263

Patil, D. P., Chen, C.-K., Pickering, B. F., Chow, A., Jackson, C., Guttman, M., et al. (2016). m6A RNA Methylation Promotes XIST-Mediated Transcriptional repressionA RNA Methylation Promotes XIST-Mediated Transcriptional Repression. *Nature* 537 (7620), 369–373. doi:10.1038/nature19342

Ping, X.-L., Sun, B.-F., Wang, L., Xiao, W., Yang, X., Wang, W.-J., et al. (2014). Mammalian WTAP Is a Regulatory Subunit of the RNA N6-Methyladenosine Methyltransferase. *Cell Res* 24 (2), 177–189. doi:10.1038/cr.2014.3

Qing, Y., Dong, L., Gao, L., Li, C., Li, Y., Han, L., et al. (2021). R-2-hydroxyglutarate Attenuates Aerobic Glycolysis in Leukemia by Targeting the FTO/m6A/PFKP/LDHB axis. *Mol. Cel* 81 (5), 922–939. doi:10.1016/j.molcel.2020.12.026

Ramasamy, S. K., Kusumbe, A. P., Wang, L., and Adams, R. H. (2014). Endothelial Notch Activity Promotes Angiogenesis and Osteogenesis in Bone. *Nature* 507 (7492), 376–380. doi:10.1038/nature13146

Roignant, J.-Y., and Soller, M. (2017). m 6 A in mRNA: An Ancient Mechanism for Fine-Tuning Gene ExpressionA in mRNA: An Ancient Mechanism for Fine-Tuning Gene Expression. *Trends Genet.* 33 (6), 380–390. doi:10.1016/j.tig.2017.04.003

Rosen, C. J., Ackert-Bicknell, C., Rodriguez, J. P., and Pino, A. M. (2009). Marrow Fat and the Bone Microenvironment: Developmental, Functional, and Pathological Implications. *Crit. Rev. Eukar Gene Expr.* 19 (2), 109–124. doi:10.1615/critreveukargeneexpr.v19.i2.20

Salzman, J. (2016). Circular RNA Expression: Its Potential Regulation and Function. *Trends Genet.* 32 (5), 309–316. doi:10.1016/j.tig.2016.03.002

Scheller, E. L., and Rosen, C. J. (2014). What's the Matter with MAT? Marrow Adipose Tissue, Metabolism, and Skeletal Health. *Ann. N.Y. Acad. Sci.* 1311, 14–30. doi:10.1111/nyas.12327

Schwartz, S., Mumbach, M. R., Jovanovic, M., Wang, T., Maciag, K., Bushkin, G. G., et al. (2014). Perturbation of m6A Writers Reveals Two Distinct Classes of mRNA Methylation at Internal and 5′ Sites. *Cel Rep.* 8 (1), 284–296. doi:10.1016/j.celrep.2014.05.048

Shapiro, C. L., Van Poznak, C., Lacchetti, C., Kirshner, J., Eastell, R., Gagel, R., et al. (2019). Management of Osteoporosis in Survivors of Adult Cancers with Nonmetastatic Disease: ASCO Clinical Practice Guideline. *Jco* 37, 2916–2946. doi:10.1200/JCO.19.01696

Shen, G.-S., Zhou, H.-B., Zhang, H., Chen, B., Liu, Z.-P., Yuan, Y., et al. (2018). The GDF11-FTO-Pparγ axis Controls the Shift of Osteoporotic MSC Fate to Adipocyte and Inhibits Bone Formation during Osteoporosis. *Biochim. Biophys. Acta (Bba) - Mol. Basis Dis.* 1864 (12), 3644–3654. doi:10.1016/j.bbadis.2018.09.015

Shi, H., Wang, X., Lu, Z., Zhao, B. S., Ma, H., Hsu, P. J., et al. (2017). YTHDF3 Facilitates Translation and Decay of N6-Methyladenosine-Modified RNA. *Cel Res* 27 (3), 315–328. doi:10.1038/cr.2017.15

Shi, H., Wei, J., and He, C. (2019). Where, when, and How: Context-dependent Functions of RNA Methylation Writers, Readers, and Erasers. *Mol. Cel* 74 (4), 640–650. doi:10.1016/j.molcel.2019.04.025

Tian, C., Huang, Y., Li, Q., Feng, Z., and Xu, Q. (2019). Mettl3 Regulates Osteogenic Differentiation and Alternative Splicing of Vegfa in Bone Marrow Mesenchymal Stem Cells. *Ijms* 20 (3), 551. doi:10.3390/ijms20030551

Tian, L., Yang, R., Wei, L., Liu, J., Yang, Y., Shao, F., et al. (2017). Prevalence of Osteoporosis and Related Lifestyle and Metabolic Factors of Postmenopausal Women and Elderly Men. *Medicine (Baltimore)* 96 (43), e8294. doi:10.1097/MD.0000000000008294

Tong, X., Chen, X., Zhang, S., Huang, M., Shen, X., Xu, J., et al. (2019). The Effect of Exercise on the Prevention of Osteoporosis and Bone Angiogenesis. *Biomed. Res. Int.* 2019, 1–8. doi:10.1155/2019/8171897

Tsangari, H., Findlay, D. M., Kuliwaba, J. S., Atkins, G. J., and Fazzalari, N. L. (2004). Increased Expression of IL-6 and RANK mRNA in Human Trabecular Bone from Fragility Fracture of the Femoral Neck. *Bone* 35 (1), 334–342. doi:10.1016/j.bone.2004.02.006

van Bodegraven, A. A., and Bravenboer, N. (2019). Perspective on Skeletal Health in Inflammatory Bowel Disease. *Osteoporos. Int.* 31, 637–646. doi:10.1007/s00198-019-05234-w

Wallner, C., Schira, J., Wagner, J. M., Schulte, M., Fischer, S., Hirsch, T., et al. (2015). Application of VEGFA and FGF-9 Enhances Angiogenesis, Osteogenesis and Bone Remodeling in Type 2 Diabetic Long Bone Regeneration. *PLoS One* 10 (3), e0118823. doi:10.1371/journal.pone.0118823

Wang, H.-F., Kuang, M.-j., Han, S.-j., Wang, A.-b., Qiu, J., Wang, F., et al. (2020). BMP2 Modified by the m6A Demethylation Enzyme ALKBH5 in the Ossification of the Ligamentum Flavum through the AKT Signaling Pathway. *Calcif Tissue Int.* 106 (5), 486–493. doi:10.1007/s00223-019-00654-6

Wang, L., Song, C., Wang, N., Li, S., Liu, Q., Sun, Z., et al. (2020). NADP Modulates RNA m6A Methylation and Adipogenesis via Enhancing FTO Activity. *Nat. Chem. Biol.* 16 (12), 1394–1402. doi:10.1038/s41589-020-0601-2

Wang, W., Qiao, S.-C., Wu, X.-B., Sun, B., Yang, J.-G., Li, X., et al. (2021). Circ_0008542 in Osteoblast Exosomes Promotes Osteoclast-Induced Bone Resorption through m6A Methylation. *Cell Death Dis* 12 (7), 628. doi:10.1038/s41419-021-03915-1

Wang, X., Feng, J., Xue, Y., Guan, Z., Zhang, D., Liu, Z., et al. (2016). Structural Basis of N6-Adenosine Methylation by the METTL3-METTL14 Complex. *Nature* 534 (7608), 575–578. doi:10.1038/nature18298

Wang, X., Lu, Z., Gomez, A., Hon, G. C., Yue, Y., Han, D., et al. (2014). N6-methyladenosine-dependent Regulation of Messenger RNA Stability. *Nature* 505 (7481), 117–120. doi:10.1038/nature12730

Wang, X., Zhao, B. S., Roundtree, I. A., Lu, Z., Han, D., Ma, H., et al. (2015). N6-methyladenosine Modulates Messenger RNA Translation Efficiency. *Cell* 161 (6), 1388–1399. doi:10.1016/j.cell.2015.05.014

Wang, Y., Zeng, L., Liang, C., Zan, R., Ji, W., Zhang, Z., et al. (2019). Integrated Analysis of Transcriptome-wide m6A Methylome of Osteosarcoma Stem Cells Enriched by Chemotherapy. *Epigenomics* 11 (15), 1693–1715. doi:10.2217/epi-2019-0262

Wang, Y., Zhang, X., Shao, J., Liu, H., Liu, X., and Luo, E. (2017). Adiponectin Regulates BMSC Osteogenic Differentiation and Osteogenesis through the Wnt/β-Catenin Pathway. *Sci. Rep.* 7 (1), 3652. doi:10.1038/s41598-017-03899-z

Warda, A. S., Kretschmer, J., Hackert, P., Lenz, C., Urlaub, H., Höbartner, C., et al. (2017). Human METTL16 Is a N 6 -methyladenosine (M 6 A) Methyltransferase that Targets pre-mRNAs and Various Non-coding RNAs. *EMBO Rep.* 18 (11), 2004–2014. doi:10.15252/embr.201744940

Wei, C.-M., Gershowitz, A., and Moss, B. (1975). Methylated Nucleotides Block 5′ Terminus of HeLa Cell Messenger RNA. *Cell* 4 (4), 379–386. doi:10.1016/0092-8674(75)90158-0

Wen, J., Lv, R., Ma, H., Shen, H., He, C., Wang, J., et al. (2018). Zc3h13 Regulates Nuclear RNA m6A Methylation and Mouse Embryonic Stem Cell Self-Renewal. *Mol. Cel* 69 (6), 1028–1038. doi:10.1016/j.molcel.2018.02.015

Wu, Y., Xie, L., Wang, M., Xiong, Q., Guo, Y., Liang, Y., et al. (2018). Mettl3-mediated m6A RNA Methylation Regulates the Fate of Bone Marrow Mesenchymal Stem Cells and Osteoporosis. *Nat. Commun.* 9 (1), 4772. doi:10.1038/s41467-018-06898-4

Xu, C., Wang, X., Liu, K., Roundtree, I. A., Tempel, W., Li, Y., et al. (2014). Structural Basis for Selective Binding of m6A RNA by the YTHDC1 YTH Domain. *Nat. Chem. Biol.* 10 (11), 927–929. doi:10.1038/nchembio.1654

Xu, H., Yi, Q., Yang, C., Wang, Y., Tian, J., and Zhu, J. (2016). Histone Modifications Interact with DNA Methylation at the GATA4 Promoter during Differentiation of Mesenchymal Stem Cells into Cardiomyocyte-like Cells. *Cell Prolif.* 49 (3), 315–329. doi:10.1111/cpr.12253

Xu, K., Yang, Y., Feng, G.-H., Sun, B.-F., Chen, J.-Q., Li, Y.-F., et al. (2017). Mettl3-mediated m6A Regulates Spermatogonial Differentiation and Meiosis Initiation. *Cel Res* 27 (9), 1100–1114. doi:10.1038/cr.2017.100

Yan, G., Yuan, Y., He, M., Gong, R., Lei, H., Zhou, H., et al. (2020). m6A Methylation of Precursor-miR-320/runx2 Controls Osteogenic Potential of

Bone Marrow-Derived Mesenchymal Stem CellsA Methylation of Precursor-miR-320/runx2 Controls Osteogenic Potential of Bone Marrow-Derived Mesenchymal Stem Cells. *Mol. Ther. - Nucleic Acids* 19, 421–436. doi:10.1016/j.omtn.2019.12.001

Yao, Y., Bi, Z., Wu, R., Zhao, Y., Liu, Y., Liu, Q., et al. (2019). METTL3 Inhibits BMSC Adipogenic Differentiation by Targeting the JAK1/STAT5/C/EBPβ Pathway via an M 6 A-YTHDF2-dependent Manner. *FASEB j.* 33 (6), 7529–7544. doi:10.1096/fj.201802644R

Yu, J., Chen, M., Huang, H., Zhu, J., Song, H., Zhu, J., et al. (2018). Dynamic m6A Modification Regulates Local Translation of mRNA in Axons. *Nucleic Acids Res.* 46 (3), 1412–1423. doi:10.1093/nar/gkx1182

Yu, J., Shen, L., Liu, Y., Ming, H., Zhu, X., Chu, M., et al. (2019). The m6A Methyltransferase METTL3 Cooperates with Demethylase ALKBH5 to Regulate Osteogenic Differentiation through NF-Kb Signaling. *Mol. Cel Biochem* 463, 203–210. doi:10.1007/s11010-019-03641-5

Yu, R., Li, Q., Feng, Z., Cai, L., and Xu, Q. (2019). m6A Reader YTHDF2 Regulates LPS-Induced Inflammatory Response. *Ijms* 20 (6), 1323. doi:10.3390/ijms20061323

Zhang, C., Samanta, D., Lu, H., Bullen, J. W., Zhang, H., Chen, I., et al. (2016). Hypoxia Induces the Breast Cancer Stem Cell Phenotype by HIF-dependent and ALKBH5-Mediated m6A-Demethylation of NANOG mRNA. *Proc. Natl. Acad. Sci. USA* 113 (14), E2047–E2056. doi:10.1073/pnas.1602883113

Zhang, F., Kang, Y., Wang, M., Li, Y., Xu, T., Yang, W., et al. (2018). Fragile X Mental Retardation Protein Modulates the Stability of its m6A-Marked Messenger RNA Targets. *Hum. Mol. Genet.* 27 (22), 3936–3950. doi:10.1093/hmg/ddy292

Zhang, Q., Riddle, R. C., Yang, Q., Rosen, C. R., Guttridge, D. C., Dirckx, N., et al. (2019). The RNA Demethylase FTO Is Required for Maintenance of Bone Mass and Functions to Protect Osteoblasts from Genotoxic Damage. *Proc. Natl. Acad. Sci. USA* 116 (36), 17980–17989. doi:10.1073/pnas.1905489116

Zhang, X., Wang, Y., Zhao, H., Han, X., Zhao, T., Qu, P., et al. (2020). Extracellular Vesicle-Encapsulated miR-22-3p from Bone Marrow Mesenchymal Stem Cell Promotes Osteogenic Differentiation via FTO Inhibition. *Stem Cel Res Ther* 11 (1), 227. doi:10.1186/s13287-020-01707-6

Zhao, X., Yang, Y., Sun, B.-F., Zhao, Y.-L., and Yang, Y.-G. (2014). FTO and Obesity: Mechanisms of Association. *Curr. Diab Rep.* 14 (5), 486. doi:10.1007/s11892-014-0486-0

Zheng, G., Dahl, J. A., Niu, Y., Fedorcsak, P., Huang, C.-M., Li, C. J., et al. (2013). ALKBH5 Is a Mammalian RNA Demethylase that Impacts RNA Metabolism and Mouse Fertility. *Mol. Cel* 49 (1), 18–29. doi:10.1016/j.molcel.2012.10.015

Zheng, W., Ding, B., Li, X., Liu, D., Yokota, H., and Zhang, P. (2020). Knee Loading Repairs Osteoporotic Osteoarthritis by Relieving Abnormal Remodeling of Subchondral Bone via Wnt/β-catenin Signaling. *FASEB j.* 34, 3399–3412. doi:10.1096/fj.201902117R

Conflict of Interest: The authors declare that the research was conducted in the absence of any commercial or financial relationships that could be construed as a potential conflict of interest.

Publisher's Note: All claims expressed in this article are solely those of the authors and do not necessarily represent those of their affiliated organizations, or those of the publisher, the editors and the reviewers. Any product that may be evaluated in this article, or claim that may be made by its manufacturer, is not guaranteed or endorsed by the publisher.

frontiers in Cell and Developmental Biology

REVIEW
published: 21 January 2022
doi: 10.3389/fcell.2022.808303

Mechanical Stimulation on Mesenchymal Stem Cells and Surrounding Microenvironments in Bone Regeneration: Regulations and Applications

Yuyang Sun[1†], Ben Wan[1,2†], Renxian Wang[1], Bowen Zhang[1], Peng Luo[1], Diaodiao Wang[3], Jing-Jun Nie[1], Dafu Chen[1]* and Xinbao Wu[1]*

[1]*Laboratory of Bone Tissue Engineering, Beijing Laboratory of Biomedical Materials, Beijing Research Institute of Traumatology and Orthopaedics, Beijing Jishuitan Hospital, Beijing, China,* [2]*Department of Oral and Maxillofacial Surgery/Pathology, Amsterdam UMC and Academic Center for Dentistry Amsterdam (ACTA), Vrije Universiteit Amsterdam (VU), Amsterdam Movement Science (AMS), Amsterdam, Netherlands,* [3]*Department of Joint Surgery, Peking University Ninth School of Clinical Medicine, Beijing Shijitan Hospital, Capital Medical University, Beijing, China*

OPEN ACCESS

Edited by:
Lifang Hu,
Northwestern Polytechnical University, China

Reviewed by:
Janak L. Pathak,
Guangzhou Medical University, China
Xuehui Zhang,
Peking University Hospital of Stomatology, China
Kelvin Yeung,
The University of Hong Kong, Hong Kong SAR, China

***Correspondence:**
Jing-Jun Nie
niejingjun_jst@126.com
Dafu Chen
chendafujst@126.com

†These authors share first authorship

Specialty section:
This article was submitted to Morphogenesis and Patterning, a section of the journal Frontiers in Cell and Developmental Biology

Received: *03 November 2021*
Accepted: *03 January 2022*
Published: *21 January 2022*

Citation:
Sun Y, Wan B, Wang R, Zhang B, Luo P, Wang D, Nie J-J Chen D and Wu X (2022) Mechanical Stimulation on Mesenchymal Stem Cells and Surrounding Microenvironments in Bone Regeneration: Regulations and Applications. Front. Cell Dev. Biol. 10:808303. doi: 10.3389/fcell.2022.808303

Treatment of bone defects remains a challenge in the clinic. Artificial bone grafts are the most promising alternative to autologous bone grafting. However, one of the limiting factors of artificial bone grafts is the limited means of regulating stem cell differentiation during bone regeneration. As a weight-bearing organ, bone is in a continuous mechanical environment. External mechanical force, a type of biophysical stimulation, plays an essential role in bone regeneration. It is generally accepted that osteocytes are mechanosensitive cells in bone. However, recent studies have shown that mesenchymal stem cells (MSCs) can also respond to mechanical signals. This article reviews the mechanotransduction mechanisms of MSCs, the regulation of mechanical stimulation on microenvironments surrounding MSCs by modulating the immune response, angiogenesis and osteogenesis, and the application of mechanical stimulation of MSCs in bone regeneration. The review provides a deep and extensive understanding of mechanical stimulation mechanisms, and prospects feasible designs of biomaterials for bone regeneration and the potential clinical applications of mechanical stimulation.

Keywords: mechanical stimulations, mesenchymal stem cells, bone regeneration, mechanotransduction, immunomicroenvironment, angiogenesis

1 INTRODUCTION

Bone has extraordinary healing potential. However, approximately 5–10% of fractures cause fracture nonunion, partly because of large segmental bone defects (Holmes, 2017). Autologous transplantation of bone, though considered as a typical strategy for bone defect treatment, has shortages of limited autografts and donor-site morbidity, while the allogeneic bone graft is constrained by immune rejection (Hunziker, 2002). Therefore, tissue-engineered bone is a promising alternative to autologous bone grafting in the future. Although stem cell therapy is widely used in the bone regeneration field, the accurate regulation of stem cells remains a significant

challenge. Traditional methods induce stem cells to the ontogenetic lineage by delivering biochemical signaling molecules such as growth factors. However, the difficulties in maintaining physiological concentration gradients and controlling the release of growth factors temporally and spatially have not yet been resolved. Therefore, regulating the differentiation of stem cells through physical means (such as mechanical stimulation) deserves further study.

Organs of the locomotor system undertake continuous mechanical loading, including compression on the bone, the stretch on muscles, and the fluid shear stress on blood vessels. Mechanical stimulation with different amplitudes, modalities, and durations plays an essential role in cell growth and differentiation, providing the possibility to regulate the lineage commitment of stem cells (Horner et al., 2019; McDermott et al., 2019; Ruehle et al., 2020). Mechanobiology is an emerging field specializing in the cellular response to mechanical cues, including the reception of mechanical signals and transduction of extracellular mechanical signals into intracellular biological signals (Fu et al., 2020). Cells can respond to pericellular mechanical stimulation from external mechanical stimulation and the properties of extracellular matrix (ECM). The process that cells convert exogenous mechanical signals into biochemical signals is called mechanical transduction (Dewey et al., 1981). Superficial mechanoreceptors of cells sense the mechanical cues, which are subsequently transmitted to the nucleus *via* the actin skeleton or chemical pathways. The nucleus responds to these signals by upregulating or downregulating the expression of genes related to mechanical stimulation (Kirby and Lammerding, 2018).

Mesenchymal stem cells (MSCs) are pluripotent cells that originate from intermediate mesoderm. MSCs have the potential to differentiate into lineages, including osteoblasts, adipocytes, chondrocytes, and myocytes. In the skeleton system, MSCs reside in bone marrow and periosteum. As one of the main functional cells in bone regeneration, MSCs enhance the bone healing process through cell-cell contact and secretion of growth factors such as BMP and VEGF (Charoenpanich et al., 2014; Schreivogel et al., 2019). Endochondral ossification is the bone regeneration mechanism involved in most fractures (Einhorn and Gerstenfeld, 2015). The bone defect first triggers an inflammatory process, which leads to the recruitment of mesenchymal stem cells (MSCs) to the bone defect by inflammatory factors. These MSCs then differentiate into cartilage that gradually ossifies with the growth of blood vessels into the cartilage model. Thus, MSCs play a crucial role in bone regeneration. MSCs regulate the immuno-microenvironment by interacting with macrophages and regulating blood vessel formation by secreting angiogenic growth factors. This process involves interacting cells, including MSCs, macrophages, and vascular endothelial cells, as well as extracellular matrix molecules and cytokines, all of which constitute the MSC niche that is of great significance in regulating bone regeneration (Moore and Lemischka, 2006; Kuhn and Tuan, 2010; Vafaei et al., 2017).

Previous studies have indicated that MSC differentiation was determined by the MSC niches (Chen et al., 2020). Moreover, recent studies have shown that MSC differentiation was also affected by mechanical stimulation (Ravichandran et al., 2017). A thorough understanding of the effect of mechanical stimulation on MSC niches in bone regeneration is of great value for establishing an *in vitro* model of bone regeneration and rehabilitation training of patients after fracture surgery. Therefore, this article reviews the intracellular mechanisms by which MSCs sense and respond to mechanical stimulation, the effect of mechanical stimulation on regulating MSC surrounding microenvironments by modulating the immune, angiogenic, and osteogenic microenvironments, and the applications of mechanical stimulation in bone regeneration.

2 MECHANISM OF MESENCHYMAL STEM CELL SENSING AND RESPONDING TO MECHANICAL STIMULATION

Mechanical stimulation plays an essential role in various physiological processes of bone. Wolff's Law demonstrates that mechanical stimulation remolds the morphology of bone by the force line direction (Lanyon and Baggott, 1976; Woo et al., 1981). Bone mass increases in high stress regions and decreases in low stress regions. Wolff's Law indicates that bone can sense and respond to the external mechanical loading and adapt to it by regulating bone metabolism. The lack of loading leads to disuse osteoporosis in the clinic, which explains why bedridden patients suffer from bone loss (Qi et al., 2012). Several types of bone cells can sense mechanical stimulation, including bone marrow MSCs and osteocytes. These cells function in different physiological processes and respond to external mechanical stimuli.

2.1 Mechanism of Mesenchymal Stem Cells Sensing Mechanical Stimulation

2.1.1 Physiological Basis

It is widely accepted that osteocytes are mechanosensitive cells that respond to mechanical stimulation (Yan et al., 2020). However, recent studies proves that external mechanical stimulation regulates bone marrow mesenchymal stem cells (BMSCs) toward osteogenic lineage which is independent of osteocytes regulation (Schreivogel et al., 2019).

The lacunar-canalicular system (LCS) is filled with interstitial fluid (Timmins and Wall, 1977). Intramedullary pressurization alteration and deformation of bone matrix generate interstitial fluid flow (Kwon et al., 2010; Price et al., 2011; Ciani et al., 2014). Therefore, mechanical loading leads to variation in intramedullary pressurization, which results in shear stress generation. Shear stress applies to osteocytes in LCS and MSCs in the bone marrow. Fluid shear stress is the general form of the force applied to MSCs in the bone marrow under physiological conditions (Gurkan and Akkus, 2008). The form of the force applied to MSCs in the periosteum is mainly caused by micro-deformation of bone generated by external mechanical stimuli such as stretching and compression. MSCs respond to the stimulation indirectly by sensing the micro-deformation of the extracellular matrix. Therefore, when investigating the mechanism of the

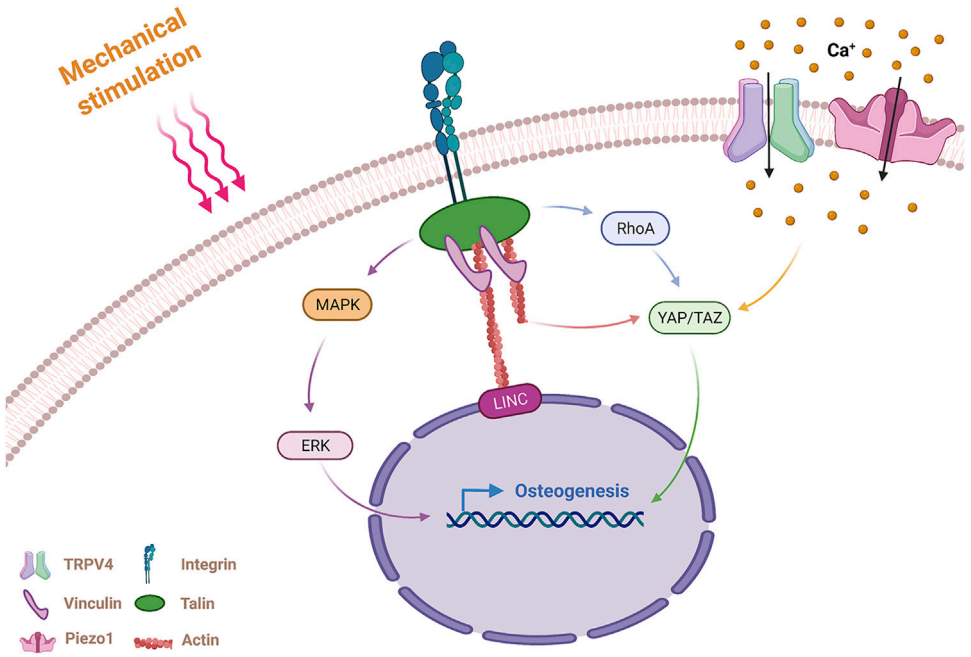

FIGURE 1 | Mechanism of MSCs sensing and responding to mechanical stimulation. MSCs sense external mechanical stimulation via integrins and mechanosensitive ion channels and transmit the mechanical signals *via* actin stress fibers and molecular pathways. Integrins activate RhoA, MAPK pathways, and actin fibers by FAs (including vinculin and talin) in response to mechanical stimulation. MAPK promotes osteogenesis through nuclear localization of ERK. The RhoA pathway and actin fibers promote osteogenesis through nuclear localization of YAP/TAZ. The mechanosensitive ion channels TRPV4 and Piezo1 generate an intracellular Ca^{2+} influx after sensing mechanical stimulation, and Piezo1 promote osteogenic differentiation through nuclear localization of YAP/TAZ. MSCs, mesenchymal stem cells; RhoA, Ras homolog gene family, member A; MAPK, Mitogen-activated protein kinases; FA, focal adhesion; ERK, extracellular signal-regulated kinase; YAP/TAZ, Yes-associated protein/transcriptional coactivator with PDZ-binding motif; TRPV4, transient receptor potential vanilloid 4.

mechanical loading effect on MSC differentiation, the function of both the direct and indirect force ought to be considered.

2.1.2 Mechanosensors

The cellular response to external mechanical stimuli involves two processes: mechanosensing and mechanotransduction (Argentati et al., 2019). Mechanosensing is the process by which cells sense physical signals from the extracellular environment by mechanoreceptors. Cells then transduce the physical signals into biochemical signals. This process results in differentiation of the cells to specific lineages and is known as mechanotransduction (Delaine-Smith and Reilly, 2011). Several typical mechanoreceptors present on the membrane are introduced here, including integrins, mechanosensitive ion channels and primary cilia (**Figure 1**).

2.1.2.1 Integrin

Integrins, widely recognized mechanical sensors, are transmembrane proteins that can take up physical signals from the ECM (Kechagia et al., 2019). Integrins mediate the adhesion and transmit the mechanical signal between cells and the ECM. One end of the integrin connects to the ligands (proteins of the extracellular matrix), and the other end connects to the intracellular actin fiber via adaptor proteins. Actin stress fiber senses mechanical signals originating from the ECM by the degree of its contraction. The link containing ECM, integrins, adaptor proteins and actin transmitting mechanical cues is known as clutches. External mechanical signals exert mechanical force on actin that tunes the integrins' alignment and reorders the actin cytoskeleton (Kechagia et al., 2019). The interactions between the ECM and the cytoskeleton alter the cells lineage and lead to remodeling of the ECM (Loebel et al., 2019).

Cells perceive external stimulation from the ECM and transmit mechanical signals to the nucleus to regulate gene expression. The adapter proteins that connect integrins and actin fibers include focal adhesion (FA) molecules, which are mainly composed of vinculin, paxillin, talin and focal adhesion kinase (FAK). The Rho and MAPK signaling pathways activated by FA lead to nuclear localization of the transcription factors Yes-associated protein/transcriptional coactivator with PDZ-binding motif (YAP/TAZ) and ERK, respectively (Nardone et al., 2017). In addition to the means of transmitting mechanical signals by chemical signals, the nuclear envelope and Linker of Nucleoskeleton and Cytoskeleton (LINC) complex also play essential roles in mechanotransduction (Bouzid et al., 2019).

2.1.2.2 Mechanosensitive Ion Channels

Studies have shown that mechanical stimulation partly impacted the concentration of intracellular calcium ions. Intracellular

calcium ions of pre-osteoblasts rapidly increase under stimulation by fluid shear stress, possibly as a result of the activation of mechanically sensitive calcium channels on cells (Chen et al., 2000). Osteoblasts contain several calcium channels, including transient receptor potential vanilloid 4 (TRPV4), multimeric L-type and T-type voltage-gated calcium channels (VSCC), and the recently discovered mechanically sensitive ion channel Piezo1. Both TRPV4 and Piezo1 are mechanically sensitive ion channels.

Ten years ago, Bertrand reported that the Piezo1 channel was a mechanically activating cation channel (Coste et al., 2010). Later, it was found that Piezo1 sensed and transduced mechanical stimuli in various cells, including endothelial cells, neural stem cells and chondrocytes (Lee et al., 2014; Li et al., 2014; Pathak et al., 2014). Piezo1 also plays an important role in the response of skeleton cells to mechanical stimulation, and governs bone homeostasis by reacting to mechanical signals. Sugimoto et al. (2017) proved that hydrostatic pressure (HP) promoted bone formation and osteogenic differentiation of MSCs through the mechanically sensitive ion channel Piezo1, which was related to the expression of bone morphogenetic protein 2 (BMP-2). Li X. et al. (2019) discovered that bone cells could also sense and respond to changes in fluid shear stress via Piezo1. After fluid shear stress is applied to bone cells, the mechanically sensitive ion channel Piezo1 partially activates YAP1 and TAZ to increase the expression of Wnt1 and regulate bone formation. In addition to investigating the mechanism of Piezo1 activation by various types of mechanical stimuli, Wang et al. recently investigated the function of Piezo1 in regulating the bone remodeling process. In this study, conditional knockout of the Piezo1 gene was found to reduce the cortical thickness and the trabecular bone volume in mice. Further studies have explained the role of Piezo1 in osteoblasts during bone remodeling. The results indicated that Piezo1 regulated osteoclast differentiation by regulating the expression of YAP type II and type IV collagen (Wang et al., 2020). The results showed that Piezo1 played an important role in maintaining bone homeostasis by regulating the crosstalk between osteoblasts and osteoclasts under mechanical stimulation conditions.

TRPV4, another mechanically sensitive calcium ion channel in MSCs, primarily localizes in the high strain regions (especially the primary cilia). TRPV4's principal function is to promote early bone formation under the stimulation of oscillatory fluid shear stress (Hu et al., 2017; Corrigan et al., 2018). Some studies have compared the roles of the two mechanically sensitive ion channels, TRPV4 and Piezo1, in sensing mechanical stimulation. Yoneda et al. found that when osteoblasts were stimulated by short term shear stress (5 s), the ion channel TRPV4 rather than Piezo1 mediated the sensing process to the mechanical stimulus (Yoneda et al., 2019). Another study of TRPV4 and Piezo1 channels in chondrocytes showed that TRPV4 channels mediated strain at the physiologic level, and Piezo2 mediated strain at the injurious level (Du G. et al., 2020). These results indicated that the magnitude and duration of shear stress required to activate the Piezo1 and TRPV4 channels of the osteoblast lineage are likely different. A recent study also showed that the activation of TRPV4 was regulated by the activation of Piezo1 in vascular endothelial cells (Swain and Liddle, 2021). However, a comprehensive comparison of the relationships between the mechanically sensitive ion channels TRPV4 and Piezo1 in osteoblast lineage has not yet been conducted.

2.1.2.3 Primary Cilium

In addition to the above two mechanoreceptors, primary cilium plays an essential role in sensing and responding to fluid shear stress in MSCs. Primary cilium was first identified and observed in osteocytes more than 40 years ago (Federman and Nichols, 1974). A laboratory in Sweden stimulated human MSCs (hMSCs) with oscillatory fluid flow (OFF) *in vitro* to simulate the fluid shear stress in the physiological environment. The results showed that OFF promoted the proliferation of hMSCs, increased the expression of osteogenic genes, and demonstrated that primary cilia mediated the response of hMSCs to fluid shear stress stimulation (Hoey et al., 2012). This laboratory then found that the mechanically reactive G protein-coupled receptor (GPCR) GRP161, located on the primary cilium, activated adenylate cyclase 6 (AC6) to respond to stimulation generated by fluid shear stress. AC6 then activates the cAMP signal, which increases the expression of PTCH1 and GLI1 in the hedgehog pathway via upregulating the expression of osteogenic genes (Johnson et al., 2021). Some ion channels, including TRPV4, are also widely localized in primary cilia, mediating fluid shear stress-induced calcium signaling and osteogenic process of MSCs (Hu et al., 2017; Corrigan et al., 2018).

2.2 Molecular Mechanism of Mesenchymal Stem Cells Responding to Different Mechanical Stimulations

2.2.1 Stretching

Previous studies have shown that mechanical stretching could promote the osteogenic differentiation of mesenchymal stem cells of multiple origins through several molecular pathways, such as BMSCs and adipose-derived stem cells (Wang et al., 2017; Fang et al., 2019). Tensile strain stimulation promotes MSC osteogenesis differentiation and inhibits differentiation toward adipogenesis mainly through the Smad signaling pathway (Li R. et al., 2015; Grier et al., 2017). The Hedgehog (Hh) signaling pathway plays an essential role in cyclic mechanical stretch (CMS). Wang et al. found that DNA methyltransferase 3b (Dnmt3b) inhibited the expression of Hedgehog signaling by binding to the Shh gene promoter to downregulate the sensitivity of MSCs to stretch stimulation (Wang et al., 2017). Jiali Tan et al. found that the osteogenic effect of mechanical stretch on MSCs was correlated with donor age. The osteogenic effect of MSCs responding to the mechanical stretch in young rats was higher than that in adult rats. Additionally, stretch also resulted in more production of ROS inhibited osteogenesis, in MSCs of adult rats than in young rats (Tan et al., 2015). However, Chen et al. suggested that appropriate levels of mechanical stretching not only promoted osteogenesis of BMSCs but also reduced ROS levels in BMSCs and induced antioxidant responses by activating the AMPK-SIRT1 pathway (Chen et al., 2018).

Stretch stimulation can also regulate the lineage differentiation of MSCs by modulating the expression of miRNA that regulating pathway molecules. Liu et al. identified differentially expressed miRNAs after stretch stimulation and found that miR-503-5p was downregulated. Therefore, it was concluded that miR-503-5p was a mechanosensitive miRNA, and miR-503-5p downregulation could promote stretch stimulation-induced osteogenic differentiation of BMSCs (Liu et al., 2017). Li J.'s (2015) work found that miR-154-5p negatively regulated the Wnt/PCP (Rhoa-Rock) pathway to induce osteogenesis of ADSCs (Li J. et al., 2015).

2.2.2 Compression

Dynamic compression can promote the differentiation and mineralization of MSCs toward osteogenesis both *in vitro* and *in vivo*, which partially replaces the role of osteogenic induction medium (Duty et al., 2007; Baas et al., 2010; Sittichokechaiwut et al., 2010; Ravichandran et al., 2017). It has been shown that dynamic compression did not directly regulate the expression of transcription factors such as RUNX2, but rather promoted MSC osteogenic differentiation in an autocrine manner by increasing BMP expression (Schreivogel et al., 2019).

Previous studies have also indicated that compression could promote both osteogenesis and chondrogenesis of MSCs (Cao et al., 2019). However, the mechanism underlying the effect of compression stimulus on MSCs and the means of controlling the differentiation of MSCs has not yet been fully explored. Possible factors include the magnitude of compression, the induction mode, and pathway activation. A previous study by Efstathios suggested that the differentiation of MSCs was related to the magnitude of compression. The study found that hMSCs differentiated toward osteogenesis under 10% dynamic compression but toward chondrogenesis under 15% (Michalopoulos et al., 2012). Moreover, Christopher et al. found that osteogenic differentiation decreased with an increase in the compression magnitude in osteogenic induction medium (Horner et al., 2018). However, another study suggested that the compression-induced MSC differentiation toward chondrogenic or osteogenic lineages depended on the activation of the ERK1/2 pathway (Pelaez et al., 2012). Dynamic compression induces chondrogenic differentiation of MSCs under normal conditions and osteogenesis differentiation when the ERK1/2 pathway is inhibited.

2.2.3 Fluid Shear Stress

MSCS residing in the periosteum and bone marrow are exposed to fluid shear stress generated by mechanical stimulation-induced deformation. Therefore, the osteogenic differentiation of MSCs induced by mechanical stimulation is also related to the fluid shear stress caused by cyclical hydrostatic pressure (CHP) *in vivo*. The ability of shear stress to promote osteogenesis of MSCs has been widely recognized, and shear stress can promote MSC osteogenesis in the absence of a chemical induction medium (Yourek et al., 2010; Yue et al., 2019). MSCs mediate fluid shear stress through primary cilia and mechanosensitive ion channels such as TRPV4 and Piezo1 (Hu et al., 2017; Johnson et al., 2018; Li X. et al., 2019). Although fluid shear stress is recognized as one of the biophysical means to promote osteogenesis, the application of shear force in bone tissue engineering requires further exploration. As Zhang et al. (2012) found in their study, MSCs from different patients showed inconsistent responses to shear stress stimulation, which may be due to the high heterogeneity of the samples. Therefore, future exploration should target at more specific populations, such as the response of osteoporotic populations MSCs to shear force.

2.2.4 Vibration

Although vibration is not a sort of mechanical stimulation in physiological condition, a great number of studies have been conducted on the vibration in osteogenesis (Chen et al., 2015; Pongkitwitoon et al., 2016). As is convenient to be applied on tissue, vibration has been used in osteoporosis treatment (Jepsen et al., 2019). Vibration stimulates skeleton with the motion of the body. Vibrations of the appropriate magnitude and frequency can trigger anabolic responses in the bones (Minematsu et al., 2019). Low magnitude vibration (LMV) is widely accepted by doctors and patients in clinic as a measure of exercise therapy based on the vibration (Wysocki et al., 2011). Thus, it is necessary to explore the mechanism of vibration in bone regeneration.

Vibration regulates and coordinates MSC bone resorption and formation via multiple signaling pathways. Previous studies have shown that vibration regulated the Wnt signaling pathway to promote MSC osteogenesis (Gao et al., 2017). Chen et al. (2016) demonstrated that vibration increased the adhesion and osteogenesis of MSCs on HA-coated surfaces by activating the Wnt/β-catenin signaling pathway. They supposed that the vibration may provide a means to promote the osseointegration of bone implants. Vibration enhances β-catenin function through inhibiting the β-catenin destruction complex element GSK3β (glycogen synthase kinase 3β), which promotes the Linker of Cytoskeleton and Nucleoskeleton (LINC) function (Uzer et al., 2018). Another study found that the expression of miR-335-5p was upregulated *via* vibration. miR-335-5p induces osteogenic differentiation by suppressing the expression of Dickkopf-related protein 1, a Wnt signaling inhibitor (Zhao et al., 2019). In addition to the Wnt pathway, vibration can also regulate the bone formation process by up-regulating the expression of estrogen receptor α (Li H. et al., 2019). Estrogen receptor α is known to be a mediator in bone remodeling and is significant in estrogen-deprived osteoporotic (Jessop et al., 2004). ERK1/2 pathway and p38 MAPK signaling have also been shown to play an essential role in vibration-induced osteogenesis of MSCs (Zhou et al., 2011; Lu et al., 2018). Recent research illustrated the effect of vibration on the YAP, a transcription factor that was significant to MSC osteogenesis. Thompson et al. (2020) discovered that the application of vibration increased the YAP nuclear shuttling and restored the basal nuclear levels of YAP, which led to MSC osteogenesis. In addition to differentiation, MSC migration is also regulated by

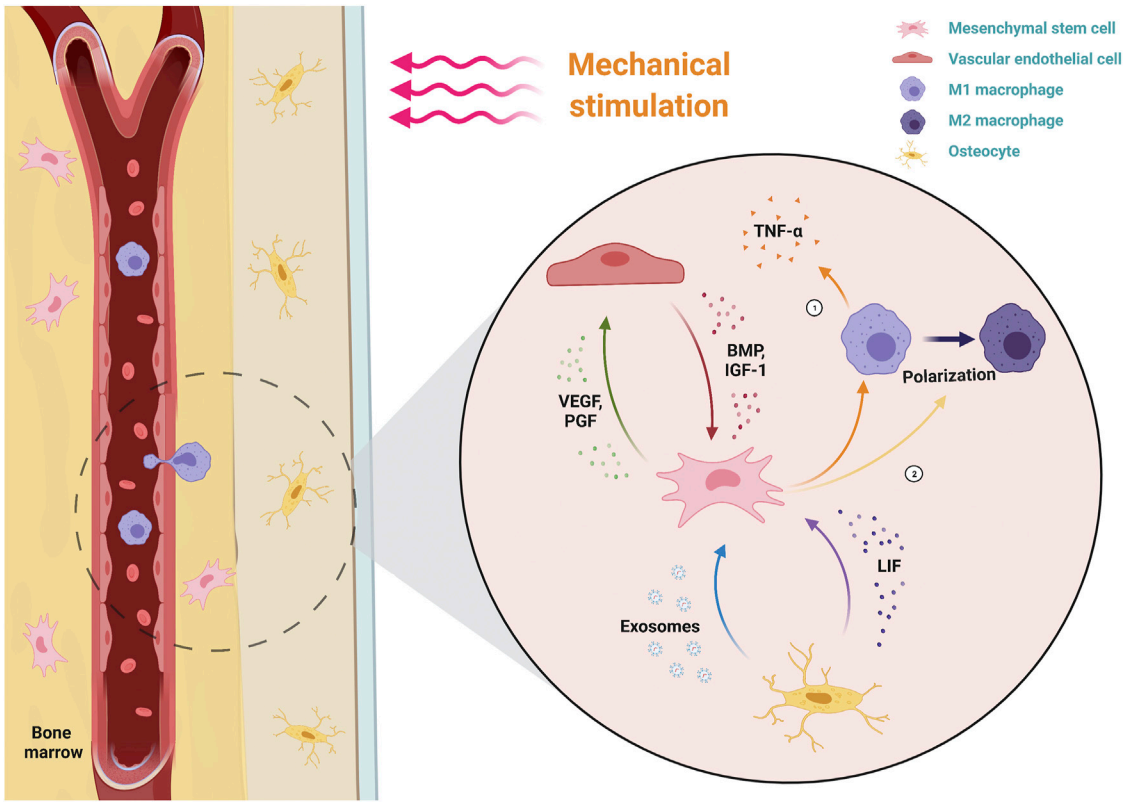

FIGURE 2 | Dynamic interactions of MSCs with their microenvironment under mechanical stimulation. MSCs perceive the mechanical stimulation applied to the bone, which downregulates the inflammatory response by decreasing macrophage secretion of pro-inflammatory TNF-α and promoting the polarization of M1 macrophages (pro-inflammatory type) to M2 macrophages (anti-inflammatory type). Simultaneously, MSCs promote VEC angiogenesis by secreting angiogenic factors (VEGF, PGF). Osteogenic factors (BMP, IGF-1) secreted by mechanical activated-VECs, as well as LIF and exosomes secreted by mechanical activated-osteocytes, together promote the osteogenic differentiation of MSCs. TNF-α, tumor necrosis factor alpha; VECs, vascular endothelial cells; VEGF, vascular endothelial growth factor; PlGF, placental growth factor; BMP, bone morphogenetic protein; IGF-1, insulin-like growth factor 1; LIF, leukemia inhibitory factor.

vibration. Wei et al. (2016) discovered that the SDF-1/CXCR4 pathway enhanced the MSC migration in response to the vibration which promoted fracture healing.

2.2.5 Low Intensity Pulsed Ultrasound

Besides stretching, compression, fluid shear stress and vibration, LIPUS is also found to be a type of force to promote bone formation (Uddin and Qin, 2013). Gao et al. (2016) discussed the distinct pathways of MSCs from different sources in LIPUS-stimulated proliferation. LIPUS increased all MSC types proliferation. ERK1/2 was activated in dental pulp stem cells (DPSCs) and JNK MAPK signaling was activated in BMSCs after LIPUS application. However, in PDLSCs, JNK MAPK signaling was stimulated immediately after the application of LIPUS and p-p38 MAPK was increased subsequently. In spite of proliferation, LIPUS also promotes the MSCs migration in bone healing possibly through activating the SDF-1/CXCR4 signaling (Wei et al., 2014). In addition to the proliferation and migration, several studies illustrated that LIPUS led to a better osteointegration (Hui et al., 2011). The possibly osteogenic differentiation mechanism is activating of Rho-associated kinase-Cot/Tpl2-MEK-ERK signaling pathway (Kusuyama et al., 2014). However, the effectiveness of LIPUS in osteogenesis is open to debate. A recent study suggested that according to multiple randomized controlled trials in clinic, LIPUS possibly has no effect on radiographic bone healing (Schandelmaier et al., 2017).

3 MECHANICAL STIMULATION REGULATES MESENCHYMAL STEM CELL SURROUNDING MICROENVIRONMENTS IN BONE REGENERATION

Mscniches provide a microenvironment to support MSC self-renewal and multi-lineage differentiation. Bone regeneration involves the inflammatory responses of immune cells, blood vessel formation of endothelial cells and osteogenic process of MSCs. Thus, intercellular communication within the niche is crucial for bone regeneration and investigating the crosstalk between MSCs and other cells, including macrophages,

vascular endothelial cells and osteocytes. As the crucial components of bone regeneration, blood vessel formation and inflammation are regulated by mechanical stimulation (Charoenpanich et al., 2014). Thus, it is important to ascertain the role of mechanical stimulation in the crosstalk of the osteogenic process (**Figure 2**).

3.1 Mechanical Stimulation Regulates the Immunoenvironment by Regulating the Crosstalk Between Mesenchymal Stem Cells and Macrophages

Some immune-inflammatory diseases, such as arthritis, suggest a correlation between mechanical force and the inflammatory response. Arthritis is characterized by inflammation that localized to the joints (such as the knee joint) when exposed to prolonged mechanical force. Therefore, mechanical force may be a factor that determines the transition of inflammation from systemic autoimmunity to local inflammation. According to Cambré's research, MSCs in the mechanosensitive region of joints could sense mechanical stimulation and convert mechanical signals into chemical signals to trigger local inflammation and bone destruction, which ultimately led to the occurrence of arthritis (Cambre et al., 2018). Therefore, mechanical stimulation plays an essential role in inflammatory response (Hao et al., 2015).

Bone regeneration involves multiple stages and cell interactions. The formation of fracture hematoma and the subsequent acute inflammatory phase are key steps to determine the success of bone regeneration. The acute inflammatory phase begins with the activation of neutrophils that secrete inflammatory factors and chemokines to recruit monocytes and macrophages (Xing et al., 2010). In addition to cleaning up the necrotic tissue, macrophages secrete inflammatory cytokines and chemokines (such as TNF-α, IL-1β, IL-6, and CCL2) to recruit MSCs. Subsequently, MSC-rich granulation tissue replaces the hematoma. Immediately after, MSCs are stimulated by various factors in the environment to trigger osteogenic differentiation by either endochondral ossification or intramembranous ossification. Therefore, it is evident that an appropriate acute inflammatory phase duration is important for bone regeneration. The interactions between MSCs and macrophages dynamically regulate this phase. Macrophages have two phenotypes. The first is classically activated M1 macrophages, which function in initiating and sustaining inflammation, and the second is alternatively activated M2 macrophages, which function in resolving inflammation. The transformation of macrophages from M1 to M2 is known as macrophage polarization (Pugin et al., 1998). The main method of anti-inflammation in bone regeneration at this stage is the early polarization of pro-inflammatory M1 macrophages to anti-inflammatory M2 macrophages, which serves to promote the resolution of inflammation and the osteogenesis process.

Following the occurrence of a fracture, MSCs are mobilized into the peripheral blood by transforming growth factor-beta (TGF-β) (Wan et al., 2012). MSCs are exposed to fluid shear stresses, one of which is wall shear stress (WSS). WSS can stimulate MSCs to produce antioxidant and anti-inflammatory mediators. Additionally, the application of WSS to MSCs facilitates the recruitment of chemokines, including prostaglandin E2 (PEG2) and cyclooxygenase-2 (COX2), to inhibit the synthesis of tumor necrosis factor α (TNF-α) generated by immune cells and the inflammatory response (Diaz et al., 2017). The mechanism by which WSS stimulates MSCs to produce inflammatory mediators may be related to the FAK-COX2 signaling pathway. Lee et al.'s (2017) study showed that WSS could promote Ca^{2+} release and activate the Akt, MAPK and FAK signaling pathways of MSCs. When inhibited the above factors respectively, only FAK disrupted the induction of COX2 and decreased the production of MSC inflammatory mediators. Thus, the FAK-COX2 signaling pathway is significant for MSCs to respond to mechanical stimulation for immunomodulatory functions. In addition to shear stress, dynamic compression regulates the crosstalk between MSCs and macrophages. Zhang et al. (2021) developed an extracellular matrix-based hydroxyapatite scaffold fabricated by freeze-drying the ECM of compression-stimulated MSCs. This biofabricated scaffold could accelerate the polarization of macrophages from the pro-inflammatory M1 phenotype to the anti-inflammatory M2 phenotype to promote bone regeneration. These findings suggested that compression could promote the secretion of anti-inflammatory mediators in MSCs. However, recent studies have found that MSCs maintained their physiological levels through TNF-α endocytosis. Cyclic stretching promoted the proliferation and osteogenic differentiation of MSCs by TNFα endocytosis, which downregulated TNFα secretion in MSCs, rather than directly downregulating TNFα gene expression (Yu et al., 2021). Additionally, mechanical stimulation of adipose tissue modulates the anti-inflammatory properties of human adipose-derived stem cells (hADSCs) in adipose tissue. Carelli et al. compared the anti-inflammatory properties of hADSCs in mechanically stimulated adipose tissue and the control group. It was found that the anti-inflammatory effect of mechanical stimulated-hADSCs was superior to that of the control group hADSCs (Carelli et al., 2018). However, other studies have found that mechanical stimulation could promote inflammation and osteogenesis simultaneously, likely as a result of the MSC autocrine regulation of inflammatory factor secretion (Sumanasinghe et al., 2009; He et al., 2020).

Most studies have discussed the response of MSCs to mechanical stimulation during osteogenesis. A recent research found that macrophages were also capable of responding to mechanical stimulation (Dong et al., 2021). Mechanical stretch polarizes macrophages into the M2 phenotype that secrets inflammation-related cytokines, including IL10 and TGF-β, to regulate the local inflammatory microenvironment. Mechanical stimulation activates the YAP/BMP2 axis in macrophages to increase the expression of BMP2, which promotes the osteogenesis of MSCs. As an important component of the mechanical transduction pathway, YAP induces the polarization of M2 macrophages *via* Wnt5a and TGFβ1 (Feng et al., 2018). Schoenenberger et al. (2020) found that macrophages, as

mechanosensitive cells, played an essential role in tendon repair. Mechanical stimulation was found to promote the transformation of macrophages to the M2 phenotype and subsequent tissue healing. These results suggested that future consideration might be given to exploring the role of mechanical stimulation in MSC and macrophage co-culture models.

3.2 Mechanical Stimulation Regulates the Angiogenic Microenvironment by Regulating the Crosstalk Between Mesenchymal Stem Cells and Vascular Endothelial Cells

Bone regeneration contains endochondral ossification and intramembranous ossification. Endochondral ossification is the process that stable cartilaginous soft callus first formed, followed by the formation of bone hard callus through vascular ingrowth and ossification centers (Gerstenfeld et al., 2003). The intramembranous osteogenesis process is accomplished by the differentiation of MSCs into osteoblasts at vascular-rich sites and the mineralization of osteoblasts to osteocytes. Thus, vascular formation, which is closely related to the osteogenesis process, is an important part of bone regeneration. During bone regeneration, MSCs and vascular endothelial cells (VECs) communicate with each other through paracrine mediators to promote osteogenesis (Li C.-J. et al., 2015). Mechanical stimulation is one of the biophysical factors that promote osteogenesis, and plays a crucial role in the crosstalk between MSCs and VECs.

Vascular endothelial growth factor (VEGF), a widely known signaling molecule regulating osteogenesis and vascularization, has been identified for its role in mechanical stimulation-induced osteogenesis. Charoenpanich et al. evaluated the effect of stretching on human MSC gene expression by microarray analysis. The results showed that stretching promoted the release of VEGF from human MSCs (Charoenpanich et al., 2014). Moreover, Jiang's team found that stretching-stimulated VEGF secretion of MSCs not only promoted tube formation but also promoted VECs to release growth factors associated with bone formation, such as BMP-2 and IGF-1, which in turn regulated the osteogenesis process of MSCs (Jiang et al., 2018). In addition to stretching, dynamic compression can promote increased VEGF secretion in MSCs. Dynamic compression promotes VEGF secretion by upregulating YAP signaling activity in MSCs (Bandaru et al., 2020). In addition to VEGF, the expression level of placental growth factor (PlGF) in MSCs is related to the magnitude and duration of mechanical stimulation. PlGF has a variety of functions, including promoting osteogenesis and angiogenesis, and plays an essential role in the regulation of osteogenic-angiogenic interactions by mechanical stimulation (McCoy et al., 2013). It has also been found that mechanical stimulation can stimulate H vessel formation and VEGF secretion by downregulating exosomal miR-214-3p from MSCs (Wang et al., 2021).

In addition to the above *in vitro* studies, several *in vivo* experiments have investigated the effects of mechanical stimulation on bone regeneration and vascularization. Some studies have explored the effect of the initial application time of mechanical stimulation on vessel and bone formation. Boerckel et al., 2011 found that the application of mechanical loading in the early stage of bone defects could inhibit the growth of blood vessels into the defect area and lead to the failure of bone regeneration. In contrast, the application of mechanical loading delayed for 4 weeks could promote the reconstruction of blood vessel networks and bone regeneration (Boerckel et al., 2011). This result suggested that the effect of mechanical stimulation on vascularization and bone formation depended on the initial application time. McDermott et al. (2019) speculated that the difference was due to the different origin of the vessel forming at different times. Other studies have explored the effect of the loading application mode on revascularization. Claes et al., 2018 compared the effects of compression, stretching and shear stress on the vessel density in bone regeneration. As a result, the vessel density in the compression group was significantly higher than that in the other two groups, which suggested that compression was more beneficial to the bone regeneration process.

3.3 Mechanical Stimulation Regulates the Osteogenic Microenvironment by Regulating the Crosstalk Between Mesenchymal Stem Cells and Osteocytes

Osteocytes are mechanosensitive cells that reside in the lacunar-canalicular system (LCS) of cortical bone (Timmins and Wall, 1977). Recent studies have found several critical mechanical sensors of osteocytes, such as cilia, integrin, ion channels and G-protein-coupled receptors (Uda et al., 2017). Osteocytes regulate bone remodeling, mainly by sensing fluid shear stress caused by mechanical loading and regulating osteoblast-osteoclast communication (Dallas et al., 2013). As mentioned above, osteocytes play an important role in responding to mechanical stimulation. Osteocytes function as regulators influencing bone loss and formation by modulating osteoblast-osteoclast coupling. Osteocytes are of vital importance in the reconstruction of bone defects (Robling and Bonewald, 2020). Osteocytes regulate bone regeneration in both direct and indirect ways: secreting stimulators and inhibitors that affect osteoblast activity, and modulating osteoclast activity to regulate osteoblast behavior indirectly (Robling and Bonewald, 2020). However, due to limited research methods, the role of the osteocyte response to mechanical stimulation in bone regeneration has not been fully explored.

Osteocytes respond to external mechanical stimulation by secreting soluble factors that regulate MSC gene expression. Specific communications exist between osteoblasts and MSCs under mechanical stimulation conditions. (Hoey et al., 2011) found that conditional medium for mechanical stimulation of osteocytes upregulated osteogenic gene expression in MSCs, while no upregulation was seen in osteoblasts treated with the

TABLE 1 | Applications of mechanical stimulation on MSCs in bone regeneration.

Source of MSC	Force type	Mechanical parameter	Intermittent and continuous loading	Immediate or delayed loading	Dimensionality	Discoveries	References
Mus musculus	Shear stress	1, 2, 5 Pa; 0.5, 1, 2 Hz	Intermittent: 1, 2, 4 h/day	1–3 days	2D	2 Pa and 2 Hz has a superior osteogenic effect	Stavenschi et al. (2017)
Rattus norregicus	Shear stress	1.03, 0.1, 0.01, 0.001 Pa	1) Continuous 2) Intermittent: application 1 h + Intermittent 7 h	40 h	2D	Intermittent loading for 0.01 Pa has a superior osteogenic effect	Dash et al. (2020)
Homo sapiens	Shear stress	0.01 Pa	Continuous	24 h	3D (borosilicate glass capillary tubes)	Loading regime of 0.01Pa has a superior osteogenic effect	Xue and Cartmell, (2020)
Homo sapiens	Shear stress	0.005, 0.011, 0.015 Pa; 3, 6, 9 ml/min	Continuous	24 h	3D (porous cylindrical β-TCP scaffold)	15 mPa has a superior osteogenic effect	Li et al. (2009)
Homo sapiens	Shear stress	0.34 Pa (0.3 ml/min), 0.42 Pa (4 ml/min)	1) Continuous: 0.42 Pa (4 ml/min) 2) Intermittent: 0.42 Pa (4 ml/min) 1 h + 0.34 Pa (0.3 ml/min) 11 h	4 h	3D [porous poly lactic co-glycol acid (PLGA)]	Intermittent FSS has a superior osteogenic effect	Liu et al. (2012)
Mus musculus	Tensile	10% Elongation; 0.5 Hz	Intermittent: 12 h/day	48–72 h	2D	CMS has a superior osteogenic effect	Wang et al. (2017)
Homo sapiens	Tensile	10% Elongation; 0.1%/s	Intermittent: 2 h/day	—	3D (PCL nanofibrous scaffolds)	10% Elongation enhances long-term ECM deposition and differentiation	Nathan et al. (2011)
Bos taurus	Tensile	1) Continuous: 10% elongation; 2.5%/min 2) Intermittent: 3% elongation; 1 Hz	1) Continuous: 2 h 2) Intermittent: 6 h/day	48 h	3D (PCL nanofibrous scaffolds)	Elongation stiffened and condensed MSC nuclei	Heo et al. (2016)
Homo sapiens	Tensile	10% Elongation; 0.5 Hz	Continuous	—	2D	10% Elongation has a superior osteogenic effect Tensile inhibited adipogenesis, but promoted osteogenesis	Fang et al. (2019)
Homo sapiens	Compression	0.22% strain; 1 Hz	Intermittent: 4 h/day	24 h	3D (PCL-TCP scaffold)	0.22% compressive strain has a superior osteogenic effect	Ravichandran et al. (2017)
Homo sapiens	Compression	1) 10% Elongation; 1 Hz 2) 15% strain; 1 Hz	Intermittent: 4 h/day	-	3D (collagen–alginate scaffolds)	10% compressive strain has a superior osteogenic effect 15% cyclic compressive strain has a superior chondrogenic effect	Michalopoulos et al. (2012)
Oryctolagus cuniculus	Compression	10% strain; 1 Hz	Intermittent: 2 h/day	-	3D (collagen scaffold)	0.22% compressive strain has a superior chondrogenic effect	Cao et al. (2019)
Homo sapiens	Compression	0.06–0.94 mPa; 1 Hz	Intermittent: 15 min/day	48 h	3D (hydroxyapatite scaffolds)	0.06–0.94 mPa compressive strain has a superior chondrogenic effect. And can modulating the inflammatory microenvironment	Zhang et al. (2021)

same. This suggested that mechanical stimulation played a vital role in the crosstalk between osteocytes and MSCs. Several studies have explored the paracrine mechanism by which osteocytes regulated MSC osteogenesis in response to mechanical stimulation. Du J. et al. (2020) suggested that mechanical regulating osteoblast-osteoclast coupling by promoting osteocyte secretion of leukemia inhibitory factor (LIF). Extracellular vesicles (EVs), as specific components of cell-cell

and cell-matrix communication, also play an important role in osteocyte and MSC interactions under mechanical stimulation. Eichholz et al. (2020) comprehensively characterized the proteins secreted by osteoblasts after fluid shear stress through proteomics and found that proteins associated with EVs were significantly overexpressed. Moreover, culturing MSCs with the collected EVs resulted in MSC osteogenic differentiation, suggesting that mechanical stimulation promotes osteocytes to modulate MSC behavior *via* EVs. Peiying Lv's team found that exosomes produced by osteocytes following mechanical stimulation also promoted the osteogenic differentiation of human periodontal ligament stem cells (PDLSC) (Lv et al., 2020).

4 APPLICATIONS OF MECHANICAL STIMULATION TO MESENCHYMAL STEM CELLS IN BONE REGENERATION

Different forms of mechanical force have been described previously to promote osteogenic differentiation of MSCs. However, these studies did not discuss the optimal mode of application of mechanical stimulation in detail. Therefore, several mechanical application modes will be discussed in this part, including the magnitude, frequency, intermittent or continuous, immediate or delayed application, and the dimensionalities of mechanical stimulation (**Table 1**).

4.1 Magnitude and Frequency of Mechanical Stimulation

The osteogenic differentiation of MSCs has been found to be correlated with the magnitude and frequency of mechanical stimulation. Stavenschi et al. explored the osteogenic effect of oscillatory fluid flow on MSCs of 1 Pa, 2 and 5 Pa. The results showed that the expression of osteogenic genes was significantly upregulated at the magnitude of 2 Pa and the frequency of 2 Hz (Stavenschi et al., 2017). The most effective shear stress for promoting MSC proliferation and osteogenesis has also been explored. Sanat's research showed that MSCs exhibited a high cell proliferation rate when stimulated by intermittent flow at 1.09 mPa, while 10 mPa upregulated osteogenic gene expression (Dash et al., 2020). Xue and Cartmell, (2020) suggested the osteogenic effect of shear stress on MSCs in three-dimensional culture was different from that in the plate. Lower fluid shear stress (1–10 mPa) stimulated MSCs in the scaffold used to simulate a three-dimensional environment to promote the osteogenic differentiation, whereas 100–4,000 mPa was required when the MSCs were cultured in a plate (Xue and Cartmell, 2020).

4.2 Intermittent and Continuous Mechanical Stimulation

Recent studies have shown that, compared to long-term continuous mechanical stimulation, a period of rest time during mechanical stimulation enhanced bone formation and improved the mechanical properties of bone (Robling et al., 2002; Saxon et al., 2005). Compared to continuous shear stress, intermittent application has been proven to maintain the mechanosensitivity of MSCs and osteocytes (Siller-Jackson et al., 2008; Liu et al., 2012). In addition to FSS, intermittent stretching can promote osteogenic differentiation of MSCs (Wang et al., 2017). Continuous cyclic mechanical tension (CCMT) has been found to downregulate Runx2 expression in MSCs and inhibit osteogenic differentiation (Shi et al., 2011). Another study compared the effects of intermittent compressive force (ICF) and continuous compressive force (CCF) on the behavior of PDLSCs. The results suggested that ICF upregulated TGFβ-1 and promoted the osteogenic differentiation of PDLSCs, whereas the osteogenic gene expression of the CCF group was unchanged (Manokawinchoke et al., 2019). Therefore, the intermittent mechanical stimulation mode is superior to continuous mechanical stimulation in terms of promoting bone regeneration.

At present, intermittent mechanical stimulation promotes osteogenesis in bone that needs the loading interval to recover its mechano-sensitivity to mechanical signals. Nardone et al. (2017) found that mechano-sensing switches (such as pFAK) were released from FAs into the cytoplasm during intermittent and activated YAP. This revocation of activation suggested that intermittent mechanical loading could activate integrin signaling downstream, which possibly explained the decreased mechano-sensitivity of bone tissue caused by continuous mechanical stimulation. Additionally, the mechanical environment is capable of modulating nuclear properties, and mechanical sensitivity may also be related to the nuclear biophysical properties (Heo et al., 2016). The nuclei in dynamic loading induced MSCs to stiffen and become resistant to deformation, which sensitizes MSCs to mechanical stimulated calcium signaling and differentiated marker expression (Heo et al., 2016). Thus, the nucleus plays an essential role in modulating cellular mechano-sensation during differentiation. There is limited research on the mechanisms by which MSCs respond to intermittent and continuous stimulation. However, studies on the mechanism of osteoblasts could provide hints for future research. It was suggested that mechano-sensitivity is primarily associated with actin stress fibers. Gardinier et al. suggested that osteoblasts responded to FSS through actin stress fiber formation (ASFF), and ASFF led to increased cell stiffness and decreased mechano-sensitivity (Gardinier et al., 2014). LIM kinase 2 (LIMK2) is a gene related to the reorganization of the cytoskeleton. Several studies found that inhibiting the LIMK2 increased the sensitivity of ERK1/2 to fluid shear stress and promoted the gene expression of c-fos to enhance the mechanical sensitivity of osteoblasts (Zhang et al., 2009; Xiang et al., 2012). These results suggested that the mechanism by which MSCs respond to intermittent mechanical stimulation may also be related to the actin stress fiber and cytoskeleton.

4.3 Immediate and Delayed Mechanical Stimulation

Delayed mechanical stimulation has a positive effect on osteogenesis by promoting angiogenesis. The formation of blood vessels is closely related to endochondral ossification, in

which MSCs first aggregate and differentiate into hyaline cartilage to form the cartilage model. Following growth of blood vessels, the cartilage is gradually replaced by bone tissue. Joe's laboratory investigated the effects of immediate and delayed mechanical loading on vascular ingrowth in bone regeneration (Boerckel et al., 2011; Ruehle et al., 2020). The results showed that load initiation was a key determinant of vascular network formation. Immediate loading significantly inhibited the growth of blood vessels into the bone defect area, which led to fracture nonunion. In contrast, delayed loading allowed the growth of vessels into the defect and induced vascular remodeling. The study by Anna showed that the bone accumulation rate was significantly elevated by 4-week delayed mechanical loading application, which coincided with chondrocyte hypertrophy and endochondral transition (McDermott et al., 2019). They concluded that a 4-week delay in mechanical loading better mimicked the process of endochondral ossification.

4.4 Dimensionalities of Mechanical Stimulation

The mechanical stimulation applied to cells in two-dimensional (2D) environments is unidirectional. However, mechanical stimulation is multidirectional in physiological environments. The behavior of mechanical loading-induced cells is altered by the dimensionalities of their environments. Thus, the response of cells to external mechanical forces in three-dimensional (3D) environments that mimic the physiological environments *in vivo* needs to be explored. Li and his team found that long-term compression loading induced maturation of α5-integrin-based adhesions to form 3D-matrix adhesions (3DMAs) in the 3D environment (Li et al., 2020). In contrast to the FA formed in the 2D environment, the composition and morphology of 3DMAs are found only in native tissues and cell-derived matrices, suggesting that dimensionality influences the behavior of cells under mechanical stimulation. However, the exact mechanism by which external mechanical forces regulate cell fate in different dimensionalities remains unclear.

Exploring the effects of mechanical stimulation on cells in a 3D environment involves not only mechanical stimulation of cells but also the properties of materials. In 2D conditions, mechanical stimulation is applied to the cells directly. However, in a 3D environment, the force is first applied to the substrate which then transmits the mechanical signals to the cell through the deformation generated by the stimulation (Steinmetz et al., 2015). Thus, the process by which the mechanical signals are transmitted to cells contains two steps: the deformation of scaffolds produced by mechanical stimulation and the cell sensing and responding to the deformation. The ECM is not a linearly elastic material and has complex mechanical properties, including viscoelasticity, mechanical plasticity and nonlinear elasticity (Chaudhuri et al., 2020). The ECM responds to external mechanical stimulation by remodeling the stress fiber network, such as by changing the structure of the fiber network and forming bonds between the fibers (Loebel et al., 2019). The effect of mechanical stimulation on cells is related to the interactions between ECM properties and cells, which suggests that the mechanical properties of scaffold materials are of vital importance for cell differentiation in the 3D environment.

Materials that mimic the mechanical properties of ECM have been explored. Davidson and his team developed a multifiber hydrogel network with force-responsive characteristics (Davidson et al., 2020). In this network, the fibers form covalent bonds under mechanical loading, and the interactions of the fiber increase material stiffness and plastic deformation. Davidson's design mimics the physiological process of ECM remodeling under mechanical stimulation, providing a model for exploring the effects of mechanical stimulation on cells in 3D environments (Davidson et al., 2020). Mechanical stimulation in a 3D environment fabricates the layered scaffolds with gradient mechanical properties. Horner et al. (2019) designed a 3D electrospinning scaffold with a tissue gradient that generates spatially controlled strain gradients in a scaffold depth-dependent manner under dynamic loading. MSCs in the greater compressive strain areas upregulate osteogenic gene expression, while chondrogenic markers are upregulated in the high local compressive strain areas. The formation of the mechanical gradient was maintained only under the application of dynamic loading. This study shows that regulating the local mechanical microenvironment provides a strategy to recapitulate the gradient structure of osteochondral tissues (**Table 1**).

Explorations of optimal mechanical parameters are significant for further application of mechanical stimulation in bone tissue engineering as presented above. Shear stress from 1.09 mPa to 5 Pa was applied to MSCs in previous studies, and 10–15 mPa were proved to have a superior osteogenic effect. Stretching or compression resulted 10% strain was discovered promoting osteogenesis. In comparison with continuous mechanical stimulation, the intermittent application is more efficient in inducing osteogenic differentiation *via* maintaining the mechanosensitivity of MSCs to mechanical signals. Therefore, mechanical stimulations are recommended to be performed with appropriate intervals. Application of delayed mechanical stimulation was reported to be an ideal option for facilitating angiogenesis in bone remodeling, which indicates that future researches should take the mechanical stimulation application time into consideration. Besides, in contrast to the 2D environment, MSCs showed a more bionic behavior in response to external mechanical stimulation in 3D environment that mimics physiological environments. Thus, 3D environment is recommended for the mechanical stimulation application.

5 OUTLOOK

Mechanical stimulation plays an important role in bone regeneration due to its influences on bone physiological functions. The main functional cells in bone regeneration, BMSCs, sense specific mechanical signals through mechanosensors on the cytomembrane, which results in the activation of downstream molecular pathways and altered

expression of osteogenic genes. Mechanical stimulated-MSCs regulate immune, angiogenic and osteogenic microenvironments of bone regeneration by interacting with macrophages, endothelial cells and osteocytes. Modes of mechanical stimulation including the magnitude, frequency, duration and intermittence, affect the osteogenic differentiation of MSCs. Therefore, investigations of mechanical stimulation on bone regeneration for application in regenerative medicine are of great importance.

The mechanism of mechanical stimulation for osteogenesis has been studied in two main aspects, the principle of mechanosensors on the cell membrane surface to sense mechanical stimulation and the intracellular pathways transmitting mechanical signals, which ultimately lead to changes in gene expression. The mechanism of the mechanoreceptor, including integrated proteins and primary cilia, has been widely reported (Hoey et al., 2012; Kechagia et al., 2019). However, as a recently discovered mechanosensitive calcium ion channel, the principle of the Piezo1 response to mechanical stimulation has not been fully elucidated in MSCs. Therefore, the mechanism of PIEZO1 responding to mechanical stimulation in MSCs needs to be confirmed by more researchers to provide convincing evidence for future applications in bone regeneration. Additionally, in spite of advancements in exploring mechanotransduction in 2D environment, our knowledge of the MSC behaviors in 3D environments under mechanical stimulation remains limited. 3D culture is one of the necessary factors for the construction of the tissue engineered-bone which mimics physiological environments and provides more suitable matrix for MSCs. The mechanism of MSCs responding to mechanical stimuli in 3D environments is possibly the priority for future researches.

The effect of mechanical stimulation on the cross-talk between MSCs and osteogenesis-related cells is an emerging field of vital significance for bone regeneration. 1) Osteocytes are mechanosensitive cells that resided in the mineral matrix, which play an important role in modulating bone metabolism (Timmins and Wall, 1977). And the interactions between MSCs and osteocytes under external mechanical stimulation deserve further investigation, especially the means by which paracrine regulation of the loading induced-osteocytes regulates the behavior of MSCs. Investigating the interactions between osteocytes and MSCs under mechanical stimulation contributes to a better understanding of MSC response to mechanical stimulation and the comprehensive effect of mechanical stimulation on bone. 2) Excesses of inflammatory response often result in the failure of bone repair in bone tissue engineering. A few studies have illustrated that mechanical stimulation could facilitate the resolution of inflammation through regulating the interactions between MSCs and macrophages. However, the anti-inflammatory mechanism and the optimal application paraments remain unclear. Thus, further studies on the role of mechanical stimulation in the immune microenvironment during bone regeneration may provide a new insight into the design of bone regeneration biomaterials. 3) Interactions between endothelial cells and MSCs under mechanical stimulation also attract great attention. Studies proved that delayed mechanical stimulation promotes angiogenesis in bone regeneration. However, most of the studies only adopted a single delayed time point and the temporal effect of different delayed-loading time points is not clear. Therefore, studies on the effect of mechanical stimulation loading time in interactions between MSCs and endothelial cells can provide a comprehensive understanding of angiogenesis, which further guides the weight-bearing point of the fracture patients.

Mechanical stimulation has been used as a therapy in orthopedic which is known as mechanotherapy (Huang et al., 2013). For instance, distraction osteogenesis is used to correct limb and craniofacial defects, and LIPUS is used to hasten the fracture healing process and increase bone mass. However, current approaches are applying mechanical stimulation directly to the tissue, rather than through the substrate. However, efficiencies of these mechanotherapies in bone repairing are open to debate, as a recent systematic review concluded that LIPUS did not improve outcomes important to patients (Schandelmaier et al., 2017). The potential application may combine mechanical stimulation and bone tissue engineering. As the key element of bone tissue engineering, 3D culture involves the interactions between the cells and the materials. Scientists are keeping searching for materials that are more compatible with physiological deformation, retraction and osteogenic activity in mechanical environments. And the interactions between cells and biomaterials also require continuous refinement, further work may focus on the combined effect of the substance stiffness and the external mechanical stimulation application on MSCs. Several active biomaterials offer novel approaches to apply mechanical stimulation, such as magnetically triggered systems. Due to the variable mechanical parameters and the precise controlling of the mechanical application timepoint, magnetically triggered strategies will possibly receive increasing attention.

6 CONCLUSION

External mechanical force plays an essential role in bone regeneration. And MSCs can sense and respond to mechanical signals during this process. Thus, in this review we discussed MSCs mechanotransduction mechanisms, the influences of mechanical stimulation on modulating interactions between MSCs and surrounding cells in bone regeneration including the immune, angiogenic and osteogenic microenvironments, and the applications of mechanical stimulation of MSCs in bone regeneration. The description of MSCs mechanotransduction on purpose of providing a comprehensive view and several promising mechanosensors required to be fully investigated in MSC mechanotransduction field. The regulation of mechanical stimulation on microenvironments surrounding MSC discussed in the manuscript is of great significance for the bone regenerative medicine, which offers an insight for the design of tissue engineered bone in consideration of immune response, angiogenesis and osteogenesis. Moreover, the depiction of different mechanical stimulation application modes bring insightful guidance to the design of bone regenerative

biomaterials and clinical applications of the mechanical stimulation.

AUTHOR CONTRIBUTIONS

YS and BW contributed equally to this review. YS and BW wrote and edited the original draft. RW helped in editing the figures and manuscript. BZ provided background information. PL helped edit the figures. DW reviewed the manuscript and provided feedback. J-JN reviewed and edited the manuscript. DC conceptualized the ideas and provided funding support. XW supervised the whole work.

FUNDING

This work was supported in part by the Beijing Municipal Health Commission (BMHC-2021-6, BMHC-2019-9, BMHC-2018-4, PXM 2020_026275_000002), National Key Research and Development Program of China (2018YFA0703100), and Beijing Natural Science Foundation (7192027).

REFERENCES

Argentati, C., Morena, F., Tortorella, I., Bazzucchi, M., Porcellati, S., Emiliani, C., et al. (2019). Insight into Mechanobiology: How Stem Cells Feel Mechanical Forces and Orchestrate Biological Functions. *Ijms* 20 (21), 5337. doi:10.3390/ijms20215337

Baas, E., Kuiper, J. H., Yang, Y., Wood, M. A., and El Haj, A. J. (2010). *In Vitro* bone Growth Responds to Local Mechanical Strain in Three-Dimensional Polymer Scaffolds. *J. Biomech.* 43 (4), 733–739. doi:10.1016/j.jbiomech.2009.10.016

Bandaru, P., Cefaloni, G., Vajhadin, F., Lee, K., Kim, H. J., Cho, H. J., et al. (2020). Mechanical Cues Regulating Proangiogenic Potential of Human Mesenchymal Stem Cells through YAP-Mediated Mechanosensing. *Small* 16 (25), 2001837. doi:10.1002/smll.202001837

Boerckel, J. D., Uhrig, B. A., Willett, N. J., Huebsch, N., and Guldberg, R. E. (2011). Mechanical Regulation of Vascular Growth and Tissue Regeneration *In Vivo*. *Proc. Natl. Acad. Sci.* 108 (37), E674–E680. doi:10.1073/pnas.1107019108

Bouzid, T., Kim, E., Riehl, B. D., Esfahani, A. M., Rosenbohm, J., Yang, R., et al. (2019). The LINC Complex, Mechanotransduction, and Mesenchymal Stem Cell Function and Fate. *J. Biol. Eng.* 13, 68. doi:10.1186/s13036-019-0197-9

Cambré, I., Gaublomme, D., Burssens, A., Jacques, P., Schryvers, N., De Muynck, A., et al. (2018). Mechanical Strain Determines the Site-specific Localization of Inflammation and Tissue Damage in Arthritis. *Nat. Commun.* 9 (1), 4613. doi:10.1038/s41467-018-06933-4

Cao, W., Lin, W., Cai, H., Chen, Y., Man, Y., Liang, J., et al. (2019). Dynamic Mechanical Loading Facilitated Chondrogenic Differentiation of Rabbit BMSCs in Collagen Scaffolds. *Regen. Biomater.* 6 (2), 99–106. doi:10.1093/rb/rbz005

Carelli, S., Colli, M., Vinci, V., Caviggioli, F., Klinger, M., and Gorio, A. (2018). Mechanical Activation of Adipose Tissue and Derived Mesenchymal Stem Cells: Novel Anti-inflammatory Properties. *Ijms* 19 (1), 267. doi:10.3390/ijms19010267

Charoenpanich, A., Wall, M. E., Tucker, C. J., Andrews, D. M. K., Lalush, D. S., Dirschl, D. R., et al. (2014). Cyclic Tensile Strain Enhances Osteogenesis and Angiogenesis in Mesenchymal Stem Cells from Osteoporotic Donors. *Tissue Eng. A* 20 (1-2), 67–78. doi:10.1089/ten.TEA.2013.0006

Chaudhuri, O., Cooper-White, J., Janmey, P. A., Mooney, D. J., and Shenoy, V. B. (2020). Effects of Extracellular Matrix Viscoelasticity on Cellular Behaviour. *Nature* 584 (7822), 535–546. doi:10.1038/s41586-020-2612-2

Chen, B., Lin, T., Yang, X., Li, Y., Xie, D., Zheng, W., et al. (2016). Low-magnitude, High-Frequency Vibration Promotes the Adhesion and the Osteogenic Differentiation of Bone Marrow-Derived Mesenchymal Stem Cells Cultured on a Hydroxyapatite-Coated Surface: The Direct Role of Wnt/β-Catenin Signaling Pathway Activation. *Int. J. Mol. Med.* 38 (5), 1531–1540. doi:10.3892/ijmm.2016.2757

Chen, N. X., Ryder, K. D., Pavalko, F. M., Turner, C. H., Burr, D. B., Qiu, J., et al. (2000). Ca2+ Regulates Fluid Shear-Induced Cytoskeletal Reorganization and Gene Expression in Osteoblasts. *Am. J. Physiology-Cell Physiol.* 278 (5), C989–C997. doi:10.1152/ajpcell.2000.278.5.C989

Chen, S., Jing, J., Yuan, Y., Feng, J., Han, X., Wen, Q., et al. (2020). Runx2+ Niche Cells Maintain Incisor Mesenchymal Tissue Homeostasis through IGF Signaling. *Cel Rep.* 32 (6), 108007. doi:10.1016/j.celrep.2020.108007

Chen, X., He, F., Zhong, D.-Y., and Luo, Z.-P. (2015). Acoustic-frequency Vibratory Stimulation Regulates the Balance between Osteogenesis and Adipogenesis of Human Bone Marrow-Derived Mesenchymal Stem Cells. *Biomed. Res. Int.* 2015, 1–10. doi:10.1155/2015/540731

Chen, X., Yan, J., He, F., Zhong, D., Yang, H., Pei, M., et al. (2018). Mechanical Stretch Induces Antioxidant Responses and Osteogenic Differentiation in Human Mesenchymal Stem Cells through Activation of the AMPK-SIRT1 Signaling Pathway. *Free Radic. Biol. Med.* 126, 187–201. doi:10.1016/j.freeradbiomed.2018.08.001

Ciani, C., Sharma, D., Doty, S. B., and Fritton, S. P. (2014). Ovariectomy Enhances Mechanical Load-Induced Solute Transport Around Osteocytes in Rat Cancellous Bone. *Bone* 59, 229–234. doi:10.1016/j.bone.2013.11.026

Claes, L., Meyers, N., Schülke, J., Reitmaier, S., Klose, S., and Ignatius, A. (2018). The Mode of Interfragmentary Movement Affects Bone Formation and Revascularization After Callus Distraction. *PLoS One* 13, e0202702. doi:10.1371/journal.pone.0202702

Corrigan, M. A., Johnson, G. P., Stavenschi, E., Riffault, M., Labour, M.-N., and Hoey, D. A. (2018). TRPV4-mediates Oscillatory Fluid Shear Mechanotransduction in Mesenchymal Stem Cells in Part via the Primary Cilium. *Sci. Rep.* 8 (1), 3824. doi:10.1038/s41598-018-22174-3

Coste, B., Mathur, J., Schmidt, M., Earley, T. J., Ranade, S., Petrus, M. J., et al. (2010). Piezo1 and Piezo2 Are Essential Components of Distinct Mechanically Activated Cation Channels. *Science* 330 (6000), 55–60. doi:10.1126/science.1193270

Dallas, S. L., Prideaux, M., and Bonewald, L. F. (2013). The Osteocyte: An Endocrine Cell ... and More. *Endocr. Rev.* 34 (5), 658–690. doi:10.1210/er.2012-1026

Dash, S. K., Sharma, V., Verma, R. S., and Das, S. K. (2020). Low Intermittent Flow Promotes Rat Mesenchymal Stem Cell Differentiation in Logarithmic Fluid Shear Device. *Biomicrofluidics* 14 (5), 054107. doi:10.1063/5.0024437

Davidson, M. D., Ban, E., Schoonen, A. C. M., Lee, M. H., D'Este, M., Shenoy, V. B., et al. (2020). Mechanochemical Adhesion and Plasticity in Multifiber Hydrogel Networks. *Adv. Mater.* 32 (8), 1905719. doi:10.1002/adma.201905719

Delaine-Smith, R. M., and Reilly, G. C. (2011). The Effects of Mechanical Loading on Mesenchymal Stem Cell Differentiation and Matrix Production. *Vitam Horm.* 87, 417–480. doi:10.1016/b978-0-12-386015-6.00039-1

Dewey, C. F., Jr., Bussolari, S. R., Gimbrone, M. A., Jr., and Davies, P. F. (1981). The Dynamic Response of Vascular Endothelial Cells to Fluid Shear Stress. *J. Biomech. Eng.* 103 (3), 177–185. doi:10.1115/1.3138276

Diaz, M. F., Vaidya, A. B., Evans, S. M., Lee, H. J., Aertker, B. M., Alexander, A. J., et al. (2017). Biomechanical Forces Promote Immune Regulatory Function of Bone Marrow Mesenchymal Stromal Cells. *Stem Cells* 35 (5), 1259–1272. doi:10.1002/stem.2587

Dong, L., Song, Y., Zhang, Y., Zhao, W., Wang, C., Lin, H., et al. (2021). Mechanical Stretch Induces Osteogenesis through the Alternative Activation of Macrophages. *J. Cel Physiol* 236 (9), 6376–6390. doi:10.1002/jcp.30312

Du, G., Li, L., Zhang, X., Liu, J., Hao, J., Zhu, J., et al. (2020a). Roles of TRPV4 and Piezo Channels in Stretch-Evoked Ca2+ Response in Chondrocytes. *Exp. Biol. Med. (Maywood)* 245 (3), 180–189. doi:10.1177/1535370219892601

Du, J., Yang, J., He, Z., Cui, J., Yang, Y., Xu, M., et al. (2020b). Osteoblast and Osteoclast Activity Affect Bone Remodeling upon Regulation by Mechanical Loading-Induced Leukemia Inhibitory Factor Expression in Osteocytes. *Front. Mol. Biosci.* 7, 585056. doi:10.3389/fmolb.2020.585056

Duty, A. O., Oest, M. E., and Guldberg, R. E. (2007). Cyclic Mechanical Compression Increases Mineralization of Cell-Seeded Polymer Scaffolds *In Vivo*. *J. Biomech. Eng.* 129 (4), 531–539. doi:10.1115/1.2746375

Eichholz, K. F., Woods, I., Riffault, M., Johnson, G. P., Corrigan, M., Lowry, M. C., et al. (2020). Human Bone Marrow Stem/stromal Cell Osteogenesis Is Regulated via Mechanically Activated Osteocyte-Derived Extracellular Vesicles. *Stem Cell Transl Med* 9 (11), 1431–1447. doi:10.1002/sctm.19-0405

Einhorn, T. A., and Gerstenfeld, L. C. (2015). Fracture Healing: Mechanisms and Interventions. *Nat. Rev. Rheumatol.* 11 (1), 45–54. doi:10.1038/nrrheum.2014.164

Fang, B., Liu, Y., Zheng, D., Shan, S., Wang, C., Gao, Y., et al. (2019). The Effects of Mechanical Stretch on the Biological Characteristics of Human Adipose-derived Stem Cells. *J. Cel Mol Med* 23 (6), 4244–4255. doi:10.1111/jcmm.14314

Federman, M., and Nichols, G., Jr. (1974). Bone Cell Cilia: Vestigial or Functional Organelles? *Calc. Tis Res.* 17 (1), 81–85. doi:10.1007/bf02547216

Feng, Y., Liang, Y., Zhu, X., Wang, M., Gui, Y., Lu, Q., et al. (2018). The Signaling Protein Wnt5a Promotes TGFβ1-Mediated Macrophage Polarization and Kidney Fibrosis by Inducing the Transcriptional Regulators Yap/Taz. *J. Biol. Chem.* 293 (50), 19290–19302. doi:10.1074/jbc.RA118.005457

Fu, J., Liu, X., Tan, L., Cui, Z., Liang, Y., Li, Z., et al. (2020). Modulation of the Mechanosensing of Mesenchymal Stem Cells by Laser-Induced Patterning for the Acceleration of Tissue Reconstruction through the Wnt/β-Catenin Signaling Pathway Activation. *Acta Biomater.* 101, 152–167. doi:10.1016/j.actbio.2019.10.041

Gao, H., Zhai, M., Wang, P., Zhang, X., Cai, J., Chen, X., et al. (2017). Low-level Mechanical Vibration Enhances Osteoblastogenesis via a Canonical Wnt Signaling-Associated Mechanism. *Mol. Med. Rep.* 16 (1), 317–324. doi:10.3892/mmr.2017.6608

Gao, Q., Walmsley, A. D., Cooper, P. R., and Scheven, B. A. (2016). Ultrasound Stimulation of Different Dental Stem Cell Populations: Role of Mitogen-Activated Protein Kinase Signaling. *J. Endodontics* 42 (3), 425–431. doi:10.1016/j.joen.2015.12.019

Gardinier, J., Yang, W., Madden, G. R., Kronbergs, A., Gangadharan, V., Adams, E., et al. (2014). P2Y2 Receptors Regulate Osteoblast Mechanosensitivity during Fluid Flow. *Am. J. Physiology-Cell Physiol.* 306 (11), C1058–C1067. doi:10.1152/ajpcell.00254.2013

Gerstenfeld, L. C., Cullinane, D. M., Barnes, G. L., Graves, D. T., and Einhorn, T. A. (2003). Fracture Healing as a post-natal Developmental Process: Molecular, Spatial, and Temporal Aspects of its Regulation. *J. Cel. Biochem.* 88 (5), 873–884. doi:10.1002/jcb.10435

Grier, W., Moy, A. S., Moy, A., and Harley, B. (2017). Cyclic Tensile Strain Enhances Human Mesenchymal Stem Cell Smad 2/3 Activation and Tenogenic Differentiation in Anisotropic Collagen-Glycosaminoglycan Scaffolds. *eCM* 33, 227–239. doi:10.22203/eCM.v033a1410.22203/ecm.v033a17

Gurkan, U. A., and Akkus, O. (2008). The Mechanical Environment of Bone Marrow: a Review. *Ann. Biomed. Eng.* 36 (12), 1978–1991. doi:10.1007/s10439-008-9577-x

Hao, J., Zhang, Y., Jing, D., Shen, Y., Tang, G., Huang, S., et al. (2015). Mechanobiology of Mesenchymal Stem Cells: Perspective into Mechanical Induction of MSC Fate. *Acta Biomater.* 20, 1–9. doi:10.1016/j.actbio.2015.04.008

He, D., Liu, F., Cui, S., Jiang, N., Yu, H., Zhou, Y., et al. (2020). Mechanical Load-Induced H2S Production by Periodontal Ligament Stem Cells Activates M1 Macrophages to Promote Bone Remodeling and Tooth Movement via STAT1. *Stem Cel Res Ther* 11 (1), 112. doi:10.1186/s13287-020-01607-9

Heo, S.-J., Driscoll, T. P., Thorpe, S. D., Nerurkar, N. L., Baker, B. M., Yang, M. T., et al. (2016). Differentiation Alters Stem Cell Nuclear Architecture, Mechanics, and Mechano-Sensitivity. *Elife* 5. doi:10.7554/eLife.18207

Hoey, D. A., Kelly, D. J., and Jacobs, C. R. (2011). A Role for the Primary Cilium in Paracrine Signaling Between Mechanically Stimulated Osteocytes and Mesenchymal Stem Cells. *Biochem Biophys Res Commun.* 412 (1), 182–187. doi:10.1016/j.bbrc.2011.07.072

Hoey, D. A., Tormey, S., Ramcharan, S., O'Brien, F. J., and Jacobs, C. R. (2012). Primary Cilia-Mediated Mechanotransduction in Human Mesenchymal Stem Cells. *Stem Cells* 30 (11), 2561–2570. doi:10.1002/stem.1235

Holmes, D. (2017). Non-union Bone Fracture: a Quicker Fix. *Nature* 550 (7677), S193. doi:10.1038/550S193a

Horner, C. B., Hirota, K., Liu, J., Maldonado, M., Hyle Park, B., and Nam, J. (2018). Magnitude-dependent and Inversely-related Osteogenic/chondrogenic Differentiation of Human Mesenchymal Stem Cells under Dynamic Compressive Strain. *J. Tissue Eng. Regen. Med.* 12 (2), e637–e647. doi:10.1002/term.2332

Horner, C. B., Maldonado, M., Tai, Y., Rony, R. M. I. K., and Nam, J. (2019). Spatially Regulated Multiphenotypic Differentiation of Stem Cells in 3D via Engineered Mechanical Gradient. *ACS Appl. Mater. Inter.* 11 (49), 45479–45488. doi:10.1021/acsami.9b17266

Hu, K., Sun, H., Gui, B., and Sui, C. (2017). TRPV4 Functions in Flow Shear Stress Induced Early Osteogenic Differentiation of Human Bone Marrow Mesenchymal Stem Cells. *Biomed. Pharmacother.* 91, 841–848. doi:10.1016/j.biopha.2017.04.094

Huang, C., Holfeld, J., Schaden, W., Orgill, D., and Ogawa, R. (2013). Mechanotherapy: Revisiting Physical Therapy and Recruiting Mechanobiology for a new era in Medicine. *Trends Mol. Med.* 19 (9), 555–564. doi:10.1016/j.molmed.2013.05.005

Hui, C. F. F., Chan, C. W., Yeung, H. Y., Lee, K. M., Qin, L., Li, G., et al. (2011). Low-intensity Pulsed Ultrasound Enhances Posterior Spinal Fusion Implanted with Mesenchymal Stem Cells-Calcium Phosphate Composite without Bone Grafting. *Spine* 36 (13), 1010–1016. doi:10.1097/BRS.0b013e318205c5f5

Hunziker, E. B. (2002). Articular Cartilage Repair: Basic Science and Clinical Progress. A Review of the Current Status and Prospects. *Osteoarthritis and Cartilage* 10 (6), 432–463. doi:10.1053/joca.2002.0801

Jepsen, D. B., Ryg, J., Hansen, S., Jørgensen, N. R., Gram, J., and Masud, T. (2019). The Combined Effect of Parathyroid Hormone (1-34) and Whole-Body Vibration Exercise in the Treatment of Postmenopausal OSteoporosis (PaVOS Study): a Randomized Controlled Trial. *Osteoporos. Int.* 30 (9), 1827–1836. doi:10.1007/s00198-019-05029-z

Jessop, H. L., Suswillo, R. F., Rawlinson, S. C., Zaman, G., Lee, K., Das-Gupta, V., et al. (2004). Osteoblast-Like Cells from Estrogen Receptor α Knockout Mice Have Deficient Responses to Mechanical Strain. *J. Bone Miner Res.* 19 (6), 938–946. doi:10.1359/jbmr.2004.19.6.938

Jiang, Y. N., Zhao, J., Chu, F. T., Jiang, Y. Y., and Tang, G. H. (2018). Tension-loaded Bone Marrow Stromal Cells Potentiate the Paracrine Osteogenic Signaling of Co-cultured Vascular Endothelial Cells. *Biol. Open* 7 (6), bio032482. doi:10.1242/bio.032482

Johnson, G. P., Fair, S., and Hoey, D. A. (2021). Primary Cilium-Mediated MSC Mechanotransduction Is Dependent on Gpr161 Regulation of Hedgehog Signalling. *Bone* 145, 115846. doi:10.1016/j.bone.2021.115846

Johnson, G. P., Stavenschi, E., Eichholz, K. F., Corrigan, M. A., Fair, S., and Hoey, D. A. (2018). Mesenchymal Stem Cell Mechanotransduction Is cAMP Dependent and Regulated by Adenylyl Cyclase 6 and the Primary Cilium. *J. Cel Sci* 131 (21), jcs222737. doi:10.1242/jcs.222737

Kechagia, J. Z., Ivaska, J., and Roca-Cusachs, P. (2019). Integrins as Biomechanical Sensors of the Microenvironment. *Nat. Rev. Mol. Cel Biol* 20 (8), 457–473. doi:10.1038/s41580-019-0134-2

Kirby, T. J., and Lammerding, J. (2018). Emerging Views of the Nucleus as a Cellular Mechanosensor. *Nat. Cel Biol* 20 (4), 373–381. doi:10.1038/s41556-018-0038-y

Kuhn, N. Z., and Tuan, R. S. (2010). Regulation of Stemness and Stem Cell Niche of Mesenchymal Stem Cells: Implications in Tumorigenesis and Metastasis. *J. Cel. Physiol.* 222 (2), 268–277. doi:10.1002/jcp.21940

Kusuyama, J., Bandow, K., Shamoto, M., Kakimoto, K., Ohnishi, T., and Matsuguchi, T. (2014). Low Intensity Pulsed Ultrasound (LIPUS) Influences the Multilineage Differentiation of Mesenchymal Stem and Progenitor Cell Lines through ROCK-Cot/Tpl2-MEK-ERK Signaling Pathway. *J. Biol. Chem.* 289 (15), 10330–10344. doi:10.1074/jbc.M113.546382

Kwon, R. Y., Meays, D. R., Tang, W. J., and Frangos, J. A. (2010). Microfluidic Enhancement of Intramedullary Pressure Increases Interstitial Fluid Flow and Inhibits Bone Loss in Hindlimb Suspended Mice. *J. Bone Miner Res.* 25 (8), 1798–1807. doi:10.1002/jbmr.74

Lanyon, L., and Baggott, D. (1976). Mechanical Function as an Influence on the Structure and Form of Bone. *The J. Bone Jt. Surg. Br. volume* 58-B (4), 436–443. doi:10.1302/0301-620X.58B4.1018029

Lee, H. J., Diaz, M. F., Ewere, A., Olson, S. D., Cox, C. S., Jr., and Wenzel, P. L. (2017). Focal Adhesion Kinase Signaling Regulates Anti-inflammatory Function of Bone Marrow Mesenchymal Stromal Cells Induced by Biomechanical Force. *Cell Signal.* 38, 1–9. doi:10.1016/j.cellsig.2017.06.012

Lee, W., Leddy, H. A., Chen, Y., Lee, S. H., Zelenski, N. A., McNulty, A. L., et al. (2014). Synergy between Piezo1 and Piezo2 Channels Confers High-Strain Mechanosensitivity to Articular Cartilage. *Proc. Natl. Acad. Sci. USA* 111 (47), E5114–E5122. doi:10.1073/pnas.1414298111

Li, C.-J., Madhu, V., Balian, G., Dighe, A. S., and Cui, Q. (2015a). Cross-Talk between VEGF and BMP-6 Pathways Accelerates Osteogenic Differentiation of Human Adipose-Derived Stem Cells. *J. Cel. Physiol.* 230 (11), 2671–2682. doi:10.1002/jcp.24983

Li, C. W., Lau, Y. T., Lam, K. L., and Chan, B. P. (2020). Mechanically Induced Formation and Maturation of 3D-Matrix Adhesions (3DMAs) in Human Mesenchymal Stem Cells. *Biomaterials* 258, 120292. doi:10.1016/j.biomaterials.2020.120292

Li, D., Tang, T., Lu, J., and Dai, K. (2009). Effects of Flow Shear Stress and Mass Transport on the Construction of a Large-Scale Tissue-Engineered Bone in a Perfusion Bioreactor. *Tissue Eng. Part A* 15 (10), 2773–2783. doi:10.1089/ten.TEA.2008.0540

Li, H., Wu, W., He, X., Cao, C., Yu, X., Zeng, Y., et al. (2019a). Applying Vibration in Early Postmenopausal Osteoporosis Promotes Osteogenic Differentiation of Bone Marrow-Derived Mesenchymal Stem Cells and Suppresses Postmenopausal Osteoporosis Progression. *Biosci. Rep.* 39 (9). doi:10.1042/bsr20191011

Li, J., Hou, B., Tumova, S., Muraki, K., Bruns, A., Ludlow, M. J., et al. (2014). Piezo1 Integration of Vascular Architecture with Physiological Force. *Nature* 515 (7526), 279–282. doi:10.1038/nature13701

Li, J., Hu, C., Han, L., Liu, L., Jing, W., Tang, W., et al. (2015b). MiR-154-5p Regulates Osteogenic Differentiation of Adipose-Derived Mesenchymal Stem Cells under Tensile Stress through the Wnt/PCP Pathway by Targeting Wnt11. *Bone* 78, 130–141. doi:10.1016/j.bone.2015.05.003

Li, R., Liang, L., Dou, Y., Huang, Z., Mo, H., Wang, Y., et al. (2015c). Mechanical Stretch Inhibits Mesenchymal Stem Cell Adipogenic Differentiation through TGFβ1/Smad2 Signaling. *J. Biomech.* 48 (13), 3656–3662. doi:10.1016/j.jbiomech.2015.08.013

Li, X., Han, L., Nookaew, I., Mannen, E., Silva, M. J., Almeida, M., et al. (2019b). Stimulation of Piezo1 by Mechanical Signals Promotes Bone Anabolism. *Elife* 8. doi:10.7554/eLife.49631

Liu, L., Liu, M., Li, R., Liu, H., Du, L., Chen, H., et al. (2017). MicroRNA-503-5p Inhibits Stretch-Induced Osteogenic Differentiation and Bone Formation. *Cell Biol Int* 41 (2), 112–123. doi:10.1002/cbin.10704

Liu, L., Yu, B., Chen, J., Tang, Z., Zong, C., Shen, D., et al. (2012). Different Effects of Intermittent and Continuous Fluid Shear Stresses on Osteogenic Differentiation of Human Mesenchymal Stem Cells. *Biomech. Model. Mechanobiol* 11 (3-4), 391–401. doi:10.1007/s10237-011-0319-x

Loebel, C., Mauck, R. L., and Burdick, J. A. (2019). Local Nascent Protein Deposition and Remodelling Guide Mesenchymal Stromal Cell Mechanosensing and Fate in Three-Dimensional Hydrogels. *Nat. Mater.* 18 (8), 883–891. doi:10.1038/s41563-019-0307-6

Lu, Y., Zhao, Q., Liu, Y., Zhang, L., Li, D., Zhu, Z., et al. (2018). Vibration Loading Promotes Osteogenic Differentiation of Bone Marrow-Derived Mesenchymal Stem Cells via P38 MAPK Signaling Pathway. *J. Biomech.* 71, 67–75. doi:10.1016/j.jbiomech.2018.01.039

Lv, P.-y., Gao, P.-f., Tian, G.-j., Yang, Y.-y., Mo, F.-f., Wang, Z.-h., et al. (2020). Osteocyte-derived Exosomes Induced by Mechanical Strain Promote Human Periodontal Ligament Stem Cell Proliferation and Osteogenic Differentiation via the miR-181b-5p/PTEN/AKT Signaling Pathway. *Stem Cel Res Ther* 11 (1), 295. doi:10.1186/s13287-020-01815-3

Manokawinchoke, J., Pavasant, P., Sawangmake, C., Limjeerajarus, N., Limjeerajarus, C. N., Egusa, H., et al. (2019). Intermittent Compressive Force Promotes Osteogenic Differentiation in Human Periodontal Ligament Cells by Regulating the Transforming Growth Factor-β Pathway. *Cell Death Dis* 10 (10), 761. doi:10.1038/s41419-019-1992-4

McCoy, R. J., Widaa, A., Watters, K. M., Wuerstle, M., Stallings, R. L., Duffy, G. P., et al. (2013). Orchestrating Osteogenic Differentiation of Mesenchymal Stem Cells-Identification of Placental Growth Factor as a Mechanosensitive Gene with a Pro-osteogenic Role. *Stem Cells* 31 (11), 2420–2431. doi:10.1002/stem.1482

McDermott, A. M., Herberg, S., Mason, D. E., Collins, J. M., Pearson, H. B., Dawahare, J. H., et al. (2019). Recapitulating Bone Development through Engineered Mesenchymal Condensations and Mechanical Cues for Tissue Regeneration. *Sci. Transl. Med.* 11 (495), eaav7756. doi:10.1126/scitranslmed.aav7756

Michalopoulos, E., Knight, R. L., Korossis, S., Kearney, J. N., Fisher, J., and Ingham, E. (2012). Development of Methods for Studying the Differentiation of Human Mesenchymal Stem Cells under Cyclic Compressive Strain. *Tissue Eng. C: Methods* 18 (4), 252–262. doi:10.1089/ten.TEC.2011.0347

Minematsu, A., Nishii, Y., Imagita, H., and Sakata, S. (2019). Possible Effects of Whole Body Vibration on Bone Properties in Growing Rats. *Osteoporos. Sarcopenia* 5 (3), 78–83. doi:10.1016/j.afos.2019.07.001

Moore, K. A., and Lemischka, I. R. (2006). Stem Cells and Their Niches. *Science* 311 (5769), 1880–1885. doi:10.1126/science.1110542

Nardone, G., Oliver-De La Cruz, J., Vrbsky, J., Martini, C., Pribyl, J., Skládal, P., et al. (2017). YAP Regulates Cell Mechanics by Controlling Focal Adhesion Assembly. *Nat. Commun.* 8, 15321. doi:10.1038/ncomms15321

Nathan, A. S., Baker, B. M., Nerurkar, N. L., and Mauck, R. L. (2011). Mechano-topographic Modulation of Stem Cell Nuclear Shape on Nanofibrous Scaffolds. *Acta Biomater.* 7 (1), 57–66. doi:10.1016/j.actbio.2010.08.007

Pathak, M. M., Nourse, J. L., Tran, T., Hwe, J., Arulmoli, J., Le, D. T. T., et al. (2014). Stretch-activated Ion Channel Piezo1 Directs Lineage Choice in Human Neural Stem Cells. *Proc. Natl. Acad. Sci. USA* 111 (45), 16148–16153. doi:10.1073/pnas.1409802111

Pelaez, D., Arita, N., and Cheung, H. S. (2012). Extracellular Signal-Regulated Kinase (ERK) Dictates Osteogenic And/or Chondrogenic Lineage Commitment of Mesenchymal Stem Cells under Dynamic Compression. *Biochem. Biophysical Res. Commun.* 417 (4), 1286–1291. doi:10.1016/j.bbrc.2011.12.131

Pongkitwitoon, S., Uzer, G., Rubin, J., and Judex, S. (2016). Cytoskeletal Configuration Modulates Mechanically Induced Changes in Mesenchymal Stem Cell Osteogenesis, Morphology, and Stiffness. *Sci. Rep.* 6, 34791. doi:10.1038/srep34791

Price, C., Zhou, X., Li, W., and Wang, L. (2011). Real-time Measurement of Solute Transport within the Lacunar-Canalicular System of Mechanically Loaded Bone: Direct Evidence for Load-Induced Fluid Flow. *J. Bone Miner Res.* 26 (2), 277–285. doi:10.1002/jbmr.211

Pugin, J., Dunn, I., Jolliet, P., Tassaux, D., Magnenat, J.-L., Nicod, L. P., et al. (1998). Activation of Human Macrophages by Mechanical Ventilation *In Vitro*. *Am. J. Physiology-Lung Cell Mol. Physiol.* 275 (6), L1040–L1050. doi:10.1152/ajplung.1998.275.6.L1040

Qi, W., Yan, Y.-B., Lei, W., Wu, Z.-X., Zhang, Y., Liu, D., et al. (2012). Prevention of Disuse Osteoporosis in Rats by Cordyceps Sinensis Extract. *Osteoporos. Int.* 23 (9), 2347–2357. doi:10.1007/s00198-011-1842-4

Ravichandran, A., Lim, J., Chong, M. S. K., Wen, F., Liu, Y., Pillay, Y. T., et al. (2017). *In Vitro* cyclic Compressive Loads Potentiate Early Osteogenic Events in Engineered Bone Tissue. *J. Biomed. Mater. Res.* 105 (8), 2366–2375. doi:10.1002/jbm.b.33772

Robling, A. G., and Bonewald, L. F. (2020). The Osteocyte: New Insights. *Annu. Rev. Physiol.* 82, 485–506. doi:10.1146/annurev-physiol-021119-034332

Robling, A. G., Hinant, F. M., Burr, D. B., and Turner, C. H. (2002). Improved Bone Structure and Strength after Long-Term Mechanical Loading Is Greatest if Loading Is Separated into Short Bouts. *J. Bone Miner Res.* 17 (8), 1545–1554. doi:10.1359/jbmr.2002.17.8.1545

Ruehle, M. A., Eastburn, E. A., LaBelle, S. A., Krishnan, L., Weiss, J. A., Boerckel, J. D., et al. (2020). Extracellular Matrix Compression Temporally Regulates Microvascular Angiogenesis. *Sci. Adv.* 6 (34), eabb6351. doi:10.1126/sciadv.abb6351

Saxon, L. K., Robling, A. G., Alam, I., and Turner, C. H. (2005). Mechanosensitivity of the Rat Skeleton Decreases after a Long Period of Loading, but Is Improved with Time off. *Bone* 36 (3), 454–464. doi:10.1016/j.bone.2004.12.001

Schandelmaier, S., Kaushal, A., Lytvyn, L., Heels-Ansdell, D., Siemieniuk, R. A., Agoritsas, T., et al. (2017). Low Intensity Pulsed Ultrasound for Bone Healing: Systematic Review of Randomized Controlled Trials. *Bmj* 356, j656. doi:10.1136/bmj.j656

Schoenenberger, A. D., Tempfer, H., Lehner, C., Egloff, J., Mauracher, M., Bird, A., et al. (2020). Macromechanics and Polycaprolactone Fiber Organization Drive Macrophage Polarization and Regulate Inflammatory Activation of Tendon *In Vitro* and *In Vivo*. *Biomaterials* 249, 120034. doi:10.1016/j.biomaterials.2020.120034

Schreivogel, S., Kuchibhotla, V., Knaus, P., Duda, G. N., and Petersen, A. (2019). Load-induced Osteogenic Differentiation of Mesenchymal Stromal Cells Is Caused by Mechano-regulated Autocrine Signaling. *J. Tissue Eng. Regen. Med.* 13 (11), 1992–2008. doi:10.1002/term.2948

Shi, Y., Li, H., Zhang, X., Fu, Y., Huang, Y., Lui, P. P. Y., et al. (2011). Continuous Cyclic Mechanical Tension Inhibited Runx2 Expression in Mesenchymal Stem Cells through RhoA-Erk1/2 Pathway. *J. Cel. Physiol.* 226 (8), 2159–2169. doi:10.1002/jcp.22551

Siller-Jackson, A. J., Burra, S., Gu, S., Xia, X., Bonewald, L. F., Sprague, E., et al. (2008). Adaptation of Connexin 43-hemichannel Prostaglandin Release to Mechanical Loading. *J. Biol. Chem.* 283 (39), 26374–26382. doi:10.1074/jbc.M803136200

Sittichokechaiwut, A., Edwards, J. H., Edwards, J., Scutt, A., and Reilly, G. (2010). Short Bouts of Mechanical Loading Are as Effective as Dexamethasone at Inducing Matrix Production by Human Bone Marrow Mesenchymal Stem Cells. *eCM* 20, 45–57. doi:10.22203/ecm.v020a05

Stavenschi, E., Labour, M.-N., and Hoey, D. A. (2017). Oscillatory Fluid Flow Induces the Osteogenic Lineage Commitment of Mesenchymal Stem Cells: The Effect of Shear Stress Magnitude, Frequency, and Duration. *J. Biomech.* 55, 99–106. doi:10.1016/j.jbiomech.2017.02.002

Steinmetz, N. J., Aisenbrey, E. A., Westbrook, K. K., Qi, H. J., and Bryant, S. J. (2015). Mechanical Loading Regulates Human MSC Differentiation in a Multi-Layer Hydrogel for Osteochondral Tissue Engineering. *Acta Biomater.* 21, 142–153. doi:10.1016/j.actbio.2015.04.015

Sugimoto, A., Miyazaki, A., Kawarabayashi, K., Shono, M., Akazawa, Y., Hasegawa, T., et al. (2017). Piezo Type Mechanosensitive Ion Channel Component 1 Functions as a Regulator of the Cell Fate Determination of Mesenchymal Stem Cells. *Sci. Rep.* 7 (1), 17696. doi:10.1038/s41598-017-18089-0

Sumanasinghe, R. D., Pfeiler, T. W., Monteiro-Riviere, N. A., and Loboa, E. G. (2009). Expression of Proinflammatory Cytokines by Human Mesenchymal Stem Cells in Response to Cyclic Tensile Strain. *J. Cel. Physiol.* 219 (1), 77–83. doi:10.1002/jcp.21653

Swain, S. M., and Liddle, R. A. (2021). Piezo1 Acts Upstream of TRPV4 to Induce Pathological Changes in Endothelial Cells Due to Shear Stress. *J. Biol. Chem.* 296, 100171. doi:10.1074/jbc.RA120.015059

Tan, J., Xu, X., Tong, Z., Lin, J., Yu, Q., Lin, Y., et al. (2015). Decreased Osteogenesis of Adult Mesenchymal Stem Cells by Reactive Oxygen Species under Cyclic Stretch: a Possible Mechanism of Age Related Osteoporosis. *Bone Res.* 3, 15003. doi:10.1038/boneres.2015.3

Thompson, M., Woods, K., Newberg, J., Oxford, J. T., and Uzer, G. (2020). Low-intensity Vibration Restores Nuclear YAP Levels and Acute YAP Nuclear Shuttling in Mesenchymal Stem Cells Subjected to Simulated Microgravity. *NPJ Microgravity* 6 (1), 35. doi:10.1038/s41526-020-00125-5

Timmins, P. A., and Wall, J. C. (1977). Bone Water. *Calc. Tis Res.* 23 (1), 1–5. doi:10.1007/bf02012759

Uda, Y., Azab, E., Sun, N., Shi, C., and Pajevic, P. D. (2017). Osteocyte Mechanobiology. *Curr. Osteoporos. Rep.* 15 (4), 318–325. doi:10.1007/s11914-017-0373-0

Uddin, S. M. Z., and Qin, Y.-X. (2013). Enhancement of Osteogenic Differentiation and Proliferation in Human Mesenchymal Stem Cells by a Modified Low Intensity Ultrasound Stimulation under Simulated Microgravity. *PLoS One* 8 (9), e73914. doi:10.1371/journal.pone.0073914

Uzer, G., Bas, G., Sen, B., Xie, Z., Birks, S., Olcum, M., et al. (2018). Sun-mediated Mechanical LINC between Nucleus and Cytoskeleton Regulates βcatenin Nuclear Access. *J. Biomech.* 74, 32–40. doi:10.1016/j.jbiomech.2018.04.013

Vafaei, R., Nassiri, S. M., and Siavashi, V. (2017). β3-Adrenergic Regulation of EPC Features through Manipulation of the Bone Marrow MSC Niche. *J. Cel. Biochem.* 118 (12), 4753–4761. doi:10.1002/jcb.26143

Wan, M., Li, C., Zhen, G., Jiao, K., He, W., Jia, X., et al. (2012). Injury-Activated Transforming Growth Factor β Controls Mobilization of Mesenchymal Stem Cells for Tissue Remodeling. *Stem Cells* 30 (11), 2498–2511. doi:10.1002/stem.1208

Wang, C., Shan, S., Wang, C., Wang, J., Li, J., Hu, G., et al. (2017). Mechanical Stimulation Promote the Osteogenic Differentiation of Bone Marrow Stromal Cells through Epigenetic Regulation of Sonic Hedgehog. *Exp. Cel Res.* 352 (2), 346–356. doi:10.1016/j.yexcr.2017.02.021

Wang, L., You, X., Lotinun, S., Zhang, L., Wu, N., and Zou, W. (2020). Mechanical Sensing Protein PIEZO1 Regulates Bone Homeostasis via Osteoblast-Osteoclast Crosstalk. *Nat. Commun.* 11 (1), 282. doi:10.1038/s41467-019-14146-6

Wang, X., Li, X., Li, J., Zhai, L., Liu, D., Abdurahman, A., et al. (2021). Mechanical Loading Stimulates Bone Angiogenesis through Enhancing Type H Vessel Formation and Downregulating Exosomal miR-214-3p from Bone Marrow-derived Mesenchymal Stem Cells. *FASEB j.* 35 (1), e21150. doi:10.1096/fj.202001080RR

Wei, F.-Y., Chow, S. K., Chow, S., Leung, K.-S., Qin, J., Guo, A., et al. (2016). Low-magnitude High-Frequency Vibration Enhanced Mesenchymal Stem Cell Recruitment in Osteoporotic Fracture Healing through the SDF-1/CXCR4 Pathway. *eCM* 31, 341–354. doi:10.22203/ecm.v031a22

Wei, F.-Y., Leung, K.-S., Li, G., Qin, J., Chow, S. K.-H., Huang, S., et al. (2014). Low Intensity Pulsed Ultrasound Enhanced Mesenchymal Stem Cell Recruitment through Stromal Derived Factor-1 Signaling in Fracture Healing. *PLoS One* 9 (9), e106722. doi:10.1371/journal.pone.0106722

Woo, S. L., Kuei, S. C., Amiel, D., Gomez, M. A., Hayes, W. C., White, F. C., et al. (1981). The Effect of Prolonged Physical Training on the Properties of Long Bone. *J. Bone Jt. Surg.* 63 (5), 780–787. doi:10.2106/00004623-198163050-00013

Wysocki, A., Butler, M., Shamliyan, T., and Kane, R. L. (2011). Whole-body Vibration Therapy for Osteoporosis: State of the Science. *Ann. Intern. Med.* 155 (10), 680w206–686613. doi:10.7326/0003-4819-155-10-201111150-00006

Xiang, Y. H., Shao, M. F., Song, Y., Yang, Z., Chen, X. D., and Fu, Q. (2012). Effect of Cytoskeleton Reorganization Inhibition on the Activation of Extracellular Signal-Regulated Kinase in Osteoblasts by Fluid Shear Stress. *Zhonghua Kou Qiang Yi Xue Za Zhi* 47 (11), 680–683. doi:10.3760/cma.j.issn.1002-0098.2012.11.010

Xing, Z., Lu, C., Hu, D., Yu, Y.-y., Wang, X., Colnot, C., et al. (2010). Multiple Roles for CCR2 during Fracture Healing. *Dis. Model. Mech.* 3 (7-8), 451–458. doi:10.1242/dmm.003186

Xue, R., and Cartmell, S. (2020). A Simple *In Vitro* Biomimetic Perfusion System for Mechanotransduction Study. *Sci. Tech. Adv. Mater.* 21 (1), 635–640. doi:10.1080/14686996.2020.1808432

Yan, Y., Wang, L., Ge, L., and Pathak, J. L. (2020). Osteocyte-Mediated Translation of Mechanical Stimuli to Cellular Signaling and its Role in Bone and Non-bone-related Clinical Complications. *Curr. Osteoporos. Rep.* 18 (1), 67–80. doi:10.1007/s11914-020-00564-9

Yoneda, M., Suzuki, H., Hatano, N., Nakano, S., Muraki, Y., Miyazawa, K., et al. (2019). PIEZO1 and TRPV4, Which Are Distinct Mechano-Sensors in the Osteoblastic MC3T3-E1 Cells, Modify Cell-Proliferation. *Ijms* 20 (19), 4960. doi:10.3390/ijms20194960

Yourek, G., McCormick, S. M., Mao, J. J., and Reilly, G. C. (2010). Shear Stress Induces Osteogenic Differentiation of Human Mesenchymal Stem Cells. *Regenerative Med.* 5 (5), 713–724. doi:10.2217/rme.10.60

Yu, W., Chen, C., Kou, X., Sui, B., Yu, T., Liu, D., et al. (2021). Mechanical Force-Driven TNFα Endocytosis Governs Stem Cell Homeostasis. *Bone Res.* 8 (1), 44. doi:10.1038/s41413-020-00117-x

Yue, D., Zhang, M., Lu, J., Zhou, J., Bai, Y., and Pan, J. (2019). The Rate of Fluid Shear Stress Is a Potent Regulator for the Differentiation of Mesenchymal Stem Cells. *J. Cel Physiol* 234, 16312–16319. doi:10.1002/jcp.28296

Zhang, H., Kay, A., Forsyth, N. R., Liu, K.-K., and El Haj, A. J. (2012). Gene Expression of Single Human Mesenchymal Stem Cell in Response to Fluid Shear. *J. Tissue Eng.* 3 (1), 204173141245198. doi:10.1177/2041731412451988

Zhang, P., Liu, X., Guo, P., Li, X., He, Z., Li, Z., et al. (2021). Effect of Cyclic Mechanical Loading on Immunoinflammatory Microenvironment in Biofabricating Hydroxyapatite Scaffold for Bone Regeneration. *Bioactive Mater.* 6 (10), 3097–3108. doi:10.1016/j.bioactmat.2021.02.024

Zhang, Y. P., Qin, F., Wu, C. J., Li, Y. R., Chen, R., Shao, M. F., et al. (2009). Effects of LIMK2 RNA Interference on the Mechanosensitivity of C-Fos Gene in Osteoblast. *Zhonghua Yi Xue Za Zhi* 89 (44), 3143–3146. doi:10.3760/cma.j.issn.0376-2491.2009.44.012

Zhao, W., Tang, Y., Yang, Y., Wang, M., and Yu, H. (2019). Low-Magnitude, High-Frequency Vibration Promotes Osteogenic Differentiation via Intensifying miRNA-335-5p Expression. *J. Environ. Pathol. Toxicol. Oncol.* 38 (3), 271–283. doi:10.1615/JEnvironPatholToxicolOncol.2019030625

Zhou, Y., Guan, X., Guan, X., Zhu, Z., Gao, S., Zhang, C., et al. (2011). Osteogenic Differentiation of Bone Marrow-Derived Mesenchymal Stromal Cells on Bone-Derived Scaffolds: Effect of Microvibration and Role of ERK1/2 Activation. *eCM* 22, 12–25. doi:10.22203/ecm.v022a02

Conflict of Interest: The authors declare that the research was conducted in the absence of any commercial or financial relationships that could be construed as a potential conflict of interest.

Publisher's Note: All claims expressed in this article are solely those of the authors and do not necessarily represent those of their affiliated organizations, or those of the publisher, the editors and the reviewers. Any product that may be evaluated in this article, or claim that may be made by its manufacturer, is not guaranteed or endorsed by the publisher.

frontiers in Cell and Developmental Biology

REVIEW
published: 25 January 2022
doi: 10.3389/fcell.2022.770931

Heterotopic Ossification: Clinical Features, Basic Researches, and Mechanical Stimulations

*Yili Xu[1], Mei Huang[1], Wenzhen He[1], Chen He[1], Kaixuan Chen[1], Jing Hou[1], Min Huang[1], Yurui Jiao[1], Ran Liu[1], Nanyu Zou[1], Ling Liu[1] and Changjun Li[1,2,3]**

[1]Department of Endocrinology, Endocrinology Research Center, The Xiangya Hospital of Central South University, Changsha, China, [2]National Clinical Research Center for Geriatric Disorders (Xiangya Hospital), Changsha, China, [3]Key Laboratory of Organ Injury, Aging and Regenerative Medicine of Hunan Province, Changsha, China

Heterotopic ossification (HO) is defined as the occurrence of extraskeletal bone in soft tissue. Although this pathological osteogenesis process involves the participation of osteoblasts and osteoclasts during the formation of bone structures, it differs from normal physiological osteogenesis in many features. In this article, the primary characteristics of heterotopic ossification are reviewed from both clinical and basic research perspectives, with a special highlight on the influence of mechanics on heterotopic ossification, which serves an important role in the prophylaxis and treatment of HO.

Keywords: heterotopic ossification, mechanical loading, bone, stem cell fate, bone formation

OPEN ACCESS

Edited by:
Airong Qian, Northwestern Polytechnical University, China

Reviewed by:
Chong Yin, Affiliated Hospital of North Sichuan Medical College, China

****Correspondence:***
Changjun Li
lichangjun@csu.edu.cn

Specialty section:
This article was submitted to Morphogenesis and Patterning, a section of the journal Frontiers in Cell and Developmental Biology

Received: *05 September 2021*
Accepted: *03 January 2022*
Published: *25 January 2022*

Citation:
Xu Y, Huang M, He W, He C, Chen K, Hou J, Huang M, Jiao Y, Liu R, Zou N, Liu L and Li C (2022) Heterotopic Ossification: Clinical Features, Basic Researches, and Mechanical Stimulations. Front. Cell Dev. Biol. 10:770931. doi: 10.3389/fcell.2022.770931

INTRODUCTION

Heterotopic ossification (HO) is a complicated pathologic process causing the formation of extra-skeletal bone in soft tissues, such as muscle, peri-articulations, ligaments, and tendons. It is commonly recognized as a complication after trauma, surgery, blast, spinal cord injury, and other stress damages (Shimono et al., 2011; Regard et al., 2013; Ranganathan et al., 2015; Wang et al., 2016). Heterotopic ossification was first labeled as "paraosteoarthropathy" by French physicians Dejerne and Ceillier, being a consequence of traumatic paraplegia of patients during World War I, and was further observed among soldiers returning from Iraq and Afghanistan (Naraghi et al., 1996; Forsberg et al., 2009; Potter et al., 2010; Forsberg et al., 2014). In severe cases, complete bony ankylosis as a result of HO is quite common, and more than 20% of patients appear overt dysfunction in soft-tissue, joint, or suffer from chronic pain; The HO morbidity of patients with traumatic brain injury almost reach 50% (Vanden Bossche and Vanderstraeten, 2005; Balboni et al., 2006; Zhang et al., 2014; Xu et al., 2018).

Inquiry about the underlying mechanism, such as cellular and mechanical processes, and earlier diagnoses as well as more effective treatments, is the hotspot of current research. Scientists analyze the proteomic biomarkers to identify early diagnostic indexes based on high-throughput mass spectrometry and antibody arrays; Doctors seek to develop efficacious prophylactic management and specific treatments via physical therapy, pharmaceutical intervention, operation, and radiation

Abbreviations: AHO, Albright's hereditary osteodystrophy; BMP, bone morphogenetic protein; BNB, blood-nerve barrier; FOP, fibrodysplasia ossificans progressive; HIFs, Hypoxia-inducible factors; HO, Heterotopic ossification; MSPCs, mesenchymal stromal/progenitor cells; NSAIDs, Nonsteroidal Antiinflammatory Drugs; POH, progressive osseous heteroplasia; TDPCs, tendon-derived progenitor cells; TMJA, temporomandibular joint ankylosis; TMJ, temporomandibular joint.

(Yuan et al., 2009; Coons and Godleski, 2013; Cheng et al., 2017; Gomez-Puerto et al., 2019; Botman et al., 2020). Moreover, patients with a high incidence of traumatic heterotopic ossification, such as fractures and hip joint arthroplasty, need to undergo prolonged postoperative immobilization or early rehabilitation exercises. Post-traumatic motion and mechanical loading are closely related to the occurrence of heterotopic ossification. The role of passive motion rehabilitative therapy after trauma, fracture, or invasive surgery for heterotopic ossification is still controversial. In this review, we elaborate on the clinical features and the fundamental biological mechanisms of HO, and for the first time summarize the separate influences of mechanical stimulations on HO based on up-to-date researches.

CLINICAL FEATURES OF HETEROTOPIC OSSIFICATION

Epidemiology

HO is often divided into three categories: traumatic, neurogenic, and genetic. The prevalence of traumatic-induced HO following burn injury has been reported to range from 0.2 to 4%, and up to 90% following the total hip joint arthroplasty or acetabular fractures (Cipriano et al., 2009; Maender et al., 2010; Rath et al., 2013; Medina et al., 2014; Medina et al., 2015). The predilection age of trauma-induced HO is 20–40 years old. Approximately half of HO occurs at this age. However, the other half of the HO could present dispersedly from infancy to late adulthood (Ackerman, 1958; Elmas and Shrestha, 2017; Xu et al., 2017; Meyers et al., 2019; Kaliya-Perumal et al., 2020). The morbidity of heterotopic ossification following central neurologic injury has been calculated to range from 10 to 53% (Teasell et al., 2010). Most studies regard traumatic brain-injured patients and spinal cord injured patients as the same category. And the prevalence of genetic HO, including fibrodysplasia ossificans progressiva (FOP), progressive osseous heteroplasia (POH), and Albright's hereditary osteodystrophy (AHO) (Shore and Kaplan, 2010), is extremely rare, affecting 1 in 2,000,000 people (Baujat et al., 2017). However, genetic HO is consensually regarded as the most severe HO disease in humans (Qi et al., 2017; Kaliya-Perumal et al., 2020). Male sex, the amount, and the type of motion could also raise the risk of HO. Men are slightly more vulnerable to HO with a sex ratio of 3:2 (Meyers et al., 2019), perhaps due to the various muscle mass, differential level of physical activity, repetitive mechanical stress working as "microtrauma", and distinct hormonal signaling pathways affecting osteogenesis (Ranganathan et al., 2015; Ko et al., 2016; Malca et al., 2018; Dowdell et al., 2020; Rüdiger et al., 2020).

Clinical Presentation

The typical clinical features of HO include the limited range of motion around the involved joint, complete bony ankylosis in severe cases, and deformity in the cervical spine, elbow, shoulder, fingers, jaw exostosis, or temporomandibular joint ankylosis (TMJA) (Zhao et al., 2020). HO could occur almost anywhere in the body, as long as it is associated with the periosteum. Typically, HO initiates away from the periosteum, and then fuse to the periosteum as a secondary feature (Meyers et al., 2019). But it is rare to observe HO in some anatomic tissues, such as the viscera or the diaphragm. This might be due to the lack of pluripotent stem cells in these sites or because these sites are not mechanically stimulated as often as the peri-articular areas prone to heterotopic ossification. Moreover, HO can only be detected as an asymptomatic finding on a radiograph. It is quite challenging to identify the potential biomarkers for early disease detection and monitoring, let alone the symptom present with complications that usually confound diagnosis (Crowgey et al., 2018). There are several ways to classify HO diseases. Four levels of classification for HO around the hip were set by Brooker to indicate the severity (Brooker et al., 1973). The Hastings and Graham classification system classifies HO at the elbow into three grades based on clinical and radiographic data (Hastings and Graham, 1994).

The presentations of genetic HO are more serious than traumatic-induced HO. Almost all FOP patients reported to date were caused by *Acvr1* mutation, and showing abnormality early. *Acvr1* gene locates on chromosome 2 (2q23-24) and encodes a bone morphogenetic protein (BMP) type 1 receptor, which is generally considered to be the major regulator in HO pathophysiology (Wang et al., 2016; Haupt et al., 2019; Meyers et al., 2019; Pearson et al., 2019; Stanley et al., 2019; Botman et al., 2020; Kaliya-Perumal et al., 2020). *Acvr1* mutation results in abnormally enhanced sensitivity of this receptor to BMPs, allowing for overexcitation of the BMP/SMAD pathway and heterotopic ossification. The typical feature of FOP is multiple skeletal deformities, involving fingers, toes, and cervical spine, and eventually resulting in pain, movement, and function limitation. POH is a genetic HO caused by inactivating mutations in the *GNAS1* gene, which result in decreased expression or function of the alpha subunit of the stimulatory G protein (Gsα) of adenylyl cyclase (Zhang et al., 2018). POH is characterized by intramembranous and cutaneous ossification, and could occur on the ear or fingers as an atypical phenotype (Kaplan et al., 1994; Zhang et al., 2018).

However, HO may be alleviated by physical intervention for traumatic-induced patients such as immobilization or Long-term bedridden. Doctors routinely use immobilization for extremity trauma patients (Kunz et al., 2014). But the mechanism that how immobilization protects the injury site reduces pain and improves healing remains unknown (Huber et al., 2020). Conversely, heterotopic ossification may become more severe in patients with insufficient immobilization and bed rest after fracture injury or joint surgery.

Clinical Risk Factors

Physical Factors

There is a positive correlation between the formation of heterotopic ossification and force application. People who are over-exercised are more likely to develop heterotopic ossification (Jones et al., 2019). The explanation may be that more active people also have a higher probability of injury, excessive stretching of soft tissues leads to abnormal activation and

differentiation of stem cells in local tissues, or that greater muscle mass leads to mechanical signal stimulation (Coons and Godleski, 2013; Dowdell et al., 2020; Rüdiger et al., 2020). Manifestations of heterotopic ossification due to mechanical stimulation can also occur in the temporomandibular joint (TMJ). Disturbance of occlusal forces will lead to TMJ disorder, while chronic abnormal forces and malposition of the joint will lead to heterotopic ossification of the TMJ (Jensen et al., 2010). Mechanics-based two- and three-dimensional finite element analysis and clinical findings indicate that the occurrence of heterotopic ossification after cervical total intervertebral disc replacement is characterized by a strong correlation with regional stress. Compressive force induces HO on the uncovered vertebral endplates, while shear force causes HO in the anterior upper and lower parts of vertebrae (Ganbat et al., 2014; Ganbat et al., 2016).

It is also quite common to apply some physical interventions, such as immobilization, physical therapy, intermittent activity, or massage for convalescent patients. However, the effect of those physical interventions on HO remains controversial. The transitory periods of forcible passive movements on immobilized arthrosis could produce HO in the soft tissues around the arthrosis within two to 5 weeks (O'Connor, 1998; Michelsson and Rauschning, 1983). The bone volume of HO was positively correlated with the duration of chronic bed rest and the frequency of forcible movement. Interestingly, HO was not induced when the limbs were merely immobilized without forcible movement, or merely passively movement without immobilization (Ellerin et al., 1999). Some researchers found that immobilization totally inhibited the formation of HO (Huber et al., 2020). Some researchers reported that surgery combined with postoperative physical therapy and rehabilitation program was effective to treat patients with heterotopic ossification of the elbow (Salazar et al., 2014). The reasons for this variation may be due to differences in the specific method, time of implementation, and duration of immobilization or rehabilitation exercises, besides the differences in the patients themselves collected in those clinical studies. It takes approximately 5–6 weeks for CT-visible heterotopic ossification to develop at the injury site, and early rehabilitation activities performed at inappropriate time points or approaches that apply additional forces to the injury site will likely result in a higher incidence of HO.

Spinal Cord and Brain Injuries

Neurogenic HO usually occurs following central nerve injuries, such as spinal cord injuries and cerebral lesions, and the prevalence has been reported to range from 10 to 53% (Teasell et al., 2010; Ranganathan et al., 2015). However, the mechanism that how the nervous system regulates HO formation remains incompletely understood. It has been demonstrated that peripheral neurotransmitters influence osteoblast formation, and the cortical bone density can be modulated by mechanistic-neural pathways (Huang et al., 2019; Zhu et al., 2019). Central neural signaling could precisely modulate bone metabolism and homeostasis. Leptin, as well as neuropeptide Y and cannabinoids, play an important role in the neural regulation of bone (Idris et al., 2005; Yue et al., 2016). However, it is unclear whether neural regulation of osteogenesis and osteolysis occurs in the same way as heterotopic ossification. The current researches are primarily devoted to the findings that osteogenic precursor cells in heterotopic ossification originate from the endoneurium and are strongly associated with local neuroinflammation leading to the blood-nerve barrier (BNB) penetration (Lazard et al., 2015; Olmsted-Davis et al., 2017; Davis et al., 2018). In general, thoracic and cervical spine injury can lead to more severe heterotopic ossification, which usually develops caudally at the level of injury, most commonly in the hip joint (Brady et al., 2018). Unlike spinal cord injuries, brain injuries often cause generalized heterotopic ossification, including hip, knee, and elbow or shoulder joints (Garland, 1988).

Empyrosis

In the case of burn patients, in addition to the typical clinical phenomenon of thermal injury, the occurrence of heterotopic ossification is also frequently observed. Heterotopic ossification is highly probable when the burned area is more than 20% of the body surface area (Mujtaba et al., 2019). In addition to the burn-induced cascade reaction that promotes heterotopic ossification formation, the scar tissue that forms around the periarticular will also limit the range of motion of the joint, which in turn may simultaneously influence heterotopic ossification from a biomechanical approach. Theoretically, the inflammatory cascades due to burns promote heterotopic ossification; the limited fixation due to burning scars may inhibit heterotopic ossification, or the mechanical force from small movements pulls on a large area of tissue due to scars, thus promoting heterotopic ossification. Furthermore, limited joint motion due to scar tissue may also confuse the clinical diagnosis of heterotopic ossification, which could also lead to restricted joint motion. Distinguishing between the two commonly relies on radiographic studies (Suito et al., 2018; Chen et al., 2019).

Surgery

Surgery that irritates the joint and its surrounding soft tissues may lead to the occurrence of heterotopic ossification. Following hip arthroplasty, the rate of heterotopic ossification occurrence could approach approximately 40% (Ranganathan et al., 2015). Surgery on the other joints, such as the knee, elbow, and temporomandibular joint, may also result in heterotopic ossification of the soft tissues surrounding them (Meyers et al., 2019). Surgery, especially invasive surgery, can lead to local tissue damage and pathologies such as ischemia and inflammation, which are high-risk factors predisposing to the development of heterotopic ossification. Generally, minimally invasive surgery (MIS), including MIS anterolateral (MIS-AL) and minimally invasive direct anterior approach (AMIS), could reduce the risk of HO compared with the standard modified anterolateral (STD-Watson-Jones) approach (Hürlimann et al., 2017).

Fracture

Fractures are an important risk factor for heterotopic ossification. Fractures usually result from trauma, and surgery to treat fractures is in turn invasive trauma to local tissues. HO following orthopedic injury occurs most frequently after acetabular fractures and elbow fractures. Interestingly, injury

severity score, sex, and fracture type do not affect this risk, but long-term mechanical ventilation is the specific risk of HO (Firoozabadi et al., 2014). This is perhaps because of the impact of mechanical ventilation itself on the patient, such as anoxia; or because mechanically ventilated patients are typically bedridden for long periods, which may influence the traditional regulation of bone metabolism and the formation of heterotopic ossification from the mechanism of mechanical signal stimulation.

Management and Treatment

Physical Therapy

The effect of physical therapy on heterotopic ossification is controversial, but physical factors, including postoperative rehabilitation exercises, joint immobilization, and prolonged bed rest, indeed influence heterotopic ossification. It has been shown that complete joint fixation can eliminate heterotopic ossification at the Achilles tendon in the mouse model (Huber et al., 2020). Others, however, believe that early postoperative exercise facilitates recovery and prevents the development of heterotopic ossification (Aronen et al., 2006; Ranganathan et al., 2015; Meyers et al., 2019). Physical therapy and continuous passive motion machines have been used for the postoperative management of total knee arthroplasty, for which a commonly encountered surgical complication is heterotopic ossification. Physical therapy has been found to be moderately beneficial at 3 months after total knee arthroplasty (Lowe et al., 2007; Manrique et al., 2015). A randomized controlled trial also found that physical therapy was superior for total hip replacement management (Mikkelsen et al., 2014). However, burn surgeons often find an increased incidence of HO in patients who are subjected to overly passive range of motion exercises at the elbow to prevent skin contracture (Meyers et al., 2019). The key to the discrepancy may lie in the duration and timing of the immobilization. In the early post-traumatic phase, immobilization facilitates the normal recovery of local tissues, while repetitive passive movements may lead to an aggravation of local micro-injuries, which in turn may lead to organization and ossification of soft tissues. However, in the late stage of trauma, the local micro-injury and inflammatory environment have been almost recovered, at this time the appropriate passive movement is conducive to the local tissue blood supply and physiological metabolic activities, and is beneficial to the normal recovery of soft tissues. On the contrary, long-term bed rest or immobilization may lead to the deterioration of local microcirculation status, and the abnormal local microenvironment may induce the aberrant differentiation of soft tissue stem cells into bone tissue, resulting in the occurrence of heterotopic ossification.

Pharmaceutical Prophylaxis

The development of traumatic heterotopic ossification, as previously mentioned, is in part secondary to surgery. It is necessary to take some appropriate clinical interventions to reduce the risk of postoperative heterotopic ossification. Currently, the preventive medications that are more routinely used for HO in clinical practice are NSAIDs and Bisphosphonates (Ranganathan et al., 2015; Meyers et al., 2019). Essentially, the origin of heterotopic ossification is the abnormal osteogenic differentiation of stem cells in soft tissues. NSAIDs could prevent heterotopic ossification by inhibiting the osteogenic differentiation of progenitor cells (Chang et al., 2007; Chang et al., 2009). However, the negative impact of NSAIDs on fracture healing while preventing heterotopic ossification has to be taken into account. Indomethacin increases the potential risk of long-bone nonunion after orthopedic injuries (Marquez-Lara et al., 2016; Duchman et al., 2019). Balancing the risk of heterotopic ossification with malunion fractures is the key to appropriate NSAID delivery.

Bisphosphonates are generally considered to be antiresorptive agents that induce osteoclast apoptosis and inhibit calcification. Yet some studies have indicated that it may have some preventive effect on heterotopic ossification, although this conclusion is still controversial (Vasileiadis et al., 2010; Zaman, 2012). Aside from the first generation, subsequent bisphosphonates generally only affect osteoclasts and thus are less likely to be able to inhibit the production of heterotopic ossification. However, bisphosphonates have indeed been found to be specifically effective in patients with burns and spinal cord injuries (Teasell et al., 2010; Ranganathan et al., 2015). This may be due to the anti-angiogenic effect of bisphosphonates, which reduces the occurrence of HO by depleting angiogenesis, or because the binding of bisphosphonates to calcium affects the mineralization of the bone matrix.

Some recent studies have also found that non-coding RNAs may have a therapeutic effect on heterotopic ossification, although the effect has yet to be demonstrated in large-scale clinical trials. MicroRNAs targeting DKK1 and vascular endothelial growth factor (VEGF), such as miR-17-5p, can alleviate the heterotopic ossification present in Ankylosing spondylitis (Qin et al., 2019). Similarly, microRNAs that can regulate osteogenic genes, such as miR-203, which targets RUNX2, can also inhibit heterotopic ossification (Tu et al., 2016). Further studies of these non-coding RNAs could contribute to the development of medicines that work precisely at the post-transcriptional level for the treatment of heterotopic ossification.

Radiation

Radiation therapy can be effective in preventing heterotopic ossification after hip arthroplasty. The incidence of heterotopic ossification without radiation after hip arthroplasty is up to 90%, while the rate decreases to about 25% after radiation therapy (Popovic et al., 2014). Appropriate prophylactic doses generally range from 400 to 800 cGy and are given 24 h before or 72 h after surgery, and 700 cGy (25%) administered postoperatively was more effective in preventing HO than 400 cGy (42%) (Popovic et al., 2014; Liu et al., 2017). Higher doses do not demonstrate increased prophylactic benefit, and may bring additional side effects, including progressive soft tissue contracture, delayed wound healing, non-union fracture, joint stiffness, potential oncogenesis, or inhibition of growth of hip implants (Hamid et al., 2010; Milakovic et al., 2015). However, the efficacy of radiation

TABLE 1 | Cells types contributing to heterotopic ossification.

Study	Cell types	Findings
Feng et al. (2020)	Tendon-derived progenitor cells (Ctsk-Cre)	Ctsk could label progenitor cells of HO in tendon
Kan et al. (2018)	Interstitial/perivascular cells (Gli1-Cre)	Gli1-Cre lineage cells contribute to endochondral HO
Agarwal et al. (2017)	Tendon/periosteum/fascia (Scx-Cre)	Scx-cre lineage cells contribute to trauma-induced and BMP-induced HO
Olmsted-Davis et al. (2017)	Endoneurium (Wnt1-CreERT)	PS^+ and $SP7^+$ cells from peripheral nerves contribute to HO
Dey et al. (2016)	Endothelial/bone marrow/muscle interstitial cells (Mx1-Cre)	Mx1-Cre lineage cells contribute to intramuscular HO
Agarwal et al. (2015)	Mesenchymal progenitor cells (Nfatc1-Cre)	ca-$ACVR1^{fx/WT}$/Nfatc1-Cre^+ mice develop heterotopic ossification
Regard et al. (2013)	Mesenchymal progenitor cells (Prx1-Cre; Dermo1-Cre; Ap2-Cre)	Loss of Gnas mice resulted in PHO
Kan et al. (2013)	Pericyte/adipocyte/connective tissue interstitium (Glast-CreERT)	Glast-creERT labeled progenitors contribute to HO at all stages
Medici et al. (2010)	Endothelium/muscle satellite cells (Tie2-Cre/VE-Cadherin-Cre)	Endothelium/muscle satellite-derived cells contribute to HO

prevention in joints other than the hip has not been adequately studied.

Surgery

For heterotopic ossification antecedent to Booker IV Classification, complete surgical resection is achievable as the aberrant bone is free-standing with the hard bone tissue at the joint. Surgical removal is the ultimate treatment for patients who have limited effectiveness with other treatments and are unable to be completely cured (Łęgosz et al., 2019). However, it should be considered that surgical resection itself is an invasive stimulus, which may lead to the recurrence of heterotopic ossification after surgery, especially in susceptible subjects. Otherwise, despite the successful removal of the heterotopic ossified tissue, there is still a risk of recurrence after the surgery.

BIOLOGICAL MECHANISMS OF HO

The type of ossification that occurs in heterotopic ossification differs depending on the origin of the HO. Among the hereditary HO, Progressive Osseous Heteroplasia (POH) and Albright hereditary osteodystrophy (AHO) are considered to be intramembranous ossification, while fibrodysplasia ossificans progressiva (FOP) is considered to be endochondral ossification (Kaplan and Shore, 2000). This is due to their different pathogenesis. In trauma-induced HO, it is generally accepted that this process occurs through endochondral osteogenesis (Wong et al., 2020). Although the precise mechanism has not been fully investigated, pathological staining such as SOFG on traumatic HO shows that cartilage formation occurs first and then ossification is formed based on it (Yu et al., 2021). However, it is worth exploring whether there is direct differentiation of MSC into osteogenic progenitor cells resulting in intramembranous ossification in traumatic HO. The single-cell sequencing results from the traumatic HO injury site showed that some of the MSCs differentiated into osteoblasts rather than chondrogenic cells (Huber et al., 2020). Moreover, this injury is usually accompanied by nerve and vascular damage. This osteogenesis of neuro- and vascular-derived cells may also affect the frequency of intramembranous vs. endochondral ossification (Wong et al., 2020).

Cell Precursors of HO

One of the most significant differences between pathological heterotopic ossification and physiological osteogenesis is the distinct cellular source. The cellular origin of physiological osteogenesis is the differentiation of preosteoblast, but the precursor cellular origin of pathological heterotopic ossification has not been fully investigated. **Table 1** summarizes the cell types that contribute to heterotopic ossification based on currently published studies. In general, the cellular origin of pathological osteogenesis is not limited to the osteoblast lineage, but potentially results from the pluripotent differentiation of a diverse range of stem cells.

To be more specific, Ctsk was previously found to be able to label osteoclasts and periosteum stem cells. Recently, a subgroup of tendon-derived progenitor cells (TDPCs) was also found to be labeled by Ctsk (Feng et al., 2020). TDPCs, as stem cells in tendon tissue, are capable of multidirectional differentiation and would differentiate towards osteogenesis under certain conditions resulting in heterotopic ossification. In addition, mesenchymal stem cells in tendon areas could also be activated to osteogenic differentiation, which can be labeled by Nfatc1-Cre, Prx1-Cre, and Dermo1-Cre. It is possible that some other cells with proliferative capacity may also shift to osteogenic differentiation in some conditions. For example, perivascular cells (Gli1-Cre), PS^+ and $SP7^+$ cells from peripheral nerves, and muscle satellite cells (Tie2-Cre/VE-Cadherin-Cre) all contribute to HO. In conclusion, the cellular origin of HO is relatively complicated, and a variety of cells have the potential to shift to osteogenic differentiation in response to some specific stimulus, which in turn promotes HO formation.

Inflammation and HO

Inflammation serves as an important microenvironmental alteration in the development of heterotopic ossification. Trauma leads to a state of local and systemic inflammation, resulting in elevated inflammatory cytokines, such as TNFα, IL-1β, IL-6, and MCP-1, which could cause abnormal activation of mesenchymal stem cells in the soft tissues (Sung Hsieh et al., 2017). Inflammation-associated cells, such as macrophages and mast cells, also accumulate at the site of trauma-induced heterotopic ossification and promote heterotopic ossification (Convente et al., 2018). Lymphoid tissues also contribute to the cellular niche in Heterotopic Ossification (Loder et al., 2016). The main role of inflammation is to turn MSCs, such

as normal fibroblast lineage, into the osteogenic lineage, initiating the onset of heterotopic ossification.

Hypoxia and HO

The hypoxic state of local tissues after trauma may also initiate heterotopic ossification. Regional tissue hypoxia causes the activation of Hypoxia-inducible factors (HIFs), consisting of 1 of 3 α subunits bound to HIFβ (Meyers et al., 2019). HIFs could increase the production of pro-angiogenic cytokines such as VEGF, facilitating localized pathological bone tissue formation (Dilling et al., 2010; Hwang et al., 2019). The inhibition of HIFs could attenuate HO formation in experimental models (Agarwal et al., 2016).

Signaling Pathways and HO

Most of the fundamental research on heterotopic ossification is presently based on traumatic and genetic mouse models. In general, hyperactivation of bone morphogenetic protein (BMP) and consequent cascading activation of activin type-1 receptor (ACVR1) is thought to lead to abnormal endochondral osteogenesis, resulting in heterotopic ossification. The dysregulation of Hedgehog (Hh) signaling also contributes to many HO. However, recent studies have suggested that this pathological osteogenic process may share similar biological mechanisms with physiological osteogeneses, such as RUNX2, a classical osteogenic transcription factor (Kim et al., 2020). CK2/HAUSP pathway is a critical regulator of RUNX2 stability because Casein kinase 2 (CK2) phosphorylates RUNX2 and recruits the deubiquitinase herpesvirus-associated ubiquitin-specific protease (HAUSP) to stabilize RUNX2 away from ubiquitin-dependent proteasomal degradation. Meanwhile, regional osteoclast activities are also enhanced during the formation of heterotopic ossification, as the formation of the bone marrow cavities depends on a dynamic balance between osteogenesis and bone resorption. Furthermore, osteogenic-osteoclastic crosstalk, such as the transforming growth factor-beta (TGF-β) released after augmented osteoclastic activity that recruits mesenchymal stromal/progenitor cells (MSPCs) in the HO microenvironment for bone remodeling activities, also plays an important role in heterotopic ossification (Wang et al., 2018). PDGF-BB concentration was also increased during HO progression. Therefore, the bone formation process of heterotopic ossification is different but correlated to that of normal physiological osteogenesis.

Some proteins that affect bone morphology and bone development also influence the formation of heterotopic ossification. Bone morphogenetic proteins (BMPs) are required for multiple developmental processes, including bone and cartilage formation (Kaliya-Perumal et al., 2020). BMPs bind to ACVR1, which locates on the cell membrane surface phosphorylating SMAD1/5/9(8). Phosphorylated SMAD1/5/9(8) combine with SMAD4 and import into the nucleus, regulating transcription that drives endochondral ossification (Nosho et al., 2020). When BMP receptors bonded with Activin A, SMAD2/3 is activated to regulate inflammation (Rautela et al., 2019). The occurrence of FOP is also associated with the R206H mutant substitution of *Acvr1*, enhancing the response to various BMP ligands (Alessi Wolken et al., 2018). Retinoic acid receptors (RARs) are morphogens that impact both osteogenesis and chondrogenesis. There is a hypothesis that RAR agonism could impede HO formation by preventing the differentiation of prechondrogenic cells, and was partly tested in a subcutaneous rBMP2-induced HO model in mice (Cash et al., 1997; Shimono et al., 2010; Riedl et al., 2020). The Hedgehog (Hh) pathway also plays an important role in HO. Hh protein inhibits the GPCR-like protein Smoothened (SMO) by binding to the Patched (PTCH1) receptor, leading to SMO aggregation in cilia and phosphorylation of the cytoplasmic tail. SMO mediates downstream signaling and induces GLI protein detachment from SUFU. GLI1 and GLI2 proteins translocate to the nucleus to activate the transcription of Hh target genes (Regard et al., 2013; Feng et al., 2020). From this viewpoint, it can be inferred that biomolecules such as microRNAs, LncRNAs, and exosomes could also regulate heterotopic ossification by influencing some specific key proteins that regulate bone morphology and development, but this remains to further study.

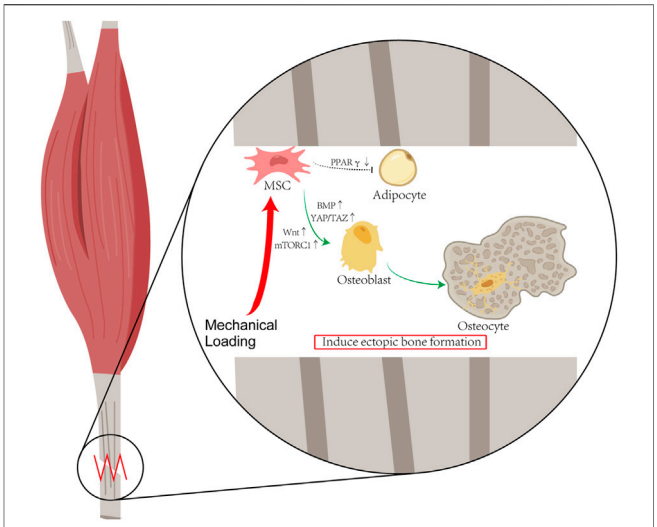

FIGURE 1 | Hypothesis of Mechanical Stimulation of HO: Mechanical stress initiates osteogenic differentiation of mesenchymal stem cells (MSCs) in soft tissue. Stem cell fate of MSCs shifts from favoring lipogenic cells to osteogenic cells under mechanical loading. According to the published literature about HO, after the mechanical loading, the activations of the YAP/TAZ and mTORC1 pathway enable MSCs to differentiate into osteoblasts, and the decrease in PPARγ expression reduces the differentiation of MSC into adipocytes.

MECHANICS AND HO

Mechanical Signals of HO

Heterotopic ossification can be modulated by mechanical signals. It is generally acknowledged that mechanical stress stimulation serves an important function in the physiological osteogenesis process. Osteocytes can sense local mechanical cues and thus induce bone formation, disuse-induced bone loss, and skeletal fragility (Qin et al., 2020). The primary mechanosensors in

osteocytes include osteocyte cytoskeleton, dendritic processes, integrin-based focal adhesions, connexin-based intercellular junctions, primary cilium, ion channels, and extracellular matrix (Uda et al., 2017). It is now generally accepted that the traditional regulation of bone metabolism is deeply affected by mechanical stimulation signals. Current studies suggest that heterotopic ossification, a pathological osteogenic process, is modulated by mechanical signals as well. Mechanical stress initiates osteogenic differentiation of mesenchymal stem cells (MSCs) in soft tissue. Stem cell fate of MSCs shifts from favoring lipogenic cells to osteogenic cells under mechanical loading (**Figure 1**).

In the genetic-induced heterotopic ossification murine model, *Acvr1* mutant cells change the local microenvironment, resulting in the skewing of the threshold for mechanical stimuli and becoming more sensitive to the fate of chondral/osteogenic lineages (Haupt et al., 2019). Stanley's study revealed that mechanistic signalings of *Acvr1* mutant cells in the soft matrix resemble that of non-mutant cells in the hard matrix, and are dependent on RhoA and YAP1 signaling (Stanley et al., 2019). Huber's study found that mechanical stress can be transmitted to mechanosignaling receptors on heterotopic ossified mesenchymal progenitor cells through the extracellular matrix and cell adhesion, such as through focal adhesion kinase signaling and nuclear translocation of the transcription coenzyme TAZ, which regulates the progression of heterotopic ossification (Huber et al., 2020). However, the specific mechanism of Acvr1 in the mechanical signaling process is not clear, and no literature suggests a direct action in the mechanical signaling cascades. Because mutations in Acvr1 result in increased sensitivity to BMP, it is reasonable to believe that the Acvr1 response to mechanical stimulation is BMP-dependent.

Early studies have found that BMP-2, 4, 6, and 7 are differentially expressed depending on the mechanical stimulation (Rui et al., 2011). However, how BMPs can sense mechanical signals has been unclear for a long time, and only recently some studies have made advances. BMP-2 signaling senses mechanical signs because of the cross-talk with YAP/TAZ at the transcriptional level. In C2C12 cells, it was shown that Smad1/5/8 can be phosphorylated and translocated into the nucleus in the presence of BMP-2 signaling alone. However, activation of osteogenic genes requires cytoskeletal tension-induced nuclear accumulation of YAP/TAZ. BMP-2 signaling responds to mechanical cues by sensing nucleocytoplasmic shuttling of YAP/TAZ (Wei et al., 2020).

YAP and TAZ (also known as WWTR1) are two protooncogene proteins that are widely known as mechanosensors and mechanotransducers in various cell types (Dupont et al., 2011). The link between YAP/TAZ and mechanical signals is extensively explored in physiological osteogenesis as well as in osteogenic lineage. YAP/TAZ translocates from the cytoplasm to the nucleus depending on ECM stiffness in MSCs (Panciera et al., 2017), and mechanical niches trigger YAP/TAZ translocation contributing to osteoblastogenesis (Xiong et al., 2018). MST1/2 complexes with the scaffolding protein MOB kinase activator 1 (MOB1) to phosphorylate many proteins involved in chromatin condensation, apoptosis, and proliferation regulation, including cytoplasmic large tumor suppressor kinases 1 and 2 (LATS1 and LATS2). Activated LATS1/2, in turn, binds to YAP/TAZ and phosphorylates its serine, resulting in its retention in the cytoplasm and non-entry into the nucleus for function (Kovar et al., 2020). This part of YAP/TAZ pathway can interact with multiple signaling pathways at different levels, such as Hippo. In the process of heterotopic ossification, mesenchymal stem cells in soft tissues could be activated for osteogenic differentiation and become osteoblast rather than fibroblast after mechanical stimulation by YAP/TAZ conduction. Moreover, once MSC pluripotent differentiation leads to the initiation of the osteogenic procedure, mechanical stimulation further promotes the proliferation and differentiation of osteoblasts, resulting in enhanced heterotopic ossification (Yu et al., 2018). Simultaneously, osteoclast, as well as bone resorption activity, can also be affected by mechanical stresses, and even osteoclast-osteoblast crosstalk based on PIEZO1 could occur in response to mechanical forces (Wang et al., 2020). However, it is still unclear whether these osteoclast and osteoblast characteristics of normal bone tissue are completely identical in heterotopic ossification.

LRP5/6 is a key receptor in the Wnt signaling pathway. Wnt signaling plays a central role in the mechanotransduction of bone. But the mechanisms by which wnt signaling senses mechanotransduction signals specifically may be multi-pathway and multi-level. YAP/TAZ is still an important part of the Wnt pathway to sense mechanical signals. At the cell membrane, YAP/TAZ binds to Axin on LRP6, allowing the recruitment of β-transducin repeatase containing E3 ubiquitin-protein ligase (BTRC) to the β-catenin disruption complex (Azzolin et al., 2014). In the cytoplasm, YAP/TAZ binds to the cytoplasmic Wnt signaling transducer disheveled segment polarity protein 1 (DVL1) and inhibits its phosphorylation, thereby abrogating its translocation to the nucleus (Barry et al., 2013). Serine phosphorylated YAP and TAZ can also bind directly to β-catenin (Zhou et al., 2017). In addition, it can also function as a transcriptional co-activator. How the Wnt pathway specifically senses mechanical signals in bone metabolism has not been completely understood, but there is no doubt that the wnt pathway plays an important role in the biomechanics of bone.

In addition, mTORC1 signaling pathway serves as a mechanosensor modulating HO. Rodgers found that mTORC1 could activate quiescent stem cells into an "alert state" thus responding quickly to injury and stress conditions (Rodgers et al., 2014). The activation of mTORC1 promotes chondrogenesis and osteogenesis. Several studies have demonstrated that mechanical loading could activate the mTORC1 signaling pathway via inducing the phosphorylation of p70 S6 kinase (Lin and Liu, 2019). Chen found mechanical loading modulated HO of the tendon through the mTORC1 signaling pathway, furthermore, low elongation mechanical loading attenuated HO, while high elongation mechanical loading accelerated HO *in vivo* (Chen et al., 2017). Stimulated by mechanistic signaling, mTORC1 activates Sirtuin 1 (Sirt1) in the nucleus. Sirt1 is a histone deacetylase that acts as a novel bone regulator and represses the expression of sclerostin gene SOST,

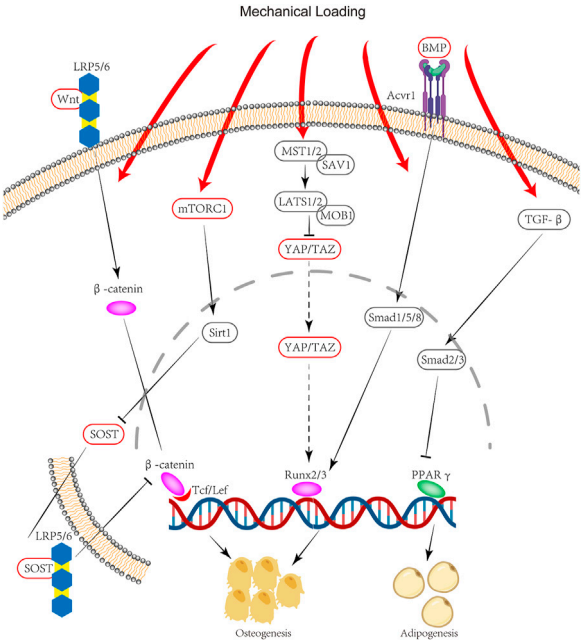

FIGURE 2 | Signaling pathway of HO due to mechanical stimulation: Mechanical stimulation through mTORC1 leads to an increase in Sirt1 translocation into the nucleus, followed by a decrease in SOST secretion. SOST can bind to LRP5/6 to inhibit β-catenin. Mechanical loading can also activate Runx2/3 gene expression through YAP/TAZ. Thus mechanical stimulation promotes osteogenic gene expression through mTORC1 and YAP/TAZ. Meanwhile, mechanical stimulation can inhibit PPARγ gene expression through the TGF-β pathway, thereby suppressing lipogenic differentiation. These combined effects lead to a stem cell fate shift.

which is usually regarded as a strong negative regulator of osteoblast differentiation and bone formation (Liu et al., 2019). SOST inhibits β-catenin and osteogenic gene expression after binding to LRP5/6. Therefore, rapamycin, a selective mTORC1 signaling pathway inhibitor, is a potential therapeutic agent for heterotopic ossification.

Mechanics and Stem Cell Fate

Mechanical interventions may affect HO formation by altering stem cell fate. Stem cells are able to sense their mechanical environments through various mechanosensors, including the cytoskeleton, focal adhesions, and primary cilia (Chen and Jacobs, 2013). The cytoskeletal tension could be generated by the interacts between myosin and actin, which is important for mechanically induced osteogenesis of stem cells. Focal adhesion is formed by the adapter proteins linking the cytoskeleton to integrins. Forces are transmitted based on these intact focal adhesions (Nardone et al., 2017). The primary cilium is a single, non-motile, antenna-like transmembrane structure, acting as a microdomain to promote biochemical signaling (Pala et al., 2017). Joint immobilization could reduce mechanotransduction signaling (Kunz et al., 2014). In the immobilized murine model, the fate of mesenchymal progenitor cells was altered. Mobile MPCs expressed more genes related to osteogenesis and chondrogenesis, such as *Sox9*, *Runx2*, *Spp1*, and differentiated more into osteogenic cells; immobile MPCs expressed more genes related to lipogenesis, e.g. *Fabp4*, *Pltp*, *Lrp1*, and differentiated more into lipogenic cells (Huber et al., 2020). In the osteogenic-lipogenic fate shifting of MSCs caused by mechanical stimulation, sclerostin signaling potentially serves as a significant regulator. Unloading makes the expression of the sclerostin increase, which downregulates two key osteogenic procedures: Wnt/β-catenin signaling and YAP/TAZ transcriptional activity. The crosstalks between Wnt/β-catenin and PPARγ influence the physiological balance between osteogenesis and adipogenesis (Benayahu et al., 2019). As the MSCs are mechanically stimulated and favor osteogenic differentiation, heterotopic ossification becomes severe. Conversely, when they favor lipogenic differentiation, the amount of heterotopic ossified bone decreases. Therefore, joint immobility after injury promotes adipogenesis rather than osteogenesis, leading to reduced HO formation. And the use of pharmacologic inhibitors altering mechanical signaling may prove to be an effective therapy that spontaneously induces adipogenesis at sites prone to osteogenesis. The accumulation of fatty tissue in the joint near the site of injury is much less severe than HO, leading to a more favorable outcome (McTighe and Chernev, 2014).

Mechanical loading has also been demonstrated to cause stem cell fate shift at the cellular level (**Figure 2**). Mechanical loading appears to favor osteogenesis whereas unloading conditions seem to promote adipogenesis. Passive stimuli including stiffness and viscoelasticity, as well as active stimuli including tensile/compressive stress and fluid shear stress, can affect cells through the extracellular matrix (Benayahu et al., 2019). Mechanical signals are conducted from the extracellular matrix through the cytoskeleton to regulate intracellular actions. Some important signaling pathways interact with mechanistic signals. For example, Wnt ligand binding to low-density lipoprotein receptor-related protein 5/6 (LRP5/6) coreceptors results in the translocation of β-catenin to the nucleus and the enhanced transcription of genes that govern osteogenesis, and its interaction with the Hippo pathway that governs the activity of YAP/TAZ, which is regarded as an important mechanistic signaling transcription factor (Benayahu et al., 2019; García de Herreros and Duñach, 2019). Even cells that already have terminally differentiated into the myogenic lineage may be reconverted to the osteoblast lineage under certain conditions: C2C12, a myoblast cell line, can be converted to osteoblasts under the combined effect of BMP and mechanical stimulation (Wei et al., 2020). Although these studies demonstrate that cells of other lineages are capable of osteogenic differentiation, it is not clear whether the same phenotype occurs *in vivo*, resulting in heterotopic ossification.

Beyond biological experiments, a significant influence of local loading on the formation of heterotopic ossification has been found through the mechanobiological algorithm system. By designing a computational model of physiology that takes into account both mechanical and biological factors, Rosenberg found that modifications to the mechanical environment significantly alter the shape and production of heterotopic bone. Adjustment of load orientation, skin material characteristics, and location of

maximum trauma resulted in four characteristic HO types. Simulation of negative pressure dressings and tourniquet application also served to highlight the behavioral characteristics of HO (Rosenberg and Bull, 2018). Still, the mechanobiological algorithm system needs further development to make it more compatible with the real world.

These basic studies suggest that mechanical signals contribute to the formation and development of heterotopic ossification, not only initiate heterotopic ossification through the activation of pluripotent differentiation of MSCs, but also influence the osteogenic program during HO by affecting osteocytes, osteoblasts, and osteoclasts. However, there are only a few studies related to mechanical stimulation and heterotopic ossification. Representative basic studies have only applied fixed models for attenuated mechanical stimulation, but elaborate force-added models also need to be investigated. Relevant clinical studies are even more lacking. Further studies in this direction would have guiding values for the development of new drug targets for the treatment of HO, as well as for the development of more effective clinical methods of physical therapy and prophylaxis for HO.

In summary, the effects of mechanics on heterotopic ossification could be considered from early, middle, and late stages, respectively. In the early stage of HO, mechanical stimulation may activate pluripotent differentiation of MSCs in soft tissues, e.g., mTORC1 could activate quiescent stem cells into an "alert state", and promote chondrogenesis and osteogenesis, leading to HO initiation. Mechanical stimulation can alter stem cell fate, causing chromatin regions around osteogenic genes to open. This results in more expression of osteogenic-related proteins and promotes stem cell differentiation toward osteogenesis. Clinically, early post-trauma immobilization can attenuate or even prevent heterotopic ossification. In the middle stage of HO, which means heterotopic ossification has been triggered and pathologic ossification is in the process of formation. Since physiological osteogenesis and pathological osteogenesis have some commonalities, they both require stem cells to differentiate into osteoblasts, and the eventual ossifications are dependent on the function of osteoblasts performing osteogenic functions. Many fundamental signaling pathway, such as CK2/HAUSP/RUNX2 are necessary for both physiologic bone formation and HO. It can be assumed that the effects of mechanics on HO may be similar to that on the osteogenesis process. From the clinical perspective, patients at this stage may still need as much bed rest as possible to avoid stress on the trauma site and to prevent pathological osteogenesis. Conversely, for the late stage, prolonged immobilization may instead lead to local tissue inflammation and hypoxia, both of which are risk factors for heterotopic ossification, and may lead to tissue ischemia and necrosis along with malfunctioning. Therefore, for patients potentially suffering from heterotopic ossification in the initial stages of injury, early and adequate immobilization is essential to avoid stress on the injured area. For those patients who have been adequately immobilized after trauma, appropriate rehabilitation exercises are recommended in the late stages to prevent heterotopic ossification as well as promote functional recovery.

SUMMARY

HO is a diverse pathologic process. We still do not fully understand the cellular origin, pathogenesis, and underlying mechanisms of HO, and have not yet developed a specific treatment for HO beyond surgical resection. HO as a pathological osteogenic activity involving pluripotent differentiation of stem cells has many remaining aspects to be explored, although it has similarities to physiological osteogenic activity in some ways. This paper reviews the features of heterotopic ossification according to the established literature, with particular emphasis on the effect of mechanical stimuli on HO. However, the specific biological mechanism of this effect needs to be further investigated.

AUTHOR CONTRIBUTIONS

CL contributed to concepts, review article revising, and final approval of article; YX draft the review article and prepared the figures; KC and CH helped in preparing the figures. MeH, WH, YJ, JH, MiH, NZ, LL, and RL and helped in the writing and submission of the article. All authors have read and agreed to the published version of the manuscript.

FUNDING

This work was supported by the National Key R&D Program of China (Grant No. 2019YFA0111900), the National Natural Science Foundation of China (Grant Nos 81922017, 81873669, 81802209), the Hunan Province Natural Science Foundation of China (Grant No. 2018JJ3863), Hunan Provincial Science and Technology Department (Grant No. 2018RS3030), the Innovation Driven Project of Central South University (Grant No. 20170033010017).

REFERENCES

Ackerman, L. V. (1958). Extra-Osseous Localized Non-neoplastic Bone and Cartilage Formation (So-Called Myositis Ossificans). *J. Bone Jt. Surg.* 40, 279–298. doi:10.2106/00004623-195840020-00004

Agarwal, S., Loder, S. J., Brownley, C., Eboda, O., Peterson, J. R., Hayano, S., et al. (2015). BMP Signaling Mediated by Constitutively Active Activin Type 1 Receptor (ACVR1) Results in Ectopic Bone Formation Localized to Distal Extremity Joints. *Develop. Biol.* 400, 202–209. doi:10.1016/j.ydbio.2015.02.011

Agarwal, S., Loder, S., Brownley, C., Cholok, D., Mangiavini, L., Li, J., et al. (2016). Inhibition of Hif1α Prevents Both Trauma-Induced and Genetic Heterotopic Ossification. *Proc. Natl. Acad. Sci. USA* 113, E338–E347. doi:10.1073/pnas.1515397113

Agarwal, S., Loder, S. J., Cholok, D., Peterson, J., Li, J., Breuler, C., et al. (2017). Scleraxis-Lineage Cells Contribute to Ectopic Bone Formation in Muscle and Tendon. *Stem Cells* 35, 705–710. doi:10.1002/stem.2515

Alessi Wolken, D. M., Idone, V., Hatsell, S. J., Yu, P. B., and Economides, A. N. (2018). The Obligatory Role of Activin A in the Formation of Heterotopic Bone in Fibrodysplasia Ossificans Progressiva. *Bone* 109, 210–217. doi:10.1016/j.bone.2017.06.011

Aronen, J. G., Garrick, J. G., Chronister, R. D., and McDevitt, E. R. (2006). Quadriceps Contusions: Clinical Results of Immediate Immobilization in 120 Degrees of Knee Flexion. *Clin. J. Sport Med.* 16, 383–387. doi:10.1097/01.jsm.0000244605.34283.94

Azzolin, L., Panciera, T., Soligo, S., Enzo, E., Bicciato, S., Dupont, S., et al. (2014). YAP/TAZ Incorporation in the β-Catenin Destruction Complex Orchestrates the Wnt Response. *Cell* 158, 157–170. doi:10.1016/j.cell.2014.06.013

Balboni, T. A., Gobezie, R., and Mamon, H. J. (2006). Heterotopic Ossification: Pathophysiology, Clinical Features, and the Role of Radiotherapy for Prophylaxis. *Int. J. Radiat. Oncol. Biol. Phys.* 65, 1289–1299. doi:10.1016/j.ijrobp.2006.03.053

Barry, E. R., Morikawa, T., Butler, B. L., Shrestha, K., de la Rosa, R., Yan, K. S., et al. (2013). Restriction of Intestinal Stem Cell Expansion and the Regenerative Response by YAP. *Nature* 493, 106–110. doi:10.1038/nature11693

Baujat, G., Choquet, R., Bouée, S., Jeanbat, V., Courouve, L., Ruel, A., et al. (2017). Prevalence of Fibrodysplasia Ossificans Progressiva (FOP) in France: an Estimate Based on a Record Linkage of Two National Databases. *Orphanet J. Rare Dis.* 12, 123. doi:10.1186/s13023-017-0674-5

Benayahu, D., Wiesenfeld, Y., and Sapir-Koren, R. (2019). How Is Mechanobiology Involved in Mesenchymal Stem Cell Differentiation toward the Osteoblastic or Adipogenic Fate? *J. Cel Physiol.* 234, 12133–12141. doi:10.1002/jcp.28099

Botman, E., Treurniet, S., Lubbers, W. D., Schwarte, L. A., Schober, P. R., Sabelis, L., et al. (2020). When Limb Surgery Has Become the Only Life-Saving Therapy in FOP: A Case Report and Systematic Review of the Literature. *Front. Endocrinol.* 11, 570. doi:10.3389/fendo.2020.00570

Brady, R. D., Shultz, S. R., McDonald, S. J., and O'Brien, T. J. (2018). Neurological Heterotopic Ossification: Current Understanding and Future Directions. *Bone* 109, 35–42. doi:10.1016/j.bone.2017.05.015

Brooker, A. F., Bowerman, J. W., Robinson, R. A., and Riley, L. H., Jr (1973). Ectopic Ossification Following Total Hip Replacement. *J. Bone Jt. Surg.* 55, 1629–1632. doi:10.2106/00004623-197355080-00006

Cash, D. E., Bock, C. B., Schughart, K., Linney, E., and Underhill, T. M. (1997). Retinoic Acid Receptor α Function in Vertebrate Limb Skeletogenesis: a Modulator of Chondrogenesis. *J. Cel Biol.* 136, 445–457. doi:10.1083/jcb.136.2.445

Chang, J.-K., Li, C.-J., Wu, S.-C., Yeh, C.-H., Chen, C.-H., Fu, Y.-C., et al. (2007). Effects of Anti-inflammatory Drugs on Proliferation, Cytotoxicity and Osteogenesis in Bone Marrow Mesenchymal Stem Cells. *Biochem. Pharmacol.* 74, 1371–1382. doi:10.1016/j.bcp.2007.06.047

Chang, J.-K., Li, C.-J., Liao, H.-J., Wang, C.-K., Wang, G.-J., and Ho, M.-L. (2009). Anti-inflammatory Drugs Suppress Proliferation and Induce Apoptosis through Altering Expressions of Cell Cycle Regulators and Pro-apoptotic Factors in Cultured Human Osteoblasts. *Toxicology* 258, 148–156. doi:10.1016/j.tox.2009.01.016

Chen, J. C., and Jacobs, C. R. (2013). Mechanically Induced Osteogenic Lineage Commitment of Stem Cells. *Stem Cel Res. Ther.* 4, 107. doi:10.1186/scrt318

Chen, G., Jiang, H., Tian, X., Tang, J., Bai, X., Zhang, Z., et al. (2017). Mechanical Loading Modulates Heterotopic Ossification in Calcific Tendinopathy through the mTORC1 Signaling Pathway. *Mol. Med. Rep.* 16, 5901–5907. doi:10.3892/mmr.2017.7380

Chen, J.-Y., Fu, C.-W., Ho, H.-Y., and Lu, Y.-C. (2019). Surgical Treatment of Postburn Heterotopic Ossification Around the Elbow. *Medicine (Baltimore)* 98, e14403. doi:10.1097/md.0000000000014403

Cheng, L., Long, H.-T., Sun, B.-H., Zhao, S.-s., and Zhu, Y. (2017). The Efficacy of a Multimodal Analgesia Protocol in Preventing Heterotopic Ossification after Acetabular Fractures Surgery. *Int. J. Clin. Pharm.* 39, 826–830. doi:10.1007/s11096-017-0476-9

Cipriano, C. A., Pill, S. G., and Keenan, M. A. (2009). Heterotopic Ossification Following Traumatic Brain Injury and Spinal Cord Injury. *J. Am. Acad. Orthop. Surg.* 17, 689–697. doi:10.5435/00124635-200911000-00003

Convente, M. R., Chakkalakal, S. A., Yang, E., Caron, R. J., Zhang, D., Kambayashi, T., et al. (2018). Depletion of Mast Cells and Macrophages Impairs Heterotopic Ossification in an Acvr1R206H Mouse Model of Fibrodysplasia Ossificans Progressiva. *J. Bone Miner Res.* 33, 269–282. doi:10.1002/jbmr.3304

Coons, D., and Godleski, M. (2013). Range of Motion Exercises in the Setting of Burn-Associated Heterotopic Ossification at the Elbow: Case Series and Discussion. *Burns* 39, e34–e38. doi:10.1016/j.burns.2012.10.014

Crowgey, E. L., Wyffels, J. T., Osborn, P. M., Wood, T. T., and Edsberg, L. E. (2018). A Systems Biology Approach for Studying Heterotopic Ossification: Proteomic Analysis of Clinical Serum and Tissue Samples. *Genomics Proteomics Bioinformatics* 16, 212–220. doi:10.1016/j.gpb.2018.04.006

Davis, E. L., Davis, A. R., Gugala, Z., and Olmsted-Davis, E. A. (2018). Is Heterotopic Ossification Getting Nervous?: The Role of the Peripheral Nervous System in Heterotopic Ossification. *Bone* 109, 22–27. doi:10.1016/j.bone.2017.07.016

Dey, D., Bagarova, J., Hatsell, S. J., Armstrong, K. A., Huang, L., Ermann, J., et al. (2016). Two Tissue-Resident Progenitor Lineages Drive Distinct Phenotypes of Heterotopic Ossification. *Sci. Transl. Med.* 8, 366ra163. doi:10.1126/scitranslmed.aaf1090

Dilling, C. F., Wada, A. M., Lazard, Z. W., Salisbury, E. A., Gannon, F. H., Vadakkan, T. J., et al. (2010). Vessel Formation Is Induced Prior to the Appearance of Cartilage in BMP-2-Mediated Heterotopic Ossification. *J. Bone Miner. Res.* 25, 1147–1156. doi:10.1359/jbmr.091031

Dowdell, J. E., Kim, J. S., Mikhail, C., Overley, S. C., Levin, J. M., McAnany, S. J., et al. (2020). The Rate of Heterotopic Ossification Following Cervical Disc Arthroplasty. *Spine* 45, E1197–E1202. doi:10.1097/brs.0000000000003524

Duchman, K. R., Lemmex, D. B., Patel, S. H., Ledbetter, L., Garrigues, G. E., and Riboh, J. C. (2019). The Effect of Non-steroidal Anti-inflammatory Drugs on Tendon-To-Bone Healing: A Systematic Review with Subgroup Meta-Analysis. *Iowa Orthop. J.* 39, 107–119.

Dupont, S., Morsut, L., Aragona, M., Enzo, E., Giulitti, S., Cordenonsi, M., et al. (2011). Role of YAP/TAZ in Mechanotransduction. *Nature* 474, 179–183. doi:10.1038/nature10137

Ellerin, B. E., Helfet, D., Parikh, S., Hotchkiss, R. N., Levin, N., Nisce, L., et al. (1999). Current Therapy in the Management of Heterotopic Ossification of the Elbow. *Am. J. Phys. Med. Rehabil.* 78, 259–271. doi:10.1097/00002060-199905000-00016

Elmas, F., and Shrestha, B. L. (2017). Eagle's Syndrome. *N. Engl. J. Med.* 377, e18. doi:10.1056/nejmicm1703542

Feng, H., Xing, W., Han, Y., Sun, J., Kong, M., Gao, B., et al. (2020). Tendon-derived Cathepsin K-Expressing Progenitor Cells Activate Hedgehog Signaling to Drive Heterotopic Ossification. *J. Clin. Invest.* 130, 6354. doi:10.1172/jci132518

Firoozabadi, R., O'Mara, T. J., Swenson, A., Agel, J., Beck, J. D., and Routt, M. (2014). Risk Factors for the Development of Heterotopic Ossification after Acetabular Fracture Fixation. *Clin. Orthop. Relat. Res.* 472, 3383–3388. doi:10.1007/s11999-014-3719-2

Forsberg, J. A., Pepek, J. M., Wagner, S., Wilson, K., Flint, J., Andersen, R. C., et al. (2009). Heterotopic Ossification in High-Energy Wartime Extremity Injuries: Prevalence and Risk Factors. *J. Bone Jt. Surg. Am.* 91, 1084–1091. doi:10.2106/jbjs.h.00792

Forsberg, J. A., Davis, T. A., Elster, E. A., and Gimble, J. M. (2014). Burned to the Bone. *Sci. Transl. Med.* 6, 255fs37. doi:10.1126/scitranslmed.3010168

Ganbat, D., Kim, K., Jin, Y. J., and Kim, Y. H. (2014). Heterotopic Ossification in Cervical Total Disk Replacement: a Finite Element Analysis. *Proc. Inst. Mech. Eng. H* 228, 200–205. doi:10.1177/0954411914522024

Ganbat, D., Kim, Y. H., Kim, K., Jin, Y. J., and Park, W. M. (2016). Effect of Mechanical Loading on Heterotopic Ossification in Cervical Total Disc Replacement: a Three-Dimensional Finite Element Analysis. *Biomech. Model. Mechanobiol.* 15, 1191–1199. doi:10.1007/s10237-015-0752-3

García de Herreros, A., and Duñach, M. (2019). Intracellular Signals Activated by Canonical Wnt Ligands Independent of GSK3 Inhibition and β-Catenin Stabilization. *Cells* 8, 1148. doi:10.3390/cells8101148

Garland, D. E. (1988). Clinical Observations on Fractures and Heterotopic Ossification in the Spinal Cord and Traumatic Brain Injured Populations. *Clin. Orthop. Relat. Res.* 233, 86–101. doi:10.1097/00003086-198808000-00011

Gomez-Puerto, M. C., Iyengar, P. V., García de Vinuesa, A., Ten Dijke, P., and Sanchez-Duffhues, G. (2019). Bone Morphogenetic Protein Receptor Signal Transduction in Human Disease. *J. Pathol.* 247, 9–20. doi:10.1002/path.5170

Hamid, N., Ashraf, N., Bosse, M. J., Connor, P. M., Kellam, J. F., Sims, S. H., et al. (2010). Radiation Therapy for Heterotopic Ossification Prophylaxis Acutely after Elbow Trauma. *J. Bone Jt. Surg Am* 92, 2032–2038. doi:10.2106/jbjs.i.01435

Hastings, H., 2nd, and Graham, T. J. (1994). The Classification and Treatment of Heterotopic Ossification about the Elbow and Forearm. *Hand Clin.* 10, 417–437. doi:10.1016/s0749-0712(21)01180-x

Haupt, J., Stanley, A., McLeod, C. M., Cosgrove, B. D., Culbert, A. L., Wang, L., et al. (2019). ACVR1R206H FOP Mutation Alters Mechanosensing and Tissue Stiffness during Heterotopic Ossification. *MBoC* 30, 17–29. doi:10.1091/mbc.e18-05-0311

Huang, S., Li, Z., Liu, Y., Gao, D., Zhang, X., Hao, J., et al. (2019). Neural Regulation of Bone Remodeling: Identifying Novel Neural Molecules and Pathways between Brain and Bone. *J. Cel Physiol.* 234, 5466–5477. doi:10.1002/jcp.26502

Huber, A. K., Patel, N., Pagani, C. A., Marini, S., Padmanabhan, K. R., Matera, D. L., et al. (2020). Immobilization after Injury Alters Extracellular Matrix and Stem Cell Fate. *J. Clin. Invest.* 130, 5444–5460. doi:10.1172/jci136142

Hürlimann, M., Schiapparelli, F. F., Rotigliano, N., Testa, E., Amsler, F., and Hirschmann, M. T. (2017). Influence of Surgical Approach on Heterotopic Ossification after Total Hip Arthroplasty - Is Minimal Invasive Better? A Case Control Study. *BMC Musculoskelet. Disord.* 18, 27. doi:10.1186/s12891-017-1391-x

Hwang, C., Marini, S., Huber, A. K., Stepien, D. M., Sorkin, M., Loder, S., et al. (2019). Mesenchymal VEGFA Induces Aberrant Differentiation in Heterotopic Ossification. *Bone Res.* 7, 36. doi:10.1038/s41413-019-0075-6

Idris, A. I., van 't Hof, R. J., Greig, I. R., Ridge, S. A., Baker, D., Ross, R. A., et al. (2005). Regulation of Bone Mass, Bone Loss and Osteoclast Activity by Cannabinoid Receptors. *Nat. Med.* 11, 774–779. doi:10.1038/nm1255

Jensen, A. W., Viozzi, C. F., and Foote, R. L. (2010). Long-term Results of Radiation Prophylaxis for Heterotopic Ossification in the Temporomandibular Joint. *J. Oral Maxillofac. Surg.* 68, 1100–1105. doi:10.1016/j.joms.2009.12.018

Jones, N. A., Bentley, B. C., and Wahl, L. (2019). Nonsurgical Management of Heterotopic Ossification in a Runner. *J. Orthop. Sports Phys. Ther.* 49, 676. doi:10.2519/jospt.2019.8491

Kaliya-Perumal, A. K., Carney, T. J., and Ingham, P. W. (2020). Fibrodysplasia Ossificans Progressiva: Current Concepts from Bench to Bedside. *Dis. Model. Mech.* 13, dmm046441. doi:10.1242/dmm.046441

Kan, L., Peng, C.-Y., McGuire, T. L., and Kessler, J. A. (2013). Glast-expressing Progenitor Cells Contribute to Heterotopic Ossification. *Bone* 53, 194–203. doi:10.1016/j.bone.2012.12.008

Kan, C., Chen, L., Hu, Y., Ding, N., Li, Y., McGuire, T. L., et al. (2018). Gli1-labeled Adult Mesenchymal Stem/progenitor Cells and Hedgehog Signaling Contribute to Endochondral Heterotopic Ossification. *Bone* 109, 71–79. doi:10.1016/j.bone.2017.06.014

Kaplan, F. S., and Shore, E. M. (2000). Progressive Osseous Heteroplasia. *J. Bone Miner Res.* 15, 2084–2094. doi:10.1359/jbmr.2000.15.11.2084

Kaplan, F. S., Hahn, G. V., and Zasloff, M. A. (1994). Heterotopic Ossification: Two Rare Forms and what They Can Teach Us. *J. Am. Acad. Orthop. Surg.* 2, 288–296. doi:10.5435/00124635-199409000-00007

Kim, J.-M., Yang, Y.-S., Park, K. H., Ge, X., Xu, R., Li, N., et al. (2020). A RUNX2 Stabilization Pathway Mediates Physiologic and Pathologic Bone Formation. *Nat. Commun.* 11, 2289. doi:10.1038/s41467-020-16038-6

Ko, J.-W. K., Tompson, J. D., Sholder, D. S., Black, E. M., and Abboud, J. A. (2016). Heterotopic Ossification of the Long Head of the Triceps after Reverse Total Shoulder Arthroplasty. *J. Shoulder Elbow Surg.* 25, 1810–1815. doi:10.1016/j.jse.2016.03.006

Kovar, H., Bierbaumer, L., and Radic-Sarikas, B. (2020). The YAP/TAZ Pathway in Osteogenesis and Bone Sarcoma Pathogenesis. *Cells* 9, 972. doi:10.3390/cells9040972

Kunz, R. I., Coradini, J. G., Silva, L. I., Bertolini, G. R. F., Brancalhão, R. M. C., and Ribeiro, L. F. C. (2014). Effects of Immobilization and Remobilization on the Ankle Joint in Wistar Rats. *Braz. J. Med. Biol. Res.* 47, 842–849. doi:10.1590/1414-431x20143795

Lazard, Z. W., Olmsted-Davis, E. A., Salisbury, E. A., Gugala, Z., Sonnet, C., Davis, E. L., et al. (2015). Osteoblasts Have a Neural Origin in Heterotopic Ossification. *Clin. Orthop. Relat. Res.* 473, 2790–2806. doi:10.1007/s11999-015-4323-9

Łęgosz, P., Otworowski, M., Sibilska, A., Starszak, K., Kotrych, D., Kwapisz, A., et al. (2019). Heterotopic Ossification: A Challenging Complication of Total Hip Arthroplasty: Risk Factors, Diagnosis, Prophylaxis, and Treatment. *Biomed. Res. Int.* 2019, 3860142. doi:10.1155/2019/3860142

Lin, S.-S., and Liu, Y.-W. (2019). Mechanical Stretch Induces mTOR Recruitment and Activation at the Phosphatidic Acid-Enriched Macropinosome in Muscle Cell. *Front. Cel Dev. Biol.* 7, 78. doi:10.3389/fcell.2019.00078

Liu, J. Z., Frisch, N. B., Barden, R. M., Rosenberg, A. G., Silverton, C. D., and Galante, J. O. (2017). Heterotopic Ossification Prophylaxis after Total Hip Arthroplasty: Randomized Trial of 400 vs 700 cGy. *J. Arthroplasty* 32, 1328–1334. doi:10.1016/j.arth.2016.10.030

Liu, W., Wang, Z., Yang, J., Wang, Y., Li, K., Huang, B., et al. (2019). Osteocyte TSC1 Promotes Sclerostin Secretion to Restrain Osteogenesis in Mice. *Open Biol.* 9, 180262. doi:10.1098/rsob.180262

Loder, S., Agarwal, S., Sorkin, M., Breuler, C., Li, J., Peterson, J., et al. (2016). Lymphatic Contribution to the Cellular Niche in Heterotopic Ossification. *Ann. Surg.* 264, 1174–1180. doi:10.1097/sla.0000000000001619

Lowe, C. J. M., Barker, K. L., Dewey, M., and Sackley, C. M. (2007). Effectiveness of Physiotherapy Exercise after Knee Arthroplasty for Osteoarthritis: Systematic Review and Meta-Analysis of Randomised Controlled Trials. *BMJ* 335, 812. doi:10.1136/bmj.39311.460093.be

Maender, C., Sahajpal, D., and Wright, T. W. (2010). Treatment of Heterotopic Ossification of the Elbow Following Burn Injury: Recommendations for Surgical Excision and Perioperative Prophylaxis Using Radiation Therapy. *J. Shoulder Elbow Surg.* 19, 1269–1275. doi:10.1016/j.jse.2010.05.029

Malca, N., Serror, K., Mimoun, M., Chatelain, S., Kaplan, J., Chaouat, M., et al. (2018). Our 35 years' Experience on Postburn Heterotopic Ossification: A Three-step Treatment. *Ann. de Chirurgie Plastique Esthétique* 63, 316–322. doi:10.1016/j.anplas.2017.11.009

Manrique, J., Gomez, M. M., and Parvizi, J. (2015). Stiffness after Total Knee Arthroplasty. *J. Knee Surg.* 28, 119–126. doi:10.1055/s-0034-1396079

Marquez-Lara, A., Hutchinson, I. D., Nuñez, F., Jr., Smith, T. L., and Miller, A. N. (2016). Nonsteroidal Anti-inflammatory Drugs and Bone-Healing: A Systematic Review of Research Quality. *JBJS Rev.* 4, e4. doi:10.2106/JBJS.RVW.O.00055

McTighe, S., and Chernev, I. (2014). Intramuscular Lipoma: a Review of the Literature. *Orthop. Rev. (Pavia)* 6, 5618. doi:10.4081/or.2014.5618

Medici, D., Shore, E. M., Lounev, V. Y., Kaplan, F. S., Kalluri, R., and Olsen, B. R. (2010). Conversion of Vascular Endothelial Cells into Multipotent Stem-like Cells. *Nat. Med.* 16, 1400–1406. doi:10.1038/nm.2252

Medina, A., Shankowsky, H., Savaryn, B., Shukalak, B., and Tredget, E. E. (2014). Characterization of Heterotopic Ossification in Burn Patients. *J. Burn Care Res.* 35, 251–256. doi:10.1097/bcr.0b013e3182957768

Medina, A., Ma, Z., Varkey, M., Liu, H., Iwashina, T., Ding, J., et al. (2015). Fibrocytes Participate in the Development of Heterotopic Ossification. *J. Burn Care Res.* 36, 394–404. doi:10.1097/bcr.0000000000000102

Meyers, C., Lisiecki, J., Miller, S., Levin, A., Fayad, L., Ding, C., et al. (2019). Heterotopic Ossification: A Comprehensive Review. *JBMR Plus* 3, e10172. doi:10.1002/jbm4.10172

Michelsson, J.-E., and Rauschning, W. (1983). Pathogenesis of Experimental Heterotopic Bone Formation Following Temporary Forcible Exercising of Immobilized Limbs. *Clin. Orthop. Relat. Res.* 176, 265–272. doi:10.1097/00003086-198306000-00039

Mikkelsen, L. R., Mechlenburg, I., Søballe, K., Jørgensen, L. B., Mikkelsen, S., Bandholm, T., et al. (2014). Effect of Early Supervised Progressive Resistance Training Compared to Unsupervised home-based Exercise after Fast-Track Total Hip Replacement Applied to Patients with Preoperative Functional Limitations. A Single-Blinded Randomised Controlled Trial. *Osteoarthr. Cartil.* 22, 2051–2058. doi:10.1016/j.joca.2014.09.025

Milakovic, M., Popovic, M., Raman, S., Tsao, M., Lam, H., and Chow, E. (2015). Radiotherapy for the Prophylaxis of Heterotopic Ossification: A Systematic Review and Meta-Analysis of Randomized Controlled Trials. *Radiother. Oncol.* 116, 4–9. doi:10.1016/j.radonc.2015.05.022

Mujtaba, B., Taher, A., Fiala, M. J., Nassar, S., Madewell, J. E., Hanafy, A. K., et al. (2019). Heterotopic Ossification: Radiological and Pathological Review. *Radiol. Oncol.* 53, 275–284. doi:10.2478/raon-2019-0039

Naraghi, F. F., DeCoster, T. A., Moneim, M. S., Miller, R. A., and Rivero, D. (1996). Heterotopic Ossification. *Orthopedics* 19, 145–152. doi:10.3928/0147-7447-19960201-10

Nardone, G., Oliver-De La Cruz, J., Vrbsky, J., Martini, C., Pribyl, J., Skládal, P., et al. (2017). YAP Regulates Cell Mechanics by Controlling Focal Adhesion Assembly. *Nat. Commun.* 8, 15321. doi:10.1038/ncomms15321

Nosho, S., Tosa, I., Ono, M., Hara, E. S., Ishibashi, K., Mikai, A., et al. (2020). Distinct Osteogenic Potentials of BMP-2 and FGF-2 in Extramedullary and Medullary Microenvironments. *Int. J. Mol. Sci.* 21, 7967. doi:10.3390/ijms21217967

O'Connor, J. P. (1998). Animal Models of Heterotopic Ossification. *Clin. Orthop. Relat. Res.*, 71–80.

Olmsted-Davis, E. A., Salisbury, E. A., Hoang, D., Davis, E. L., Lazard, Z., Sonnet, C., et al. (2017). Progenitors in Peripheral Nerves Launch Heterotopic Ossification. *Stem Cell Transl. Med.* 6, 1109–1119. doi:10.1002/sctm.16-0347

Pala, R., Alomari, N., and Nauli, S. M. (2017). Primary Cilium-dependent Signaling Mechanisms. *Int. J. Mol. Sci.* 18, 2272. doi:10.3390/ijms18112272

Panciera, T., Azzolin, L., Cordenonsi, M., and Piccolo, S. (2017). Mechanobiology of YAP and TAZ in Physiology and Disease. *Nat. Rev. Mol. Cel Biol.* 18, 758–770. doi:10.1038/nrm.2017.87

Pearson, H. B., Mason, D. E., Kegelman, C. D., Zhao, L., Dawahare, J. H., Kacena, M. A., et al. (2019). Effects of Bone Morphogenetic Protein-2 on Neovascularization during Large Bone Defect Regeneration. *Tissue Eng. A* 25, 1623–1634. doi:10.1089/ten.tea.2018.0326

Popovic, M., Agarwal, A., Zhang, L., Yip, C., Kreder, H. J., Nousiainen, M. T., et al. (2014). Radiotherapy for the Prophylaxis of Heterotopic Ossification: a Systematic Review and Meta-Analysis of Published Data. *Radiother. Oncol.* 113, 10–17. doi:10.1016/j.radonc.2014.08.025

Potter, B. K., Forsberg, J. A., Davis, T. A., Evans, K. N., Hawksworth, J. S., Tadaki, D., et al. (2010). Heterotopic Ossification Following Combat-Related Trauma. *J. Bone Jt. Surg Am* 92 (Suppl. 2), 74–89. doi:10.2106/JBJS.J.00776

Qi, Z., Luan, J., Zhou, X., Cui, Y., and Han, J. (2017). Fibrodysplasia Ossificans Progressiva: Basic Understanding and Experimental Models. *Intractable Rare Dis. Res.* 6, 242–248. doi:10.5582/irdr.2017.01055

Qin, X., Zhu, B., Jiang, T., Tan, J., Wu, Z., Yuan, Z., et al. (2019). miR-17-5p Regulates Heterotopic Ossification by Targeting ANKH in Ankylosing Spondylitis. *Mol. Ther. Nucleic Acids* 18, 696–707. doi:10.1016/j.omtn.2019.10.003

Qin, L., Liu, W., Cao, H., and Xiao, G. (2020). Molecular Mechanosensors in Osteocytes. *Bone Res.* 8, 23. doi:10.1038/s41413-020-0099-y

Ranganathan, K., Loder, S., Agarwal, S., Wong, V. W., Forsberg, J., Davis, T. A., et al. (2015). Heterotopic Ossification: Basic-Science Principles and Clinical Correlates. *J. Bone Jt. Surg.* 97, 1101–1111. doi:10.2106/jbjs.n.01056

Rath, E., Sherman, H., Sampson, T. G., Ben Tov, T., Maman, E., and Amar, E. (2013). The Incidence of Heterotopic Ossification in Hip Arthroscopy. *Arthrosc. J. Arthrosc. Relat. Surg.* 29, 427–433. doi:10.1016/j.arthro.2012.10.015

Rautela, J., Dagley, L. F., de Oliveira, C. C., Schuster, I. S., Hediyeh-Zadeh, S., Delconte, R. B., et al. (2019). Therapeutic Blockade of Activin-A Improves NK Cell Function and Antitumor Immunity. *Sci. Signal.* 12, eaat7527. doi:10.1126/scisignal.aat7527

Regard, J. B., Malhotra, D., Gvozdenovic-Jeremic, J., Josey, M., Chen, M., Weinstein, L. S., et al. (2013). Activation of Hedgehog Signaling by Loss of GNAS Causes Heterotopic Ossification. *Nat. Med.* 19, 1505–1512. doi:10.1038/nm.3314

Riedl, M., Witzmann, C., Koch, M., Lang, S., Kerschbaum, M., Baumann, F., et al. (2020). Attenuation of Hypertrophy in Human MSCs via Treatment with a Retinoic Acid Receptor Inverse Agonist. *Int. J. Mol. Sci.* 21, 1444. doi:10.3390/ijms21041444

Rodgers, J. T., King, K. Y., Brett, J. O., Cromie, M. J., Charville, G. W., Maguire, K. K., et al. (2014). mTORC1 Controls the Adaptive Transition of Quiescent Stem Cells from G0 to GAlert. *Nature* 510, 393–396. doi:10.1038/nature13255

Rosenberg, N. M., and Bull, A. M. J. (2018). Application of a Mechanobiological Algorithm to Investigate Mechanical Mediation of Heterotopic Bone in Transfemoral Amputees. *Sci. Rep.* 8, 14196. doi:10.1038/s41598-018-32414-1

Rüdiger, H., Dittrich, M., Robinson, J., Mansour, T., Schwab, T., Stadelmann, V., et al. (2020). The Impact of Heterotopic Ossification on Self-Reported Outcomes after Total Hip Arthroplasty Using the Direct Anterior Approach. *J. Bone Jt. Surg. Am.* 102, 91. doi:10.2106/JBJS.20.00071

Rui, Y. F., Lui, P. P. Y., Ni, M., Chan, L. S., Lee, Y. W., and Chan, K. M. (2011). Mechanical Loading Increased BMP-2 Expression Which Promoted Osteogenic Differentiation of Tendon-Derived Stem Cells. *J. Orthop. Res.* 29, 390–396. doi:10.1002/jor.21218

Salazar, D., Golz, A., Israel, H., and Marra, G. (2014). Heterotopic Ossification of the Elbow Treated with Surgical Resection: Risk Factors, Bony Ankylosis, and Complications. *Clin. Orthop. Relat. Res.* 472, 2269–2275. doi:10.1007/s11999-014-3591-0

Shimono, K., Morrison, T. N., Tung, W.-e., Chandraratna, R. A., Williams, J. A., Iwamoto, M., et al. (2010). Inhibition of Ectopic Bone Formation by a Selective Retinoic Acid Receptor α-agonist: A New Therapy for Heterotopic Ossification? *J. Orthop. Res.* 28, 271–277. doi:10.1002/jor.20985

Shimono, K., Tung, W.-e., Macolino, C., Chi, A. H.-T., Didizian, J. H., Mundy, C., et al. (2011). Potent Inhibition of Heterotopic Ossification by Nuclear Retinoic Acid Receptor-γ Agonists. *Nat. Med.* 17, 454–460. doi:10.1038/nm.2334

Shore, E. M., and Kaplan, F. S. (2010). Inherited Human Diseases of Heterotopic Bone Formation. *Nat. Rev. Rheumatol.* 6, 518–527. doi:10.1038/nrrheum.2010.122

Stanley, A., Heo, S. j., Mauck, R. L., Mourkioti, F., and Shore, E. M. (2019). Elevated BMP and Mechanical Signaling through YAP1/RhoA Poises FOP Mesenchymal Progenitors for Osteogenesis. *J. Bone Miner Res.* 34, 1894–1909. doi:10.1002/jbmr.3760

Suito, M., Yuzuriha, S., Iwasawa, M., Yanagisawa, D., Kinjo, Y., Takashimizu, I., et al. (2018). Therapeutic Strategies for Elbow Ankylosis Due to Heterotopic Ossification in Patients with Severe burns. *JPRAS Open* 17, 24–30. doi:10.1016/j.jpra.2018.06.004

Sung Hsieh, H. H., Chung, M. T., Allen, R. M., Ranganathan, K., Habbouche, J., Cholok, D., et al. (2017). Evaluation of Salivary Cytokines for Diagnosis of Both Trauma-Induced and Genetic Heterotopic Ossification. *Front. Endocrinol.* 8, 74. doi:10.3389/fendo.2017.00074

Teasell, R. W., Mehta, S., Mehta, S., Aubut, J. L., Ashe, M. C., Sequeira, K., et al. (2010). A Systematic Review of the Therapeutic Interventions for Heterotopic Ossification after Spinal Cord Injury. *Spinal Cord* 48, 512–521. doi:10.1038/sc.2009.175

Tu, B., Liu, S., Yu, B., Zhu, J., Ruan, H., Tang, T., et al. (2016). miR-203 Inhibits the Traumatic Heterotopic Ossification by Targeting Runx2. *Cell Death Dis.* 7, e2436. doi:10.1038/cddis.2016.325

Uda, Y., Azab, E., Sun, N., Shi, C., and Pajevic, P. D. (2017). Osteocyte Mechanobiology. *Curr. Osteoporos. Rep.* 15, 318–325. doi:10.1007/s11914-017-0373-0

Vanden Bossche, L., and Vanderstraeten, G. (2005). Heterotopic Ossification: a Review. *J. Rehabil. Med.* 37, 129–136. doi:10.1080/16501970510027628

Vasileiadis, G. I., Sakellariou, V. I., Kelekis, A., Galanos, A., Soucacos, P. N., Papagelopoulos, P. J., et al. (2010). Prevention of Heterotopic Ossification in Cases of Hypertrophic Osteoarthritis Submitted to Total Hip Arthroplasty. Etidronate or Indomethacin? *J. Musculoskelet. Neuronal. Interact* 10, 159–165.

Wang, G., Kang, Y., Chen, F., and Wang, B. (2016). Cervical Intervertebral Disc Calcification Combined with Ossification of Posterior Longitudinal Ligament in An-11-Year Old Girl: Case Report and Review of Literature. *Childs Nerv. Syst.* 32, 381–386. doi:10.1007/s00381-015-2840-1

Wang, X., Li, F., Xie, L., Crane, J., Zhen, G., Mishina, Y., et al. (2018). Inhibition of Overactive TGF-β Attenuates Progression of Heterotopic Ossification in Mice. *Nat. Commun.* 9, 551. doi:10.1038/s41467-018-02988-5

Wang, L., You, X., Lotinun, S., Zhang, L., Wu, N., and Zou, W. (2020). Mechanical Sensing Protein PIEZO1 Regulates Bone Homeostasis via Osteoblast-Osteoclast Crosstalk. *Nat. Commun.* 11, 282. doi:10.1038/s41467-019-14146-6

Wei, Q., Holle, A., Li, J., Posa, F., Biagioni, F., Croci, O., et al. (2020). BMP-2 Signaling and Mechanotransduction Synergize to Drive Osteogenic Differentiation via YAP/TAZ. *Adv. Sci.* 7, 1902931. doi:10.1002/advs.201902931

Wong, K. R., Mychasiuk, R., O'Brien, T. J., Shultz, S. R., McDonald, S. J., and Brady, R. D. (2020). Neurological Heterotopic Ossification: Novel Mechanisms, Prognostic Biomarkers and Prophylactic Therapies. *Bone Res.* 8, 42. doi:10.1038/s41413-020-00119-9

Xiong, J., Almeida, M., and O'Brien, C. A. (2018). The YAP/TAZ Transcriptional Co-activators Have Opposing Effects at Different Stages of Osteoblast Differentiation. *Bone* 112, 1–9. doi:10.1016/j.bone.2018.04.001

Xu, J., Zeng, M., Xie, J., Wen, T., and Hu, Y. (2017). Cementless Total Hip Arthroplasty in Patients with Ankylosing Spondylitis. *Medicine (Baltimore)* 96, e5813. doi:10.1097/md.0000000000005813

Xu, R., Hu, J., Zhou, X., and Yang, Y. (2018). Heterotopic Ossification: Mechanistic Insights and Clinical Challenges. *Bone* 109, 134–142. doi:10.1016/j.bone.2017.08.025

Yu, K.-W., Yao, C.-C., Jeng, J.-H., Shieh, H.-Y., and Chen, Y.-J. (2018). Periostin Inhibits Mechanical Stretch-Induced Apoptosis in Osteoblast-like MG-63 Cells. *J. Formos. Med. Assoc.* 117, 292–300. doi:10.1016/j.jfma.2017.12.008

Yu, T., Zhang, J., Zhu, W., Wang, X., Bai, Y., Feng, B., et al. (2021). Chondrogenesis Mediates Progression of Ankylosing Spondylitis through Heterotopic Ossification. *Bone Res.* 9, 19. doi:10.1038/s41413-021-00140-6

Yuan, P., Wang, W.-C., Li, Z.-H., and Mao, X.-Z. (2009). Could Insertion of the Particles that Induce Osteolysis Be a New Treatment Option in Heterotopic Ossification? *Med. Hypotheses* 73, 27–28. doi:10.1016/j.mehy.2009.02.016

Yue, R., Zhou, B. O., Shimada, I. S., Zhao, Z., and Morrison, S. J. (2016). Leptin Receptor Promotes Adipogenesis and Reduces Osteogenesis by Regulating Mesenchymal Stromal Cells in Adult Bone Marrow. *Cell Stem Cell* 18, 782–796. doi:10.1016/j.stem.2016.02.015

Zaman, S. R. (2012). Heterotopic Ossification of the Elbows in a Major Petrol Burn. *BMJ Case Rep.* 2012. doi:10.1136/bcr.03.2012.6027

Zhang, X., Jie, S., Liu, T., and Zhang, X. (2014). Acquired Heterotopic Ossification in Hips and Knees Following Encephalitis: Case Report and Literature Review. *BMC Surg.* 14, 74. doi:10.1186/1471-2482-14-74

Zhang, S.-D., Xie, Z.-l., Zhang, K.-Q., Nh-Tseung, K., and Zhao, J.-J. (2018). Progressive Osseous Heteroplasia in a Chinese Infant and a Novel Mutation in the GNAS Gene. *J. Eur. Acad. Dermatol. Venereol.* 32, e209–e211. doi:10.1111/jdv.14743

Zhao, Y., Ouyang, N., Chen, L., Zhao, H., Shen, G., and Dai, J. (2020). Stimulating Factors and Origins of Precursor Cells in Traumatic Heterotopic Ossification Around the Temporomandibular Joint in Mice. *Front. Cel Dev. Biol.* 8, 445. doi:10.3389/fcell.2020.00445

Zhou, X., Chadarevian, J. P., Ruiz, B., and Ying, Q.-L. (2017). Cytoplasmic and Nuclear TAZ Exert Distinct Functions in Regulating Primed Pluripotency. *Stem Cel Rep.* 9, 732–741. doi:10.1016/j.stemcr.2017.07.019

Zhu, S., Zhu, J., Zhen, G., Hu, Y., An, S., Li, Y., et al. (2019). Subchondral Bone Osteoclasts Induce Sensory Innervation and Osteoarthritis Pain. *J. Clin. Invest.* 129, 1076–1093. doi:10.1172/jci121561

Conflict of Interest: The authors declare that the research was conducted in the absence of any commercial or financial relationships that could be construed as a potential conflict of interest.

Publisher's Note: All claims expressed in this article are solely those of the authors and do not necessarily represent those of their affiliated organizations, or those of the publisher, the editors and the reviewers. Any product that may be evaluated in this article, or claim that may be made by its manufacturer, is not guaranteed or endorsed by the publisher.

frontiers in Cell and Developmental Biology

ORIGINAL RESEARCH
published: 08 February 2022
doi: 10.3389/fcell.2022.831894

Uncovering Hidden Mechanisms of Different Prescriptions Treatment for Osteoporosis *via* Novel Bioinformatics Model and Experiment Validation

Yujie Liu[1,2†], Qinwen Liu[1,2†], Chuanhui Yin[1,2†], Yi Li[3], Jie Wu[1,2], Quanlin Chen[1,2], Hailang Yu[1], Aiping Lu[4,5] and Daogang Guan[1,2]**

[1]Department of Biochemistry and Molecular Biology, School of Basic Medical Sciences, Southern Medical University, Guangzhou, China, [2]Guangdong Key Laboratory of Biochip Technology, Southern Medical University, Guangzhou, China, [3]Department of Radiology, Nanfang Hospital, Southern Medical University, Guangzhou, China, [4]Institute of Integrated Bioinformedicine and Translational Science, Hong Kong Baptist University, Hong Kong SAR, China, [5]Guangdong-Hong Kong-Macau Joint Lab on Chinese Medicine and Immune Disease Research, Guangzhou, China

OPEN ACCESS

Edited by:
Airong Qian,
Northwestern Polytechnical University, China

Reviewed by:
Youqiang Sun,
Guangzhou University of Chinese Medicine, China
Chunli Zheng,
Northwest University, China

***Correspondence:**
Aiping Lu
aipinglu@hkbu.edu.hk
Daogang Guan
guandg0929@hotmail.com

†These authors have contributed equally to this work

Specialty section:
This article was submitted to Morphogenesis and Patterning, a section of the journal Frontiers in Cell and Developmental Biology

Received: 09 December 2021
Accepted: 06 January 2022
Published: 08 February 2022

Citation:
Liu Y, Liu Q, Yin C, Li Y, Wu J, Chen Q, Yu H, Lu A and Guan D (2022) Uncovering Hidden Mechanisms of Different Prescriptions Treatment for Osteoporosis via Novel Bioinformatics Model and Experiment Validation. Front. Cell Dev. Biol. 10:831894. doi: 10.3389/fcell.2022.831894

Osteoporosis (OP) is a systemic disease susceptible to fracture due to the decline of bone mineral density and bone mass, the destruction of bone tissue microstructure, and increased bone fragility. At present, the treatments of OP mainly include bisphosphonates, hormone therapy, and RANKL antibody therapy. However, these treatments have observable side effects and cannot fundamentally improve bone metabolism. Currently, the prescription of herbal medicine and their derived proprietary Chinese medicines are playing increasingly important roles in the treatment of OP due to their significant curative effects and few side effects. Among these prescriptions, Gushukang Granules (GSK), Xianling Gubao Capsules (XLGB), and Er-xian Decoction (EXD) are widely employed at the clinic on therapy of OP, which also is in line with the compatibility principle of "different treatments for the same disease" in herbal medicine. However, at present, the functional interpretation of "different treatments for the same disease" in herbal medicine still lacks systematic quantitative research, especially on the detection of key component groups and mechanisms. To solve this problem, we designed a new bioinformatics model based on random walk, optimized programming, and information gain to analyze the components and targets to figure out the Functional Response Motifs (FRMs) of different prescriptions for the therapy of OP. The distribution of high relevance score, the number of reported evidence, and coverage of enriched pathways were performed to verify the precision and reliability of FRMs. At the same time, the information gain and target influence of each component was calculated, and the key component groups in all FRMs of each prescription were screened to speculate the potential action mode of different prescriptions on the same disease. Results show that the relevance score and the number of reported evidence of high reliable genes in FRMs were higher than those of the pathogenic genes of OP. Furthermore, the gene enrichment

Abbreviations: OP, osteoporosis; GSK, Gushukang Granules; XLGB, Xianling Gubao Capsules; EXD, Er-xian Decoction; SDFM, Significant Different Functional Modes; FRMs, FRM, Functional Response Motif; C-T network, component-target network.

pathways in FRMs could cover 79.6, 81, and 79.5% of the gene enrichment pathways in the component-target (C-T) network. Functional pathway enrichment analysis showed that GSK, XLGB, and EXD all treat OP through osteoclast differentiation (hsa04380), calcium signaling pathway (hsa04020), MAPK signaling pathway (hsa04010), and PI3K-Akt signaling pathway (hsa04151). Combined with experiments, the key component groups and the mechanism of "different treatments for the same disease" in the three prescriptions and proprietary Chinese medicines were verified. This study provides methodological references for the optimization and mechanism speculation of Chinese medicine prescriptions and proprietary Chinese medicines.

Keywords: osteoporosis, Gushukang Granules, Xianling Gubao Capsules, Er-xian Decoction, herbal medicine, functional response motif

INTRODUCTION

Osteoporosis (OP) is the most common bone disease characterized by decreased bone mass and degradation of bone microstructure. The main clinical manifestations are decreased bone density, chronic pain, decreased mobility, and so on (Miller, 2016). The common pathogenic factors include aging, decreased estrogen, nutritional disorders, poor living habits, and long-term use of steroids, anti-cancer drugs, diuretics, and so on. The main manifestations of OP are the decline of bone mineral density and bone quality. Its symptoms are most prone to systemic metabolic diseases such as fracture, low back pain, shortening of body length, bone pain, and even weakening of respiratory function (Zhao and Wang, 2003). It has a significant influence on the quality of life of patients and brings a heavy economic burden to families and society. OP is universal and can affect men and women of all races, especially older women who have passed menopause (Lane et al., 2000).

The current treatment drugs for OP mainly include estrogen (Stefanick, 2005), bisphosphonates (Delmas, 2005), calcitonin (Silverman, 2003), and parathyroid hormone (Neer et al., 2001; Srivastava and Deal, 2002). After treatment, the symptoms of osteoporosis patients will be alleviated, but these treatments cannot radically enhance bone metabolism and maintain the balance between osteoclasts and osteogenesis. In addition, the side effects of drugs also bring multiple risks to patients, including some side effects, even toxicity to the kidney, blood, and liver; gastrointestinal side effects; and immunosuppression (Tella and Gallagher, 2014). After taking estrogen receptor modulator drugs, it can also cause endometrial hyperplasia and uterine bleeding (Papapoulos and Makras, 2008).

Herbal medicine has been diffusely used at the clinic on OP therapy due to its fewer side effects and irritation (Zhang et al., 2016). It is known that Gushukang Granules (GSK), Xianling Gubao Capsules (XLGB), Er-xian Decoction (EXD), Liuwei Dihuang Pills, and Guishen Pill are effective in treating OP. In the treatments of OP, different prescriptions have the same and different targets and pathways, which fully figure out the action mode of "multi-components-multi-targets-multi-pathways" on the clinical therapy of complex diseases. How to systematically quantify the hidden mode of action in herbal prescriptions is the foundation and crux to interpret the principle of "different treatments for the same disease" in herbal medicine.

Among these prescriptions, GSK, XLGB, and EXD are widely used in the clinic. GSK contains seven herbs: *Epimedium brevicornum* Maxim., *Radix Rehmanniae Preparata*, *Auricularia auricular* (L.) Underw., *Astragalus mongholicus* Bunge, *Cucumis sativus* L., *Davallia mariesii* Moore ex Bak., and *Salvia miltiorrhiza* Bge. XLGB consists of six herbs: *Epimedium brevicornum* Maxim., *Rehmannia glutinosa* (Gaetn.) Libosch. ex Fisch. et Mey., *Salvia miltiorrhiza* Bge., *Dipsacales*, *Anemarrhena asphodeloides* Bunge, and *Psoralea corylifolia* Linn. EXD has six kinds of herbs: *Curculigo orchioides* Gaertn., *Epimedium brevicornum* Maxim., *Angelica sinensis* (Oliv.) Diels, *Morinda officinalis* How., *Phellodendron chinense* Schneid., and *Anemarrhena asphodeloides* Bunge. Clinical studies have shown that GSK can increase sex hormones (estrogen and androgen), inhibit bone absorption, effectively improve bone mineral density (BMD), reduce bone loss, increase osteocalcin (OC) and blood alkaline phosphatase (ALP) levels, and enhance osteoblast activity, which can effectively prevent and treat OP (Li et al., 2001; Wang et al., 2007; Wang et al., 2018a). Pharmacological research has shown that XLGB can improve bone metabolism, promote osteogenic effects, inhibit osteoclasts, increase bone density, and facilitate bone formation (Zhu and Hou, 2020). Clinical studies have also shown that XLGB has a therapeutic effect on BMD in patients with OP, which can effectively increase BMD, improve bone metabolism, and control bone loss (Wu et al., 2017). Pharmacological studies have shown that EXD not only increases the proliferation of osteoblasts and alkaline phosphatase (ALP) activity but also reduces the tartrate resistant acid phosphatase (TRAP) activity of osteoclasts (Li et al., 2017). Additionally, EXD affects the calcium signaling pathway and mediates apoptosis by activating the expression of downstream CAMK and activates downstream JNK, AKT, and ERK through upstream TNF-α, affecting the apoptosis process of bone-related cells (Yang et al., 2021). However, the pharmacodynamic material foundation and related molecular mechanism of different prescriptions in the therapy of OP under the concept of "different treatments for same disease" are still indistinct. Therefore, it is necessary to scientifically decipher the material basis and molecular mechanism of the efficacy of different prescriptions on the same disease.

Herbal informatics is an interdisciplinary subject that integrates Chinese medicine, computer science, biology, mathematics, multi-directional pharmacology, and other disciplines. It researches complex herbal medicine systems by systematically observing the response and effect of drugs on pathogenetic gene networks (Wang et al., 2021). Herbal informatics and network pharmacology have been diffusely used in the "same disease and different treatments" of herbal medicine. For example, Wang Kexin et al. clarified the molecular mechanism of DSD, GFD, and HGWD in treating rheumatoid arthritis based on herbal informatics (Wang et al., 2020a). Gao Yao et al. used the method of herbal informatics to analyze the mechanism of Xiaoyao Powder and Kaixin powder in the treatment of depression (Gao et al., 2018). Zhao Can et al. discussed the possible mechanism of Fuling Xingren Gancao Decoction and Ju-Zhijiang Decoction in treating coronary atherosclerotic heart disease based on the herbal informatics method (Zhao et al., 2019). With the continuous in-depth intersection of life sciences, chemistry, computer and information sciences, and other disciplines with drug research and the optimization and upgrading of network visualization tools and network construction analysis technologies, the research ideas and technical methods of herbal informatics will be better used. The study of the mechanism of the "different treatments for the same disease" of Chinese medicine provides more reference for the study of modernization of Chinese medicine (Li and Zhang, 2013).

In this study, a computational model based on herbal informatics was designed to discover the Significant Different Functional Modes (SDFMs) of different prescriptions in the therapy of OP. In order to further decode the key components group of different prescriptions on OP, a genetic algorithm-based optimization model was designed to figure out the FRMs from SDFMs. The distribution of high relevance score, the number of reported evidence, and the coverage of the enrichment pathway of target genes in FRMs were used to evaluate the accuracy and reliability of the FRMs detection model. Then, the effective proteins in the FRMs of each prescription were employed to screen the key components group of each prescription. The importance scores of the components in the key components group of each prescription were obtained based on information gain and target influence, and the effects of these key components were verified by cell experiments. Finally, the potential action mode of different prescriptions in treating the same disease was speculated based on the key components group of each prescription.

In conclusion, according to the herbal informatics strategy proposed in this study, the main mechanisms and relevant pharmacological effects of different treatments of OP can be detected through FRMs, which provide a new network-based method for herbal medicine in the clinic therapy of complex diseases.

MATERIALS AND METHODS

Flowchart

The schematic diagram of the whole process is shown in **Figure 1**, and the detailed procedure is described as follows: 1) chemical compounds of GSK, XLGB, and EXD were extracted from the published databases, and a widely used ADME screening model was used to screen potential active components in these compounds. Then, the online webserver is used to predict the targets of these active components. 2) The discovery model of the functional response motif was designed to optimize the C-T network and obtain Significant SDFMs. SDFMs were optimized by a genetic-based optimization model to obtain FRMs. 3) The reliability and accuracy of the FRMs detection model were validated by the distribution of the relevance score, the number of reported evidence, and coverage of functional pathways. 4) The information gain and target influence were combined to score the components in the key components group of each prescription. 5) The effectiveness of high-scored and randomly selected components in the key components group were performed in the *in vitro* experiments to confirm the precision of our proposed key components group selection model. 6) Finally, the potential action mode of different prescriptions treating the same disease mechanism was inferred by function analysis of the key components group in each prescription.

Component Collection

The original components in the three prescriptions were extracted by searching the Traditional Chinese Medicine Integrated Database (TCMID 2.0), TCM Database@Taiwan, and Traditional Chinese Medicine Systems Pharmacology Database and Analysis Platform (TCMSP) with the herbs in GSK, XLGB, and EXD as keywords. Open Babel (version 2.4.1) was used to convert the structures of all chemical components into canonical SMILES. The Similarity Ensemble Approach (SEA), Hit Identification and Target Prediction (HitPick), and SwissTargetPrediction were used to predict the drug targets of GSK, XLGB, and EXD.

SwissADME Screening

Lipinski's Rule of Five is the five elementary principles for selecting drug-like molecules, put forward by the pharmaceutical chemist Christopher Lipinski in 1997. Compounds that conform to the Lipinski Rule of Five will have better pharmacokinetic features and higher bioavailability during metabolism *in vivo*, so they tend more to become oral drugs. In drug research and development, the Lipinski Rule of Five is used in the preliminary screening of the compound library to exclude those molecules that are unfit for drugs, narrow the range of selecting, and economize the cost of drug research and development. The detailed description of Lipinski's Rule of Five is that the molecular weight of the compound is less than 500 Da. The number of hydrogen bond donors (including hydroxyl groups and amino groups) in the structure of the compound does not exceed 5. The number of hydrogen bond receptors in the compound does not exceed 10. The logarithmic value (logP) of the lipid-water partition coefficient of the compound is between −2 and 5. The quantity of rotatable bonds in the compound does not exceed 10 (Lipinski et al., 2001). The bioavailability score indicates the probability that a compound has at least 10% oral bioavailability or a measurable Caco-2 permeability in rats. Gastrointestinal absorption (GI absorption) indicates that the drug has good oral bioavailability (Daina et al.,

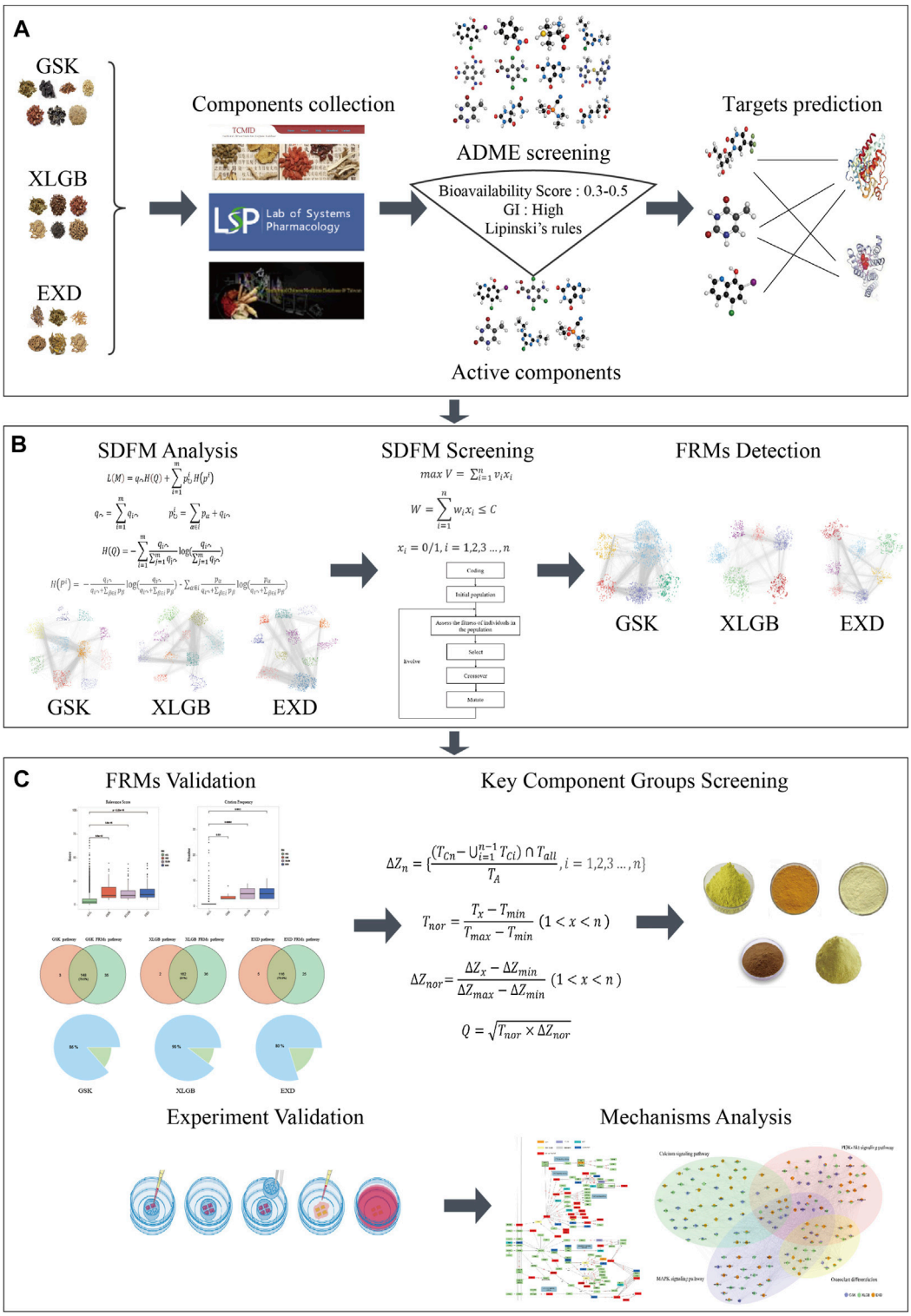

FIGURE 1 | The flowchart of our network pharmacology approach, including component collection and target prediction **(A)**. Using the function motif discovery model to find Significant Different Functional Modes (SDFMs) in the three prescriptions and then using the genetic-based optimization model to figure out the Functional Response Motifs (FRMs) **(B)**. Validation of FRMs, screening key component groups, and experiment validation and potential mechanism analysis **(C)**.

2017). Our research screened the active components of GSK, XLGB, and EXD according to Lipinski's Rule of Five, bioavailability, and gastrointestinal absorption. Among them, the bioavailability is defined between 0.3 and 0.55.

Network Construction

Cytoscape (version 3.7.2) was employed to build a C-T network, and its plug-in NetworkAnalyzer was used to analyze network topology parameters.

Functional Enrichment Analysis

Function enrichment is conducted based on KEGG (Kyoto Encyclopedia of Genes and Genomes). The hypergeometric distribution model is employed to calculate the significance of the biological pathway containing the target gene. The Benjamini–Hochberg method was used to correct the *p*-value. All statistical analysis was performed using the R language (version 4.0.5).

Explore the Significant Different Functional Modes

In order to find SDFMs in the three prescriptions for treating OP, we designed the below function motif discovery model.

The function motif discovery model is based on the combination of random walk and information compression. It uses the double-layer Huffman coding method to associate community discovery with information coding, records the paths generated by a random walk in the graph, and finds the community division with the shortest length. The average coding length of each step described in the random walk can be measured by the following prescription:

$$L(M) = q_{\curvearrowright} H(Q) + \sum_{i=1}^{m} p_{\circlearrowright}^{i} H(p^{i}),$$

where M indicates the way of community division and M indicates that nodes are divided into M communities.

$q_{\curvearrowright} = \sum_{i=1}^{m} q_{i\curvearrowright}$ means the proportion of all codes representing the community's name in the code, and $q_{\curvearrowright}$ is equal to the probability of jumping out of community i.

$H(Q) = -\sum_{i=1}^{m} \frac{q_{i\curvearrowright}}{\sum_{j=1}^{m} q_{j\curvearrowright}} log\left(\frac{q_{i\curvearrowright}}{\sum_{j=1}^{m} q_{j\curvearrowright}}\right)$ stands for the average length of bytes required to encode a community name.

$p_{\circlearrowright}^{i} = \sum_{\alpha \in i} p_{\alpha} + q_{i\curvearrowright}$ shows the code proportion of all nodes (including jump nodes) belonging to community i in the code.

$H(P^{i})$ denotes the average byte length required by all nodes in the coding community i. The average coding length $L(M)$ of each step is the weighted sum of two parts. One part is the average byte length required by the coding community name, and the other part is the average byte length required by the coding node in each community. The prescription can be expressed as

$$H(P^{i}) = -\frac{q_{i\curvearrowright}}{q_{i\curvearrowright} + \sum_{\beta \in i} p_{\beta}} log\left(\frac{q_{i\curvearrowright}}{q_{i\curvearrowright} + \sum_{\beta \in i} p_{\beta}}\right) - \sum_{\alpha \in i} \frac{p_{\alpha}}{q_{i\curvearrowright} + \sum_{\beta \in i} p_{\beta}} log\left(\frac{p_{\alpha}}{q_{i\curvearrowright} + \sum_{\beta \in i} p_{\beta}}\right),$$

Detection of Functional Response Motifs

In order to further screen the SDFM, we designed a novel genetic-based optimization model, which is described in detail as follows:

$$max\ V = \sum_{i=1}^{n} v_i x_i,$$

$$W = \sum_{i=1}^{n} w_i x_i \leq C,$$

$$x_i = 0/1,\ i = 1, 2, 3 \ldots, n,$$

The genetic algorithm (GA) is a random walk method that simulates the evolution of the genetic mechanism of the evolutionary laws of nature. It takes all individuals in a population as the object and efficiently searches a coded parameter space through genetic operations of selection, crossover, and mutation. As a new global optimization search algorithm, the genetic algorithm has the obvious characteristics of simplicity and generality, strong robustness, high efficiency, and practicality. It can be applied in all kinds of fields, has achieved good results, and has become one of the critical, intelligent algorithms by degrees. The calculation process is as follows:

1) Random generation of the initial population: the chromosome coding method is represented by a binary column code of length n. When $x_i = 0$, the binary code is 0. Otherwise, the binary code is 1. A binary column is a chromosome.
2) Individual evaluation: under the premise of not exceeding C, v_i and $\sum_{i=1}^{n} v_i x_i$ were used to evaluate individual fitness.
3) Individual selection: the roulette model is used to convert individual fitness into the area of the roulette wheel in proportion and rotate the roulette wheel. Finally, the individual corresponding to the landing position is selected.
4) Two points cross: two points are randomly set in the individual code, and some genes are exchanged in the middle of the two intersection points.
5) Basic mutation, a number is randomly generated for each chromosome, indicating whether the chromosome needs to be mutated. If a mutation is needed, a random variable is generated, indicating which bit of the chromosome to modify.
6) A new population is formed, and the iteration continues until the termination condition is met: $W = C$.

Pathway Network Integrating

Cytoscape (version 3.7.2) was used to combine osteoclast differentiation, calcium signaling pathway, MAPK signaling pathway, and PI3K-Akt signaling pathway into an integrated pathway.

Key Component Groups Screening

In order to screen the key component groups in different prescriptions, we designed a novel component importance calculation method that combined the information gain and target influence. We sort all the components in descending order of the corresponding target number and calculate the information gain Z of each component. The degree of information gain represents the contribution of increased coverage to the whole targets after adding the component. Higher information gain score

indicates the influence and the importance of the component in the C-T network of each prescription. There are n components, the corresponding target set of the components is denoted by T_{Ci}, the target set of all FRMs is denoted by T_{all}, and the target number of all FRMs is denoted by T_A. The information gain Z of components is calculated according to the following prescription. Then, we standardize the target number T of the component and the information gain Z and calculate the Q score. That is,

$$\Delta Z_n = \left\{ \frac{\left(T_{Cn} - \cup_{i=1}^{n-1} T_{Ci}\right) \cap T_{all}}{T_A}, i = 1, 2, 3 \ldots, n \right\},$$

$$T_{nor} = \frac{T_x - T_{min}}{T_{max} - T_{min}} \ (1 < x < n),$$

$$\Delta Z_{nor} = \frac{\Delta Z_x - \Delta Z_{min}}{\Delta Z_{max} - \Delta Z_{min}} \ (1 < x < n),$$

$$Q = \sqrt{T_{nor} \times \Delta Z_{nor}}.$$

Experiment Validation

Cell Culture and Drug Treatment

Mouse preosteoblastic MC3T3-E1 cells were purchased from the American Type Culture Collection (ATCC) and stored in Minimal Essential Medium, Alpha (α-MEM), supplemented with 10% fetal bovine serum (FBS), 100 units/mL of penicillin G, and 100 μg/ml of streptomycin at 37°C under 5% CO_2. Cells were seeded into 96-well plates (1×10^3 cells per/well) for 24 h and then treated with 5 μM quercetin, isoliquiritigenin, rutaecarpine, isofraxidin, and secoisolariciresinol for 24 and 48 h. Quercetin, isoliquiritigenin, rutaecarpine, isofraxidin, and secoisolariciresinol (≥98% purity by HPLC) were dissolved in DMSO.

Cell Viability Assay

Cell Count Kit-8 (CCK-8) assay was utilized to measure cell viability. After cell culture, add 10 μl CCK8 to the culture medium and incubate at 37°C for 2 h. The absorbance was measured at 450 nm with a microplate reader (*TECAN, infiniteM200*).

RESULTS

Collection of Chemical Components and Determination of High-Concentration Components

We collected the herbal components and concentrations of GSK, XLGB, and EXD from the reported literature. The detailed information is shown in **Table 1** and **Supplementary Table S1**. The results show that the chemical composition and concentration of the herbal medicine provide experimental auxiliary evidence for searching for active components and provide a valuable reference for further analysis.

Screening of Active Components for GSK, XLGB, and EXD

Seven herbs of GSK with 672 components, six herbs of XLGB with 540 components, and six herbs of EXD with 752 components were extracted from the Traditional Chinese Medicine Integrated Database (TCMID 2.0), TCM@TAIWAN, and Traditional Chinese Medicine Systems Pharmacology Database and Analysis Platform (TCMSP). Generally speaking, each Chinese medicine compound contains multiple herbal medicines, and each herbal medicine contains a series of chemical components. The pharmacological properties of these components are closely related to their therapeutic effects. Ingredients with better pharmacological properties may have positive therapeutic effects. Therefore, before analyzing the pharmacological effects, we first screen for pharmacological properties. SwissADME was used to screen the components in accordance with Lipinski's Rule of Five, gastrointestinal absorption, and bioavailability. After SwissADME screening, 271, 242, and 344 active components were obtained in GSK, XLGB, and EXD, respectively (**Table 2**, **Supplementary Table S2**). Our further analysis revealed 88 common components in the three prescriptions, 65, 37, and 232 specific components in GSK, XLGB, and EXD, respectively. In addition, we found that each of the herbs from GSK, XLGB, and EXD had its own chemical composition. There were many common components among the three prescriptions, while there were few common components in the prescriptions. Each prescription depended on its unique components (**Figure 2**). These results indicated that three prescriptions may play a role in treating OP by influencing both the common and specific components.

Target Prediction and C-T Network Construction

Cytoscape was used to construct a C-T network to analyze the relationships between the active components and targets of the three prescriptions (**Supplementary Figure S1**). The results showed 271, 240, and 339 active components; 1,264, 1,157, and 1,445 targets; and 9,701, 7,001, and 10,333 interactions in the GSK network, XLGB network, and EXD network, respectively. Then, we use the Cytoscape plug-in tool NetworkAnalyzer to further analyze the topological parameters of the three prescription C-T networks. After analyzing the network topology in the C-T network of GSK, the average degree of the components was 35.80. Among them, phenylalanine had the highest node degree, acting on 207 drug targets (degree: 207), and tyrosine acted on 128 targets in descending order (degree: 128). Quercetin acted on 120 targets (degree: 120). Studies have shown that high phenylalanine levels can affect bones, cause bone-related diseases, and affect bone mineral density (BMD) in a lower way (Mendes et al., 2012). Phosphorylation of tyrosine residues is key to the regulation of osteoclast production and bone resorption activity (Shalev and Elson, 2019). Phenylalanine can be converted to tyrosine, and the metabolic state of phenylalanine is related to normal body growth and maintenance of normal physiological functions (Westbroek et al., 2001). In addition, phenylalanine interacts with the calcium-sensing receptor (CaSR), affecting the body's calcium metabolism and bone balance (Conigrave et al., 2008). Animal experiments have proved that OP can be prevented by intervening phenylalanine metabolism in rats (Liu et al., 2012).

TABLE 1 | The experiments confirmed high concentration components of GSK, XLGB, and EXD.

Herb	Method	Component	Concentration (mg/g)	Prescription	References
Epimedium brevicornum Maxim.	HPLC	Icariin	2.025	GSK	SZ Sun, HE Yan-Li, YW Wen, & YT Chen. (2019). Simultaneous determination of six components in Gushukang Granula and Gushukang Capsules by HPLC-ms/ms. Chinese Journal of Pharmaceutical Analysis
Radix Rehmanniae Preparata		Acteoside	0.043		
Astragalus mongholicus Bunge		Calycosin-7-glucoside	0.06		
Salvia miltiorrhiza Bge.		Tanshinone IIA	0.0858		
Davallia mariesii Moore ex Bak		Naringin	0.1049		
Epimedium brevicornum Maxim	HPLC	Icariin	2.119	GSK	YE Guangming, Y. Jiang, Y. Chen, GU Liping, & X. Xue. (2010). Simultaneous determination of contents of icariin and naringin in Gushukang Granules by HPLC method. Pharmaceutical Care and Research
Davallia mariesii Moore ex Bak.		Naringin	0.163		
Epimedium brevicornum Maxim.	HPLC	Icariin	1.164	XLGB	Chen, Z., Xiaoxia, L., Chen, G., & Chen, J. (2017). One-step assay for five components in Xianling Gubao Capsule by HPLC method. Journal of Pharmaceutical Practice
Dipsacales		Epimedin C	7.068		
Psoralea corylifolia Linn.		Asperosaponin VI	8.458		
		Psoralen	0.776		
		Angelicin	0.838		
Dipsacales	HPLC	Asperosaponin VI	8.458	XLGB	Gong, QD, Chen, ZL, and Chen, G. Q. (2016). Determination of asperosaponin VI, psoralen, and angelicin in Xianling Gubao Capsule by HPLC. Chinese Traditional and Herbal Drugs
Psoralea corylifolia Linn.		Psoralen	0.776		
		Angelicin	0.838		
Epimedium brevicornum Maxim.	HPLC	Epimedin B	0.89	EXD	Gao, F., Liu, Y., H Li, Fan, F., & Pharmacy, D. O. (2019). Determination of epimedium flavonoids in Er-xian Decoction by high-performance liquid chromatography. World Chinese Medicine
		Epimedin C	0.701		
		Icariin	0.487		
		Icariside II	1.027		

TABLE 2 | The number of active components before and after SwissADME screening in GSK, XLGB, and EXD.

Formula	Chemical composition quantity before SwissADME screening	Chemical composition quantity after SwissADME screening
GSK	672	271
XLGB	540	242
EXD	752	344

Quercetin can restrain the expression of ERK1/2, MAPK mRNA, and protein, thereby inhibiting the conduction of the ERK1/2-MAPK signaling pathway, promoting the expression of specific genes in bone and osteoblast generation, increasing bone mineral density, and preventing OP (Casado-Díaz et al., 2016). In the C-T network of GSK, the average degree of the target was 7.67. Among them, the highest degree of the node was Microtubule Associated Protein Tau (MAPT), which targeted 172 compounds (degree: 172), followed by Tyrosyl-DNA phosphodiesterase 1 (TDP1), which targeted 135 compounds (degree: 135). Muscleblind Like Splicing Regulator 1 (MBNL1) targeted 83 compounds (degree: 83).

In the C-T network of XLGB, the average degree of the components was 30.48. Among them, phenylalanine had the highest node degree, acting on 202 drug targets (degree: 202), and tyrosine acted on 124 targets in descending order (degree: 124). Quercetin acted on 106 targets (degree: 106). The average degree of the target was 6.05. Among them, the highest degree of the node was Microtubule Associated Protein Tau (MAPT), which targeted 105 compounds (degree: 105), followed by Tyrosyl-DNA phosphodiesterase 1 (TDP1), which targeted 74 compounds (degree: 74). Carbonic anhydrase 7 (CA7) targeted 63 compounds (degree: 63).

In the C-T network of EXD, the average degree of the components was 30.58. Among them, asperglaucide had the highest node degree, acting on 267 drug targets (degree: 267), and phenylalanine acted on 197 targets in descending order (degree: 197). n-cis-Feruloyltyramine acted on 177 targets (degree: 177). The average degree of the target was 7.16. Among them, the highest degree of the node was cytochrome P450 family 1 subfamily B member 1 (CYP1B1), which targeted 94 compounds (degree: 94), followed by carbonic anhydrase 3 (CA3), which targeted 90 compounds (degree: 90). Carbonic anhydrase 7 (CA7) targeted 86 compounds (degree: 86). Through the comparative analysis of the number of targeted genes, it can be seen that GSK had a stronger control rate on the C-T network.

The results showed that, in the three prescriptions, there were a relationship between one component corresponding to multiple targets and a phenomenon of different components acting on the same target, consistent with the function of "multi-components-multi-targets-multi-pathways" in herbal medicine, reflecting the complicacy of the underlying mechanism of herbal medicine.

Screening Significant Different Functional Modes and Functional Response Motifs

Due to the large and complex C-T network of the three prescriptions, it is difficult to quickly extract the most important active ingredient information. Therefore, we designed a novel function motif discovery model to screen the C-T network to filter the modes that can represent the complete C-T network. The results showed that we predicted 22, 23, and 30 SDFM in GSK, XLGB, and EXD, respectively

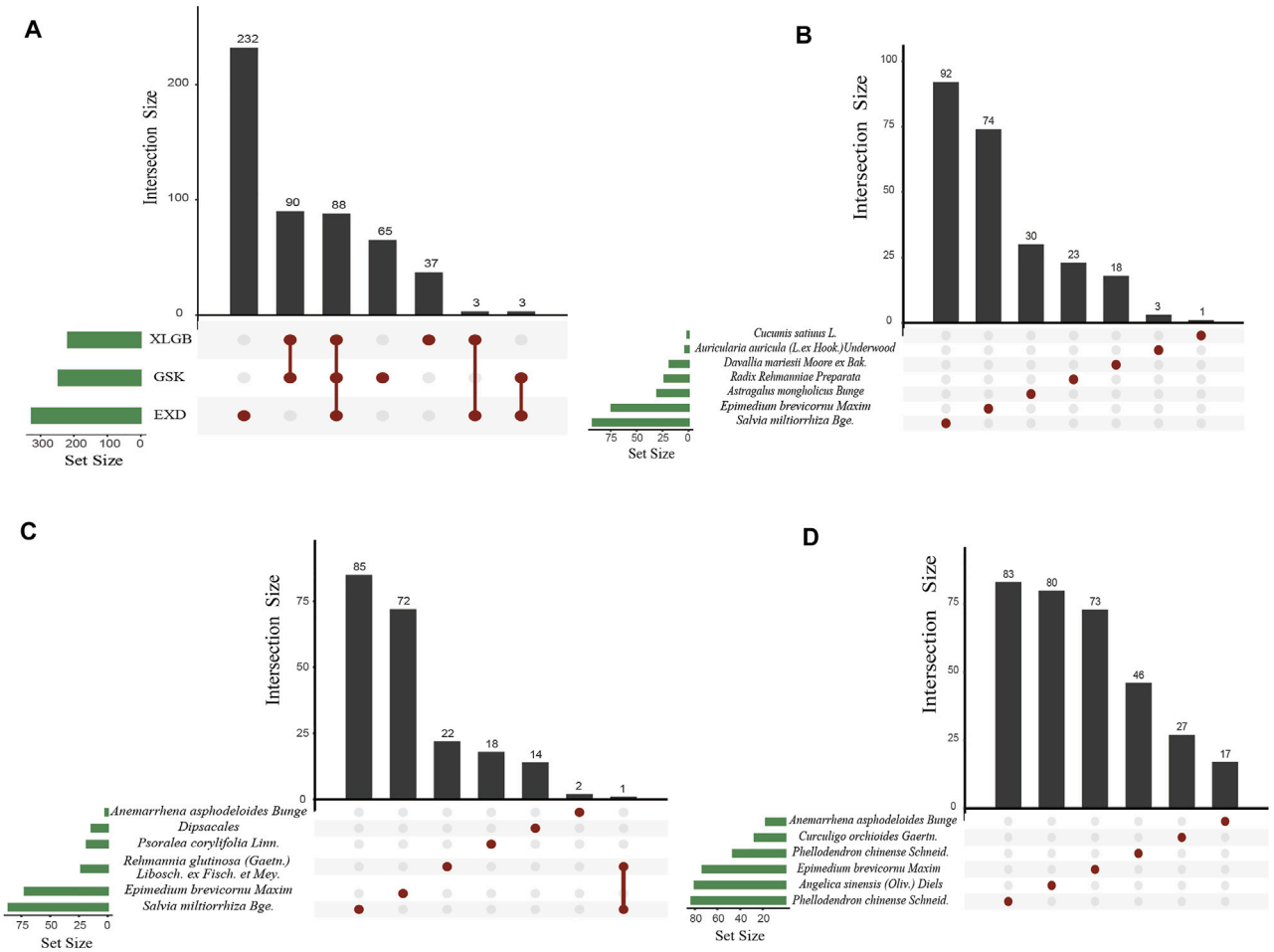

FIGURE 2 | Distribution map of active components in GSK, XLGB, and EXD **(A)**. Common components of GSK, XLGB, and EXD **(B–D)**. Distribution map of herbs in GSK **(B)**. XLGB **(C)**. and EXD **(D)**.

($p < 0.05$). In order to figure out the FRMs and remove the noise in the SDFM in each prescription. We designed another genetic-based optimization model to optimize the SDFM and finally obtained 11, 13, and 15 FRMs in GSK, XLGB, and EXD, respectively (**Figures 3–5**).

Validating FRMs

In order to verify whether the entire C-T network can be replaced by the predicted FRMs, we propose two criteria to evaluate the accuracy and dependability of FRMs. The first criterion is whether the relevance score and the number of reported evidence of FRMs-related high reliable genes, defined in the following section, are higher than those of the pathogenic genes of OP. High relevance score and the high number of reported evidence indicate that the genes in FRMs can cover the high reliable pathogenic genes to the maximum extent. The second criterion is whether the gene enrichment pathways in FRMs can cover the gene enrichment pathways in the C-T network as much as possible. The high pathway coverage indicates that FRMs can cover most of the gene enrichment pathways in the C-T network and have the most likely function of the prescription. Details of the results are as follows:

Validating FRMs Based Relevance Score and the Number of Reported Evidence

We extracted the pathogenic genes of OP with relevance score and the number of reported evidence from GeneCards database and DisGeNet database.

Herein, we set a criterion for screening two high reliable pathogenic gene sets by calculating the average relevance score and the number of reported evidence of pathogenic genes, respectively. The first high reliable pathogenic gene set was defined as the genes with higher relevance score than the average of all pathogenic genes. The second high reliable pathogenic gene set was defined as the genes with higher number of reported evidence than the average of all pathogenic genes. According to this criterion, the average relevance score and the number of reported evidence of pathogenic genes of OP collected from the database are 5.13 and 2.7, respectively. Thus, in the first high reliable pathogenic

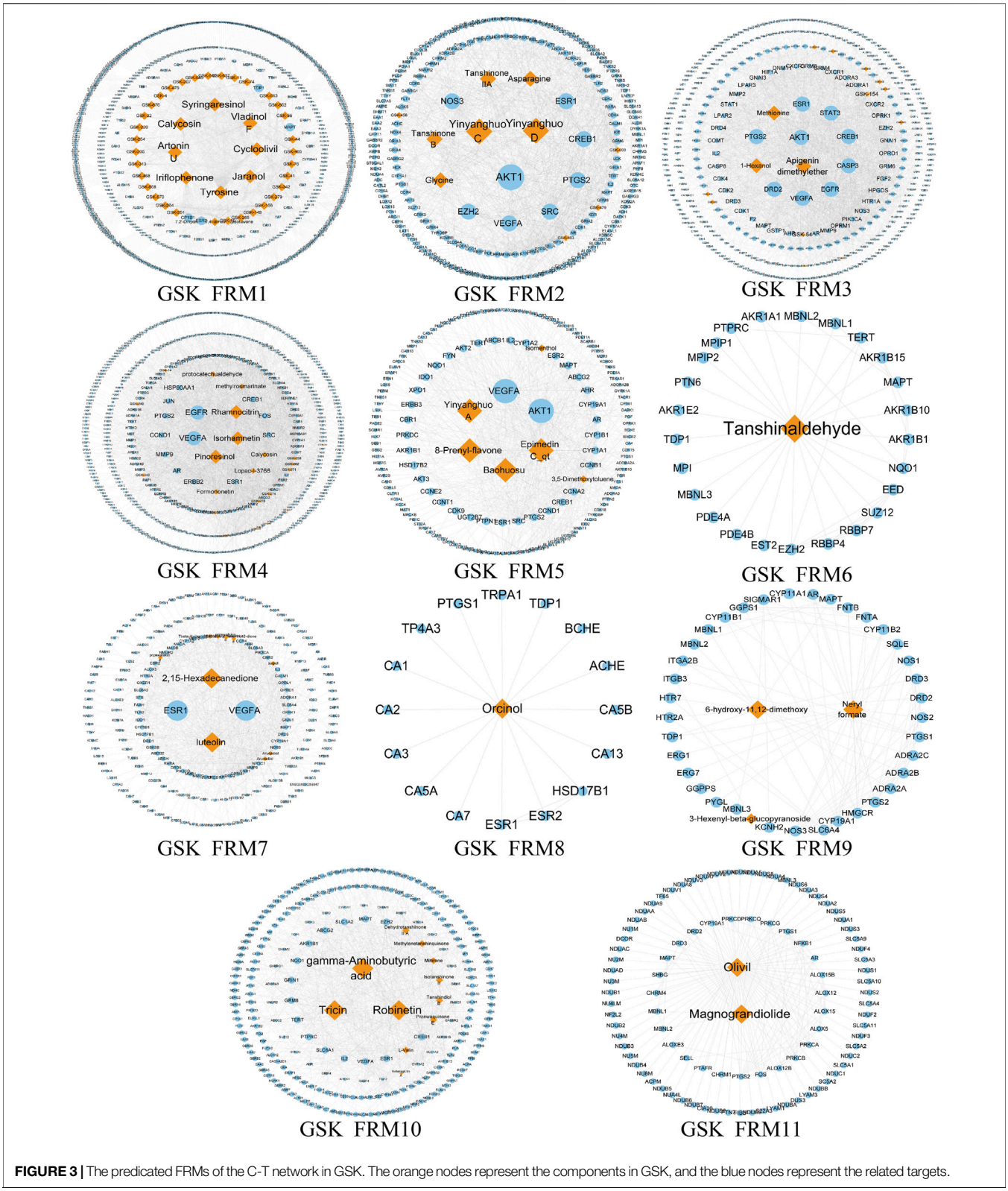

FIGURE 3 | The predicated FRMs of the C-T network in GSK. The orange nodes represent the components in GSK, and the blue nodes represent the related targets.

gene set, the relevance score of each gene was higher than 5.13. While in the second high reliable pathogenic gene set, the number of reported evidence of each gene was higher than 2.7. The average relevance scores of FRMs in GSK, XLGB, and EXD were 14.22, 12.98, and 14.43, respectively, while the average numbers of reported evidence were 10.5, 7.75, and 8.17,

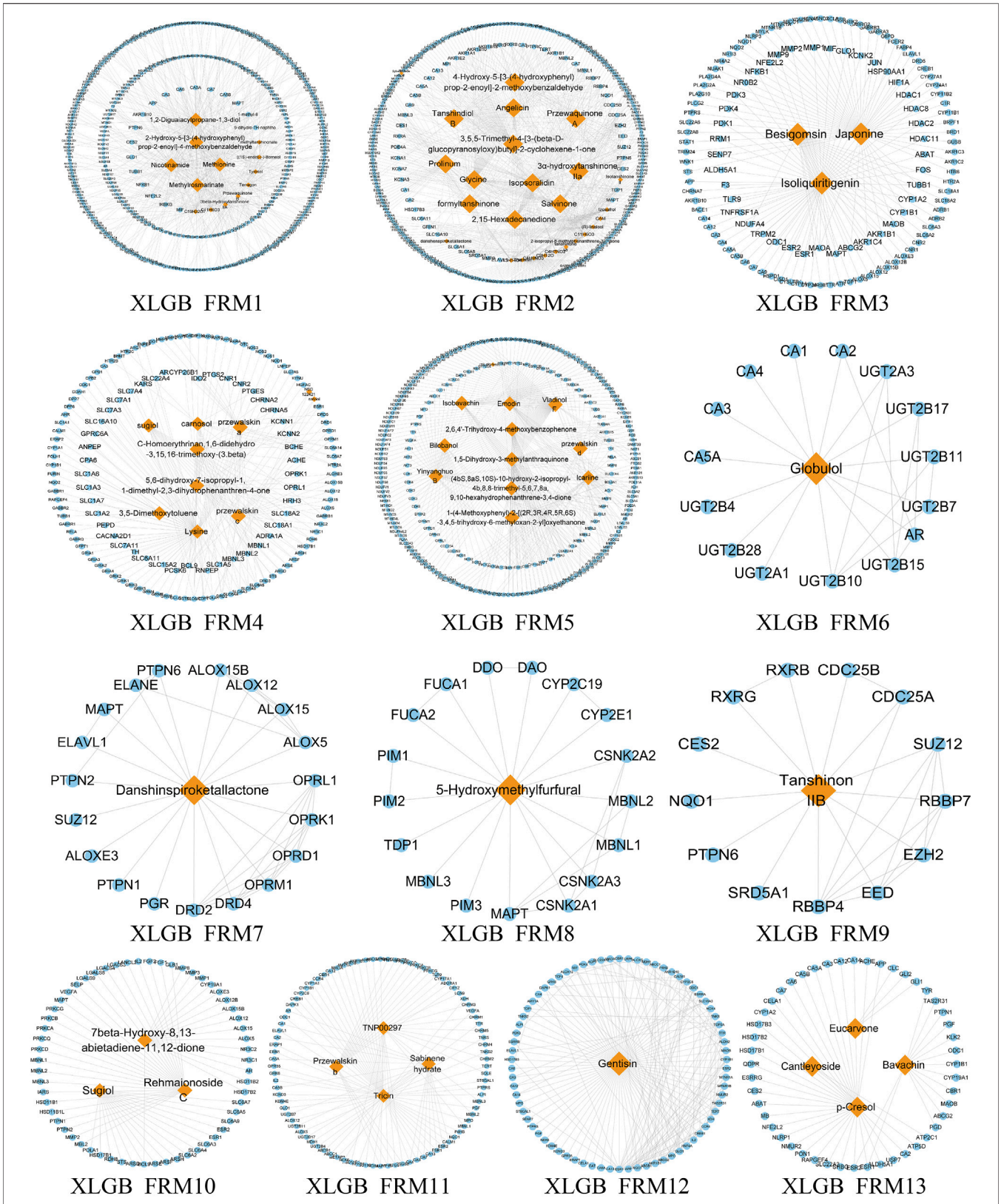

FIGURE 4 | The predicated FRMs of the C-T network in XLGB. The orange nodes represent the components in XLGB, and the blue nodes represent the related targets.

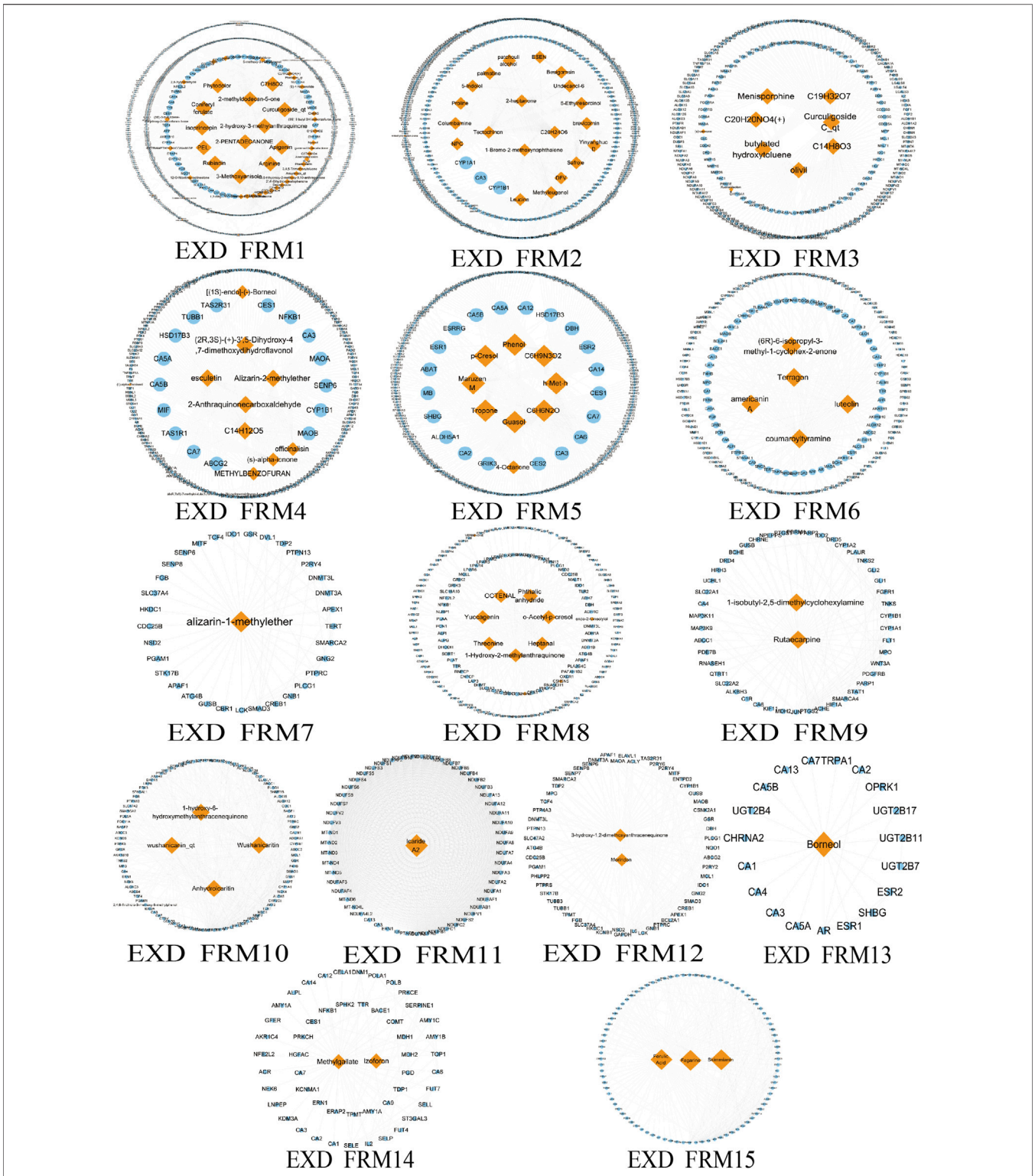

FIGURE 5 | The predicated FRMs of the C-T network in EXD. The orange nodes represent the components in EXD, and the blue nodes represent the related targets.

respectively, which were significantly higher than the two high reliable pathogenic gene sets, respectively (**Figure 6**). The high relevance score and the number of reported evidence can represent a higher degree of association between genes and disease, and the average score and the number of reported evidence of predicted FRMs in three prescriptions were

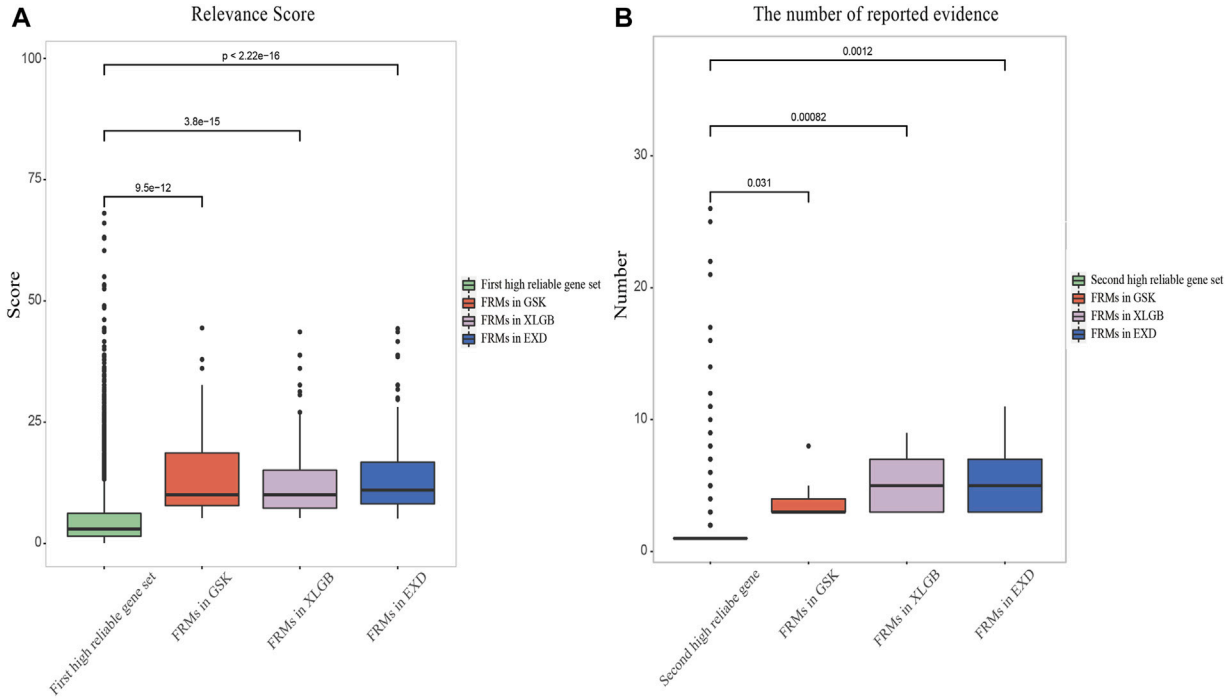

FIGURE 6 | Validation of FRMs. Relevance score **(A)** and the number of reported evidence **(B)** of FRMs and two high reliable pathogenic gene sets of OP were compared.

significantly higher than those of the two high reliable pathogenic genes sets. Results showed that the FRMs prediction model could accurately screen genes with higher disease correlation.

Validating FRMs Based on Gene Enrichment Pathways Analysis

Another criterion for evaluating the accuracy and reliability of FRMs is to evaluate their functional consistency. According to this method, we used the KEGG enrichment analysis to determine whether the gene enrichment pathways in FRMs could cover the gene enrichment pathways in the C-T network as much as possible. The high pathways coverage indicates that FRMs can represent the complete C-T network at the functional level. Our analysis showed that GSK, XLGB, and EXD FRMs gene enrichment pathways accounted for 79.6, 81, and 79.5% of GSK, XLGB, and EXD complete C-T network gene enrichment pathways, respectively (**Figure 7**). The results showed that the predicted FRMs can represent the complete C-T network at the functional level, and it also indicated that the predicted FRMs can preserve the functional pathway of herbal medicine prescriptions to the maximum extent. Additionally, to examine whether the FRMs in each prescription have the similar therapeutic function as the original prescription, we defined the prescription-related reference pathways by selecting the intersection of target gene and pathogenic gene enriched pathways. After that, we compared the enrichment pathways of genes in FRMs for each prescription to corresponding reference pathways. The results showed that the proportion of GSK, XLGB, and EXD was 86.47, 89.63, and 79.8%, respectively (**Figure 8**). It showed that screened FRMs can retain the functional information of the original prescriptions and the intervention function of the original prescriptions to the maximum extent.

Potential Mechanism Analysis

In order to reveal the potential action mode underlying the treatment of OP by different prescriptions, we performed a pathway enrichment analysis of FRMs genes. Other disease, virus-related, and drug-resistant pathways were removed, and pathways with a count number greater than 12 were retained for further analysis. We found that 40 pathways were enriched in GSK, 66 pathways in XLGB, and 48 pathways in EXD. After combination, the three prescriptions were found to be enriched in 16 identical pathways (**Figure 9**), for example, steroid hormone biosynthesis (hsa00140), osteoclast differentiation (hsa04380), calcium signaling pathway (hsa04020), MAPK signaling pathway (hsa04010), and PI3K-Akt signaling pathway (hsa04151). Through PubMed literature retrieval, we found that, among these common pathways, osteoclast differentiation, calcium signaling pathway, MAPK signaling pathway, and PI3K-Akt signaling pathway were most reported. Previous studies have shown that the suppression of RANKL-induced calcium signaling inhibits OP in oophorectomy (OVX) mouse models (Chen et al., 2020). MAPK pathway is a major signaling pathway regulating OP. By restraining the production of RANKL-induced ROS and increasing the expression of antioxidant enzymes, intracellular ROS levels are inhibited and the activation of the MAPK pathway is weakened, resulting in the attenuation of downstream proteins, which contributes to the

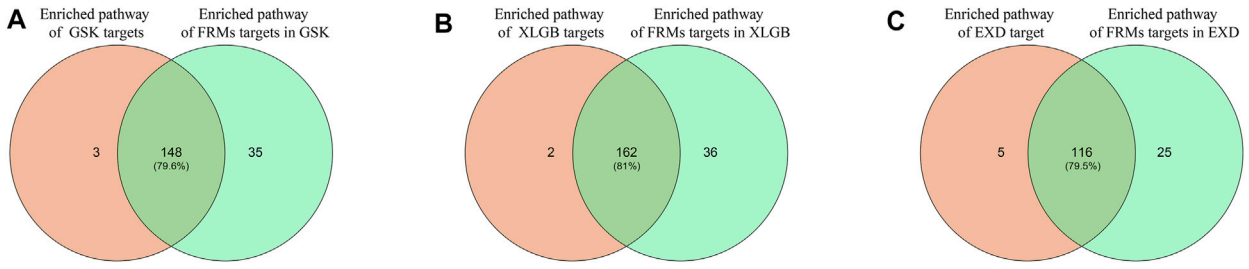

FIGURE 7 | Validation of FRMs. The intersection proportion of FRMs gene enrichment pathways and C-T network gene enrichment pathways in GSK**(A)**, XLGB**(B)**, and EXD**(C)**.

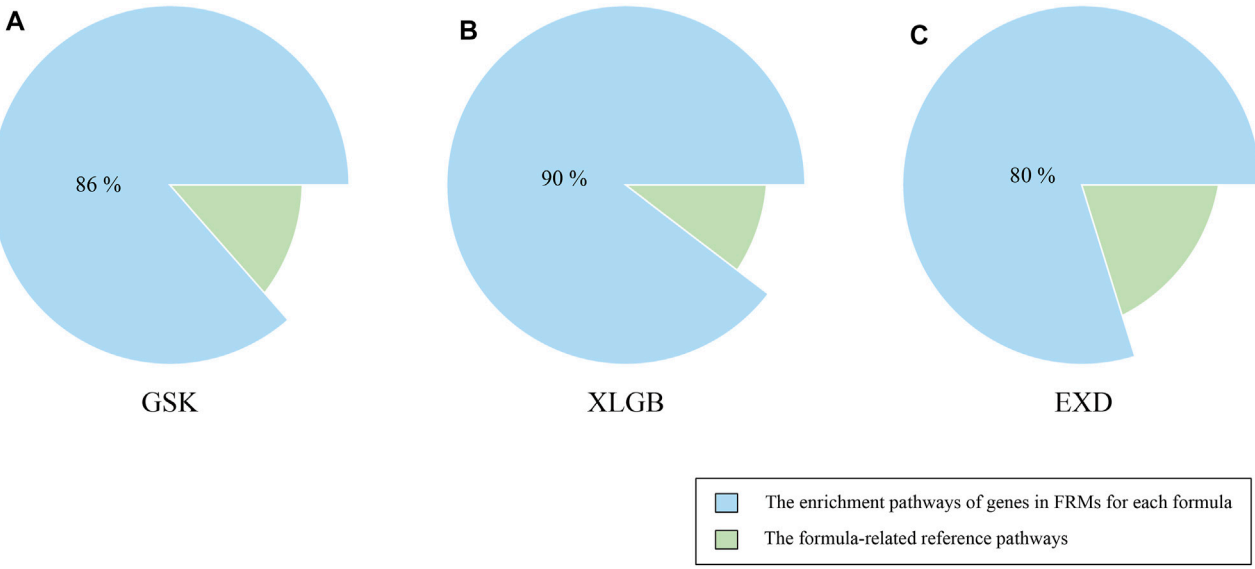

FIGURE 8 | Validation of FRMs. The proportion of the enrichment pathways of genes in FRMs for GSK **(A)**, XLGB **(B)**, and EXD **(C)** to corresponding reference pathways. The formula-related reference pathways were defined as selecting the intersection of the target gene and pathogenic gene enriched pathways.

reduction of OP (Yao et al., 2018; Chen et al., 2019). Meanwhile, the PI3K/AKT signaling pathway has been proven to be essential for all stages of bone maturation, differentiation, and bone growth. Inhabiting the PI3K/AKT signaling pathway not only injures the differentiation of chondrocytes but also inhibits the growth of longitudinal bones (Ye et al., 2019).

Next, osteoclast differentiation, calcium signaling pathway, MAPK signaling pathway, and PI3K-Akt signaling pathway were combined into a gene network (**Figure 10**). Our analysis found that, in this gene network, GSK, XLGB, and EXD had different and co-functional effects in treating OP. There were 10 genes common to GSK, XLGB, and EXD (ITGB3, IGF1R, CHRM1, GRB2, IL2, BCL2L1, ERBB4, PIK3R1, RPS6KA4, and TACR2). For example, GSK, XLGB, and EXD all have target gene ERBB4, which played a role in OP through PI3K-Akt signaling pathway, MAPK signaling pathway, and calcium signaling pathway, and common gene IL2, which only affected OP through the PI3K-Akt signaling pathway. In the gene network, 27, 37, and 44 genes were unique to GSK, XLGB, and EXD. For example, among the 27 specific genes of GSK, LCK affected OP through osteoclast differentiation; VEGFA played a role in OP through the PI3K-Akt signaling pathway, MAPK signaling pathway, and calcium signaling pathway. Among the 37 unique genes of XLGB, HRH2 simply affected OP through the calcium signaling pathway; JUN impacted OP through the MAPK signaling pathway and osteoclast differentiation pathway. Among the 44 distinct genes of EXD, CACNB1 merely affected OP through the MAPK signaling pathway; CHRM2 influenced OP through the PI3K-Akt signaling pathway and calcium signaling pathway (**Figure 10**). ITGB3 belongs to the integrin family and is a membrane receptor composed of a subunit and ß subunit, which is involved in cell cycle, cytoskeletal tissue, osteoblast differentiation, and proliferation (Rapisarda et al., 2017; Lopes et al., 2019). ITGB3 can also interact with IL1RN to activate ß-catenin signaling and regulate osteoblast differentiation (Zou et al., 2021). In addition, IGF1R signaling plays an important role in osteoblast-mediated bone formation and promotes osteoblasts differentiation and maturation. During the

FIGURE 9 | The specific and the common enrichment pathway of FRMs in GSK, XLGB, and EXD.

differentiation of bone marrow stromal cells, IGF1R signaling pathway is controlled by PI3K/Akt and inhibits osteoblast apoptosis (Fang et al., 2019).

Among the specific genes of GSK, cyclin D1 (CCND1) is a member of the protein kinases family associated with cell cycle regulation (Guo et al., 2013). In addition, CCND1 is often overexpressed in human diseases through translocation, amplification, or post-transcriptional regulation (Xu and Lin, 2018). Studies have found that controlling the expression of CCND1 can regulate the proliferation, differentiation, mineralization, and apoptosis of osteoblasts, therefore treating OP (Wang and Cai, 2020). In addition, it was shown that chemokine receptor-4 (CXCR4) overexpression in mesenchymal stem cells can promote BMD increase, improve MSC migration to bones, enhance MSC effects, and prevent bone loss in OVX mice after oophorectomy (Cho et al., 2009).

Among the specific genes of XLGB, CD38 has been shown to play a role in bone remodeling. It is expressed in osteoclasts, and when activated, it increases IL-6 release and inhibits bone resorption (Sun et al., 1999). Meanwhile, osteoblasts and osteoclasts express P2X7R, which regulates differentiation, function, and longevity of both cell types (Agrawal and Gartland, 2015). In the mouse model of postmenopausal osteoporosis, P2X7 has been shown to hinder bone loss. After the deletion of P2X7R in ovariectomized mice, significant bone loss, osteoblast reduction, and osteoclast increase were observed. Under normal physiological conditions, the loss of P2X7R leads to osteopenic-like bone phenotype (Wang et al., 2018b).

Among the specific genes of EXD, BCL2 is a gene that inhibits apoptosis. Studies have shown that upregulation of BCL2 may inhibit bone loss, while upregulation of BCL2 in osteoblasts can restrain osteoblast differentiation and cause osteocyte apoptosis (Moriishi et al., 2011). Colony stimulating factor 1 receptor (CSF-1R or c-FMS) is a tyrosine kinase receptor, a receptor for CSF-1, which is delivered by osteoblasts and promotes the proliferation of osteoclast progenitor cells through the combination of CSF-1R and receptor activator of nuclear factor-kappaB ligand (RANKL), leading to the formation of mature osteoclasts (Wittrant et al., 2009). Previous studies have shown that the CSF-1/CSF-1R signaling pathway affects the expression of RANK in osteoclasts and RANKL binds to RANK to induce the cascade of MAPKs, PI3K, and NF-κB signaling and finally generates NFATc1, which is the major regulator of osteoclast differentiation. The inhibition of CSF-1R on osteoclasts hinders the proliferation, differentiation, and survival of osteoclasts and downregulates the formation of osteoclast markers (TRAP) (Zinnia and Khademul Islam, 2021).

The above results indicate that the FRMs of different prescriptions have different and co-functional effects in treating OP. They provide a possible mechanism reference for us to reveal multiple treatments for the same disease.

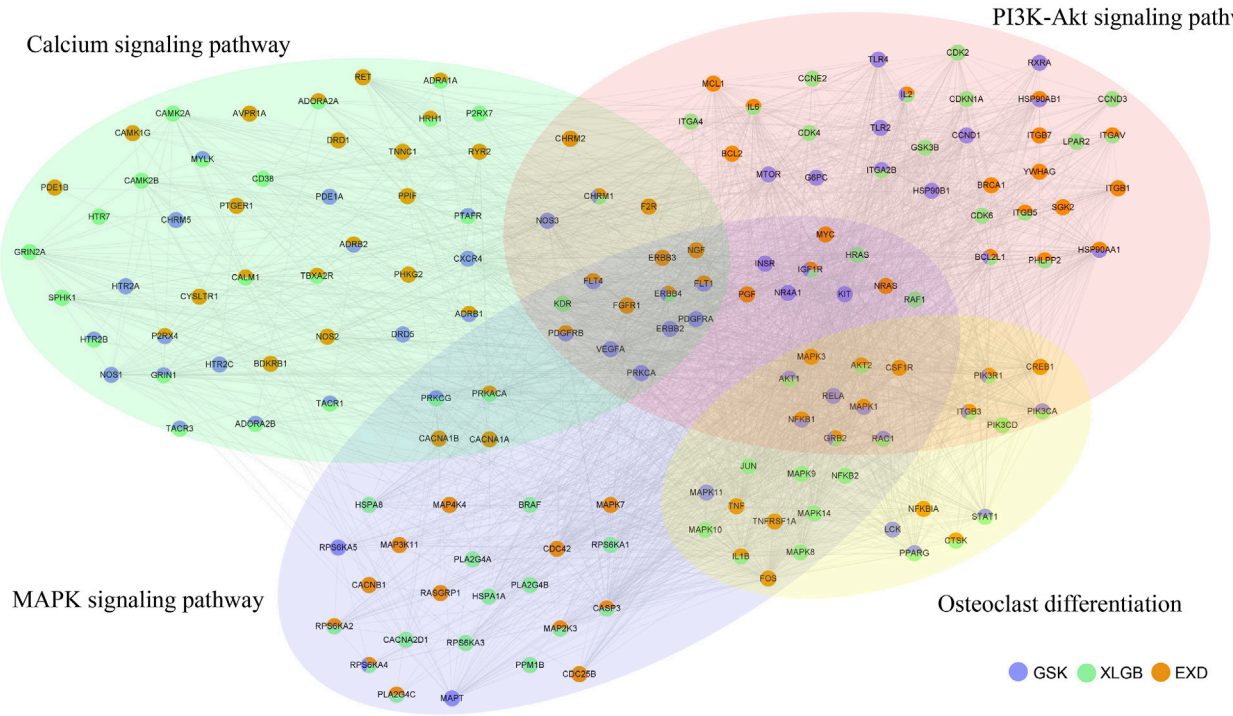

FIGURE 10 | Gene network in the osteoclast differentiation, calcium signaling pathway, MAPK signaling pathway, and PI3K-Akt signaling pathway. Blue nodes represent targets in GSK. Green nodes represent targets in XLGB. Orange nodes represent targets in EXD. Nodes with three colors indicate that the gene is shared by three prescriptions. Nodes in light yellow, light green, light blue, and light red circles represent genes of osteoclast differentiation, calcium signaling pathway, MAPK signaling pathway, and PI3K-Akt signaling pathway, respectively.

Screen Key Component Groups

Osteoclast differentiation, calcium signaling pathway, PI3K-Akt signaling pathway, and MAPK signaling pathway were combined into an integrated pathway. A novel component importance calculation method that combined the information gain and target influence was designed and employed to screen the key component groups in different prescriptions. The components with a ***Q*** score of more than 0.01 were defined as potential important components in each prescription. Based on this method, we obtained 24, 23, and 22 potential important components in GSK, XLGB, and EXD, respectively. To prove the effectiveness of each potential important component screened by the model, we selected the highest ***Q*** score component in each of the three prescriptions and randomly selected one, one, and two components from GSK, XLGB, and EXD, respectively. Finally, we selected quercetin, isoliquiritigenin, rutaecarpine, isofraxidin, and secoisolariciresinol for further validation. The effectiveness of these components was further verified *in vitro* to prove the model's reliability (**Table 3**).

Experimental Validation *In Vitro*

MC3T3-E1 is an osteoblast strain constructed from C57BL/6 mouse cranial parietal cells, which has biological characteristics of osteoblasts, such as ALP active type I collagen synthesis and matrix calcification, and is often used as a cellular model for bone metabolism studies. In order to assess the reliability of our model, the CCK8 method was used to validate the effects of the key components (quercetin, isoliquiritigenin, rutaecarpine, isofraxidin, and secoisolariciresinol) on the MC3T3-E1 cells at different time points (Day 0, Day 1, Day 2). The results showed that the cell viabilities of MC3T3-E1 cells were 115.93, 119.74, 111.27, 115.11, and 117.02% after exposure to 5 μM quercetin, isoliquiritigenin, rutaecarpine, isofraxidin, and secoisolariciresinol on Day 1, respectively (**Figure 11**). On Day 2, the cell viabilities of five components were 147.88, 149.88, 132.34, 131.87, and 133.02%, respectively (**Figure 11**). Compared with the control group (DMSO), the cell viability of the MC3T3-E1 cells markedly increased after treatment with five components at Day 1 and Day 2. Our results suggested that quercetin, isoliquiritigenin, rutaecarpine, isofraxidin, and secoisolariciresinol could increase the viabilities of MC3T3-E1 cells.

DISCUSSION

OP causes fractures and other complications, which increase the physical pain of patients and bring great pressure and burden to the society and family. For the treatments of OP, drugs that promote bone mineralization, inhibit bone resorption, and promote bone formation are widely used (Das and Crockett, 2013). However, these drugs are expensive and have side effects. Thus, it is desirable to choose an alternative medicine to address this issue. Herbal medicine prescriptions have significant

TABLE 3 | The potential important components and score in GSK, XLGB, and EXD.

Formula	Name	Component	Q
GSK	Phenylalanine	GSK-430	1
GSK	Quercetin	GSK-136	0.529699172
GSK	Secoisolariciresinol	GSK-264	0.468361473
GSK	Apigenin 7,4′-dimethyl ether	GSK-51	0.349024322
GSK	Arginine	GSK-323	0.264370699
GSK	Tyrosine	GSK-435	0.211996592
GSK	Pinoresinol	GSK-263	0.21119811
GSK	Xanthogalenol	GSK-317	0.157596558
GSK	Gamma-aminobutyric acid	GSK-350	0.157417777
GSK	Isoolivil	GSK-26	0.148203935
GSK	Iriflophenone	GSK-310	0.147059487
GSK	Methionine	GSK-487	0.1389871
GSK	Artonin U	GSK-88	0.135082763
GSK	Lariciresinol	GSK-376	0.127357247
GSK	Histidine	GSK-439	0.120541692
GSK	1,2-Bis(4-hydroxy-3-methoxyphenyl)propane-1,3-diol	GSK-138	0.117705025
GSK	(2S,3S,4R,5S,6R)-2-(Hydroxymethyl)-6-[2-(4-hydroxyphenyl)ethoxy]oxane-3,4,5-triol	GSK-47	0.11770502
GSK	3,4-Dihydroxybenzaldehyde	GSK-462	0.115043307
GSK	Vladinol F	GSK-133	0.114306628
GSK	1-Hexanol	GSK-24	0.113316944
GSK	Apigenin	GSK-2	0.112568974
GSK	Methyleugenol	GSK-10	0.107187098
GSK	Methyl rosmarinate	GSK-568	0.105064369
GSK	Tanshinone IIA	GSK-606	0.100684748
XLGB	Phenylalanine	XLGB-174	1
XLGB	Tyrosine	XLGB-187	0.265722595
XLGB	Quercetin	XLGB-35	0.419289486
XLGB	Nicotinamide	XLGB-516	0.237387556
XLGB	Methionine	XLGB-337	0.161318712
XLGB	Lysine	XLGB-186	0.122755389
XLGB	Japonine	XLGB-498	0.143756394
XLGB	Isoliquiritigenin	XLGB-66	0.105348726
XLGB	Huazhongilexin	XLGB-147	0.172357865
XLGB	Histidine	XLGB-176	0.145081365
XLGB	Glycine	XLGB-165	0.181153762
XLGB	Ethyl beta-D-galactopyranoside	XLGB-164	0.179295726
XLGB	Chrysoeriol	XLGB-82	0.139191528
XLGB	Artonin U	XLGB-120	0.207032871
XLGB	Arginine	XLGB-189	0.314224575
XLGB	Apigenin 7,4′-dimethyl ether	XLGB-83	0.251858762
XLGB	Apigenin	XLGB-34	0.164693641
XLGB	3-Hexenyl-beta-glucopyranoside	XLGB-114	0.103747239
XLGB	3,4-Dihydroxybenzaldehyde	XLGB-231	0.158023093
XLGB	2-Decenal	XLGB-37	0.12526283
XLGB	2,6,4′-Trihydroxy-4-methoxybenzophenone	XLGB-510	0.267516823
XLGB	1,2-Bis(4-hydroxy-3-methoxyphenyl)propane-1,3-diol	XLGB-8	0.376297348
XLGB	1-(3,4-Dihydroxyphenyl)-2-hydroxyethanone	XLGB-350	0.118592977
EXD	Isoolivil	EXD-117	1
EXD	Vanillyl alcohol	EXD-616	0.125075771
EXD	Tyrosine	EXD-421	0.193500377
EXD	Rutaecarpine	EXD-631	0.114443255
EXD	Quercetin	EXD-226	0.350841822
EXD	Phenylalanine	EXD-400	0.204988715
EXD	Nicotinamide	EXD-751	0.107475835
EXD	N-cis-Feruloyltyramine	EXD-674	0.113378648
EXD	Methyl nonyl ketone	EXD-454	0.157576077
EXD	Methionine	EXD-316	0.262915243
EXD	Isoliquiritigenin	EXD-125	0.570518314
EXD	Isofraxidin	EXD-495	0.145679135
EXD	Dibutyl phthalate	EXD-443	0.159583501
EXD	Coniferyl ferulate	EXD-367	0.224742828
EXD	Asperglaucide	EXD-679	0.110398041
EXD	Arginine	EXD-424	0.17722632
EXD	Apigenin 7,4′-dimethyl ether	EXD-141	0.522823729

(Continued on following page)

TABLE 3 | (*Continued*) The potential important components and score in GSK, XLGB, and EXD.

Formula	Name	Component	Q
EXD	2-Phenylethanol	EXD-456	0.145887101
EXD	2-Carbomethoxy-9,10-anthraquinone	EXD-526	0.126521782
EXD	2,6,4′-Trihydroxy-4-methoxybenzophenone	EXD-745	0.108038542
EXD	1-Hydroxy-3-methoxyanthracene-9,10-dione	EXD-517	0.12688071
EXD	1,3-Dimethoxybenzene	EXD-9	0.100024253

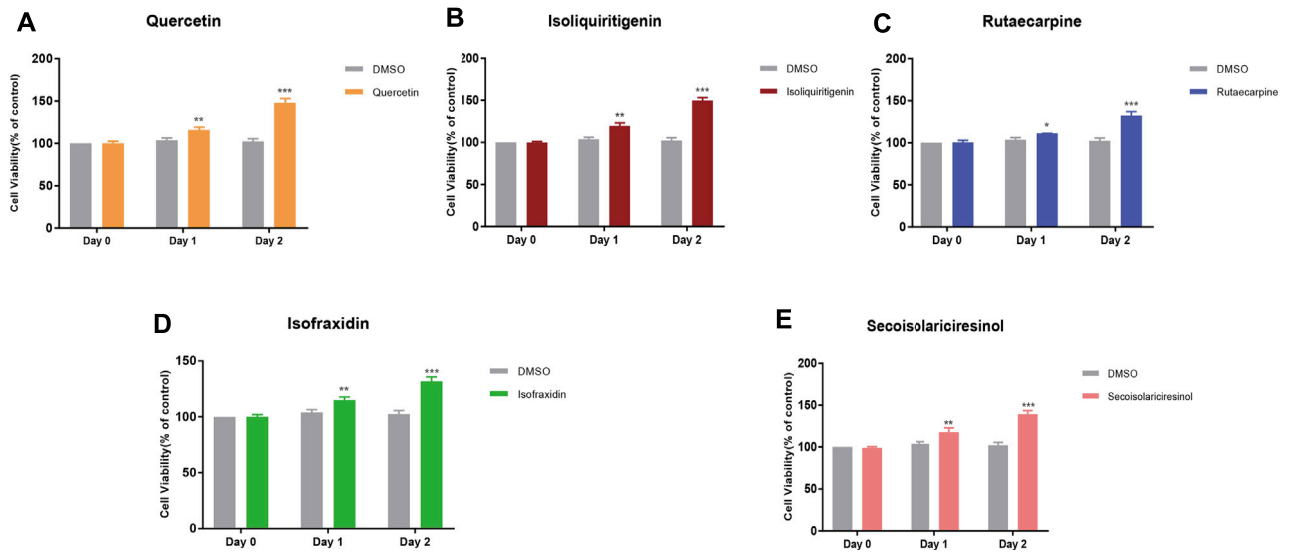

FIGURE 11 | Effects of quercetin **(A)**, isoliquiritigenin **(B)**, rutaecarpine **(C)**, isofraxidin **(D)**, and secoisolariciresinol **(E)** on cell viabilities on MC3T3-E1 cells. *p < 0.05, **p < 0.01, ***p < 0.001 compared with DMSO group.

advantages in the treatment of OP because of their remarkable efficacy and few side effects. However, due to the characteristic of "multi-components-multi-targets-multi-pathways," their mechanism of action is not yet clear. Therefore, it is required to exploit new methods to study the pharmacological material basis and molecular mechanism of herbal medicine prescriptions and make a scientific interpretation.

Herbal informatics is an interdisciplinary subject that integrates Chinese medicine, computer science, biology, mathematics, multi-directional pharmacology, and other disciplines. It researches complex herbal medicine systems by systematically observing the intervention and influence of drugs on disease networks (Guo et al., 2021). Herbal informatics has been widely used in herbal medicine. For example, Wang Kexin et al. systematically interpreted the compatibility of Huanglian Jiedu Decoction in treating diseases (Wang et al., 2020b). Gao Yao et al. used the method of herbal informatics to analyze the mechanism of LCW in treating Systemic Lupus Erythematosus (Gao et al., 2020). Yang Lang et al. designed a new network pharmacology method to decode the mechanism of EXD in treating OP (Yang et al., 2021). These studies demonstrate the reliability of herbal informatics.

In this study, after ADME screening, 517 active components were obtained. Among the three prescriptions, there were 88 common components; there were 65, 37, and 232 specific components in GSK, XLGB, and EXD, respectively. This suggests that the three prescriptions impact OP treatment through common and specific components.

To quickly extract vital information from the complex C-T networks, we designed a novel function motif discovery model and a genetic-based optimization model and obtained 11, 13, and 15 FRMs (p < 0.05). The FRMs were used to detect the latent action mode of GSK, XLGB, and EXD in the clinical therapeutics of OP.

The function motif discovery model based on a random walk adopts the idea of double-layer coding, which can greatly simplify the coding length. Nodes are divided into N categories with different numbers, and the same coding is used in each category so that the coding length can be saved. The genetic-based optimization model has good global search ability and can quickly search for all solutions in the solution space without falling into the trap of fast descent of local optimal solutions. Moreover, it can conveniently carry out distributed calculations, accelerate the solving speed, and have strong convergence using its inherent parallelism. At the same time, searching from the group has the potential to be parallel. It can compare multiple individuals at the same time and use the evaluation function to evaluate individuals. The process is simple. In the iterative

process, the probability mechanism is used to iterate, and the selection of individuals is random to avoid accidental results. The genetic algorithm (GA) can retain good individuals and maintain the group's diversity. The information gain inspects the feature's contribution to the whole system and considers both the occurrence and nonoccurrence of the feature. Meanwhile, it considers comprehensively and uses the statistical attributes of all samples to reduce the sensitivity to noise.

The accuracy and reliability of FRMs were evaluated using the relevance score, the number of reported evidence, and the coverage of functional pathways of FRMs. Results showed that the predicted FRMs overlapped with the C-T network in pathogenic genes and functional pathways at high coverage.

Next, we conducted pathway enrichment analysis for each FRMs and found that 16 enriched pathways were shared by three prescriptions. Through a literature search, we found that osteoclast differentiation, calcium signaling pathway, MAPK signaling pathway, and PI3K-Akt signaling pathway were most reported. Recent research has shown that RANKL-induced ROS signaling regulates the MAPK and NF-κB activity, and the loss of NF-κB signaling in mouse models causes bone defect formation, leading to osteoporosis (Iotsova et al., 1997). RANKL can stimulate the three main members of the MAPK signaling pathway, JNK, ERK, and P38, therefore impacting the differentiation of osteoclasts (Boyle et al., 2003). In the OVX mouse model, the reduction of ROS level and the inhibition of the MAPK signaling pathway can inhibit osteoclast differentiation and reduce bone loss (Xiao et al., 2020). PI3K/AKT signaling pathway exists in mammalian cells; is involved in cell proliferation, metastasis, and apoptosis; and regulates the functions of osteoblasts and osteoclasts by affecting their formation, proliferation, differentiation, and apoptosis (Agas et al., 2013) (Qu et al., 2014). Activating the PI3K/AKT signaling pathway affects the upregulation of the expression of osteogenic differentiation marker genes, thereby promoting the proliferation and differentiation of osteoblasts (Lu et al., 2017). Inhibition of the PI3K/AKT signaling pathway can reduce the bone resorption ability of osteoclasts (Zhang et al., 2020), thus inhibiting the occurrence of osteoporosis.

Furthermore, we found that some enriched genes were shared by four pathways, but others were specific to one pathway, and these genes all played different roles in the influence of OP, indicating that the FRMs of different prescriptions have different and co-functional effects in the treatment of OP. It provides a possible mechanism reference for us to reveal multiple treatments for the same disease.

Then, we devised a novel component importance calculation method that combined the information gain and target influence to screen the key component groups in different prescriptions. The components with a $\boldsymbol{Q}$ score more than 0.01 were defined as potential important components in each prescription. Using this new method, we obtained 24, 23, and 22 potential important components in GSK, XLGB, and EXD; selected the highest important component; and randomly selected components as the key component groups of the three prescriptions, including quercetin, isoliquiritigenin, rutaecarpine, isofraxidin, and secoisolariciresinol. The effectiveness of these components was verified by *in vitro* experiments to prove the model's reliability.

In vitro cell experiments also showed that these components can increase the viability of MC3T3-E1 cells, speculating that these components have a certain role in treating OP. Additionally, to better evaluate the dependability of our proposed network pharmacological model, we will conduct *in vivo* studies in future studies.

However, there are still some limitations in this study. First, more ingredients from key component groups should be selected for validating the reliability of our method and model. Second, the action mode of GSK, XLGB, and EXD in the clinic therapy of OP is not verified in this study. Meanwhile, the issue of drug dose should be considered in future studies.

In conclusion, we propose a new network pharmacology strategy that reveals the hidden mechanisms of different prescriptions for OP through new bioinformatics models and experimental validation, providing a new web-based approach for herbal medicine treatment of complex diseases.

DATA AVAILABILITY STATEMENT

The original contributions presented in the study are included in the article/**Supplementary Material**, further inquiries can be directed to the corresponding authors.

AUTHOR CONTRIBUTIONS

DG and AL provided the concept and designed the study. YL and DG conducted the analyses and wrote the manuscript. YL, QL, YC, YL, HY, JW, CY, QC, HY, and DG participated in data analysis. DG and YL contributed to revising and proofreading the manuscript. All authors read and approved the final manuscript.

FUNDING

This study is financially supported by the Startup fund from Southern Medical University (grant no. G619280010), the Natural Science Foundation Council of China (grant no. 32070676, 31501080), the National Key R&D Program of China (2018YFC1705205), Natural Science Foundation of Guangdong Province (grant no. 2021A1515010737), Hong Kong Baptist University Strategic Development Fund (grant no. SDF13-1209-P01, SDF15-0324-P02(b) and SDF19-0402-P02), Hong Kong Baptist University Interdisciplinary Research Matching Scheme (grant no. RC/IRCs/17-18/04), the 2020 Guangdong Provincial Science and Technology Innovation Strategy Special Fund (grant no. 2020B1212030006).

SUPPLEMENTARY MATERIAL

The Supplementary Material for this article can be found online at: https://www.frontiersin.org/articles/10.3389/fcell.2022.831894/full#supplementary-material

REFERENCES

Agas, D., Sabbieti, M. G., Marchetti, L., Xiao, L., and Hurley, M. M. (2013). FGF-2 Enhances Runx-2/Smads Nuclear Localization in BMP-2 Canonical Signaling in Osteoblasts. *J. Cel. Physiol.* 228 (11), 2149–2158. doi:10.1002/jcp.24382

Agrawal, A., and Gartland, A. (2015). P2X7 Receptors: Role in Bone Cell Formation and Function. *J. Mol. Endocrinol.* 54 (2), R75–R88. doi:10.1530/jme-14-0226

Boyle, W. J., Simonet, W. S., and Lacey, D. L. (2003). Osteoclast Differentiation and Activation. *Nature* 423 (6937), 337–342. doi:10.1038/nature01658

Casado-Díaz, A., Anter, J., Dorado, G., and Quesada-Gómez, J. M. (2016). Effects of Quercetin, a Natural Phenolic Compound, in the Differentiation of Human Mesenchymal Stem Cells (MSC) into Adipocytes and Osteoblasts. *J. Nutr. Biochem.* 32, 151–162. doi:10.1016/j.jnutbio.2016.03.005

Chen, D., Ye, Z., Wang, C., Wang, Q., Wang, H., Kuek, V., et al. (2020). Arctiin Abrogates Osteoclastogenesis and Bone Resorption via Suppressing RANKL-Induced ROS and NFATc1 Activation. *Pharmacol. Res.* 159, 104944. doi:10.1016/j.phrs.2020.104944

Chen, K., Qiu, P., Yuan, Y., Zheng, L., He, J., Wang, C., et al. (2019). Pseurotin A Inhibits Osteoclastogenesis and Prevents Ovariectomized-Induced Bone Loss by Suppressing Reactive Oxygen Species. *Theranostics* 9 (6), 1634–1650. doi:10.7150/thno.30206

Cho, S. W., Sun, H. J., Yang, J.-Y., Jung, J. Y., An, J. H., Cho, H. Y., et al. (2009). Transplantation of Mesenchymal Stem Cells Overexpressing RANK-Fc or CXCR4 Prevents Bone Loss in Ovariectomized Mice. *Mol. Ther.* 17 (11), 1979–1987. doi:10.1038/mt.2009.153

Conigrave, A. D., Brown, E. M., and Rizzoli, R. (2008). Dietary Protein and Bone Health: Roles of Amino Acid-Sensing Receptors in the Control of Calcium Metabolism and Bone Homeostasis. *Annu. Rev. Nutr.* 28, 131–155. doi:10.1146/annurev.nutr.28.061807.155328

Daina, A., Michielin, O., and Zoete, V. (2017). SwissADME: a Free Web Tool to Evaluate Pharmacokinetics, Drug-Likeness and Medicinal Chemistry Friendliness of Small Molecules. *Sci. Rep.* 7, 42717. doi:10.1038/srep42717

Das, S., and Crockett, J. C. (2013). Osteoporosis - a Current View of Pharmacological Prevention and Treatment. *Drug Des. Devel Ther.* 7, 435–448. doi:10.2147/DDDT.S31504

Delmas, P. D. (2005). The Use of Bisphosphonates in the Treatment of Osteoporosis. *Curr. Opin. Rheumatol.* 17 (4), 462–466. doi:10.1097/01.bor.0000163448.51661.87

Fang, Y., Xue, Z., Zhao, L., Yang, X., Yang, Y., Zhou, X., et al. (2019). Calycosin Stimulates the Osteogenic Differentiation of Rat Calvarial Osteoblasts by Activating the IGF1R/PI3K/Akt Signaling Pathway. *Cell Biol Int* 43 (3), 323–332. doi:10.1002/cbin.11102

Gao, Y., Wang, K.-x., Wang, P., Li, X., Chen, J.-j., Zhou, B.-y., et al. (2020). A Novel Network Pharmacology Strategy to Decode Mechanism of Lang Chuang Wan in Treating Systemic Lupus Erythematosus. *Front. Pharmacol.* 11, 512877. doi:10.3389/fphar.2020.512877

Gao, Y., Wu, D., Tian, J.-S., Zhou, Y.-Z., Gao, X., Qin, X., et al. (2018). Mechanism of Network Pharmacology of Xiaoyao Powder and Kaixin Powder in Treating Depression with "Same Disease with Different Treatments. *Chin. Traditional Herbal Drugs* 49 (15), 3483–3492. doi:10.7501/j.issn.0253-2670.2018.15.004

Guo, S., Zhou, J. Y., Tan, C., Shi, L., Shi, Y., and Shi, J. (2021). Network Pharmacology-Based Analysis on the Mechanism of Action of Ephedrae Herba-Cinnamomi Ramulus Couplet Medicines in the Treatment for Psoriasis. *Med. Sci. Monit.* 27, e927421. doi:10.12659/MSM.927421

Guo, Y., Yan, K., Fang, J., Qu, Q., Zhou, M., and Chen, F. (2013). Let-7b Expression Determines Response to Chemotherapy through the Regulation of Cyclin D1 in Glioblastoma. *J. Exp. Clin. Cancer Res.* 32, 41. doi:10.1186/1756-9966-32-41

Iotsova, V., Caamaño, J., Loy, J., Yang, Y., Lewin, A., and Bravo, R. (1997). Osteopetrosis in Mice Lacking NF-Kb1 and NF-Kb2. *Nat. Med.* 3 (11), 1285–1289. doi:10.1038/nm1197-1285

Lane, J. M., Russell, L., and Khan, S. N. (2000). Osteoporosis. *Clin. Orthopaedics Relat. Res.* 372 (372), 139–150. doi:10.1097/00003086-200003000-00016

Li, J.-Y., Jia, Y.-S., Chai, L.-M., Mu, X.-H., Ma, S., Xu, L., et al. (2017). Effects of Chinese Herbal Formula Erxian Decoction for Treating Osteoporosis: a Systematic Review. *Clin. Interv. Aging* 12, 45–53. doi:10.2147/cia.s117597

Li, S. Q., Pei, Z. G., and Liu, Y. M. (2001). Clinical Study on Effect of Gushukang Granule in Preventing and Treating Primary Osteoporosis. *Zhongguo Zhong Xi Yi Jie He Za Zhi* 21, 265–268.

Li, S., and Zhang, B. (2013). Traditional Chinese Medicine Network Pharmacology: Theory, Methodology and Application. *Chin. J. Nat. Medicines* 11 (2), 110–120. doi:10.1016/s1875-5364(13)60037-0

Lipinski, C. A., Lombardo, F., Dominy, B. W., and Feeney, P. J. (2001). Experimental and Computational Approaches to Estimate Solubility and Permeability in Drug Discovery and Development Settings. *Adv. Drug Deliv. Rev.* 46 (1-3), 3–26. doi:10.1016/s0169-409x(00)00129-0

Liu, X., Zhang, S., Lu, X., Zheng, S., Li, F., and Xiong, Z. (2012). Metabonomic Study on the Anti-osteoporosis Effect of Rhizoma Drynariae and its Action Mechanism Using Ultra-performance Liquid Chromatography-Tandem Mass Spectrometry. *J. Ethnopharmacology* 139 (1), 311–317. doi:10.1016/j.jep.2011.11.017

Lopes, H. B., Freitas, G. P., Elias, C. N., Tye, C., Stein, J. L., Stein, G. S., et al. (2019). Participation of Integrin β3 in Osteoblast Differentiation Induced by Titanium with Nano or Microtopography. *J. Biomed. Mater. Res.* 107 (6), 1303–1313. doi:10.1002/jbm.a.36643

Lu, S.-Y., Wang, C.-Y., Jin, Y., Meng, Q., Liu, Q., Liu, Z.-h., et al. (2017). The Osteogenesis-Promoting Effects of Alpha-Lipoic Acid against Glucocorticoid-Induced Osteoporosis through the NOX4, NF-kappaB, JNK and PI3K/AKT Pathways. *Sci. Rep.* 7 (1), 3331. doi:10.1038/s41598-017-03187-w

Mendes, A. B., Martins, F. F., Cruz, W. M. S., da Silva, L. E., Abadesso, C. B. M., and Boaventura, G. T. (2012). Bone Development in Children and Adolescents with PKU. *J. Inherit. Metab. Dis.* 35 (3), 425–430. doi:10.1007/s10545-011-9412-7

Miller, P. D. (2016). Management of Severe Osteoporosis. *Expert Opin. Pharmacother.* 17 (4), 473–488. doi:10.1517/14656566.2016.1124856

Moriishi, T., Maruyama, Z., Fukuyama, R., Ito, M., Miyazaki, T., Kitaura, H., et al. (2011). Overexpression of Bcl2 in Osteoblasts Inhibits Osteoblast Differentiation and Induces Osteocyte Apoptosis. *PLoS One* 6 (11), e27487. doi:10.1371/journal.pone.0027487

Neer, R. M., Arnaud, C. D., Zanchetta, J. R., Prince, R., Gaich, G. A., Reginster, J.-Y., et al. (2001). Effect of Parathyroid Hormone (1-34) on Fractures and Bone mineral Density in Postmenopausal Women with Osteoporosis. *N. Engl. J. Med.* 344 (19), 1434–1441. doi:10.1056/nejm200105103441904

Papapoulos, S., and Makras, P. (2008). Selection of Antiresorptive or Anabolic Treatments for Postmenopausal Osteoporosis. *Nat. Rev. Endocrinol.* 4 (9), 514–523. doi:10.1038/ncpendmet0941

Qu, X., Zhai, Z., Liu, X., Li, H., Ouyang, Z., Wu, C., et al. (2014). Dioscin Inhibits Osteoclast Differentiation and Bone Resorption Though Down-Regulating the Akt Signaling Cascades. *Biochem. Biophysical Res. Commun.* 443 (2), 658–665. doi:10.1016/j.bbrc.2013.12.029

Rapisarda, V., Borghesan, M., Miguela, V., Encheva, V., Snijders, A. P., Lujambio, A., et al. (2017). Integrin Beta 3 Regulates Cellular Senescence by Activating the TGF-β Pathway. *Cel Rep.* 18 (10), 2480–2493. doi:10.1016/j.celrep.2017.02.012

Shalev, M., and Elson, A. (2019). The Roles of Protein Tyrosine Phosphatases in Bone-Resorbing Osteoclasts. *Biochim. Biophys. Acta (Bba) - Mol. Cel Res.* 1866 (1), 114–123. doi:10.1016/j.bbamcr.2018.07.005

Silverman, S. L. (2003). Calcitonin. *Endocrinol. Metab. Clin. North America* 32 (1), 273–284. doi:10.1016/s0889-8529(02)00060-9

Srivastava, M., and Deal, C. (2002). Osteoporosis in Elderly: Prevention and Treatment. *Clin. Geriatr. Med.* 18 (3), 529–555. doi:10.1016/s0749-0690(02)00022-8

Stefanick, M. L. (2005). Estrogens and Progestins: Background and History, Trends in Use, and Guidelines and Regimens Approved by the US Food and Drug Administration. *Am. J. Med.* 118 (Suppl. 12B), 64–73. doi:10.1016/j.amjmed.2005.09.059

Sun, L., Adebanjo, O. A., Moonga, B. S., Corisdeo, S., Anandatheerthavarada, H. K., Biswas, G., et al. (1999). Cd38/Adp-Ribosyl Cyclase. *J. Cel Biol* 146 (5), 1161–1172. doi:10.1083/jcb.146.5.1161

Tella, S. H., and Gallagher, J. C. (2014). Prevention and Treatment of Postmenopausal Osteoporosis. *J. Steroid. Biochem. Mol. Biol.* 142, 155–170. doi:10.1016/j.jsbmb.2013.09.008

Wang, K.-X., Gao, Y., Gong, W.-X., Ye, X.-F., Fan, L.-Y., Wang, C., et al. (2020). A Novel Strategy for Decoding and Validating the Combination Principles of Huanglian Jiedu Decoction from Multi-Scale Perspective. *Front. Pharmacol.* 11, 567088. doi:10.3389/fphar.2020.567088

Wang, K.-x., Gao, Y., Lu, C., Li, Y., Zhou, B.-y., Qin, X.-m., et al. (2020). Uncovering the Complexity Mechanism of Different Formulas Treatment for Rheumatoid Arthritis Based on a Novel Network Pharmacology Model. *Front. Pharmacol.* 11, 1035. doi:10.3389/fphar.2020.01035

Wang, K., Li, K., Chen, Y., Wei, G., Yu, H., Li, Y., et al. (2021). Computational Network Pharmacology–Based Strategy to Capture Key Functional Components and Decode the Mechanism of Chai-Hu-Shu-Gan-San in Treating Depression. *Front. Pharmacol*, 12, 782060. doi:10.3389/fphar.2021.782060

Wang, L. J., and Cai, H. Q. (2020). Let-7b Downgrades CCND1 to Repress Osteogenic Proliferation and Differentiation of MC3T3-E1 Cells: An Implication in Osteoporosis. *Kaohsiung J. Med. Sci.* 36 (10), 775–785. doi:10.1002/kjm2.12236

Wang, N., Agrawal, A., Jørgensen, N. R., and Gartland, A. (2018). P2X7 Receptor Regulates Osteoclast Function and Bone Loss in a Mouse Model of Osteoporosis. *Sci. Rep.* 8 (1), 3507. doi:10.1038/s41598-018-21574-9

Wang, Q., Zhao, Y., Sha, N., Zhang, Y., Li, C., Zhang, H., et al. (2018). The Systemic Bone Protective Effects of Gushukang Granules in Ovariectomized Mice by Inhibiting Osteoclastogenesis and Stimulating Osteoblastogenesis. *J. Pharmacol. Sci.* 136 (3), 155–164. doi:10.1016/j.jphs.2018.01.007

Wang, X. J., Liang, R. X., and Zhao, L. (2007). Progress of Study on Prevention and Treatment of Osteoporosis by Compound Gushukang. *Zhongguo Zhong Xi Yi Jie He Za Zhi* 27, 282–285.

Westbroek, I., van der Plas, A., de Rooij, K. E., Klein-Nulend, J., and Nijweide, P. J. (2001). Expression of Serotonin Receptors in Bone. *J. Biol. Chem.* 276 (31), 28961–28968. doi:10.1074/jbc.m101824200

Wittrant, Y., Gorin, Y., Mohan, S., Wagner, B., and Abboud-Werner, S. L. (2009). Colony-stimulating Factor-1 (CSF-1) Directly Inhibits Receptor Activator of Nuclear Factor-Kb Ligand (RANKL) Expression by Osteoblasts. *Endocrinology* 150 (11), 4977–4988. doi:10.1210/en.2009-0248

Wu, Z., Zhu, X., Xu, C., Chen, Y., Zhang, L., and Zhang, C. (2017). Effect of Xianling Gubao Capsules on Bone mineral Density in Osteoporosis Patients. *J. Biol. Regul. Homeost. Agents* 31 (2), 359.

Xiao, L., Zhong, M., Huang, Y., Zhu, J., Tang, W., Li, D., et al. (2020). Puerarin Alleviates Osteoporosis in the Ovariectomy-Induced Mice by Suppressing Osteoclastogenesis via Inhibition of TRAF6/ROS-dependent MAPK/NF-κB Signaling Pathways. *Aging* 12 (21), 21706–21729. doi:10.18632/aging.103976

Xu, J., and Lin, D. I. (2018). Oncogenic C-Terminal Cyclin D1 (CCND1) Mutations Are Enriched in Endometrioid Endometrial Adenocarcinomas. *PLoS One* 13 (7), e0199688. doi:10.1371/journal.pone.0199688

Yang, L., Fan, L., Wang, K., Chen, Y., Liang, L., Qin, X., et al. (2021). Analysis of Molecular Mechanism of Erxian Decoction in Treating Osteoporosis Based on Formula Optimization Model. *Oxid Med. Cel Longev* 2021, 6641838. doi:10.1155/2021/6641838

Yao, H., Yao, Z., Zhang, S., Zhang, W., and Zhou, W. (2018). Upregulation of SIRT1 Inhibits H2O2-induced O-steoblast A-poptosis via FoxO1/β-catenin P-athway. *Mol. Med. Rep.* 17 (5), 6681–6690. doi:10.3892/mmr.2018.8657

Ye, C., Zhang, W., Hang, K., Chen, M., Hou, W., Chen, J., et al. (2019). Extracellular IL-37 Promotes Osteogenic Differentiation of Human Bone Marrow Mesenchymal Stem Cells via Activation of the PI3K/AKT Signaling Pathway. *Cell Death Dis* 10 (10), 753. doi:10.1038/s41419-019-1904-7

Zhang, N.-D., Han, T., Huang, B.-K., Rahman, K., Jiang, Y.-P., Xu, H.-T., et al. (2016). Traditional Chinese Medicine Formulas for the Treatment of Osteoporosis: Implication for Antiosteoporotic Drug Discovery. *J. Ethnopharmacology* 189, 61–80. doi:10.1016/j.jep.2016.05.025

Zhang, Y., Cao, X., Li, P., Fan, Y., Zhang, L., Li, W., et al. (2020). PSMC6 Promotes Osteoblast Apoptosis through Inhibiting PI3K/AKT Signaling Pathway Activation in Ovariectomy-Induced Osteoporosis Mouse Model. *J. Cel Physiol* 235 (7-8), 5511–5524. doi:10.1002/jcp.29261

Zhao, C., Yang, J., Wu, Y., and Yu, R.Hunan University of Chinese Medicine (2019). Fuling Xingren Gancao Decoction and Ju-Zhi-Jiang Decoction in Treating Coronary Heart Disease with "Treating Same Disease with Different Treatments. *Acta Chin. Med.* doi:10.16368/j.issn.1674-8999.2019.11.556

Zhao, Y. H., and Wang, M. W. (2003). Progress of Experimental Research on Prevention and Treatment of Osteoporosis by Traditional Chinese Medicine. *Zhongguo Zhong Xi Yi Jie He Za Zhi* 23 (12), 943–945.

Zhu, N., and Hou, J. (2020). Exploring the Mechanism of Action Xianlingubao Prescription in the Treatment of Osteoporosis by Network Pharmacology. *Comput. Biol. Chem.* 85 (Suppl. 4), 107240. doi:10.1016/j.compbiolchem.2020.107240

Zinnia, M. A., and Khademul Islam, A. B. M. M. (2021). Fenugreek Steroidal Saponins Hinder Osteoclastogenic Bone Resorption by Targeting CSF-1R Which Diminishes the RANKL/OPG Ratio. *Int. J. Biol. Macromolecules* 186, 351–364. doi:10.1016/j.ijbiomac.2021.06.197

Zou, Z., Liu, R., Wang, Y., Xing, Y., Shi, Z., Wang, K., et al. (2021). IL1RN Promotes Osteoblastic Differentiation via Interacting with ITGB3 in Osteoporosis. *Acta Biochim. Biophys. Sin (Shanghai)* 53 (3), 294–303. doi:10.1093/abbs/gmaa174

Conflict of Interest: The authors declare that the research was conducted in the absence of any commercial or financial relationships that could be construed as a potential conflict of interest.

Publisher's Note: All claims expressed in this article are solely those of the authors and do not necessarily represent those of their affiliated organizations, or those of the publisher, the editors, and the reviewers. Any product that may be evaluated in this article, or claim that may be made by its manufacturer, is not guaranteed or endorsed by the publisher.

frontiers | Frontiers in Cell and Developmental Biology

ORIGINAL RESEARCH
published: 20 May 2022
doi: 10.3389/fcell.2022.883228

β-Ecdysterone Enhanced Bone Regeneration Through the BMP-2/SMAD/RUNX2/Osterix Signaling Pathway

Cai-Ping Yan[1,2†], Xing-Kuan Wang[1,2†], Ke Jiang[1,2], Chong Yin[3], Chao Xiang[1,2], Yong Wang[1,2], Chaoyu Pu[1,2], Lu Chen[1] and Yu-Ling Li[1,2*]*

[1]Department of Orthopaedics, Affiliated Hospital of North Sichuan Medical College, Nanchong, China, [2]Laboratory of Biological Tissue Engineering and Digital Medicine, Affiliated Hospital of North Sichuan Medical College, Nanchong, China, [3]Laboratory for Bone Metabolism, Xi'an Key Laboratory of Special Medicine and Health Engineering, Key Lab for Space Biosciences and Biotechnology, NPU-UAB Joint Laboratory for Bone Metabolism, Research Center for Special Medicine and Health Systems Engineering, School of Life Sciences, Northwestern Polytechnical University, Xi'an, China

OPEN ACCESS

Edited by:
Cory Xian,
University of South Australia, Australia

Reviewed by:
Beth Bragdon,
Boston University, United States
Se Eun Kim,
Chonnam National University, South Korea

***Correspondence:**
Ke Jiang
jiangke2010@nsmc.edu.cn
Yu-Ling Li
lyl1987@nsmc.edu.cn

[†]These authors have contributed equally to this work and share first authorship

Specialty section:
This article was submitted to Morphogenesis and Patterning, a section of the journal Frontiers in Cell and Developmental Biology

Received: 24 February 2022
Accepted: 03 May 2022
Published: 20 May 2022

Citation:
Yan C-P, Wang X-K, Jiang K, Yin C, Xiang C, Wang Y, Pu C, Chen L and Li Y-L (2022) β-Ecdysterone Enhanced Bone Regeneration Through the BMP-2/SMAD/RUNX2/Osterix Signaling Pathway. Front. Cell Dev. Biol. 10:883228. doi: 10.3389/fcell.2022.883228

Bone defects are a global public health problem. However, the available methods for inducing bone regeneration are limited. The application of traditional Chinese herbs for bone regeneration has gained popularity in recent years. β-ecdysterone is a plant sterol similar to estrogen, that promotes protein synthesis in cells; however, its function in bone regeneration remains unclear. In this study, we investigated the function of β-ecdysterone on osteoblast differentiation and bone regeneration *in vitro* and *in vivo*. MC3T3-E1 cells were used to test the function of β-ecdysterone on osteoblast differentiation and bone regeneration *in vitro*. The results of the Cell Counting Kit-8 assay suggested that the proliferation of MC3T3-E1 cells was promoted by β-ecdysterone. Furthermore, β-ecdysterone influenced the expression of osteogenesis-related genes, and the bone regeneration capacity of MC3T3-E1 cells was detected by polymerase chain reaction, the alkaline phosphatase (ALP) test, and the alizarin red test. β-ecdysterone could upregulate the expression of osteoblastic-related genes, and promoted ALP activity and the formation of calcium nodules. We also determined that β-ecdysterone increased the mRNA and protein levels of components of the BMP-2/Smad/Runx2/Osterix pathway. DNA sequencing further confirmed these target effects. β-ecdysterone promoted bone formation by enhancing gene expression of the BMP-2/Smad/Runx2/Osterix signaling pathway and by enrichment biological processes. For *in vivo* experiments, a femoral condyle defect model was constructed by drilling a bone defect measuring 3 mm in diameter and 4 mm in depth in the femoral condyle of 8-week-old Sprague Dawley male rats. This model was used to further assess the bone regenerative functions of β-ecdysterone. The results of micro-computed tomography showed that β-ecdysterone could accelerate bone regeneration, exhibiting higher bone volume, bone surface, and bone mineral density at each observation time point. Immunohistochemistry confirmed that the β-ecdysterone also increased the expression of collagen, osteocalcin, and bone morphogenetic protein-2 in the experiment group at 4 and 8 weeks. In conclusion, β-ecdysterone is a new bone regeneration regulator that can

stimulate MC3T3-E1 cell proliferation and induce bone regeneration through the BMP-2/Smad/Runx2/Osterix pathway. This newly discovered function of β-ecdysterone has revealed a new direction of osteogenic differentiation and has provided novel therapeutic strategies for treating bone defects.

Keywords: β-ecdysterone, bone regeneration, bone morphogenetic protein-2 (BMP2), RUNX 2, Smad

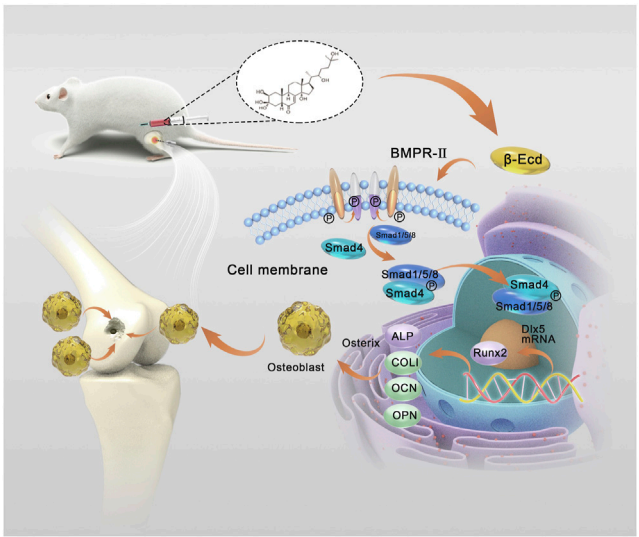

GRAPHICAL ABSTRACT | Schematic illustrations of the fabrication of the bone defect model and action of β-Ecd in promoting bone regeneration and repair of bone defects. We established a rat model of a femoral bone defect *in vivo* to evaluate the effect of β-Ecd on bone regeneration. Rats injected intraperitoneally with 72 mg/kg β-Ecd showed a higher degree of ossification of regenerated bone tissue at the site of the bone defect at weeks 4 and 8. β-ecdysterone binding to the BMP2 receptor activates SMAD1 to bind to SMAD1/5/8, promotes RUNX2 and OSTERIX replication in the nucleus, and mediates bone regeneration. This study provides a new approach to the treatment of bone injury and degenerative diseases represented by bone defects and osteoporosis.

INTRODUCTION

Bone defect refers to the destruction of the structural integrity of the phalanx, and complete or partial destruction of its continuity. Studies have shown that a variety of signal transduction mechanisms regulate bone growth metabolism and regeneration after bone injury. When these critical signal transduction mechanisms that promote bone growth are not fully activated or destroyed, bone formation is reduced and bone marrow fat accumulation increases, resulting in impaired bone regeneration (Hak et al., 2014; Yu et al., 2018). Bone regeneration is a highly complex but organized process that requires damaged bones to return to their pre-injury cellular structure and biomechanical functions (Schindeler et al., 2008). Both, intramembranous and endochondral ossification are essential forms of bone regeneration (Phillips 2005; Takigawa 2013; Ko and Sumner 2021). In the process of intramembranous ossification, bone marrow mesenchymal stem cells (BMSCs) differentiate directly into osteoblasts and deposit mineralized extracellular matrix to achieve bone regeneration (Percival and Richtsmeier 2013). BMSCs are cells with multi-differentiation potential, and have the ability to differentiate into bone, cartilage, fat, nerves, or myoblasts *in vivo* and *in vitro* (Sumer, Liu et al., 2018, Yang et al., 2019; Zhao et al., 2020). BMSCs can also secrete a variety of cytokines (such as BMP-2, IGF-1, IL-6, and M-CSF) to promote bone regeneration (Meirelles et al., 2009). On exposure to certain specific chemical mediators, cytokines, and mechanical stimulation, intracellular BMP-Smad, Wnt/β-catenin, Notch, Hedgehog, or other signaling pathways of BMSCs are activated to promote osteoblast differentiation (Abdallah et al., 2005). However, when the specific environment is destroyed due to various diseases, BMSCs show abnormal osteogenic differentiation, an imbalance of metabolic regulation, which reduces the bone remodeling rate, bone matrix, and bone mineral deficiency; eventually, this can cause bone regeneration deficiency, osteoporosis, and osteomalacia (Liu et al., 2018). It is therefore essential that strategies are identified to effectively regulate the function of BMSCs for promoting osteogenic differentiation and bone regeneration.

In recent years, researchers have tried various approaches to boost stem cell function. Basic and clinical studies are increasingly investigating the promotion of osteogenic differentiation of BMSCs and the mechanisms involved, including traditional cytokines and related physical and

chemical stimulation factors. Osteoblast growth peptide promotes osteogenic differentiation of BMSCs through the RhoA/ROCK pathway in a dose-dependent manner (Chen et al., 2011). Boron can promote the synthesis of osteogenic genes in the proliferation and differentiation of human BMSCs (Ying et al., 2011). The BMP-2 related peptides P24 (Lin et al., 2010) and simvastatin (Feng et al., 2020) also promote osteogenic differentiation and proliferation of BMSCs. BMPs are acidic proteins located in the bone matrix, and belong to the TGF-β superfamily. BMPs serve essential roles in skeletal development, bone formation, and MSC differentiation (Cai et al., 2021). Research has shown that fenofibrates induce PPARα and BMP2 expression to stimulate osteoblast differentiation; however, disruption in BMP signaling causes skeletal and vascular abnormalities (Miyazono, Kamiya and Morikawa 2010). In this context, a study showed BMP-2 and BMP-4 knockouts to be embryonically lethal in mice (Scarfì 2016). Thus, BMP2 serves an important role in inducing the osteogenic differentiation of MSCs (Toth et al., 2021).

In their study, Jian et al. (2013) applied 50, 100, and 200 μmol/L β-ecdysterone to human periodontal membrane stem cells (PDLSs) *in vitro* and confirmed that 200 μmol/L β-ecdysterone could effectively induce BMP-2 expression and osteogenic differentiation of periodontal membrane stem cells through the extracellular signal-regulated kinase pathway (Jian et al., 2013). However, it is unclear whether these positive effects of β-ecdysterone can also affect BMSCs and the specific molecular mechanisms involved and whether they can be applied to bone regeneration in animals or clinics.

β-ecdysterone is a polyhydroxylated steroid hormone, which is most abundant in insects and Anatidae plants. It is known as a phytoestrogen, because its chemical structure is similar to that of estrogen (Zou et al., 2015). β ecdysterone can not only stimulate protein synthesis (Tóth et al., 2008), promote carbohydrate and lipid metabolism (Catalán et al., 1985), control blood glucose level (Yoshida et al., 1971), inhibit cell apoptosis (Tang et al., 2018a), and improve intervertebral disc degeneration (Wen et al., 2019), but it also has good biocompatibility (Dai et al., 2017). Chinese herbal medicines such as *Achyranthe bidentata* have been used for centuries to treat osteoporosis and joint degeneration in China, and no side effects have been reported for hundreds of years. Studies have shown that β-ecdysterone can stimulate arthropod midgut stem cells (Smagghe et al., 2005) and induce osteogenic differentiation of mouse mesenchymal stem cells (Gao, Cai and Shi 2008). β-ecdysterone can regulate the proliferation and osteogenic differentiation of BMSCs by targeting estrogen receptors *in vivo* and plays an essential role in the process of bone regeneration (Abiramasundari et al., (2018). However, the specific signal transduction mechanism involved, the regulation mode of gene differential expression, and the optimal drug dose have not been discussed in depth. Therefore, a better understanding of the interactions and mechanisms between β-ecdysterone and BMSCs is expected to positively impact bone regeneration and formation.

This study aimed to explore whether β-ecdysterone can promote osteogenic differentiation and functionalization of BMSCs, enhancing their ability to promote *in situ* bone regeneration. Furthermore, it elucidated the potential signal transduction mechanism, differential regulation of gene expression, and appropriate dose of β-ecdysterone in promoting bone regeneration. During the in-vitro experiments, we treated MC3T3-E1 cells with β-ecdysterone to assess their biocompatibility and the osteogenesis-promoting effect. Cell Counting Kit-8 (CCK-8) was used to verify the excellent biocompatibility of β-ecdysterone. Immunohistochemical staining and quantitative polymerase chain reaction (q-PCR) were used to verify the excellent expression of alkaline phosphatase (ALP), collagen I, and other osteogenic proteins in MC3T3-E1 cells treated with β-ecdysterone. The alizarin red staining experiment further verified that the system could effectively form mineralized nodules from the extracellular matrix. Subsequently, MC3T3-E1 cells treated with different doses of β-ecdysterone were analyzed by gene sequencing and differential expression analysis of osteogenic-related genes. β-ecdysterone could effectively improve the replication and transcription of intracellular BMP-Smad signaling pathway genes in a dose-dependent manner. Finally, we added noggin, a BMP2 signaling pathway blocker, to explore any possible relationship between the BMP-2 signaling pathway, metabolism of BMSCs, and osteogenic differentiation after β-ecdysterone treatment; this was performed to evaluate the potential mechanism of enhanced bone regeneration. q-PCR and western blotting showed that β-ecdysterone significantly increased the expression of mRNA and proteins in the BMP2 signaling pathway, and this effect was inhibited by noggin, a BMP2 signaling pathway blocker. Furthermore, we established a rat model of femoral bone defect *in vivo* to evaluate the effect of β-ecdysterone on bone regeneration mediated by BMSCs. The animal experiments showed that at week 4 and 8 after surgery, rats injected intraperitoneally with 72 mg/kg of β-ecdysterone had a higher degree of gross bone tissue growth, bone mineral density, and degree of ossification in regenerated bone tissue at the site of the bone defect (as observed on immunohistochemical staining) than in the other groups. Overall, our data suggested that β-ecdysterone can mediate bone regeneration *via* the BMP2/Smad/Runx/Osterix signaling pathway. This study provides a new approach to the treatment of bone injury and degenerative diseases represented by bone defects and osteoporosis.

MATERIALS AND METHODS

Materials

MC3T3-E1 cells (subclone 14) were purchased from Procell (Wuhan, China), induction medium (Cyagen, Guangzhou, China), α-modified Eagle medium (α-MEM, containing 4.5 g/L D-glucose, 25 mM HEPES), fetal bovine serum, 0.25% trypsin-EDTA, penicillin/streptomycin, and phosphate buffer saline (PBS) were purchased from Hyclone (Logan, UT, United States). Triton X-100, bovine serum albumin, and alizarin red S were purchased from Sangon Biotech (Shanghai, China). The RNeasy Mini Kit was purchased from Qiagen (Duesseldorf, Germany). The PrimeScript RT Master Mix and the TB Green Premix Ex Taq were purchased from Takara

TABLE 1 | RT-qPCR primer sequences.

Gene	Primer sequences
Bmp-2	Forward: 5′-CACGAGAATGGACATGCCC-3′
	Reverse: 5′-GCTTCAGGCCAAACATGCTG-3′
Runx2	Forward: 5′-GCTGTTGTGATGCGTATTCCC-3′
	Reverse: 5′-TGAACCTGGCCACTTGGTTT-3′
Osterix	Forward: 5′-GATGGCGTCCTCTCTGCTTG-3′
	Reverse: 5′-AATGGGCTTCTTCCTCAGCC-3′
Collagen I	Forward: 5′-AAGGCTCCCCTGGAAGAGAT-3′
	Reverse: 5′-CAGGATCGGAACCTTCGCTT-3′
GAPDH	Forward: 5′-TCCATGACAACTTTGGTATCG-3′
	Reverse: 5′-TGTAGCCAAATTCGTTGTCA-3′

(Tokyo, Japan). The CCK-8, 4% paraformaldehyde, 10% cetylpyridinium chloride monohydrate, and β-ecdysterone were purchased from Solarbio (Beijing, China). The alkaline phosphatase assay kit and the goat anti-rabbit IgGDAB kit were purchased from Beyotime (Shanghai, China). Noggin, DAPI, SuperScript II reverse transcriptase, the RevertAid First Strand cDNA Synthesis Kit were purchased from Invitrogen (Thermo Fisher, United States), and 10% sodium dodecyl sulfate-polyacrylamide gel, cell lysis buffer, polyvinylidene fluoride membrane, and goat anti-rabbit antibody were purchased from Boster (Wuhan, China). All primary antibodies (type I collagen, osteopontin, BMP-2, Smad1/5, P-SMad1/5, Runx2, and Osterix) were purchased from Abcam. The animal anesthetic used was isoflurane (Jiangsu, Beikang, China), lidocaine (xylocaine 2%, Hebei Tiancheng, China).

Cell Culture

MC3T3-E1 cells were cultured in α-MEM medium supplemented with 10% fetal bovine serum, 100 U/mL penicillin, and 100 g/ml streptomycin at 37°C in 5% CO_2. The medium was replaced every 2–3 days. When cell fusion reached 80% (80% of the dish was covered by cells), 0.25% trypsin-EDTA was used for digestion, isolation, and passage culture. In our experiment, MC3T3-E1 of the third generation was used.

Cell Proliferation

The CCK-8 assay was used to detect the biocompatibility of β-ecdysterone in MC3T3-E1 cells. MC3T3-E1 cells were incubated with 5×10^3/well in 96-well plates, and 200 μl of α-MEM was added to each well. After incubation for 24 h, β-ecdysterone (Solarbio, Beijing, China) was added to 96-well plates at a final concentration of 0, 50, 100, 150, 200, and 250 μM. The cells were then incubated for 1–7 days. At each observation time point, cells were washed with PBS thrice; 10 μl CCK-8 solution and 100 μl fresh α-MEM medium were added to each well and then incubated at 37°C for 1 h. The absorbance was measured at 460 nm using a microplate reader (Thermo Fisher United States).

Alkaline Phosphatase Activity

ALP activity was measured using an ALP Assay Kit (Beyotime, Shanghai, China). MC3T3-E1 cells were cultured in 6-well plates at 2×10^4 cells/well. When the degree of cell fusion exceeded 60% (60% of the dish was covered by cells), β-ecdysterone was added to the medium at final concentrations of 0, 100, 150, and 200 μM with induction medium. After 3 or 7 days of culture, the cells were washed with PBS and fixed with 4% paraformaldehyde for 15 min. Triton X-100 was used to rupture the cell membranes and cell proteins were extracted by centrifugation at 12,000/min. According to the manufacturer's instructions for the ALP kit, extracts from the control, standard, and experimental groups were transferred to 96-well plates, at volumes of 4, 8, 16, 24, 32, and 40 μl, respectively. The protein concentration was normalized before transfer. Detection buffer and chromogenic substrate were added to achieve a total volume 100 μl, and the reaction system was incubated in darkness at 37°C for 10 min. A stop buffer was added to each well to stop the reaction and the absorbance at 405 nm was measured using a microplate reader.

Alizarin Red S Staining

To test the mineralization ability of MC3T3-E1 cells induced by β-ecdysterone, calcium nodules were detected by alizarin red S staining. MC3T3-E1 cells were incubated at a density of 1×10^4 cells/cm^2 in a dish (φ = 30 mm) and incubated in a medium containing 150 μM of β-ecdysterone or induction medium. The medium and β-ecdysterone were replaced every 3 days. On day 21, the cells were washed with PBS and fixed with 4% paraformaldehyde for 30 min; they were then stained with a 1% alizarin red S solution for 20 min. Decolorization was performed with 10% cetylpyridinium chloride monohydrate for 20 min, and absorbance was measured at 595 nm for quantitative analysis.

Immunocytochemical Staining and Immunofluorescence Staining

To investigate the effect of osteogenic-related protein expression in MC3T3-E1 cells treated with β-ecdysterone, MC3T3-E1 cells were incubated with 1.5×10^4 cells/well in 6-well plates and cultured in standard medium, medium containing 150 μM/L β-ecdysterone, and induction medium. After 14 days of culture, the cells were washed thrice with PBS and fixed in 4% paraformaldehyde solution at room temperature for 15 min. The cells were washed again with PBS and treated with 0.1% Triton X-100 for 15 min. The cells were then incubated in a 5% bovine serum albumin solution at 37°C for 1 h. After washing the cells thrice with PBS, either osteopontin antibody (1:200) or secondary antibody and hematoxylin were added; the cells were then incubated at 4°C overnight, followed by incubation with goat anti-rabbit IgG at room temperature for 30 min. The DAB horseradish peroxidase chromogenic kit was used to detect osteopontin expression in cells. The nuclei were then stained with hematoxylin for 3 min and osteopontin staining was observed under an inverted microscope (Leica Microsystems CMS, Wetzlar, Germany).

Immunofluorescence staining was used to detect type I collagen expression in cells treated with different concentrations of β-ecdysterone. MC3T3-E1 cells were incubated with 1×10^4 cells/well in 6-well plates and cultured in a medium containing 0, 100, 150, and 200 μM/L of β-

TABLE 2 | Effects of β-ecdysterone on the proliferation of MC3T3-E1 cells (*OD value*, *X* ± *SD*).

Culture (day)	β-ecdysterone concentration (μM/L)					
	0	50	100	150	200	250
1	1.00 ± 0.13	1.30 ± 0.03**	1.29 ± 0.07**	1.30 ± 0.06**	1.23 ± 0.11*	1.20 ± 0.01*
2	1.08 ± 0.09	1.64 ± 0.05***	1.69 ± 0.03***	1.88 ± 0.08***	1.54 ± 0.04***	1.54 ± 0.02***
3	1.19 ± 0.06	2.04 ± 0.05***	2.26 ± 0.06***	2.45 ± 0.08***	2.20 ± 0.01***	2.08 ± 0.05***
4	1.00 ± 0.03	1.69 ± 0.24*	2.18 ± 0.34***	2.30 ± 0.12***	2.16 ± 0.17***	2.01 ± 0.27***
5	1.06 ± 0.08	2.75 ± 0.09***	2.78 ± 0.21***	2.89 ± 0.07***	2.65 ± 0.11***	2.50 ± 0.12***
6	1.98 ± 0.03	2.89 ± 0.14***	2.96 ± 0.07***	2.94 ± 0.07***	2.77 ± 0.15***	2.82 ± 0.06***
7	1.72 ± 0.03	1.91 ± 0.05**	2.20 ± 0.26**	2.37 ± 0.09*	2.06 ± 0.09*	1.77 ± 0.14**

Values are expressed as means X ± SD *(n = 5). The control group (0 μM) was compared with each experimental group.* *p < *0.05,* **p < *0.01,* ***p < *0.001, NS, no significance.*

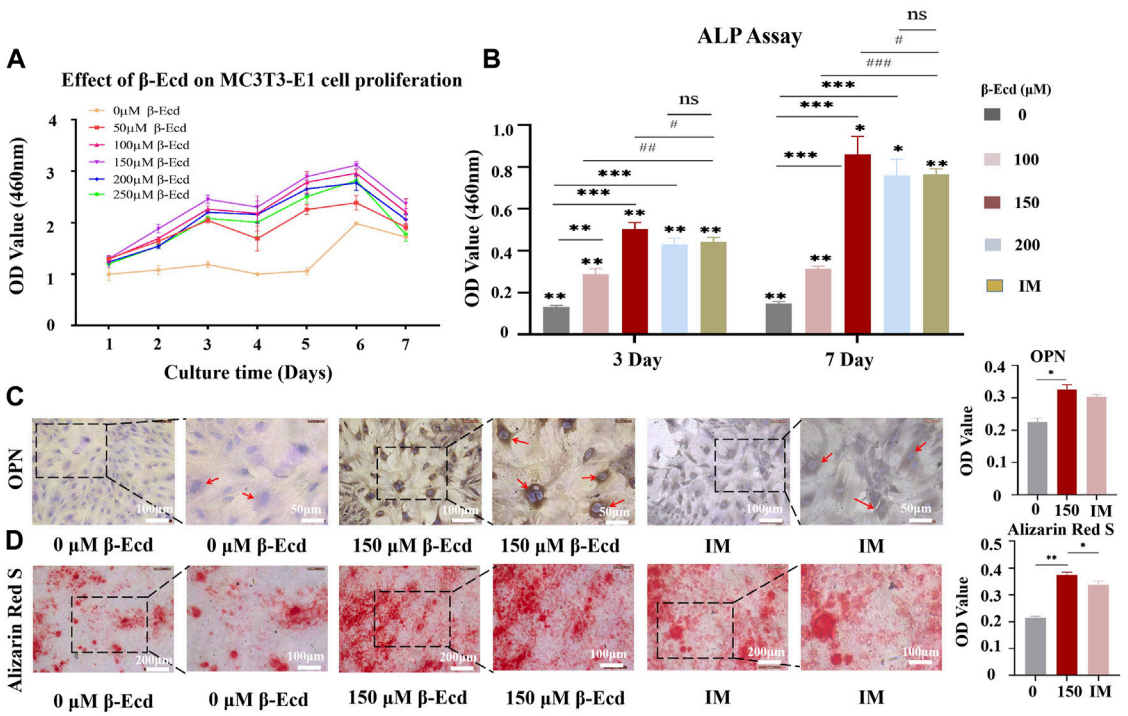

FIGURE 1 | Osteogenic effect of β-Ecd on MC3TE-E1 cells *in vitro*. **(A)** The effects of β-Ecd on the proliferation of MC3TE-E1cells. MC3TE-E1 cells were cultured with medium containing 0 μM β-Ecd (control group) and 50–250 μM β-Ecd (experimental group) and evaluated by the CCK-8 assay. The cell proliferation rate at 1–7 days is shown (*n* = 5). β-Ecd could increase the cell proliferation rate to different degrees, among which 150 μM β-Ecd was the most significant. **(B)** Alkaline phosphatase activity assay. After culturing MC3TE-E1 for 3 and 7 days with medium containing 0 μM β-Ecd (control group) and 100–200 μM β-Ecd (experiment group) or induction medium, intracellular ALP activity was measured. The results showed that the activity of ALP in cells treated with β-Ecd was higher than that of the control group and the most significant increase occurred at 150 μM β-Ecd, there was no significant difference 200 μM β-Ecd group compared with the IM group. The "*" stands for the control group (0 μM) was compared with each experimental group, $^{*}p < 0.05$, $^{**}p < 0.01$, $^{***}p < 0.001$. The "$^{\#}$" stands for the IM group was compared with each experimental group, $^{\#}p < 0.05$, $^{\#\#}p < 0.01$, $^{\#\#\#}p < 0.001$. **(C)** Immunocytochemical staining to detect the expression of osteopontin in MC3TE-E1, after treating MC3TE-E1 with 0 μM β-Ecd (control group) and 150 μM β-Ecd (experimental group) or induction mediun for 14 days, the immunochemistry of osteopontin in cells. The staining results showed that the expression level of the experimental group was significantly higher than that of the control group, there was no significant difference compared with the IM group. The yellow-brown particles in the cytoplasm are osteopontin. **(D)** Alizarin Red S staining to detect the formation of calcified nodules by MC3TE-E1 and its extracellular matrix. After 21 days of treatment with 0 μM β-Ecd (control group) and 150 μM β-Ecd (experimental group) or induction medium, the results of Alizarin Red S staining showed that the formation of calcium nodules in the experimental group was significantly higher than in the control group, there was no significant difference compared with the IM group. In red is the calcium nodule. ImageJ software was used to measure the relative expression values in the figure, and three independent experiments were carried out, and the data were expressed as *X* ± *SD*; $^{*}p < 0.05$, $^{**}p < 0.01$, $^{***}p < 0.001$.

ecdysterone; alternatively, they were cultured in induction medium. In addition, noggin (0.5 mg/ml) was added in the control group. After 10 days of induction culture, the cells were fixed at room temperature with 4% paraformaldehyde for 30 min, washed thrice with PBS, and treated with Triton X-100 for 15 min to rupture the cell membranes. The cells were washed again with PBS and blocked at room temperature with 10% normal goat serum for 1 h. The primary antibody of type I collagen was added followed by incubation overnight at 4°C; this was followed by an appropriate dose of fluorescent secondary

TABLE 3 | ALP activity detection (n = 6).

Time (days)	β-ecdysterone (μM)	$\bar{X} \pm SD$ (OD value)	DEA/mg
3	0	0.132 ± 0.01	48.73
	100	0.287 ± 0.03$^{**/\#\#}$	129.51
	150	0.503 ± 0.03$^{***/\#}$	241.37
	200	0.429 ± 0.03$^{***/NS}$	202.79
	IM	0.442 ± 0.02	211.26
7	0	0.146 ± 0.01	56.5
	100	0.314 ± 0.01$^{***/\#\#\#}$	143.49
	150	0.860 ± 0.08$^{***/\#}$	426.23
	200	0.759 ± 0.08$^{***/NS}$	373.93
	IM	0.766 ± 0.03	378.12

Values are expressed as means X ± SD *(*n *= 6). The "*" stands for the control group (0 μM), which was compared with each experimental group.* $p < 0.05$, $^{**}p < 0.01$, $^{***}p < 0.001$. *The "#" stands for the IM group, which was compared with each experimental group.* $^{\#}p < 0.05$, $^{\#\#}p < 0.01$, $^{\#\#\#}p < 0.001$. *ALP, alkaline phosphatase activity; DEA, diethanolamine enzyme activity unit.*

antibody at room temperature for 30 min. The cells were rewashed thrice with PBS and stained with DAPI nuclear stain (0.1 mg/ml; Sigma-Aldrich, St. Louis, MO, United States) for 15 min. A confocal laser scanning microscope (Olympus, Tokyo, Japan) was used to observe the distribution of type I collagen and the fluorescence intensity of type I collagen in the cytoplasm was quantified by ImageJ software (Wayne Rasband, NIH, United States). The determination was repeated thrice in each group.

RNA Sequence Analysis and Gene Enrichment Analysis

To observe and compare gene expression in MC3T3-E1 cells treated with β-ecdysterone, we performed RNA sequencing of the samples. Third generation MC3T3-E1 cells were incubated in a petri dish measuring 10 cm in diameter in a standard medium containing 0, 100, 150, and 200 μM of β-ecdysterone for 5 and 10 days. When the number of cells reached 3×10^6–5×10^6 cells/well, the RNA was extracted by TRIzol (Qiagen) lysis ($n = 3$). After the qualified samples were detected, the TruSeq RNA sample preparation kit was used to construct a sequencing gene bank (Illumina). First, magnetic beads with oligo (dT) enriched eukaryotic mRNA were used, and the mRNA was randomly interrupted by fragmentation buffer. Second, using mRNA as a template, cDNA was synthesized by reverse transcription of RNA using SuperScript II reverse transcriptase (Invitrogen) and cDNA was purified using AMPure XP beads. Third, the purified double-stranded cDNA was repaired, a-tailed, and sequenced. Finally, AMPure XP Beads were used for fragment size selection, and cDNA libraries were obtained by PCR enrichment. After the library was constructed, sequencing was performed using the Illumina platform and bioinformatics analysis was performed at Qingdao Bioscience and Technology Co., Ltd.

Real-Time-qPCR

Real-time PCR (RT-qPCR) was performed to further verify the results of gene sequencing and the impact of the β-ecdysterone on bone regeneration. MC3T3-E1 cells were incubated in 6-well plates at a density of 5×10^5 cells/well. When the cell density exceeded 60% (60% of the dish was covered by cells), induction medium with 150 μM of β-ecdysterone was added in the experimental group, and noggin (0.5 mg/ml) was added in the control group. On days 7 and 10, total RNA was extracted from MC3T3-E1 cells using TRIzol reagent and cDNA was synthesized using the RevertAid First Strand cDNA Synthesis Kit. The cDNA concentration was normalized before transfer. The RT q-PCR was performed using FastStart Universal SYBR Green Master (Rox) (Roche, Germany). The BMP2, Runx2, Osterix, Col I, and GAPDH primer sequences are shown in **Table 1**. Relative gene expression was calculated using the $2^{-\Delta\Delta CT}$ method and all experiments were repeated thrice.

Protein Electrophoresis Analysis

MC3T3-E1 cells were incubated in 6-well plates at a density of 5×10^5 cells/well. Cells cultured in a medium containing different concentrations (0–200 μM) of β-ecdysterone and noggin (0.5 mg/ml) were included in the experimental and control groups, respectively. After 7 days of induction culture, proteins were extracted with cell lysis buffer; the protein concentration was normalized before transfer. Proteins denatured in equal amounts from different samples were separated by electrophoresis on 10% sodium dodecyl sulfate-polyacrylamide gel (Beyotime) and then transferred to a polyvinylidene fluoride membrane. After the protein transfer membrane was enclosed in blocking buffer (Tris-buffered saline containing 0.1% Tween 20 and 5% fat-free milk) for 1 h, it was incubated with primary antibody at 4°C overnight. The goat anti-rabbit antibody (Boster) was then incubated at 37°C for 2 h. The ChemiDoc XRS + chemiluminescence detection system (BIO-RAD) was used for observation and the strip strength was analyzed using ImageJ software. The primary antibodies used were BMP-2 (1:1,000, Abcam), Smad1/5 (1:1,000, Abcam), P-SMad1/5 (1:1,000, Abcam), Runx2 (1:1,000, Abcam), and Osterix (1:1,000, Abcam). All experiments were repeated thrice.

Rat Model of Bone Defects

The animal experiments were approved by the Research Ethics Committee of the Affiliated Hospital of the North Sichuan Medical College (2021–26). Fifteen male Sprague Dawley rats (6–8 weeks old, weighing approximately 200 g) were selected for the animal experiments. The rat model of bone defects (Yan et al., 2019; Li and Helms 2021) was constructed after anesthetizing with inhalational isoflurane (for animals); an anesthesia ventilator was used for maintenance. The anesthesia protocol was as follows: the rat was placed in a closed glass container and anesthetized with 2.5% isoflurane in 30% oxygen (Schubert et al., 2012). During anesthesia induction, the inhalational concentration of isoflurane was raised to 1.5%–3.0% within 7–10 min. Once the four limbs of the rat were limp and no pain reflex was elicited, continuous anesthesia was initiated, oxygen inhalation was maintained *via* a mask, and the concentration of isoflurane was maintained at 1%–2.5%. Incisions were performed after subcutaneous infiltration of lidocaine for local anesthesia. After the operation, the rats were allowed to breathe air freely until they were fully awake.

The specific method of surgery was as follows: after skin preparation, the medial condyle of the femur was exposed and

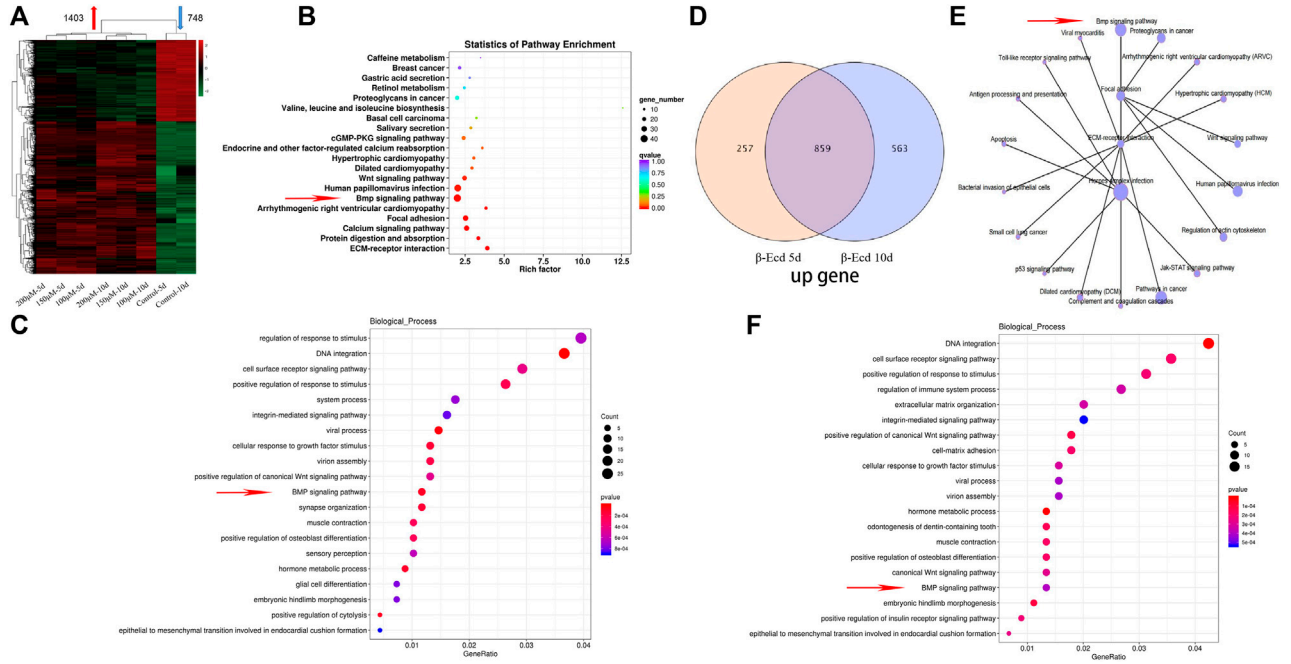

FIGURE 2 | Intracellular RNA was extracted at 5 and 10 days of culture, and transcriptome RNA sequencing analysis was performed. **(A)** Cluster analysis of differentially expressed genes |log2 ratio| > 1 and FDR < 0.05 in the 0–200 μM β-Ecd group compared to 5 and 10 days. **(B)** Differential gene enrichment of the KEGG signaling pathway. **(C)** Analysis of cell biological processes of differential gene enrichment biological processes. **(D)** Venn analysis of differentially expressed genes. **(E)** KEGG signaling pathway of mRNAs associated with osteogenic differentiation. **(F)** Analysis of the cell biology enrichment process of 859 genes upregulated in the Venn analysis.

a bone defect measuring 3 mm in diameter and 4 mm in depth was created using a K wire of 3.0 mm in diameter with a slow-speed electric drill; the site was irrigated using ice-cold saline solution to avoid thermal necrosis. The operative region was then sutured layer by layer. The sham operation group ($n = 5$) only received anesthesia and skin surgery, with no damage to the femur condyle. Rats with bone defects ($n = 10$) were categorized into 2 groups to receive intraperitoneal injections of 0 mg/kg of PBS ($n = 5$) and 72 mg/kg of β-ecdysterone ($n = 5$), respectively, every 3 days. At 4 and 8 weeks after surgery, the mice were over-anesthetized to death. The femur was harvested and fixed with a 4% paraformaldehyde solution for inspection.

In Vivo Toxicology Studies

The animals were segregated into three groups. The group of animals administered 72 mg/kg of intraperitoneal β-ecdysterone for 4 weeks comprised the experimental group; the group administered PBS served as the control group. The untreated mice served as the sham group. After 4 weeks of treatment, the animals were sacrificed by over-anesthesia. The liver and kidney tissues of rats were sectioned and stained with hematoxylin and eosin to observe toxicities *in vivo*.

Micro-Computed Tomography Analysis

All samples collected from rat models with femoral condylar defects were fixed in 4% paraformaldehyde at room temperature for 24 h. Micro-computed tomography (CT) (u-ct80, SCANCO, Switzerland) was used to test the samples (Clark and Badea 2021). Three-dimensional reconstruction was performed using the processed images (Scanco® software) and the bone volume, trabecular thickness, and bone mineral density of each group were detected and analyzed.

Immunohistochemical Analysis

All femoral condyle samples were decalcified and embedded in paraffin after micro-CT analysis. A 5-μm-thick tissue section was analyzed at the bone defect site for histomorphological analysis and the detection of new site-specific proteins of bone tissue (including BMP2 and Runx2). The sections were then stained with hematoxylin and eosin for histochemistry. Images of the histological specimen were obtained using a microscope (Eclipse E800; Nikon, Japan).

Statistical Analysis

Statistical analysis was performed using SPSS 23.0 (IBM Corp., Armonk, NY, United States) and Graphpad Prism 9 (GraphPad Software, United States). The independent sample *t*-test was used to evaluate statistical differences between the two groups and one-way analysis of variance (ANOVA) was used for multiple data groups. Data have been presented as means ± standard deviation. $p < 0.05$ was considered statistically significant.

RESULTS

β-Ecdysterone Promoted the Proliferation of MC3T3-E1 Cells *In Vitro*

To understand the biocompatibility of β-ecdysterone on MC3T3-E1 cells, we treated MC3T3-E1 cells with different concentrations of β-ecdysterone (0, 50, 100, 150, 200, and 250 μM); the CCK-8 assay was used to detect its effect on cell proliferation. The results showed that β-ecdysterone did not significantly inhibit the proliferation of MC3T3-E1 cells at different concentrations, but showed different proliferative abilities (**Table 2**; **Figure 1A**). Cell proliferation activity gradually increased with an increase in drug concentrations from 0 to 150 μM; however, this activity did not continue to increase when drug concentrations increased from 150 to 250 μM. Therefore, we treated cells with β-ecdysterone concentrations of 100, 150, and 200 μM in subsequent experiments.

β-Ecdysterone Enhance Osteogenic Differentiation of MC3T3-E1 Cells *In Vitro*

ALP is an osteoblast marker secreted at the beginning of osteogenic differentiation. To explore the role of β-ecdysterone in promoting osteogenic differentiation of MC3T3-E1 cells, we examined ALP activity in MC3T3-E1 cells. The results showed that intracellular ALP activity increased after treatment with different concentrations of β-ecdysterone (0, 100, 150, and 200 μM) for 3 and 7 days and the effect was dose- and time-dependent. In addition, 150 μM β-ecdysterone induced the most significant increase in ALP activity, which was significantly higher on day 7 than on day 3 (**Table 3**; **Figure 1B**).

Osteopontin (OPN) is an osteogenic marker secreted by osteoblasts in the middle and late stages of osteogenic differentiation. Immunocytochemical staining was performed on MC3T3-E1 cells treated with β-ecdysterone (0 and 150 μM) to investigate whether it also promoted MC3T3-E1 cells in the middle and late stages of osteogenic differentiation. The results showed that the brownish-yellow granules in the cytoplasm of the experimental group were significantly higher than those of the control group. There was no significant difference between the 150 μM β-ecdysterone and IM groups (**Figure 1C**). However, the nucleus was observed in the cells of the antibody controls (OPN group) in our study; no OPN expression was observed in the cytoplasm (**Supplementary Figure S1**).

During osteogenesis, osteoblasts undergo proliferation and gradually differentiate into osteocytes. Calcium salts are deposited in bone cells before they form bone tissue. The cells then fuse, mineralize, and form mineralized nodules. In our study, alizarin red staining was used to compare cells cultured for 21 days to investigate the effect of β-ecdysterone on mineralized nodule formation in MC3T3-E1 cells at the end stage of differentiation. The results showed that MC3T3-E1 cells cultured in osteoblast induction medium under β-ecdysterone intervention had more mineralized nodules than those cultured in osteoblast induction medium alone (**Figure 1D**). These results suggest that β-ecdysterone can enhance osteogenic differentiation of MC3T3-E1 cells and improve their ability to form bone tissue *in vitro*.

Gene Sequencing Analysis of MC3T3-E1 Cells Treated With β-Ecdysterone

To understand the specific effects of β-ecdysterone on nucleic acid transcription and expression in MC3T3-E1 cells, we used mRNA-seq to study the gene expression of MC3T3-E1 cells treated with β-ecdysterone at days 5 and 10. As shown in **Figure 2A**, among all detected mRNAs, 29,583 genes were found to be involved in gene expression analysis compared to the known mouse genome. In the experimental group, 1403 and 748 genes were up- and down-regulated, respectively; log2 > 1 and Q < 0.05 were established as indicators of significant difference. Further analysis of biological processes enriched by these differentially expressed genes using Kyoto Encyclopedia of Genes and Genomes clustering analysis and Gene Ontology functional enrichment analysis showed that genes of the BMP signaling pathway were among the top 20 upregulated genes; the differences were significant (**Figures 2B,C**). We analyzed the intersection of gene expression in MC3T3-E1 cells treated with β-ecdysterone for 5 and 10 days using Venn diagrams. A total of 1310 genes were up- or downregulated, including 859 upregulated genes (**Figure 2D**). We analyzed these 859 upregulated genes (**Figure 2F**) and found that osteogenesis-related genes (BMP and Wnt) were almost all upregulated; related signal transduction genes, including those associated with DNA integration and cell membrane receptors, were significantly upregulated. Kyoto Encyclopedia of Genes and Genomes analysis of signaling pathways of osteogenic target genes revealed that genes of the BMP, Wnt, and extracellular matrix-receptor interaction signaling pathways were enriched (**Figure 2E**).

β-Ecdysterone Induced the Expression of BMP-2, Runx2, and Osterix mRNA in MC3T3-E1 Cells *In Vitro*

BMP-2 has been shown to induce osteoblast differentiation rapidly and effectively *in vitro*. Furthermore, BMP-2 plays a vital role in bone formation and remodeling. Using mRNA sequencing analysis, our study found that β-ecdysterone enhanced the enrichment of genes from the osteogenic signaling pathway, including the BMP signaling pathway. To investigate the effect of genes of the BMP-2 signaling pathway on β-ecdysterone-mediated (0/150 μM) osteogenic differentiation of MC3T3-E1 cells, we performed RT-qPCR to measure the expression of osteogenic-related genes. The RT-qPCR results showed that β-ecdysterone significantly increased the expression of BMP-2, Runx2, Col I, and Osterix (**Figure 3A**). To further verify the involvement of BMP-2 in β-ecdysterone induced osteogenic differentiation, we used the BMP-2 receptor antagonist noggin to block BMP-2 signaling in MC3T3-E1 cells. Noggin treatment of MC3T3-E1 cells reduced the

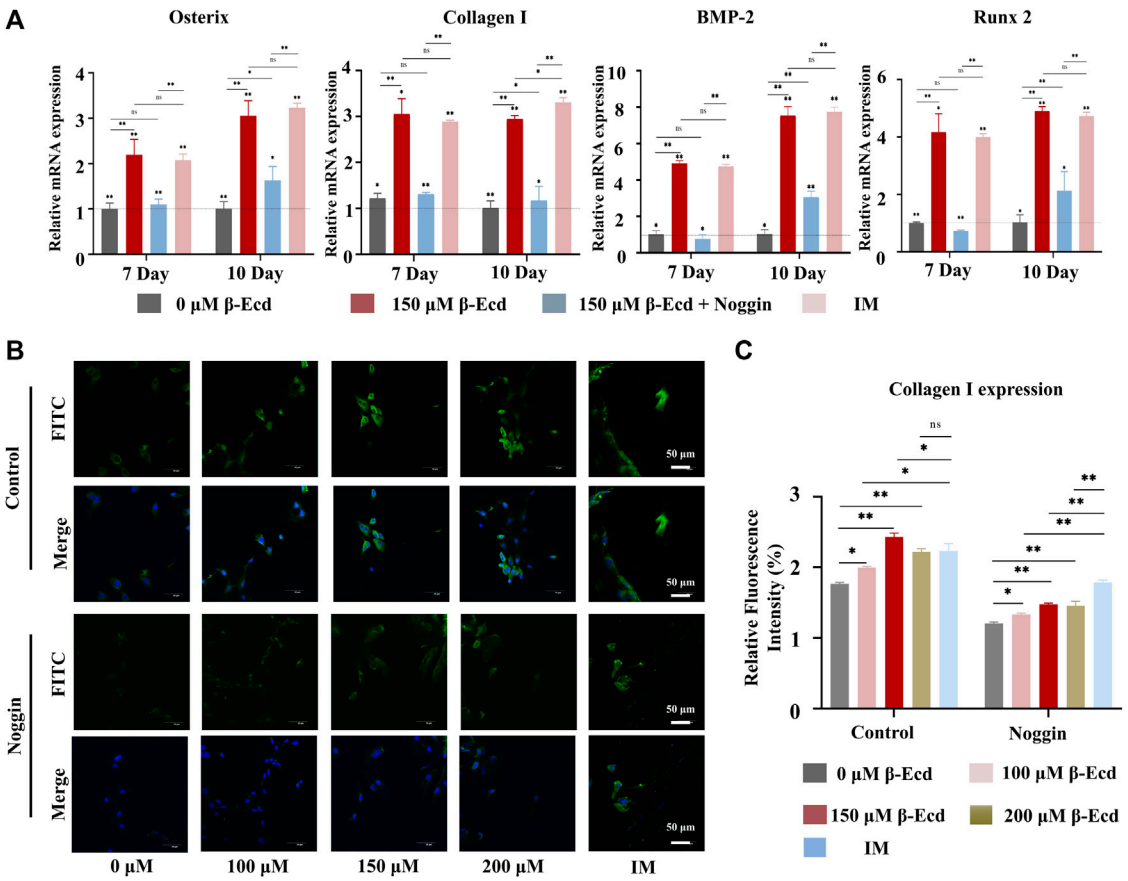

FIGURE 3 | β-Ecd promotes the expression of osteogenic proteins and genes. **(A)** The relative expression levels of osteogenic differentiation-related genes in MC3TE-E1 treated with induction medium, β-Ecd and noggin were determined by RT-qPCR. The results showed that β-Ecd could significantly increase the expression of osterix mRNA, Collagen I mRNA, BMP-2 mRNA, and Runx2 mRNA in cells; however, this effect could be inhibited by exposure to noggin. There was no significant difference compared with the IM group and 150 μM β-Ecd group. The experiments were repeated three times and the results were normalized by the expression level of GAPDH. $^{*}p < 0.05$, $^{**}p < 0.01$. **(B,C)** Immunofluorescence (IF) staining to detect type I collagen expression in MC3T3-E1. After treating MC3TE-E1 with 0 μM β-Ecd (control group) and 100–200 μM β-Ecd (experimental group) or iduction medium for 10 days, the IF results showed that the expression of type I collagen in the experimental group increased significantly compared to the control group, but this effect could be explained by inhibition of noggin, type I collagen is shown in green and nuclei are shown in blue. There was no significant difference compared with the IM group and 150 μM β-Ecd group. ImageJ software was used to measure the relative expression values in the figure, and three independent experiments were carried out, $^{*}p < 0.05$, $^{**}p < 0.05$.

expression of BMP-2, Runx2, Osterix, and Collagen I mRNA. These data suggested that the BMP-2 signaling pathway plays a significant role in osteogenic differentiation of MC3T3-E1 cells mediated by β-ecdysterone (**Figure 3A**).

β-Ecdysterone Regulated Osteogenic Differentiation of MC3T3-E1 Cells Through the BMP-2/Smad/Runx2/Osterix Signaling Pathway

Western blotting was used to detect the expression of the BMP-2, Smad1/5, phosphorylated (p)-Smad1/5, RUNX2, and osterix proteins induced by β-ecdysterone. We confirmed the role of the BMP-2/SMAD/RUNX2/Osterix pathway in β-ecdysterone-mediated osteogenic differentiation of MC3T3-E1 cells. Our data showed that β-ecdysterone significantly increased intracellular BMP-2, Smad1/5, p-Smad1/5, Runx2, and osterix proteins; the ratio of protein to phos-protein also increased significantly, with the most significant increase observed at 150 μM (**Figure 4**). Furthermore, there was no effect on the levels of the GAPDH protein. The protein expression of BMP-2, Smad1/5, phosphorylated (p)-Smad1/5, Runx2, and Osterix were significantly decreased in MC3T3-E1 cells treated with noggin. Therefore, these data suggested that the BMP-2/Smad/Runx2/Osterix signaling pathway is involved in the regulation of osteogenic differentiation of MC3T3-E1 cells by β-ecdysterone.

Immunofluorescence was used to detect the expression of collagen I in the cytoplasmic region and the effect induced by exposure to noggin. The results showed that collagen I immunofluorescence aggregation differed significantly between the experimental and control groups ($p < 0.05$). Collagen I expression was most significant in the experimental group when the concentration of β-ecdysterone was 150 μM. In contrast, collagen I expression

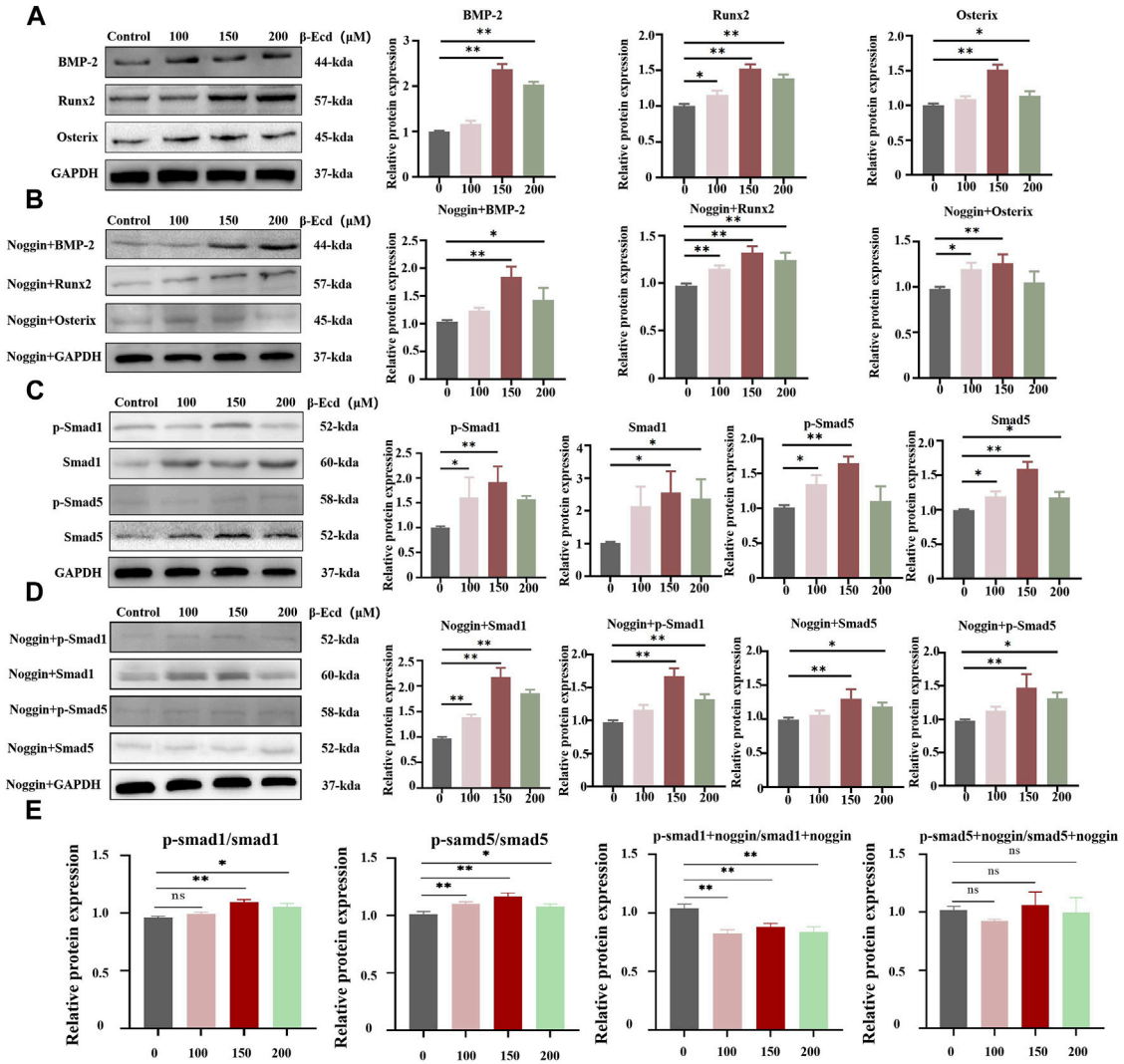

FIGURE 4 | Western blotting detection of BMP-2, Smad1/5, p-Smad1/5, Runx2 and Osterix protein expression levels in MC3TE-E1 cultured with β-Ecd and noggin. **(A,B)**, BMP-2, Runx2, Osterix protein expression levels, **(C,D)**, Smad1/5, phosphorylated (p)-Smad1/5 protein expression levels. **(E)** the ratio of the protein to phos-protein, β-Ecd could increased the ratio of the protein to phos-protein, but, the noggin inhibit this. ImageJ software was used to calculate the densitometric analysis of the protein bands ($N = 3$; $^{*}p < 0.05$, $^{**}p < 0.001$).

in cells treated with noggin was generally decreased ($p < 0.05$), as shown in **Figures 3B,C**. These data suggest that noggin may inhibit the positive regulation of collagen I expression in MC3T3-E1 cells.

Therapeutic Effect of β-Ecdysterone on Femoral Bone Defects in Rats

The bone defect model was established in this study by drilling the femoral condyle in rats. According to the results of the *in vitro* experiment, the rats were divided into three groups: the control group (0 mg/kg of β-ecdysterone was injected intraperitoneally), experimental group (72 mg/kg of β-ecdysterone was injected intraperitoneally), and the sham operation group. Rats were injected intraperitoneally with the corresponding drugs every 3 days after surgery and were sacrificed at the eighth week for micro-CT scanning, reconstruction, and immunohistochemical staining.

Table 4 and **Figure 5** show the results of weight and histopathology analysis of different tissues in the control, sham, and experimental groups. Tissue sections of the liver and kidney of rats treated with 72 mg/kg of β-ecdysterone for 4 weeks showed no signs of abnormality and toxicity, respectively. This further confirmed that β-ecdysterone did not exert any undesirable toxic effects on the animals at low doses.

As shown in **Figure 6**, micro-CT was used to evaluate changes in the femoral condylar defect in rats. On micro-CT reconstruction analysis, the images clearly showed characteristics of changes in the bone regeneration process.

TABLE 4 | The weight of rats in different groups (0 and 4 weeks after surgery; $n = 5$).

Time (days)	PBS group	Sham group	β-ecdysterone group	Statistics (F, p)
0 weeks	204.7 ± 2.48	204.4 ± 2.96	203.9 ± 2.76	F = 0.13, $p = 0.89$
4 weeks	306.9 ± 4.86	308.5 ± 3.59	311.0 ± 4.87	F = 1.66, $p = 0.23$
Statistics (t, p)	$t = 33.6$, $p < 0.01$	$t = 35.9$, $p < 0.01$	$t = 39.8$, $p < 0.01$	

Values are expressed by means X ± SD *(n = 5). **p < 0.01, ***p < 0.001, NS, no significance.*

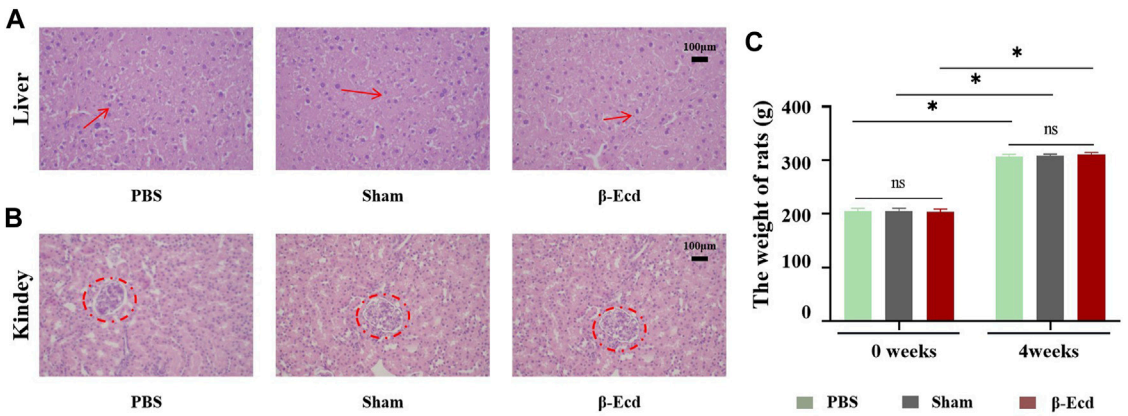

FIGURE 5 | Effect of β-ecdysterone on tissue architecture of rats 4 weeks after surgery was compared with that before surgery. **(A)** Depicts the hematoxylin and eosin stained section of liver from control rat, sham rat and rat treated with 92 mg/kg β-ecdysterone showing no signs of hepatotoxicity (shown in arrow). **(B)** Depicts the hematoxylin and eosin stained section of kidney from control rat, sham rat and rat treated with 92 mg/kg β-ecdysterone showing no signs of nephrotoxicity (shown in circle). **(C)** 4 weeks after surgery, the weight of rats in different groups increased respectly, and β-ecdysterone showing no signs of weight loss. *$p < 0.05$ and NS, no significant.

Compared to the control/PBS group, more new bone tissue had regenerated in the experimental group (**Figure 6**). On quantitative analysis, the volume and density of new bone tissue increased in the experimental group at 4 and 8 weeks ($p < 0.05$); however, there was no significant difference between the sham and experimental groups ($p > 0.05$) at 8 weeks. In addition to micro-CT, HE staining was used to detect histological changes in newly formed bone tissue. Unlike in the control group, the calcium phosphorus crystals in the bone tissue of the experimental group were arranged in a regular shape and the collagenous fibers were arranged in a circular shape. The direction of arrangement of the collagenous fibers was consistent with that of the bone cavities; this is a typical histomorphological characteristic of newly formed bone. Immunohistochemistry was used to detect the protein expression levels of BMP2, Smad4, Runx2, and Osterix. Compared to the control group, the expression of target protein in the experimental group was significantly increased. In addition, there was no significant difference in expression between the sham and control groups at 4 and 8 weeks (**Figure 7**).

DISCUSSION

Fractures, traumatic bone defects, and osteoporosis are increasingly prominent and common diseases worldwide, and adequate bone regeneration is the key their successful treatment. To our knowledge, bone regeneration is a common process of intramembranous ossification and endochondral ossification, initiated by periosteal bone progenitor cells, which first form avascular cartilage tissue and is then replaced by bone tissue (Slade and Chou 1998). BMSCs play an essential role in bone repair (Wang et al., 2013). Among the cytokines involved in bone formation, the transcription factor BMP2 is the most studied, but its induction mechanism in bone progenitor cells is poorly understood. This study showed that β-ecdysterone promotes bone formation and improves cell proliferation and differentiation by activating the BMP2/Smad/Runx2/Osterix signaling pathway, suggesting that β-ecdysterone can effectively improve bone volume and quality. Mechanistically, BMP2 binds to the BMPR-II receptor on the cell membrane and activates the BMPR-II receptor and BMPR-I receptor, regulates the binding of the downstream transcription factor Smad1/5/8 to the transcription factor Smad4, which is transferred to the nucleus and activates the downstream nuclear transcription factor Runx2. Runx2 further enhances Osterix fragment transcription and translation in the nucleic acid chain, promoting osteogenic proteins, extracellular matrix deposition, and calcium mineralization, leading to fracture regeneration. In general, our study suggests that β-ecdysterone is a positive regulator of bone regeneration, promoting BMSC proliferation and osteogenic differentiation.

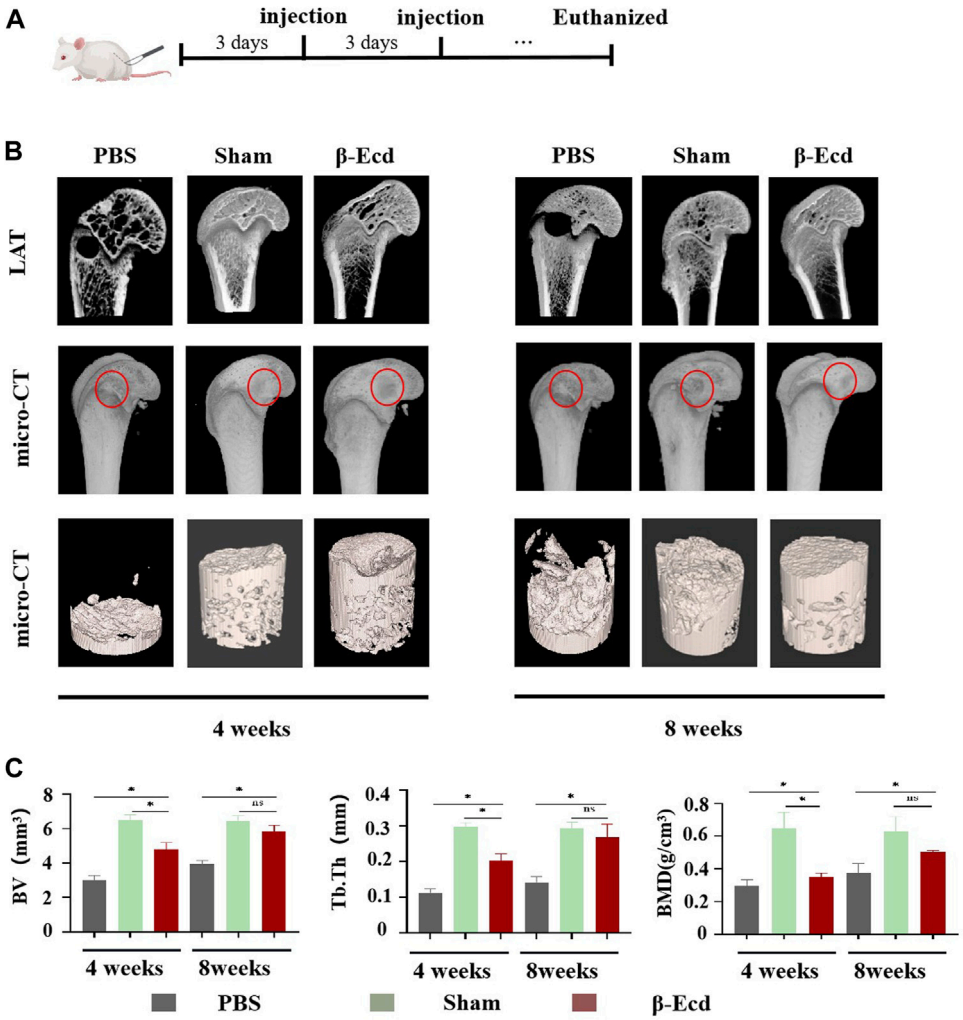

FIGURE 6 | The results of the Micro-CT test show that β-Ecd accelerates bone healing in rats. **(A)** Critical size bone defect model of the distal femur and β-Ecd injection; **(B)** Micro-CT analysis of new bone formation, CT-vox software to identify new bone and analyze the distribution of new bone at 8 weeks. It can be seen that the new bone formation in the sham operation group and the β-Ecd group was significantly increased compared to the PBS group at 4 and 8 weeks, but there were no significant differences between the sham operation group and the β-Ecd group; **(C)** Statistics of new bone microstructural parameters in the 4 week and eighth week, including bone mineral density (BMD), bone tissue volume (BV), trabecular bone thickness (Tb.Th). Each group contained three replicates, and the data were analyzed by one-way ANOVA for multiple comparisons. *$p < 0.05$, ns, nosignificant.

β-ecdysterone has been shown to effectively protect mouse osteoblasts from glucocorticoid-induced apoptosis and autophagy (Tang et al., 2018a). It also blocks IL-1β-induced chondrocyte apoptosis and the inflammatory response by inhibiting NF-κB signaling (Zhang et al., 2014). In their *in vitro* study, Jian et al. (2013) (Xu et al., 2009) demonstrated that β-ecdysterone can induce BMP-2 dependent osteogenic differentiation and proliferation of human periodontal ligament stem cells through the extracellular signal-regulated kinase pathway. However, the results only evaluated the toxicity of β-ecdysterone and did not determine whether it promoted osteogenic differentiation of BMSCs. Data regarding the connection between estrogen receptors and BMP signaling are lacking. Studies have shown that cytokine sensitivity screening considers the BMP4 signaling pathway to be crucial for treating ER + breast cancer (Shee et al., 2019). In addition, dehydrodiconiferyl alcohol has been found to promote BMP-2-induced osteoblastogenesis through its agonistic effects on estrogen receptors (Lee et al., 2018). In their study, Pang et al. found that quercetin stimulates BMSC differentiation through an estrogen receptor-mediated pathway (Pang et al., 2018). We therefore suspect the presence of an interaction between BMP signaling and estrogen receptors; β-ecdysterone may have promoted osteogenic differentiation of BMSCs in our study by activating estrogen receptors *in vivo*.

Considering the importance of BMSCs in bone repair and reconstruction, we investigated the effects of β-ecdysterone on BMSCs *in vitro* and *in vivo*. *In vitro*, we used the MC3T3-E1 cell line, which includes osteogenic precursor cells cloned from the skull of C57BL/6 mice, to replace BMSC cells. Repeated

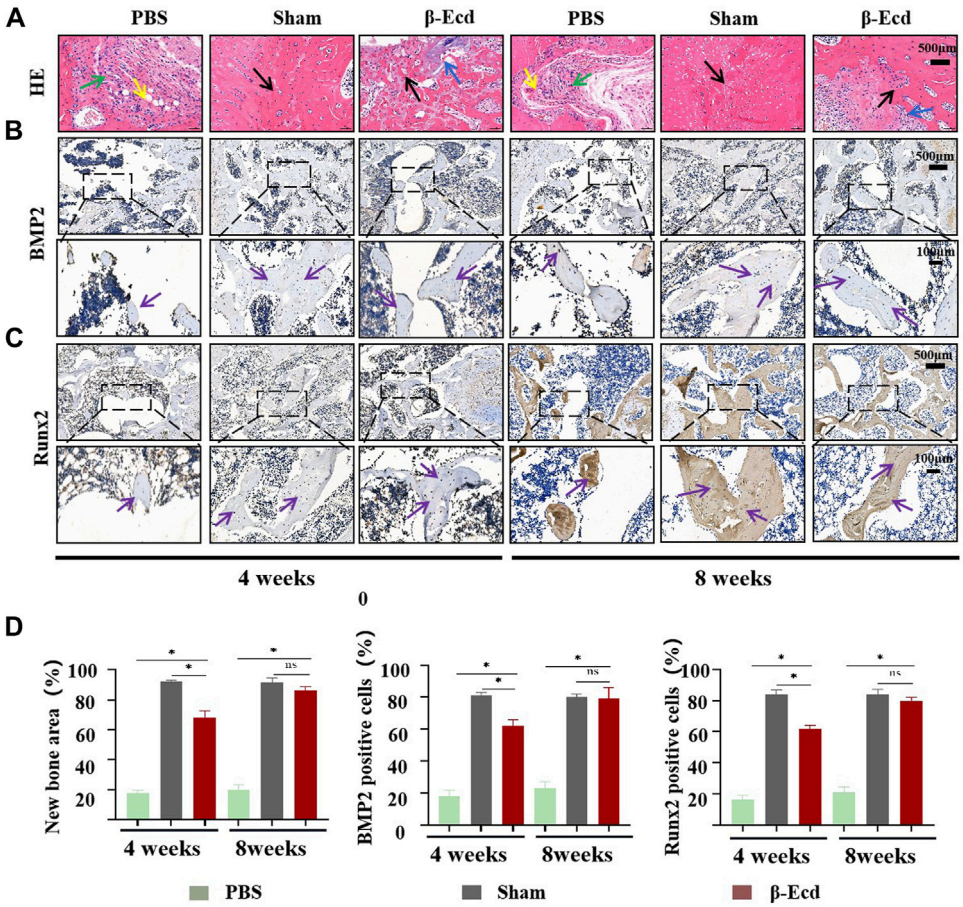

FIGURE 7 | Histomorphological analysis of newly formed bone tissue in bone defect area and immunohistochemical evaluation of osteogenesis-related proteins in newly formed bone. **(A)** HE staining of bone tissue sections around the bone defect at 4 and 8 weeks; Green arrow: fibrous tissue; Yellow arrow: new capillary formation; Black arrow: bone tissue. **(B,C)** immunohistochemical detection of the expression of the BMP2/Runx2 protein in the new tissue in the area of the bone defect, the enlarged images in the black box are bone trabeculae or osteocytes; **(D)** The area of new bone tissue and the expression of the BMP2 protein in the three groups were statistically analyzed using ImageJ software. At 4 weeks, the expression of the BMP2/Runx2 protein was significantly increased in the bone defect area; At 8 weeks, the expression of the BMP2/Runx2 protein was significantly increased in the bone defect area, but there was no significant difference between the β-Ecd group and the sham-operated group. Each group contained three replicates, and the data were analyzed by one-way ANOVA for multiple comparisons. Purple arrow: BMP2/Runx2 protein positive site. *$p < 0.05$, ns, not significant.

subculture of this cell line has been reported to maintain the phenotype of high ALP activity of osteoblasts; it also promotes differentiation into osteoblasts and osteocytes *in vitro*, forming calcified bone tissue and mineral deposits of hydroxyapatite (Kunimatsu et al., 2018). This cell line has proven to be a viable model for exploring osteoblast proliferation, maturation, and differentiation (Gal et al., 2000) and is commonly used to study the effects of drugs on osteoblasts.

In vitro cell proliferation experiments showed that β-ecdysterone promoted MC3T3-E1 cell proliferation at 25–200 mM. In contrast, MC3T3-E1 cell proliferation and metabolism were inhibited after 7 days of culture or when the concentration was greater than 400 mM. Microscopically, cells reached fusion after 7 days of culture; this may explain why the effect of β-ecdysterone on the proliferation of MC3T3-E1 cells was limited to the early stage of cell culture. Our results also indicate that higher levels of β-ecdysterone exert a specific toxic effect on MC3T3-E1 cells. *In vivo* experiments were performed using 0 and 150 μM of β-ecdysterone (72 mg/kg), which was injected intraperitoneally in femoral condylar defect model rats. The results showed that the bone defect regenerated to different degrees after 8 weeks and the effect was most significant at 72 mg/kg. This result demonstrates that β-ecdysterone can promote osteoblast proliferation *in vivo* and has obvious biosafety. In previous in-vivo and in-vitro studies, the effect of β-ecdysterone on cell proliferation was complex (Tang et al., 2018b). In our study, β-ecdysterone at an appropriate concentration showed the ability to promote bone progenitor cell proliferation, which is essential for bone tissue regeneration; this is because the body needs enough bone cells to rebuild after fracture, and the number of cells that can be transplanted by autologous or allograft is limited.

Bone formation is a complex process. In addition to cell proliferation, deposition and mineralization of the extracellular matrix are also important (Jia et al., 2003). Therefore, ideal methods for bone regeneration must promote bone progenitor

cell proliferation and stimulate osteogenic differentiation. In this study, MC3T3-E1 cells were cultured with different concentrations of β-ecdysterone to further verify the effect of β-ecdysterone on osteoprogenitor cell differentiation. The final data showed that β-ecdysterone significantly increased ALP activity in MC3T3-E1 cells, and the increase was more pronounced at a concentration of 200 mM Runx2 is an early phenotypic marker of mature osteoblasts similar to ALP, while COL-1 and OPN are late phenotypic markers of osteoblast differentiation (Zhang et al., 2010; Zhou et al., 2014). We demonstrated that β-ecdysterone induced significantly higher expression of the COL-1, OPN, and Runx2 gene or protein in MC3T3-E1 cells than in nonstimulated controls. These results suggest that β-ecdysterone stimulates early and late differentiation of bone progenitor cells.

For the in-vivo experiments, we selected a rat partial femoral condyle defect model. In the partial defect model, a defect is usually drilled into the side of the bone to create an area of injury. Drilling through the cortical bone may extend to the underlying cancellous bone or marrow cavity. In this model, only one bone is usually injured; notably, certain cortical bone defects are simple to operate and can simulate the steps of stable fracture healing (McGovern et al., 2018). They offer many advantages over other closed and open fractures, including reduced morbidity in animals and better histomorphometric analysis. Micro-CT values and immunohistochemical staining results of the rat bone defect model showed greater new bone formation (based on mineralization measurement) in the group treated with β-ecdysterone than in the control/PBS group. In conjunction, these results suggest that β-ecdysterone stimulates osteogenic differentiation of bone progenitors at different stages *in vitro* and *in vivo*.

BMPs play a vital role in the osteogenic differentiation of different cell lines (Urist and Strates 2009; Long 2011). Through gene sequencing and differential expression analysis of osteogenic related genes in different treatment groups of MC3T3-E1 cells, we found that the genes detected in different groups of cells had significant differences in signal pathway enrichment and cell function. The BMP signaling pathway genes were ranked among the top 20 and the differences were statistically significant. BMP-2 has been reported to be a crucial regulatory factor in the BMP pathway, which can enhance the osteogenic differentiation of human BMSCs (Peng et al., 2003). Therefore, our analysis of the results of gene sequencing suggested that β-ecdysterone-enhanced osteogenic differentiation of bone progenitor cells was closely related to the BMP2 signaling pathway. Similarly, we found that β-ecdysterone upregulates BMP-2 expression at mRNA and protein levels, and the BMP-2 signaling pathway inhibitor noggin can counteract this effect *in vitro*. Although noggin has been observed to be nonspecific for BMP-2 (Secondini et al., 2011), genetic tests showed that β-ecdysterone did not significantly increase BMP signaling in MC3T3-E1 cells. These results suggest that the BMP-2 signaling pathway plays an essential role in β-ecdysterone-induced osteogenic differentiation of bone progenitor cells.

Regarding the induction mechanism of BMP-2, many studies have shown that it is related to the MAPK signaling pathway (Park et al., 2019). Previous studies have reported that the ERK pathway is involved in the differentiation of periodontal ligament cells and osteoblasts (Tóth et al., 2008), but our results suggest that the increased expression of BMP-2 and other osteogenic proteins and genes is directly related to the BMP2/Smad/Runx2/Osterix pathway. The noggin inhibitor can abrogate this effect. According to our data and previous studies (Qiao et al., 2005; Wang et al., 2012; Fischerauer et al., 2013), we speculate that the mechanism of action involves BMP-2 active the BMP type 2 receptor, but it interacts and activates the BMP type 1 receptor which then the BMP type 1 receptor activates downstream signaling pathways, by phosphorylation of Smad1, Smad5, or Smad8. Smad1/5/8 activates and binds to Smad4 and enters the cell nucleus to regulate the transcription function of specific genes. The Smad protein, as a coregulatory, interacts with Runx2 to participate in osteoblast phenotypic gene expression and differentiation (Phimphilai et al., 2006). In addition, Runx2 can interact with osteoblast specifics acting element 2 in the osteocalcin promoter region to stimulate osteocalcin expression. There are osteoblast specifics acting element 2-like elements in the promoter regions of osteoblast-related genes such as type I collagen, osteocalcin, and osteopontin, and Runx2 can bind to these osteoblast specifics acting element 2-like elements to activate gene expression (Liu and Lee 2013); however, this mechanism requires further study.

In summary, β-ecdysterone can be used as a safe and effective agent for bone regeneration to resolve insufficient bone regeneration and severe osteoporosis caused by decreased osteogenic capacity. Thus, β-ecdysterone has excellent research value and application prospects. Furthermore, it remains to be explored whether β-ecdysterone can be incorporated into bone regeneration biomaterials to promote bone tissue regeneration for the treatment of critical bone defects in the future.

CONCLUSION

This study is the first to demonstrate that β-ecdysterone has good biosafety in mammals *in vitro* and *in vivo* and can promote proliferation and induce osteogenic differentiation of bone progenitors through the BMP2/Smad/Runx2/Osterix signaling pathway. This indicates its considerable potential as a therapeutic agent for bone regeneration and repair.

DATA AVAILABILITY STATEMENT

The datasets presented in this study can be found in online repositories. The names of the repository/repositories and accession number(s) can be found in the article/ **Supplementary Material**.

ETHICS STATEMENT

The animal study was reviewed and approved by The Research Ethics Committee of the Affiliated Hospital of the North Sichuan Medical College (2021–26).

AUTHOR CONTRIBUTIONS

C-PY and X-KW: Methodology, Resources, Investigation, Writing-original manuscript. KJ: Supervision, Writing-review and editing. CY: Investigation. CX, YW, and CP: Investigation, Resources. LC: Supervision, Validation. Y-LL: Conceptualization, Supervision, Writing-reviewing and editing.

FUNDING

This work was supported by the National Science Foundation of China (Grant Nos. 82102578 and 82102571), Applied Basic Research Programs of the Science and Technology Department of Sichuan Province (2021YJ0467), Research Project of the Affiliated Hospital of North Sichuan Medical College (2021ZK001), and the Research Project of the North Sichuan Medical College (CBY20-QA-Z04).

SUPPLEMENTARY MATERIAL

The Supplementary Material for this article can be found online at: https://www.frontiersin.org/articles/10.3389/fcell.2022.883228/full#supplementary-material

REFERENCES

Abdallah, B. M., Haack-Sørensen, M., Burns, J. S., Elsnab, B., Jakob, F., Hokland, P., et al. (2005). Maintenance of Differentiation Potential of Human Bone Marrow Mesenchymal Stem Cells Immortalized by Human Telomerase Reverse Transcriptase Gene Despite of Extensive Proliferation. *Biochem. biophysical Res. Commun.* 326, 527–538. doi:10.1016/j.bbrc.2004.11.059

Abiramasundari, G., Mohan Gowda, C. M., and Sreepriya, M. (2018). Selective Estrogen Receptor Modulator and Prostimulatory Effects of Phytoestrogen β-ecdysone in Tinospora Cordifolia on Osteoblast Cells. *J. Ayurveda Integr. Med.* 9, 161–168. doi:10.1016/j.jaim.2017.04.003

Cai, H., Zou, J., Wang, W., and Yang, A. (2021). BMP2 Induces hMSC Osteogenesis and Matrix Remodeling. *Mol. Med. Rep.* 23, 11764. doi:10.3892/mmr.2020.11764

Catalán, R. E., Martinez, A. M., Aragones, M. D., Miguel, B. G., Robles, A., and Godoy, J. E. (1985). Alterations in Rat Lipid Metabolism Following Ecdysterone Treatment. *Comp. Biochem. physiology. B, Comp. Biochem.* 81, 771

Chen, Z., Wang, X., Shao, Y., Shi, D., Chen, T., Cui, D., et al. (2011). Synthetic Osteogenic Growth Peptide Promotes Differentiation of Human Bone Marrow Mesenchymal Stem Cells to Osteoblasts via RhoA/ROCK Pathway. *Mol. Cell Biochem.* 358, 221–227. doi:10.1007/s11010-011-0938-7

Clark, D. P., and Badea, C. T. (2021). Advances in Micro-CT Imaging of Small Animals. *Phys. Medica* 88, 175–192. doi:10.1016/j.ejmp.2021.07.005

da Silva Meirelles, L., Fontes, A. M., Covas, D. T., and Caplan, A. I. (2009). Mechanisms Involved in the Therapeutic Properties of Mesenchymal Stem Cells. *Cytokine & growth factor Rev.* 20, 419–427. doi:10.1016/j.cytogfr.2009.10.002

Dai, W.-W., Wang, L.-B., Jin, G.-Q., Wu, H.-J., Zhang, J., Wang, C.-L., et al. (2017). Beta-Ecdysone Protects Mouse Osteoblasts from Glucocorticoid-Induced Apoptosis *In Vitro*. *Planta Med.* 83, 888–894. doi:10.1055/s-0043-107808

Feng, C., Xiao, L., Yu, J. C., Li, D. Y., Tang, T. Y., Liao, W., et al. (2020). Simvastatin Promotes Osteogenic Differentiation of Mesenchymal Stem Cells in Rat Model of Osteoporosis through BMP-2/Smads Signaling Pathway. *Eur. Rev. Med. Pharmacol. Sci.* 24, 434–443. doi:10.26355/eurrev_202001_19943

Fischerauer, E. E., Manninger, M., Seles, M., Janezic, G., Pichler, K., Ebner, B., et al. (2013).BMP-6 and BMPR-1a Are Up-Regulated in the Growth Plate of the Fractured Tibia. *J. Orthop. Res.*, 31, 357–363. doi:10.1002/jor.22238

Gal, T. J., Munoz-Antonia, T., Muro-Cacho, C. A., and Klotch, D. W. (2000). Radiation Effects on Osteoblasts *In Vitro*: a Potential Role in Osteoradionecrosis. *Arch. Otolaryngol. Head. Neck Surg.* 126, 1124–1128. doi:10.1001/archotol.126.9.1124

Gao, L., Cai, G., and Shi, X. (2008). BETA.-Ecdysterone Induces Osteogenic Differentiation in Mouse Mesenchymal Stem Cells and Relieves Osteoporosis. *Biol. Pharm. Bull.* 31, 2245–2249. doi:10.1248/bpb.31.2245

Hak, D. J., Fitzpatrick, D., Bishop, J. A., Marsh, J. L., Tilp, S., Schnettler, R., et al. (2014). Delayed Union and Nonunions: Epidemiology, Clinical Issues, and Financial Aspects. *Injury* 45 (Suppl. 2), S3–S7. doi:10.1016/j.injury.2014.04.002

Jia, T.-L., Wang, H.-Z., Xie, L.-P., Wang, X.-Y., and Zhang, R.-Q. (2003). Daidzein Enhances Osteoblast Growth that May Be Mediated by Increased Bone Morphogenetic Protein (BMP) Production. *Biochem. Pharmacol.* 65, 709–715. doi:10.1016/s0006-2952(02)01585-x

Jian, C.-X., Liu, X.-F., Hu, J., Li, C.-J., Zhang, G., Li, Y., et al. (2013). 20-Hydroxyecdysone-induced Bone Morphogenetic Protein-2-dependent Osteogenic Differentiation through the ERK Pathway in Human Periodontal Ligament Stem Cells. *Eur. J. Pharmacol.* 698, 48–56. doi:10.1016/j.ejphar.2012.07.044

Ko, F. C., and Sumner, D. R. (2021). How Faithfully Does Intramembranous Bone Regeneration Recapitulate Embryonic Skeletal Development? *Dev. Dyn.* 250, 377–392. doi:10.1002/dvdy.240

Kunimatsu, R., Gunji, H., Tsuka, Y., Yoshimi, Y., Awada, T., Sumi, K., et al. (2018). Effects of High-Frequency Near-Infrared Diode Laser Irradiation on the Proliferation and Migration of Mouse Calvarial Osteoblasts. *Lasers Med. Sci.* 33, 959–966. doi:10.1007/s10103-017-2426-0

Lee, W., Ko, K. R., Kim, H.-K., Lim, S., and Kim, S. (2018). Dehydrodiconiferyl Alcohol Promotes BMP-2-Induced Osteoblastogenesis through its Agonistic Effects on Estrogen Receptor. *Biochem. biophysical Res. Commun.* 495, 2242–2248. doi:10.1016/j.bbrc.2017.12.079

Li, Z., and Helms, J. A. (2021). Drill Hole Models to Investigate Bone Repair. *Methods Mol. Biol. Clift. N.J.)* 2221, 193–204. doi:10.1007/978-1-0716-0989-7_12

Lin, Z.-Y., Duan, Z.-X., Guo, X.-D., Li, J.-F., Lu, H.-W., Zheng, Q.-X., et al. (2010). Bone Induction by Biomimetic PLGA-(PEG-ASP)n Copolymer Loaded with a Novel Synthetic BMP-2-Related Peptide *In Vitro* and *In Vivo*. *J. Control. Release* 144, 190–195. doi:10.1016/j.jconrel.2010.02.016

Liu, Q., Zhang, X., Jiao, Y., Liu, X., Wang, Y., Li, S. L., et al. (2018). *In Vitro* cell Behaviors of Bone Mesenchymal Stem Cells Derived from Normal and Postmenopausal Osteoporotic Rats. *Int. J. Mol. Med.* 41, 669–678. doi:10.3892/ijmm.2017.3280

Liu, T. M., and Lee, E. H. (2013). Transcriptional Regulatory Cascades in Runx2-dependent Bone Development. *Tissue Eng. Part B Rev.* 19, 254–263. doi:10.1089/ten.teb.2012.0527

Long, F. (2011). Building Strong Bones: Molecular Regulation of the Osteoblast Lineage. *Nat. Rev. Mol. Cell Biol.* 13, 27–38. doi:10.1038/nrm3254

McGovern, J. A., Griffin, M., and Hutmacher, D. W. (2018). Animal Models for Bone Tissue Engineering and Modelling Disease. *Dis. Model. Mech.* 11. doi:10.1242/dmm.033084

Miyazono, K., Kamiya, Y., and Morikawa, M. (2010). Bone Morphogenetic Protein Receptors and Signal Transduction. *J. Biochem.* 147, 35–51. doi:10.1093/jb/mvp148

Pang, X. G., Cong, Y., Bao, N. R., Li, Y. G., and Zhao, J. N. (2018). Quercetin Stimulates Bone Marrow Mesenchymal Stem Cell Differentiation through an Estrogen Receptor-Mediated Pathway. *Biomed. Res. Int.* 2018, 4178021. doi:10.1155/2018/4178021

Park, M., Choi, H. K., and An, J. H. (2019). Taurine Activates BMP-2/Wnt3a-Mediated Osteoblast Differentiation and Mineralization via Akt and MAPK Signaling. *Iran. J. Public Health* 48, 1960

Peng, Y., Kang, Q., Cheng, H., Li, X., Sun, M. H., Jiang, W., et al. (2003). Transcriptional Characterization of Bone Morphogenetic Proteins (BMPs)-Mediated Osteogenic Signaling. *J. Cell. Biochem.* 90, 1149–1165. doi:10.1002/jcb.10744

Percival, C. J., and Richtsmeier, J. T. (2013). Angiogenesis and Intramembranous Osteogenesis. *Dev. Dyn.* 242, 909–922. doi:10.1002/dvdy.23992

Phillips, A. M. (2005). Overview of the Fracture Healing Cascade. *Injury* 36 Suppl 3 (Suppl. 3), S5–S7. doi:10.1016/j.injury.2005.07.027

Phimphilai, M., Zhao, Z., Boules, H., Roca, H., and Franceschi, R. T. (2006). BMP Signaling Is Required for RUNX2-dependent Induction of the Osteoblast Phenotype. *J. Bone Min. Res.* 21, 637–646. doi:10.1359/jbmr.060109

Qiao, B., Padilla, S. R., and Benya, P. D. (2005). Transforming Growth Factor (TGF)-β-activated Kinase 1 Mimics and Mediates TGF-β-Induced Stimulation of Type II Collagen Synthesis in Chondrocytes Independent of Col2a1 Transcription and Smad3 Signaling. *J. Biol. Chem.* 280, 17562–17571. doi:10.1074/jbc.m500646200

Scarfì, S. (2016). Use of Bone Morphogenetic Proteins in Mesenchymal Stem Cell Stimulation of Cartilage and Bone Repair. *World J. Stem Cells* 8, 1–12. doi:10.4252/wjsc.v8.i1.1

Schindeler, A., McDonald, M. M., Bokko, P., and Little, D. G. (2008). Bone Remodeling during Fracture Repair: The Cellular Picture. *Seminars Cell & Dev. Biol.* 19, 459–466. doi:10.1016/j.semcdb.2008.07.004

Schubert, H., Eiselt, M., Walter, B., Fritz, H., Brodhun, M., and Bauer, R. (2012). Isoflurane/nitrous Oxide Anesthesia and Stress-Induced Procedures Enhance Neuroapoptosis in Intrauterine Growth-Restricted Piglets. *Intensive Care Med.* 38, 1205–1214. doi:10.1007/s00134-012-2576-2

Secondini, C., Wetterwald, A., Schwaninger, R., Thalmann, G. N., and Cecchini, M. G. (2011). The Role of the BMP Signaling Antagonist Noggin in the Development of Prostate Cancer Osteolytic Bone Metastasis. *PloS one* 6, e16078. doi:10.1371/journal.pone.0016078

Shee, K., Jiang, A., Varn, F. S., Liu, S., Traphagen, N. A., Owens, P., et al. (2019). Cytokine Sensitivity Screening Highlights BMP4 Pathway Signaling as a Therapeutic Opportunity in ER + Breast Cancer. *FASEB J.* 33, 1644–1657. doi:10.1096/fj.201801241r

Slade, J. F., and Chou, K. H. (1998). Bony Tissue Repair. *J. Hand Ther.* 11, 118–124. doi:10.1016/s0894-1130(98)80008-2

Smagghe, G., Vanhassel, W., Moeremans, C., De Wilde, D., Goto, S., Loeb, M. J., et al. (2005). Stimulation of Midgut Stem Cell Proliferation and Differentiation by Insect Hormones and Peptides. *Ann. N. Y. Acad. Sci.* 1040, 472–475. doi:10.1196/annals.1327.094

Takigawa, M. (2013). CCN2: a Master Regulator of the Genesis of Bone and Cartilage. *J. Cell Commun. Signal.* 7, 191–201. doi:10.1007/s12079-013-0204-8

Tang, Y. H., Yue, Z. S., Li, G. S., Zeng, L. R., Xin, D. W., Hu, Z. Q., et al. (2018a). Effect of βecdysterone on Glucocorticoidinduced Apoptosis and Autophagy in Osteoblasts. *Mol. Med. Rep.* 17, 158–164. doi:10.3892/mmr.2017.7840

Tang, Y. H., Yue, Z. S., Xin, D. W., Zeng, L. R., Xiong, Z. F., Hu, Z. Q., et al. (2018b). βEcdysterone Promotes Autophagy and Inhibits Apoptosis in Oteoporotic Rats. *Mol. Med. Rep.* 17, 1591–1598. doi:10.3892/mmr.2017.8053

Tóth, N., Szabó, A., Kacsala, P., Héger, J., and Zádor, E. (2008). 20-Hydroxyecdysone Increases Fiber Size in a Muscle-specific Fashion in Rat. *Phytomedicine* 15, 691–698. doi:10.1016/j.phymed.2008.04.015

Toth, Z., Ward, A., Tang, S. Y., and McBride-Gagyi, S. (2021). Sexual Differences in Bone Porosity, Osteocyte Density, and Extracellular Matrix Organization Due to Osteoblastic-specific Bmp2 Deficiency in Mice. *Bone* 150, 116002. doi:10.1016/j.bone.2021.116002

Urist, M. R., and Strates, B. S. (2009). The Classic: Bone Morphogenetic Protein. *Clin. Orthop. Relat. Res.* 467, 3051–3062. doi:10.1007/s11999-009-1068-3

Wang, X., Wang, Y., Gou, W., Lu, Q., Peng, J., and Lu, S. (2013). Role of Mesenchymal Stem Cells in Bone Regeneration and Fracture Repair: a Review. *Int. Orthop. (SICOT)* 37, 2491–2498. doi:10.1007/s00264-013-2059-2

Wang, Y., Li, L., Zheng, Y., Yuan, G., Yang, G., He, F., et al. (2012). BMP Activity Is Required for Tooth Development from the Lamina to Bud Stage. *J. Dent. Res.* 91, 690–695. doi:10.1177/0022034512448660

Wen, F., Yu, J., He, C. J., Zhang, Z. W., and Yang, A. F. (2019). Becdysterone Protects against Apoptosis by Promoting Autophagy in Nucleus Pulposus Cells and Ameliorates Disc Degeneration. *Mol. Med. Rep.* 19, 2440–2448. doi:10.3892/mmr.2019.9861

Xu, J., Wang, W., Kapila, Y., Lotz, J., and Kapila, S. (2009). Multiple Differentiation Capacity of STRO-1+/CD146$^+$PDL Mesenchymal Progenitor Cells. *Stem cells Dev.* 18, 487–496. doi:10.1089/scd.2008.0113

Yan, Y., Chen, H., Zhang, H., Guo, C., Yang, K., Chen, K., et al. (2019). Vascularized 3D Printed Scaffolds for Promoting Bone Regeneration. *Biomaterials* 190, 197. doi:10.1016/j.biomaterials.2018.10.033

Yang, C., Liu, X., Zhao, K., Zhu, Y., Hu, B., Zhou, Y., et al. (2019). miRNA-21 Promotes Osteogenesis via the PTEN/PI3K/Akt/HIF-1α Pathway and Enhances Bone Regeneration in Critical Size Defects. *Stem Cell Res Ther.* 10, 65. doi:10.1186/s13287-019-1168-2

Ying, X., Cheng, S., Wang, W., Lin, Z., Chen, Q., Zhang, W., et al. (2011). Effect of Boron on Osteogenic Differentiation of Human Bone Marrow Stromal Cells. *Biol. Trace Elem. Res.* 144, 306–315. doi:10.1007/s12011-011-9094-x

Yoshida, T., Otaka, T., Uchiyama, M., and Ogawa, S. (1971). Effect of Ecdysterone on Hyperglycemia in Experimental Animals. *Biochem. Pharmacol.* 20, 3263–3268. doi:10.1016/0006-2952(71)90431-x

Yu, B., Huo, L., Liu, Y., Deng, P., Szymanski, J., Li, J., et al. (2018). PGC-1α Controls Skeletal Stem Cell Fate and Bone-Fat Balance in Osteoporosis and Skeletal Aging by Inducing TAZ. *Cell stem Cell* 23, 615–623. doi:10.1016/j.stem.2018.09.001

Zhang, L., Hu, Y., Sun, C.-y., Li, J., Guo, T., Huang, J., et al. (2010). Lentiviral shRNA Silencing of BDNF Inhibitsin Vivomultiple Myeloma Growth and Angiogenesis via Down-Regulated Stroma-Derived VEGF Expression in the Bone Marrow Milieu. *Cancer Sci.* 101, 1117–1124. doi:10.1111/j.1349-7006.2010.01515.x

Zhang, X., Xu, X., Xu, T., and Qin, S. (2014). β-Ecdysterone Suppresses Interleukin-1β-Induced Apoptosis and Inflammation in Rat Chondrocytes via Inhibition of NF-Kb Signaling Pathway. *Drug Dev. Res.* 75, 195–201. doi:10.1002/ddr.21170

Zhao, S. J., Kong, F. Q., Jie, J., Li, Q., Liu, H., Xu, A. D., et al. (2020). Macrophage MSR1 Promotes BMSC Osteogenic Differentiation and M2-Like Polarization by Activating PI3K/AKT/GSK3β/β-Catenin Pathway. *Theranostics* 10, 17–35. doi:10.7150/thno.36930

Zhou, P. R., Liu, H. J., Liao, E. Y., Zhang, Z. L., Chen, D. C., Liu, J., et al. (2014). LRP5 Polymorphisms and Response to Alendronate Treatment in Chinese Postmenopausal Women with Osteoporosis. *Pharmacogenomics* 15, 821–831. doi:10.2217/pgs.14.12

Zou, Y., Wang, R., Guo, H., and Dong, M. (2015). Phytoestrogen β-Ecdysterone Protects PC12 Cells against MPP+-Induced NeurotoxicityIn Vitro: Involvement of PI3K-Nrf2-Regulated Pathway. *Toxicol. Sci.* 147, 28–38. doi:10.1093/toxsci/kfv111

Conflict of Interest: The authors declare that the research was conducted in the absence of any commercial or financial relationships that could be construed as a potential conflict of interest.

Publisher's Note: All claims expressed in this article are solely those of the authors and do not necessarily represent those of their affiliated organizations, or those of the publisher, the editors and the reviewers. Any product that may be evaluated in this article, or claim that may be made by its manufacturer, is not guaranteed or endorsed by the publisher.

frontiers | Frontiers in Cell and Developmental Biology

ORIGINAL RESEARCH
published: 27 May 2022
doi: 10.3389/fcell.2022.892229

Connexin 43 Hemichannels Regulate Osteoblast to Osteocyte Differentiation

*Rui Hua, Sumin Gu and Jean X. Jiang**

Department of Biochemistry and Structural Biology, University of Texas Health Science Center, San Antonio, TX, United States

Connexin 43 (Cx43) is the predominant connexin subtype expressed in osteocytes. Osteocytes, accounting for 90%–95% of total bone cells, function as orchestrators coordinating balanced activity between bone-resorbing osteoclasts and bone-forming osteoblasts. In this study, two newly developed osteocytic cell lines, OCY454 and IDG-SW3, were used to determine the role of Cx43 gap junctions and hemichannels (HCs) in the regulation of osteoblast to osteocyte differentiation. We found that the Cx43 level was substantially increased during the differentiation of IDG-SW3 cells and is also much higher than that of OCY454 cells. We knocked down Cx43 expression using the lentiviral CRISPR/Cas9 approach and inhibition of Cx43 HCs using Cx43 (E2) antibody in IDG-SW3 cells. Cx43 knockdown (KD) or Cx43 HC inhibition decreased gene expression for osteoblast and osteocyte markers, including alkaline phosphatase, type I collagen, dentin matrix protein 1, sclerostin, and fibroblast growth factor 23, whereas increasing the osteoclastogenesis indicator and the receptor activator of nuclear factor kappa-B ligand (RANKL)/osteoprotegerin (OPG) ratio at early and late differentiation stages. Moreover, mineralization was remarkably attenuated in differentiated Cx43-deficient IDG-SW3 cells compared to ROSA26 control. The conditioned medium collected from fully differentiated IDG-SW3 cells with Cx43 KD promoted osteoclastogenesis of RAW264.7 osteoclast precursors. Our results demonstrated that Cx43 HCs play critical roles in osteoblast to osteocyte differentiation process and regulate osteoclast differentiation *via* secreted factors.

Keywords: IDG-SW3 cells, Cx43, CRISPR/Cas9, osteoblast differentiation, mineralization, osteoclastogenesis

OPEN ACCESS

Edited by:
Airong Qian,
Northwestern Polytechnical University, China

Reviewed by:
Lilian Irene Plotkin,
Indiana University Bloomington School of Medicine, United States
Lingxin Zhu,
Wuhan University, China

****Correspondence:***
Jean X. Jiang
jiangj@uthscsa.edu

Specialty section:
This article was submitted to Morphogenesis and Patterning, a section of the journal Frontiers in Cell and Developmental Biology

Received: *08 March 2022*
Accepted: *18 April 2022*
Published: *27 May 2022*

Citation:
Hua R, Gu S and Jiang JX (2022) Connexin 43 Hemichannels Regulate Osteoblast to Osteocyte Differentiation. Front. Cell Dev. Biol. 10:892229. doi: 10.3389/fcell.2022.892229

INTRODUCTION

Osteocytes are the most abundant cell type in bone tissue, comprising 90–95% of bone cells. They are buried within the mineral bone matrix and form an extensive network through long dendritic processes, which allows osteocytes to communicate with neighboring osteocytes, bone-forming osteoblasts, and bone-resorbing osteoclasts (Creecy et al., 2020; Robling and Bonewald, 2020). Emerging studies suggest that osteocytes function as master orchestrators of bone remodeling (Dallas et al., 2013; Schaffler et al., 2014). Osteocytes are shown to sense mechanical loading to coordinate adaptive responses of the skeleton (Qin et al., 2020) and actively secrete factors that regulates phosphate homeostasis and mineral metabolism (Chande and Bergwitz, 2018).

Osteocytes are derived from osteoblasts through osteogenesis. During this transition process, osteoblasts lay down osteoid (non-mineralized bone matrix), accompanied by a morphology change from polygonal to highly dendritic with reduced cell volume, and eventually transform into

osteocytes embedded in the mineralized bone matrix (Franz-Odendaal et al., 2006; Dallas and Bonewald, 2010). Since osteocytes reside within the mineralized lacuno-canalicular network, their isolation has been difficult, generating low yields and high heterogeneity. In addition, osteocytes, as terminally differentiated cells, tend to lose phenotype when isolated from their natural mineralized environment (Dallas et al., 2013; Wang et al., 2019). Despite the abundance and importance, osteocytes have been a challenge to study due to lack of appropriate *in vitro* cell models. It is not until the past 2 decades or so that significant osteocyte cell models have been developed. MLO-Y4 is the first established osteocyte-like cell line, which has been one of the most widely used for studying osteocyte functions (Kato et al., 1997). This cell line was derived from the long bones of transgenic mice expressing the immortalizing SV40 T antigen driven by the osteocalcin promoter. However, several limitations of MLO-Y4 cells include the absence of mineralized matrix, constitutive expression of the large T antigen, and very low levels of the mature osteocyte markers fibroblast growth factor 23 (FGF23) and sclerostin (SOST) (Yang et al., 2009; Woo et al., 2011).

There are two pre-osteocyte cell models, IDG-SW3 (Woo et al., 2011) and OCY454 (Spatz et al., 2015). These two cell lines were generated by crossing the dentin matrix protein 1 (DMP1)–GFP transgenic mice (Kalajzic et al., 2004) with the "immortomouse", which carries a temperature-sensitive SV40 T antigen (Jat et al., 1991). When cultured at 33°C, both IDG-SW3 and OCY454 cells proliferate rapidly. However, at 37°C, they no longer express the SV40 T antigen and differentiate from the late osteoblast to the late osteocyte, closely recapitulating the phenotype of primary cells. These two cell lines provide valuable tools for studying the transition from osteoblast to mature osteocyte. The expression of FGF23 mRNA is elevated in response to 1,25-dihydroxyvitamin D_3 treatment, while the SOST expression with parathyroid hormone (PTH) treatment is downregulated in IDG-SW3 cells (Woo et al., 2011). OCY454 cells express SOST at earlier time points than IDG-SW3 cells after the induction of differentiation, and the expression is upregulated in response to microgravity *in vitro* (Spatz et al., 2015).

Connexin 43 (Cx43) is the most abundant connexin present in osteocytes, acting as a key modulator for skeletal homeostasis (Batra et al., 2012; Stains and Civitelli, 2016; Hua et al., 2021). Cx43 forms gap junctions, which mediate direct cell–cell communication. Cx43 hemichannels (HCs) are unpaired gap junction channels, mediating communication between cells and their extracellular environment. Connexin-formed gap junctions and HCs allow the passage of small molecules (MW < 1 kDa) such as ions, essential metabolites, and secondary messengers, including Ca^{2+}, NAD^{+}, prostaglandin E_2 (PGE_2), cAMP, ADP, and ATP (Goodenough et al., 1996). Deficiency of Cx43 causes heart deficits and death of animals soon after birth (Reaume et al., 1995; Ya et al., 1998), accompanied by osteoblast dysfunction and delayed intramembranous and endochondral ossification in fetuses or newborn pups (Lecanda et al., 2000; Chaible et al., 2011). Using osteoblast- and osteocyte-specific Cx43 knockout mouse models, it has been reported that Cx43 contributes to bone cell proliferation, survival, and differentiation (Plotkin et al., 2008; Watkins et al., 2011; Bivi et al., 2012). Our previous work showed that impairment of Cx43 HCs in osteocytes negatively affect bone formation, remodeling, and osteocyte viability (Xu et al., 2015).

In this study, we aim to investigate the role of Cx43 in regulating osteoblast to osteocyte differentiation, and its impact on osteoclastogenesis. Taking advantage of the newly developed *in vitro* osteocytic cell models, we established a Cx43 knockdown (KD) stable cell line using lentiviral-mediated CRISPR/Cas9 genome editing technology and specifically inhibited Cx43 HCs using Cx43 (E2) antibody. We evaluated osteoblastic and osteocytic marker genes expression and mineralization at different differentiation stages as well as the regulation on osteoclastogenesis. This study will help gain new insights into the basic regulatory mechanisms of osteocyte differentiation and implications for the pathogenesis and treatment of osteoporosis.

MATERIALS AND METHODS

Cell Culture

IDG-SW3 cells, a gift from Dr. Lynda Bonewald (Indiana University), were cultured on collagen-coated (rat tail collagen type I, Corning, 354236, 0.15 mg/ml) plates (Woo et al., 2011). Cells were expanded in immortalizing conditions in an α-MEM medium (Thermo Fisher Scientific, Waltham, MA, United States) supplemented with 10% fetal bovine serum (FBS), 50 U/mL of IFN-γ (Sigma-Aldrich, IF005, St. Louis, MO, United States), and 1% penicillin/streptomycin at 33°C and 5% CO_2. For osteogenesis induction, cells were cultured in the α-MEM medium supplemented with 10% FBS, 50 μg/ml ascorbic acid, and 4 mM β-glycerophosphate at 37°C and 5% CO_2. For Cx43 (E2) antibody treatment, IDG-SW3 cells were supplied with 2 μg/ml Cx43 (E2) antibody upon differentiation, the medium was changed every 2 days.

OCY454 cells were kindly provided by Dr. Paola Divieti Pajevic (Boston University). Cells were expanded in the α-MEM medium supplemented with 10% FBS and 1% penicillin/streptomycin at 33°C and 5% CO_2 on collagen-coated plates, as described previously (Spatz et al., 2015). Upon confluence, cells were plated on non-collagen–coated plates to induce osteogenesis in a 5% CO_2 incubator at 37°C.

Plasmid Design and Construction

The 20-nucleotide single guide RNA (sgRNA) sequences were designed using the CRISPR design and optimization tool (CRISPR-DO) (Ma et al., 2016). SgRNA oligos were annealed and cloned into the BsmBI enzyme site of the lentiviral expression vector lentiCRISPRv2 (Addgene, plasmid #52961, Watertown, MA, United States) (Sanjana et al., 2014; Shalem et al., 2014). The sgRNA sequences used in this study are as follows: Cx43 KD-1: 5′-AAGCCTACTCCACGGCCGG-3′; Cx43 KD-2: 5′- AAAGTG GCGCAGACCGACG-3′; and ROSA26: 5′- CACCGCGCCCAT CTTCTAGAAAGAC-3′.

Lentivirus Packaging and Infection

The HEK293T cells (ATCC, CRL-11268, Manassas, VA, United States) were grown at 37°C and 5% CO_2 in Dulbecco's

modified Eagle's medium (Thermo Fisher Scientific), and lentiviruses were produced by transfecting the HEK293T cells with lentiCRISPRv2:Cx43-sgRNA or ROSA26-sgRNA, together with helper plasmids pCMV-VSV-G (Addgene, plasmid #8454) and psPAX2 (Addgene, plasmid #12260). The transfections were carried out using Lipofectamine 2000 (Thermo Fisher Scientific, 11668019), according to manufacturer's instructions. The virus-containing medium was harvested 48 and 72 h after transfection and subsequently pre-cleaned with a 0.45 μm filter (Millipore, Burlington, MA, United States), as previously described (Jiang et al., 2015; Wang et al., 2016). The viral supernatant was added to IDG-SW3 cells with polybrene. The media was changed 24 h after the infection. An antibiotic kill curve experiment was performed to determine the optimal concentration of puromycin needed to eliminate untransduced cells. At 48 h postinfection, cells were selected with 5 μg/ml puromycin (Sigma-Aldrich, P8833) for 5 days.

Preparation of Cell Membrane Extracts and Western Blotting

Cultured cells were collected in lysis buffer (5 mM Tris, 5 mM EDTA/EGTA, and proteinase inhibitors) and then ruptured by pipetting using a 20-gauge needle. Cell lysates were first centrifuged at 1,000 rpm for 5 min. The supernatant was transferred into ultracentrifuge tubes (Beckman Coulter, 357448, Brea, CA, United States) and centrifuged at 45,000 g for 45 min. The pellet was resuspended in lysis buffer, and the membrane protein was dissolved by addition of SDS to a 1% final concentration. Protein concentrations of SDS-dissolved lysates were determined by using a Micro BCA Protein Kit (Thermo Scientific, 23235), and the lysates were used for Western blotting analysis. Each protein sample was boiled in SDS loading buffer, subjected to electrophoresis on a 10% SDS-polyacrylamide gel, and electroblotted on a nitrocellulose membrane. Membranes were incubated with affinity-purified polyclonal Cx43 antibody (1:300) (Cherian et al., 2003), polyclonal GFP antibody (Abcam, ab290, 1:2000 dilution, Cambridge, United Kingdom), monoclonal β-actin antibody (Thermo Fisher Scientific, MA515739, 1:5000 dilution), or monoclonal GAPDH antibody (Thermo Fisher Scientific, AM4300, 1:5000 dilution). Primary antibodies were detected with goat anti-rabbit IgG–conjugated IRDye® 800CW and goat anti-mouse IgG–conjugated IRDye® 680RD (1:15000 dilution) using a LiCor Odyssey Infrared Imager (LI-COR, Lincoln, NE, United States), as previously described (Ma et al., 2019). The band intensity was quantified by densitometry using ImageJ software (NIH, Bethesda, MA, United States).

Immunofluorescence Staining

The cells were cultured on collagen-coated coverslips for immunofluorescence staining. Cells were rinsed three times with cold DPBS with Ca^{2+} and Mg^{2+} and fixed with 2% paraformaldehyde for 10 min. The cells were then incubated with blocking solution (2% donkey serum, 2% fish skin gelatin, 1% BSA, and 0.2% Triton X-100 in PBS) for 1 h, followed by incubation with affinity-purified polyclonal Cx43 antibody (1:100) at 4°C overnight (Cherian et al., 2003). The primary antibody was detected using 1:500 dilution of Alexa Fluor 488- or Alexa Fluor 594–conjugated donkey anti-rabbit antibody (Jackson Immuno Research Labs, 711-545-152 or 711-585-152, West Grove, PA, United States) for 1 h. Cells on coverslips were mounted using the Vectashield mounting medium (Vector Laboratories, H-1000, Burlingame, CA, United States) and sealed. Fluorescence imaging was performed using a confocal laser scanning microscope (Zeiss, LSM780, Jena, Germany) or a fluorescent microscope (Keyence, BZ-X710, Osaka, Japan).

Scrape Loading/Dye Transfer Assay

Gap junction intercellular coupling was determined at 25°C using scrape loading/dye transfer technique in undifferentiated confluent ROSA26 or Cx43 KD IDG-SW3 cells (Hua et al., 2021). In brief, cells were washed twice with DPBS containing Ca^{2+} and Mg^{2+}, and scrape-loading was performed by scraping cells with a sharp razor scraper containing the gap junction–permeable fluorescent dye (1% lucifer yellow, 457 Da) and gap junction–non-permeable fluorescent dye (1% rhodamine–dextran, 10 kDa). After 5 min, cells were washed four times with DPBS and then fixed with 2% paraformaldehyde for 10 min. Fluorescence images were captured using an inverted fluorescent microscope (Olympus IX70, Tokyo, Japan). Experiments were repeated three times, and data were quantified by averaging fluorescence areas of three fields using NIH ImageJ software. Quantification of changes in dye coupled under different groups was performed by measuring the fluorescence area in square millimeters of the lucifer yellow fluorescence minus rhodamine-–dextran fluorescence.

Fluid Flow Shear Stress (FFSS)

FFSS experiment was conducted to apply mechanical stimulation on undifferentiated ROSA26 or Cx43 KD IDG-SW3 cells. As described previously (Cheng et al., 2001; Riquelme et al., 2015), fluid flow was generated by using a parallel plate flow chamber system (Bioptechs, Butler, PA, United States). The chambers were separated by a gasket of defined thickness with gravity-driven fluid flow using a peristaltic pump (Cole-Parmer Instrument, Chicago, IL, United States). The wall shear stress experienced by cells in these chambers was related directly to the flow rate of the circulating medium through the channel and inversely to the square of the channel height. By adjusting the channel height and flow rate, stress levels of 16 dyn/cm^2 were established. Cells were cultured on collagen-coated microscope glass slides, which can be mounted on the flow chamber with the surface area of 5 cm^2 for shear stress exposure. Each test was conducted for 10 min. The circulating medium was recording media (HCO^{3-}-free α-MEM medium buffered with 10 mM HEPES, pH 7.4), and controls are consisted of ROSA26 or Cx43 KD IDG-SW3 cells in recording media but not subjected to FFSS.

Dye Uptake Assay

On completion of the flow regimen, the cell-covered slides were removed for the dye uptake assay. Cells were incubated with a mixture of 0.1 mM ethidium bromide (EtBr, MW 394 Da) and

TABLE 1 | Primers sequences for RT-PCR.

Gene	Forward primer (5′–3′)	Reverse primer (5′–3′)
ALP	GGAGATGGACCAGGCCATTG	CCGTCCACCACCTTGTAGCC
COL1A1	GCCAATGGTGCTCCTGGTATTG	TTTGGCACCAGTGTCTCCTTTG
DMP1	CCCAGTTGCCAGATACCACAATAC	GCTGTCCGTGTGGTCACTATTT
SOST	CATCCCAGGGCTTGGAGAGTA	TGTCAGGAAGCGGGTGTAGT
FGF23	CTACAGCCAGGACCAGCTATCA	GTTGCCGTGGAGATCCATACAAAG
OPG	GAATGCCGAGAGTGTAGAGAGGATAA	CGCTGCTTTCACAGAGGTCAAT
RANKL	CCGTGCAGAAGGAACTGCAA	TATGGGAACCCGATGGGATG

1 mg/ml FITC-dextran (MW 10 kDa) for 5 min. EtBr was used as a tracer to detect hemichannel activity, and FITC-dextran, which is too large to pass through hemichannels but is taken up by dying cells, was used as a negative control. Cells were then rinsed five times with PBS, followed by fixing with 2% paraformaldehyde for 10 min. At least six microphotographs of fluorescence fields were captured under a 20X fluorescent microscope (Keyence, BZ-X710, Osaka, Japan). For each image, the average intensity of EtBr fluorescence was measured and quantified from at least 30 random cells using ImageJ software (NIH, Bethesda, MD, United States). Experiments were repeated three times, and the collected data were illustrated as pixel mean in arbitrary units.

RNA Isolation and Real-Time PCR

Total RNA was isolated from differentiated IDG-SW3 cells using the TRIzol reagent (Molecular Research Center, TR118, Cincinnati, OH, United States), according to the manufacturer's instructions. After RNA quantification by using Nanodrop 2000, cDNA was synthesized from 1 μg of total RNA using the high-capacity RNA-to-cDNA kit (Applied Biosystems, 43-889-50, Bedford, MA, United States). Real-time PCR was performed using an ABI 7900 PCR device (Thermo Fisher Scientific) and SYBR Green (Bio-Rad Laboratories, 1725124, Hercules, CA, United States) with a two-step protocol (94°C for 15 s and 60°C for 60 s). The $2^{-\Delta\Delta CT}$ method was used for qPCR data analysis. GAPDH was used as a housekeeping gene control. The primers sequences used in this study are listed in **Table 1**. Experiments were run in triplicates.

Alkaline Phosphatase, Alizarin Red, and *von Kossa* Staining

For alkaline phosphatase staining, after osteogenic induction for 9 days, cells were fixed with 4% paraformaldehyde for 10 min and incubated in freshly prepared naphthol AS-MX phosphate (Sigma-Aldrich, 855) and Fast Blue BB (Sigma-Aldrich, F0500) solution. For Alizarin red staining of calcium, after osteogenic induction for 18 or 28 days, cells were fixed with 10% buffered formalin for 15 min and then stained with 2% Alizarin red solution, pH 4.2 (Sigma-Aldrich, A5533). For *von Kossa* staining of phosphate, after osteogenic induction for 28 days, cells were fixed with 10% buffered formalin for 15 min. Cells were then incubated with 5% silver nitrate solution under ultraviolet (UV) light for 20 min. Images were captured using a Keyence microscope (BZ-X710, Osaka, Japan). The stained area was calculated as a percent of total well area over a representative threshold level.

Conditioned Medium Treatment and Tartrate-Resistant Acid Phosphatase (TRAP) Staining

RAW264.7 osteoclast precursors were grown in the RPMI-1640 medium (Thermo Fisher Scientific) supplemented with 10% FBS and 1% penicillin/streptomycin. The conditioned medium collected from differentiated IDG-SW3 cells was aliquoted and stored at −80°C before use. RAW264.7 cells were seeded in 48-well plates for osteoclastogenesis induction. RAW264.7 cells were supplied with the conditioned medium and RAW264.7 growth media mixed in the ratio of 1:1, with 10 ng/ml or 50 ng/ml recombinant RANKL (R&D Systems, 462-TEC-010, Minneapolis, MN, United States). After 7 days of differentiation, osteoclasts were visualized using a leukocyte acid phosphatase staining kit (Sigma, 387A-1 KT). Images were captured using a Keyence microscope (BZ-X710, Osaka, Japan).

Statistical Analysis

Statistical analysis was performed using GraphPad Prism8 statistics software (GraphPad, San Diego, United States). All data are presented as mean ± SEM. *t*-test, one-way ANOVA, and two-way ANOVA with Tukey's test was used for statistical analysis. Asterisks indicate the degree of significant differences compared with the controls (*, $p < 0.05$; **, $p < 0.01$; ***, $p < 0.001$; ****, $p < 0.0001$).

RESULTS

Cx43 Expression is Increased During Osteogenic Differentiation

OCY454 and IDG-SW3 cell lines are two cell models of differentiated osteocytes, which are derived from long bones of double transgenic mice expressing DMP1-GFP and thermolabile large T antigen that enables conditional immortalization of cells (Woo et al., 2011; Spatz et al., 2015). At 33°C, OCY454 and IDG-SW3 cells showed continuous proliferation and were GFP-negative (**Figure 1A**, Day 0). After osteogenic induction, they exhibited late osteoblast to osteocyte phenotype, with expression of a DMP1-GFP reporter as a marker for osteocytic differentiation (**Figure 1A**, Day 6–Day 15). The percentage of GFP-positive cells increased along with the differentiation process in both cell lines. Cx43 expression in OCY454 and IDG-SW3 cells were examined by immunofluorescence

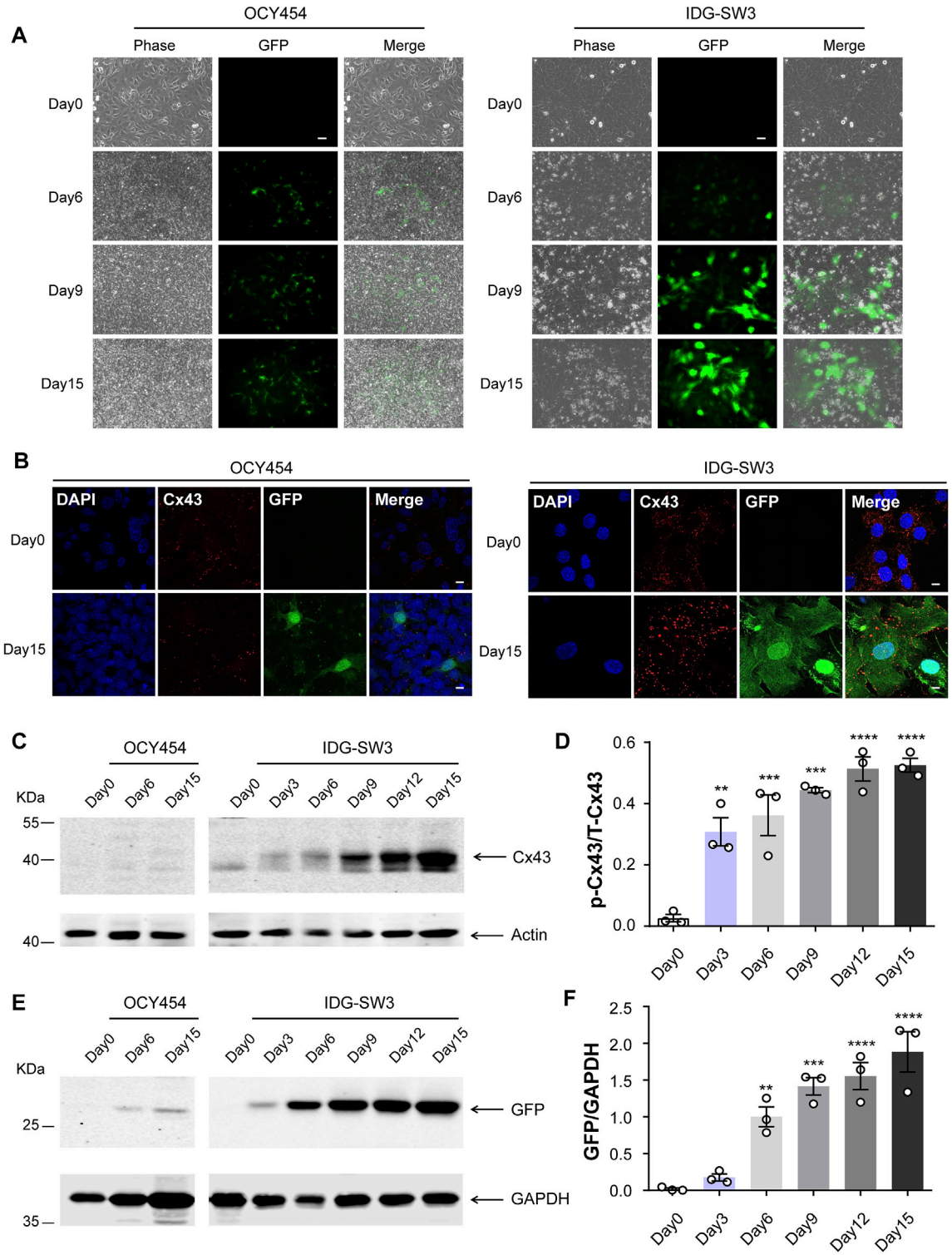

FIGURE 1 | Cx43 expression is increased during osteogenic differentiation in DMP1-GFP–expressing IDG-SW3 and OCY454 cells **(A)** Representative images of DMP1-GFP expression in OCY454 (left panels) and IDG-SW3 cells (right panels) under fluorescent and phase-contrast microscopy during the time course from immortalizing (Day 0) to osteogenic differentiation (Day 15). Scale bar, 50 μm. **(B)** Immunofluorescence staining of Cx43 in OCY454 (left panels) and IDG-SW3 cells (right panels) under immortalizing (Day 0) and osteogenic differentiation (Day 15) conditions. Nuclei were stained with DAPI (blue). Scale bar, 10 μm. **(C)** Membrane extracts were prepared from OCY454 and IDG-SW3 cells and subjected to immunoblotting using Cx43 (CT) or β-actin antibodies. **(D)** Densitometry measurement ratio of phosphorylated Cx43 (p-Cx43) to total Cx43 (T-Cx43). **(E)** Soluble protein extract was isolated from OCY454 and IDG-SW3 cells and subjected to immunoblotting using GFP or GAPDH antibodies. **(F)** Densitometry measurement ratios of GFP to GAPDH. Data shown are mean ± SEM. **, $p < 0.01$, ***, $p < 0.001$, ****, $p < 0.0001$.

staining (**Figure 1B**). Under proliferating conditions, the subcellular localization of Cx43 was mainly in the cytoplasmic region, which is consistent with a previous report in osteoblasts (Yang et al., 2021). The differentiated IDG-SW3 cells displayed a clustered punctate spot-like distribution of Cx43 toward the cell surface (**Figure 1B**, right panels). However, the difference of Cx43 distribution patterns between proliferating and differentiated OCY454 cells was not evident (**Figure 1B**, left panels). To further quantitatively evaluate the Cx43 expression level, Western blot was performed using crude membrane extracts isolated from both cell lines at different time point of differentiation. As shown in **Figure 1C**, there was a minimal level of Cx43 in proliferating OCY454 cells revealed by the affinity-purified Cx43 antibody. In addition, Cx43 expression in differentiated OCY454 cells is very low. In contrast, the amount of Cx43 protein increased dramatically in IDG-SW3 cells along with the differentiation process. The posttranslational phosphorylation of Cx43 was increased associated with differentiation of IDG-SW3 cells (**Figure 1C**), showing the band with decreased electrophoretic mobility due to the addition of phosphate (Musil and Goodenough, 1991; Cheng et al., 2001). The quantification of the phosphorylated Cx43 (p-Cx43)/total Cx43 (T-Cx43) ratio showed a marked elevation during differentiation (**Figure 1D**). We next probed GFP expression in soluble protein prepared at different time point of differentiation. In **Figure 1E**, GFP was increased in differentiated OCY454 cells compared to proliferation condition. However, GFP increase was more profound in IDG-SW3 cells during differentiation. The changes can also be reflected in the densitometry analysis for the GFP level (**Figure 1F**). Taken together, during the osteogenic differentiation process, Cx43 protein was significantly increased and differentiated IDG-SW3 cells expressed more Cx43 than OCY454 cells.

Generation of Cx43 Knockdown IDG-SW3 Cells Using CRISPR/Cas9 Genome Editing Technology

We next focused on the IDG-SW3 cells to study the role of Cx43 in regulating osteoblast to osteocyte differentiation process. Using lentiviral-mediated CRISPR/Cas9 genome editing technology, we generated Cx43 KD cells after lentivirus infection of two pairs of sgRNA followed by puromycin selection. ROSA26, as a preferred site for the integration of transgenes and reporter constructs, is ubiquitously expressed in all cell types and developmental stages (Irion et al., 2007; Chu et al., 2016). In our study, sgRNA targeting ROSA26 was designed for lentivirus infection and puromycin selection in IDG-SW3 cells, which could serve as a reference control (Bäck et al., 2019; Riggan et al., 2020). The expression of Cx43 was determined by Western blot. There was a remarkably band intensity reduction after CRISPR/Cas9-mediated ablation of Cx43, and the Cx43 level is comparable between ROSA26 and non-targeting control groups (**Figure 2A**, upper panel). Quantification of the Cx43/actin ratio showed a 90% decrease in Cx43 KD groups compared to ROSA26 or control (**Figure 2A**, lower panel). The immunofluorescence staining further validated the successful generation of Cx43 KD strains in proliferating IDG-SW3 cells (**Figure 2B**). During the osteoblast to osteocyte transition, IDG-SW3 cells undergo several differentiation stages: early osteoblast (day 4), osteoid osteocyte (day 9), mineralizing osteocyte (day 18), and mature osteocyte (day 28) (Woo et al., 2011). We cultured IDG-SW3 cells from ROSA26 and Cx43 KD groups for differentiation to examine whether the CRISPR/Cas9-mediated Cx43 deficiency could be maintained throughout the differentiation process. Membrane extracts collected at different differentiation stages were subjected to Western blot analysis. As shown in **Figure 2C**, compared to the ROSA26 group, Cx43 KD groups had minimal Cx43 expression at each time point. These results demonstrated the generation of stable Cx43 KD IDG-SW3 cell lines by using lentiviral-mediated CRISPR/Cas9 genome editing technology.

Cx43 Knockdown in IDG-SW3 Cells Inhibits Gap Junction Intercellular Communication and the Opening of Cx43 Hemichannels

The scrape loading/dye transfer assay is a commonly used approach to study intercellular coupling *via* functional gap junction channels (el-Fouly et al., 1987). Gap junction intercellular communication (GJIC) was evaluated in undifferentiated ROSA26 and Cx43 KD IDG-SW3 cells. Cells were grown to reach confluence before performing the scrape loading/dye transfer assay. As illustrated in **Figure 3A** and quantified in **Figure 3B**, the ROSA26 group was much more efficient in transferring LY in comparison with Cx43 KD groups. Carbenoxolone (CBX) acts as a potent and effective blocker of GJIC (Connors, 2012). After CBX inhibition, the ROSA26 group showed decreased intercellular coupling compared to that of the Cx43 KD level (**Figure 3A,B**). There was no difference between Cx43 KD IDG-SW3 cells with or without CBX blocking, indicating the CRISPR/Cas9-mediated Cx43 deficiency inhibited GJIC. The activity of Cx43 HCs was further evaluated using the EtBr dye uptake assay. Cells were grown at a low-cell density to ensure that the majority of the cells were not physically in contact. Our previous study has demonstrated that Cx43 HCs open when subjected to mechanical stimulation in the form of FFSS (Cherian et al., 2005). Under FFSS, the ROSA26 group showed a 2-fold increase in arbitrary units (AU) of fluorescence intensity, reflective of the hemichannel dye uptake level, compared to that of the basal level (**Figure 3C,D**). In contrast, Cx43 KD groups were not responding to FFSS-induced HCs opening, indicating an impaired Cx43 HCs activity in undifferentiated IDG-SW3 cells with Cx43 KD.

Cx43 Knockdown in IDG-SW3 Cells Decreases Alkaline Phosphatase and Type I Collagen Expression at Early Differentiation Stage

IDG-SW3 cells express osteoblastic markers including alkaline phosphatase (ALP) and type I collagen (COL1A1) at the early stage of differentiation. To evaluate the osteoblastic activity of ROSA26 and Cx43 KD IDG-SW3 cells, ALP staining was performed after 9 days of differentiation. Cx43 KD groups had significantly reduced the level of positive ALP staining (**Figure 4A,B**). Using real-time PCR, we also observed lower abundance of ALP and COL1A1 mRNA with Cx43 deficiency

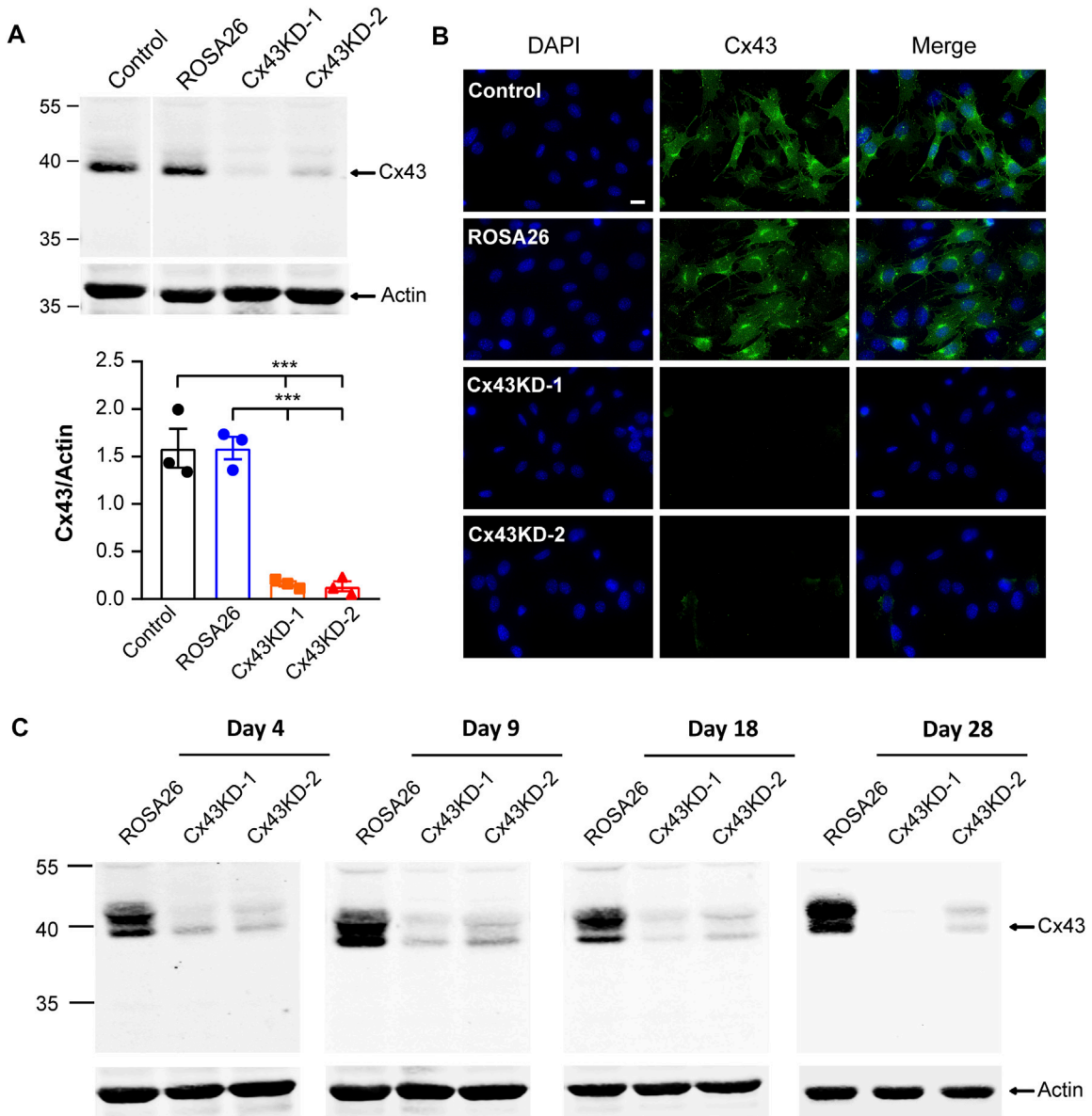

FIGURE 2 | Ablation of Cx43 expression using CRISPR/Cas9 gene editing technology in IDG-SW3 cell line. **(A)** Immortalizing (Day 0) IDG-SW3 cells were subjected to specified ROSA26 or Cx43-sgRNA lentivirus transduction and puromycin selection. Membrane extracts were immunoblotted by Cx43 or β-actin antibodies (upper panel). The lower panel shows the densitometric measurement ratios of Cx43 to β-actin. **(B)** Representative images of Cx43 immunofluorescence staining in control, ROSA26, or Cx43 KD IDG-SW3 cells. Scale bar, 20 μm. **(C)** Membrane extracts were isolated from ROSA26 or Cx43 KD groups during the time course from Day 4 to Day 28 after differentiation. Cx43 expression was analyzed by using Western blot probed with Cx43 and β-actin antibodies. Data shown are mean ± SEM. ***, $p < 0.001$.

(**Figure 4C**), further suggesting that Cx43 KD in IDG-SW3 cells decreases osteoblastic marker expression.

Cx43 Knockdown in IDG-SW3 Cells Decreases Mineralization and Osteocytic Genes Expression at Late Differentiation Stage

We then tested whether Cx43 plays a major role in mineralization and calcium deposition during osteogenic differentiation. ROSA26 and Cx43 KD IDG-SW3 cells were cultured in a mineralizing medium containing ascorbic acid and β-glycerophosphate for 18 and 28 days. Alizarin red staining for calcium deposition showed that the staining area was substantially lower in Cx43 KD groups than that in ROSA26 cells at both 18 days (**Figure 5A,B**) and 28 days (**Figures 5C,D**) after differentiation. In addition, *von Kossa* staining for focal nodular mineralization was performed at 28 days. The number of mineralized nodules was reduced by 80% in IDG-SW3 cells with Cx43 KD (**Figure 5E,F**). The mRNA expression of DMP1, SOST, FGF23, osteoprotegerin (OPG), and receptor

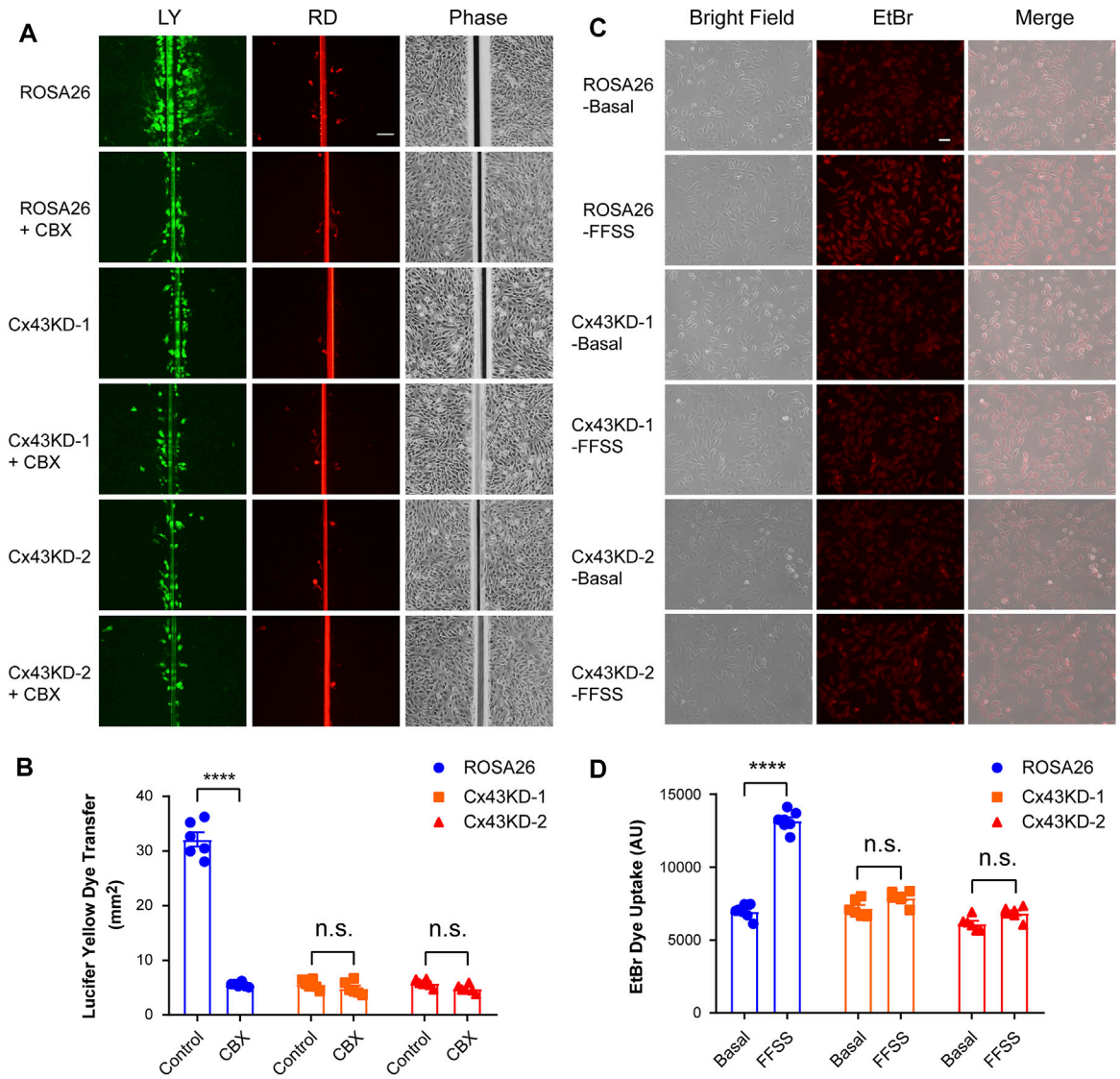

FIGURE 3 | Cx43 deficiency in IDG-SW3 cell line inhibits gap junction intercellular communication and the opening of Cx43 hemichannels. **(A)** Dye transfer was determined in ROSA26 or Cx43 KD IDG-SW3 cells in absence or presence of 100 μM CBX. The scrape loading assay was performed with LY and RD for 5 min. Scale bar, 200 μm. **(B)** Area of dye transfer was determined and quantified by fluorescence microcopy and NIH ImageJ software. **(C)** ROSA26 or Cx43 KD IDG-SW3 cells were subjected to FFSS for 10 min or non-FFSS basal conditions, followed by incubation with 100 μM EtBr for 5 min. Scale bar, 50 μm. **(D)** Level of EtBr dye uptake was determined and quantified by fluorescence microcopy and NIH ImageJ software. Data shown are mean ± SEM. ****, $p < 0.0001$.

activator of nuclear factor kappa-B ligand (RANKL) was determined. After 28 days of osteogenic differentiation, DMP1, SOST, FGF23, and OPG showed significant decrease in both Cx43 KD groups compared to that in the ROSA26 group (**Figure 5G**). In contrast, the level of RANKL mRNA was elevated up to almost 2-fold in Cx43 KD IDG-SW3 cells. Correspondingly, the ratio of RANKL/OPG, which is indicative of the propensity to generate osteoclasts during bone remodeling (Boyce and Xing, 2008), was significantly elevated in IDG-SW3 cells with Cx43 KD (**Figure 5G**). The aforementioned results indicated delayed osteogenic differentiation caused by Cx43 deficiency, along with a decrease in DMP1, SOST, and FGF23, and an increase in the RANKL/OPG ratio.

Blocking Cx43 Hemichannels in IDG-SW3 Cells Reduces Osteoblastic and Osteocytic Genes Expression During Differentiation

We then assessed whether Cx43 HCs could play a role in regulating the osteoblastic genes expression. To specifically target the Cx43 HCs, we utilized the Cx43 (E2) antibody, which was previously generated by our lab (Siller-Jackson et al., 2008). This blocking antibody targets the second extracellular loop (E2) of Cx43. IDG-SW3 cells were treated with or without Cx43 (E2) antibody for 9 days during differentiation. The ALP-stained area was significantly decreased in Cx43 (E2)-treated cells (**Figure 6A,B**).

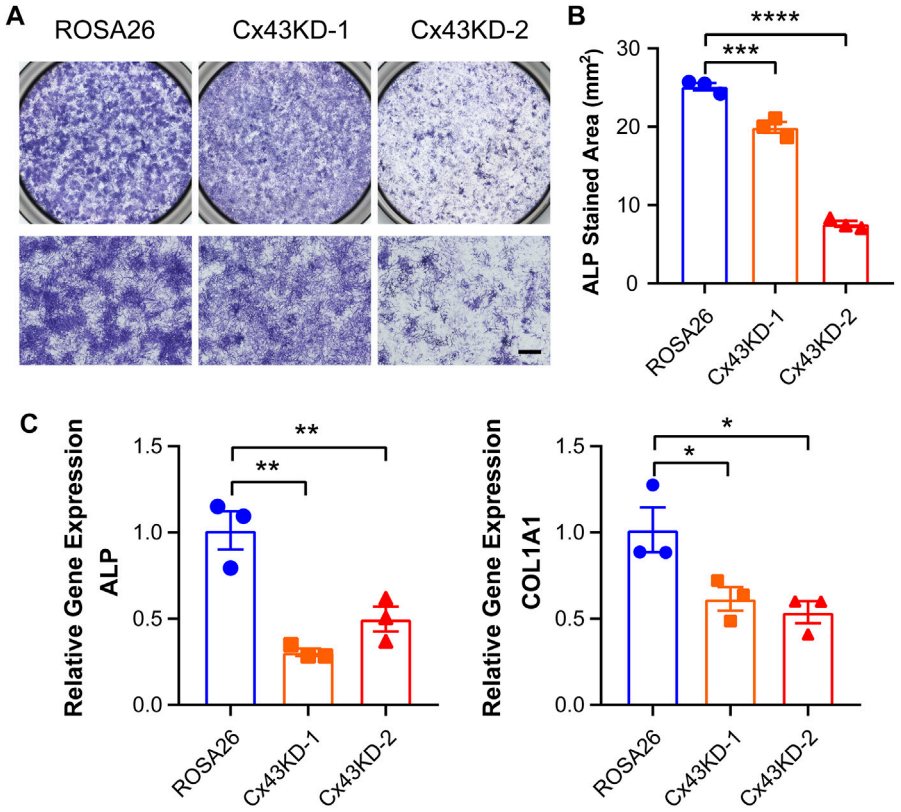

FIGURE 4 | Cx43 knockdown decreased alkaline phosphatase and type I collagen expression in IDG-SW3 cells. **(A)** Representative images of ALP staining in ROSA26 or Cx43 KD IDG-SW3 cells at day 9 of the induction of differentiation. Lower panels show an enlarged view of the center regions of upper panels. Scale bar, 500 μm. **(B)** Quantification of ALP-stained area by NIH ImageJ software. **(C)** Total RNA was prepared from ROSA26 or Cx43 KD IDG-SW3 cells. The mRNA levels of ALP and COL1A1 were determined by real-time PCR normalized to GAPDH. Data shown are mean ± SEM. *, $p < 0.05$, **, $p < 0.01$, ***, $p < 0.001$, ****, $p < 0.0001$.

Consistently, ALP and COL1A1 mRNA levels were much lower in the Cx43 (E2) group than those in the control group (**Figure 6C**).

To study the role of Cx43 HCs in the regulation of mineralization and osteocytic marker genes expression, we incubated IDG-SW3 cells with Cx43 (E2) antibody for 28 days during differentiation. There was no significant difference of calcium deposition evaluated by Alizarin red–stained area after Cx43 (E2) treatment (**Figure 7A,B**). The mRNA expression of DMP1, SOST, FGF23, OPG, and RANKL was also determined. The Cx43 (E2) antibody–treated IDG-SW3 cells showed significant downregulation of DMP1, SOST, FGF23, and OPG. With the Cx43 (E2) inhibition of Cx43 HC activity, the RANKL mRNA exhibited a trend of elevation, resulting in a significantly increased RANKL/OPG ratio compared to the control group.

Conditioned Medium From Cx43 Knockdown IDG-SW3 Cells Promotes Osteoclastogenesis of RAW264.7 Cells

Osteocytes express essential bone modulating factors which could act directly to regulate osteoclast formation and bone resorption (Kitaura et al., 2020). Given the impaired osteogenesis function under Cx43 deficiency condition, we next investigated whether the secreted factors from ROSA26 and Cx43 KD osteocytes could influence osteoclastogenesis. The conditioned medium (CM) was collected from IDG-SW3 cells with or without Cx43 deficiency after 28 days of differentiation. RAW264.7 osteoclast precursors were cultured using CM supplemented with 10 ng/ml or 50 ng/ml RANKL for 1 week. As shown in **Figure 8A,B**, there was a 1.7-fold elevation in TRAP-positive cell percentage in RAW264.7 cells treated with Cx43 KD CM and 10 ng/ml RANKL. The treatment with Cx43 KD CM and 50 ng/ml RANKL showed more large osteoclasts with multi-nuclei (**Figure 8C**, red arrows), and quantification further demonstrated a significant increase of mature osteoclasts numbers compared to the ROSA26 control (**Figure 8D**). These results indicate that Cx43 channels in IDG-SW3 cells may secrete factors that inhibit osteoclast differentiation.

DISCUSSION

In this study, we found that during IDG-SW3 cell differentiation process, Cx43 expression increased dramatically, and their Cx43 expression level is much higher than OCY454 cells. We effectively deleted Cx43 in IDG-SW3 cell model using lentiviral-based CRISPR/Cas9 genome editing technique. IDG-SW3 cells with

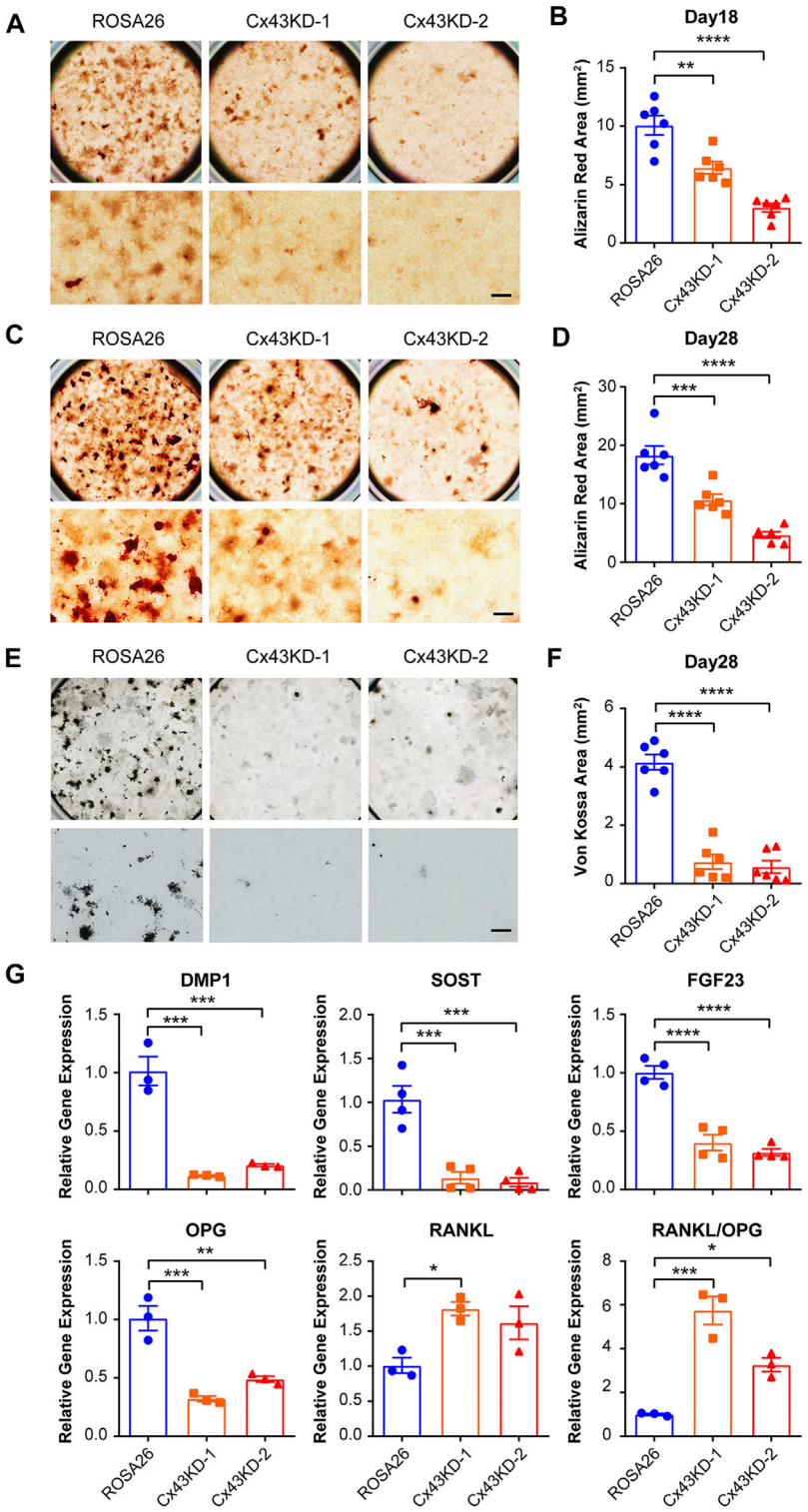

FIGURE 5 | Cx43 knockdown decreased matrix mineralization and osteocytic markers expression in IDG-SW3 cells. Representative images of Alizarin red staining in ROSA26 or Cx43 KD IDG-SW3 cells at day 18 **(A)** or 28 **(C)** of the induction of differentiation. Lower panels show an enlarged view of the center regions of upper panels. Scale bar, 500 μm. **(B,D)** Quantification of Alizarin red–stained area by NIH ImageJ software. **(E)** Representative images of *von Kossa* staining in ROSA26 or Cx43 KD IDG-SW3 cells after 28 days of differentiation. Lower panels show an enlarged view of the center regions of upper panels. Scale bar, 500 μm. **(F)** Quantification of *von Kossa*-stained area by NIH ImageJ software. **(G)** Total RNA was prepared from ROSA26 or Cx43 KD IDG-SW3 cells after 28 days of differentiation. The mRNA levels of DMP1, SOST, FGF23, OPG, and RANKL were determined by real-time PCR normalized to GAPDH. Data shown are mean ± SEM. *, $p < 0.05$, **, $p < 0.01$, ***, $p < 0.001$, ****, $p < 0.0001$.

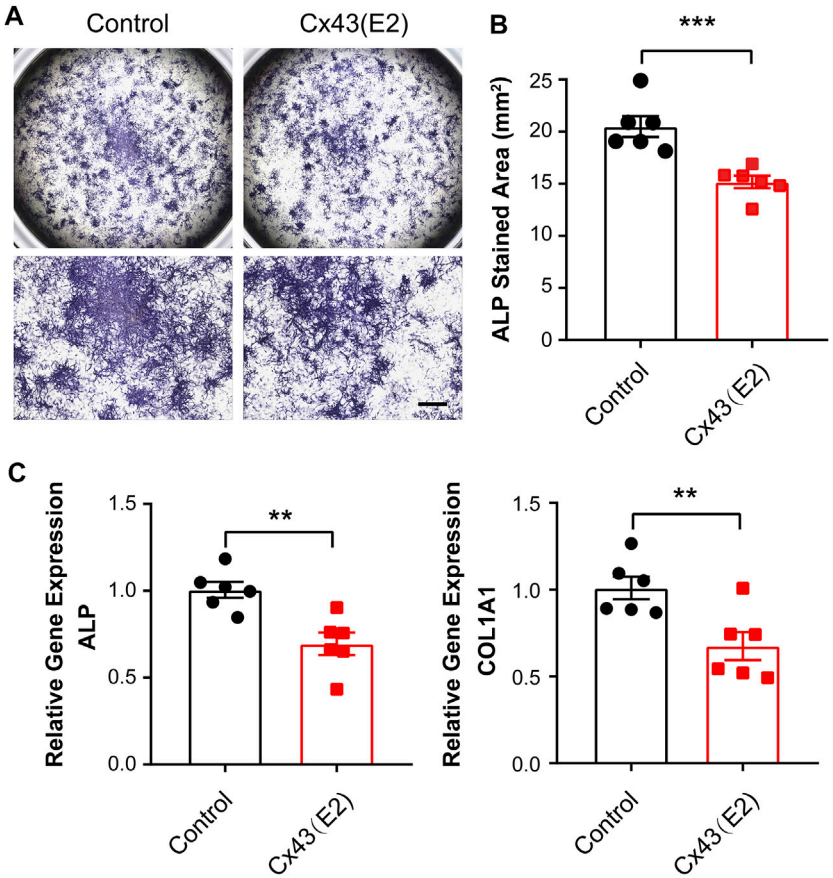

FIGURE 6 | Inhibition of Cx43 hemichannels decreased alkaline phosphatase and type I collagen expression in IDG-SW3 cells. **(A)** Representative images of ALP staining in control or Cx43 (E2) antibody–treated IDG-SW3 cells at day 9 of the induction of differentiation. Lower panels show enlarged view of the center regions of upper panels. **(B)** Quantification of ALP-stained area by NIH ImageJ software. **(C)** Total RNA was prepared from control or Cx43 (E2) antibody–treated IDG-SW3 cells. The mRNA levels of ALP and COL1A1 were determined by real-time PCR normalized to GAPDH. Data shown are mean ± SEM. **, $p < 0.01$, ***, $p < 0.001$.

Cx43 deficiency exhibited decreased osteoblast markers, ALP and COL1A1, expression at the osteoid–osteocyte stage compared to control. With the progression from mineralization to maturation of osteocytes, Cx43 deficiency resulted in a reduction in matrix-forming protein—DMP1, mature osteocyte markers—SOST and FGF23, and a significant increase in the RANKL/OPG level. Moreover, blocking Cx43 HCs using a specific Cx43 antibody resulted in downregulation of ALP, COL1A1, DMP1, SOST, and FGF23, with an increase of RANKL/OPG. Interestingly, RAW264.7 osteoclast precursors were more prone to osteoclastogenesis after treatment with CM from Cx43 KD IDG-SW3 cells. Our findings suggest that Cx43 HCs plays an essential role in osteoblast to osteocyte differentiation and mineralization process as well as in regulating osteoclast differentiation *via* secreted factors.

The CRISPR/Cas9 system is a fast and efficient tool to conduct genomic modification (Wang et al., 2018). In combination with the lentivirus infection, the sgRNA and Cas9 sequences can be integrated into the genome of target cells. Our results showed that the lentiviral-mediated CRISPR/Cas9 expression was steadily maintained, which can continuously exert excision functions throughout the IDG-SW3 cell differentiation process. Cx43 consists of two exons: exon1 encodes most of the 5'-untranslated region (5'-UTR) and exon2 contains complete coding sequence and 3′-UTR (Pfeifer et al., 2004). To silence the Cx43 gene, two sgRNA oligonucleotides targeting the exon2 were designed and validated to avoid the effects of potential off-target activities. Both pairs of sgRNAs led to remarkable reduction of GJIC and HC opening induced by FFSS in IDG-SW3 cells. The ROSA26 locus is often referred to as a "safe harbor" locus and has been extensively used as a transgene insertion site (Irion et al., 2007; Chu et al., 2016). The sgRNA-targeted ROSA26 gene was constructed and served as a good experimental control. In addition, the validated lentiviral CRISPR/Cas9 vectors could be potentially expanded to application in other cell types.

Cx43 forms gap junctions and HCs, which play essential roles in bone development *in vivo*. The conventional Cx43 knockout mouse model is embryonically lethal, with delayed ossification and craniofacial abnormalities (Lecanda et al., 2000; Chaible et al., 2011). Cx43 conditional deletion models in osteoblasts and/or osteocytes have been developed. The COL1A1 promoter–driven

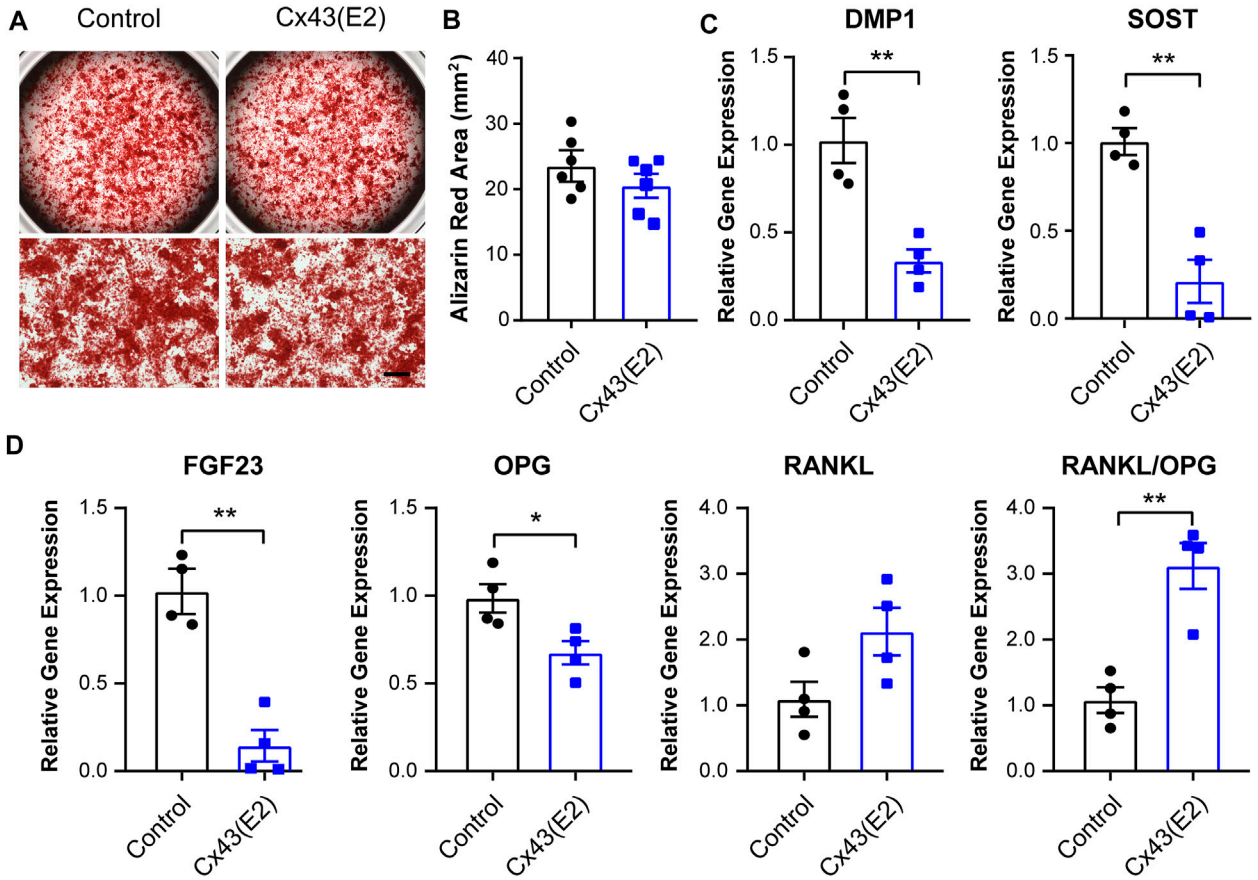

FIGURE 7 | Inhibition of Cx43 hemichannels decreased osteocytic markers expression in IDG-SW3 cells. **(A)** Representative images of Alizarin red staining in control or Cx43 (E2) antibody–treated IDG-SW3 cells at day 28 of the induction of differentiation. Lower panels show enlarged view of the center regions of upper panels. Scale bar, 500 μm. **(B)** Quantification of Alizarin red–stained area by NIH ImageJ software. **(C–D)** Total RNA was prepared from control or Cx43 (E2) antibody–treated IDG-SW3 cells after 28 days of differentiation. The mRNA levels of DMP1, SOST, FGF23, OPG, and RANKL were determined by real-time PCR normalized to GAPDH. Data shown are mean ± SEM. *, $p < 0.05$, **, $p < 0.01$.

Cx43 deletion results in low bone mineral density (BMD) and compromised bone strength (Chung et al., 2006; Grimston et al., 2008). The human osteocalcin promoter- or DMP1 promoter–driven Cx43 deletion leads to increased osteocytic apoptosis, endocortical bone resorption, and periosteal bone formation (Zhang et al., 2011; Bivi et al., 2012). Studies with osteoblastic cell lines have demonstrated the importance of Cx43 channels in osteoblast proliferation (Gramsch et al., 2001) and in mediating the antiapoptotic effects of bisphosphonates and parathyroid hormone (Plotkin et al., 2002; Bivi et al., 2011). Moreover, Cx43 potentiates osteoblast responsiveness to FGF2 (Lima et al., 2009). Previous reports also reveal the roles of gap junctions in osteoblast differentiation (Jiang et al., 2007). Cx43 expression and gap junction function are shown to increase along with osteoblast differentiation process (Donahue et al., 2000). Overexpression of Cx43 promotes osteoblasts proliferation and differentiation (Lecanda et al., 1998; Gramsch et al., 2001). In contrast, using inhibitors of gap junctions or transfection with antisense Cx43 cDNA/dominant negative Cx43 construct attenuates osteoblast differentiation, which is associated with a reduction in ALP activity, COL1A1 expression, and decreased bone nodule formation (Li et al., 1999; Schiller et al., 2001; Upham et al., 2003). Our study generated CRISPR/Cas9-mediated Cx43 deficiency in a newly developed osteocytic cell model and specifically targeted Cx43 HCs to investigate the regulation from pre-osteocyte to mature osteocyte differentiation. Our results highlighted the unrecognized role of Cx43 HCs in this differentiation process.

To dissect the differential functions of gap junctions vs. HCs formed by Cx43 *in vivo*, we have generated two transgenic mouse models driven by DMP1 promoter with Cx43-dominant negative mutants (Xu et al., 2015). R76W mutant has an impaired gap junction, while both the gap junction and HCs were impaired in Δ130-136 mice. Cx43 HCs play a dominant role in regulating osteocyte survival, endocortical bone resorption, and periosteal apposition. We also showed that functional HCs protect osteocytes against catabolic effects during estrogen deficiency (Ma et al., 2019). In this study, to delineate the role of Cx43 HCs in the regulation of osteoblast to osteocyte differentiation, we adopted the Cx43 (E2) antibody developed in our lab (Siller-

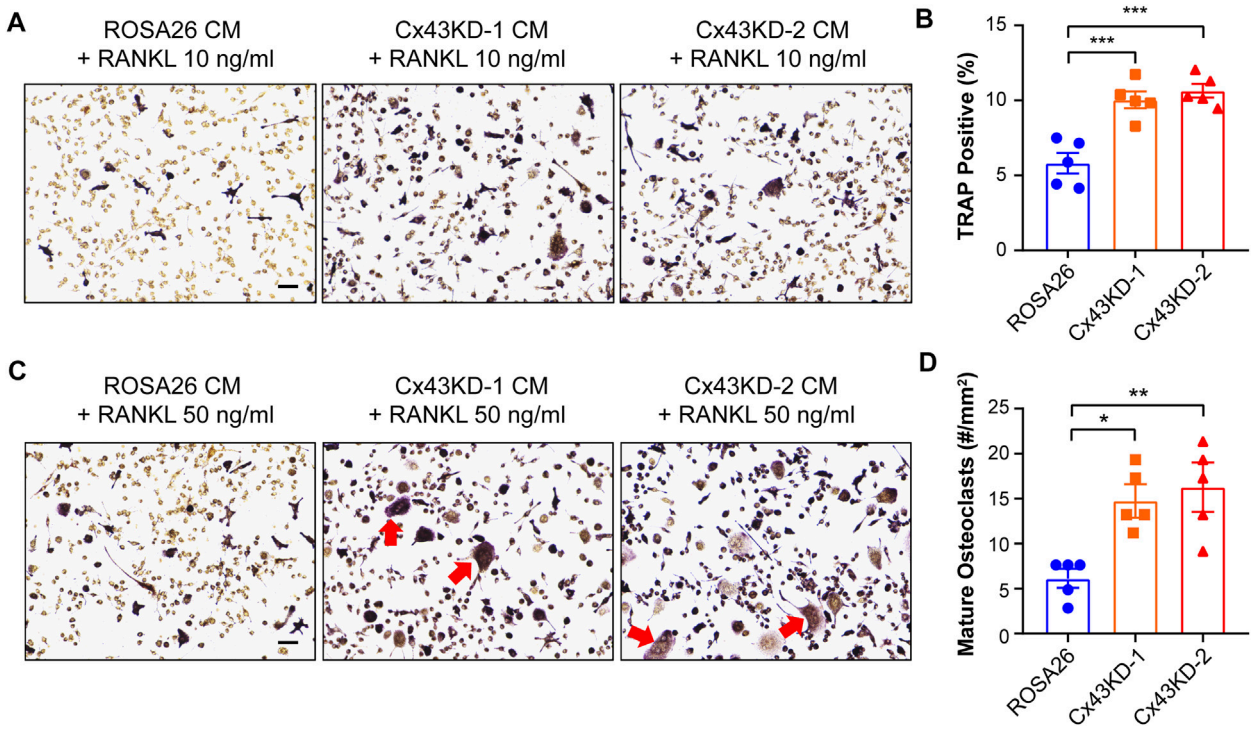

FIGURE 8 | Conditioned medium collected from differentiated IDG-SW3 cells with Cx43 knockdown promoted osteoclastogenesis of RAW264.7 cells. Representative images **(A,C)** of TRAP staining in differentiated RAW264.7 cells cultured in CM from ROSA26 or Cx43 KD IDG-SW3 cells with 10 ng/ml **(A,B)** or 50 ng/ml RANKL **(C,D)** for 7 days. Scale bar, 50 μm. **T**he percentage of TRAP-stained cells **(B)** and numbers of mature osteoclasts **(D)** were quantified by NIH ImageJ software. Data shown are mean ± SEM. *, $p < 0.05$, **, $p < 0.01$, ***, $p < 0.001$.

Jackson et al., 2008; Riquelme et al., 2013). This polyclonal antibody specifically binds to the E2 domain of Cx43, detects cell surface–expressed Cx43, and impedes the opening of Cx43 HCs, without affecting the docking and function of the gap junction channels. The Cx43 (E2) antibody has been widely used by various groups to determine the function of Cx43 HCs (Bao et al., 2011; Orellana et al., 2012; Tarzemany et al., 2017). Our results demonstrated that blocking Cx43 HCs decreased osteoblastic markers at an early differentiation stage; downregulated DMP1, SOST, and FGF23; and increased RANKL/OPG at the late differentiation stage, which were also observed under Cx43 deficiency condition. These findings indicate that Cx43 HCs play important roles in regulating the differentiation markers expression, possibly through mediating the release of anabolic factors that are elicited during differentiation process. After Cx43 (E2) antibody treatment, the calcium deposition only showed a trend of reduction. One of the possible reasons could be that the matrix accumulated around differentiated cells may impede the accessibility of the antibody to the cell.

RANKL secreted by osteocytes is the key factor for osteoclast formation and bone resorption (Kitaura et al., 2020). OPG acts as a decoy receptor, which protects bone from excessive resorption by binding to RANKL and preventing it from interacting with RANK. Thus, the relative concentration of RANKL and OPG is a major determinant of bone mass and strength (Boyce and Xing, 2008). Blocking Cx43 gap junctions and HCs resulted in an elevated RANKL/OPG ratio in differentiated mature osteocytes, suggesting a potentially catabolic environment. Indeed, the CM from Cx43 KD IDG-SW3 cells induced more TRAP-positive osteoclasts and multi-nuclei mature osteoclasts after RAW264.7 cell differentiation. Previous reports have shown that the RANKL/OPG ratio increased in MLO-Y4 cells lacking Cx43 (Bivi et al., 2012; Davis et al., 2017). Osteoclast precursors cocultured with Cx43-silenced MLO-Y4 cells or treated with CM from Cx43-silenced MLO-Y4 cells enhance osteoclast differentiation (Davis et al., 2017). Consistently, one recent study reveals that Cx43 exerts protective effects against excess osteoclastogenesis *via* passing cyclic adenosine monophosphate (cAMP) between osteoblasts (Kawatsura et al., 2022). In addition, increased osteocyte apoptosis has been found in Cx43-silenced MLO-Y4 cells compared to control, which may lead to more osteoclastogenesis (Bivi et al., 2012; Davis et al., 2017). The aforementioned findings highlight the indispensable role of Cx43 in regulating both arms of bone remodeling.

Osteocytes are highly mechanosensitive cells. Our previous *in vitro* studies have shown that FFSS opens Cx43 HCs, leading to the release of anabolic factor, PGE_2 in osteocytes (Cherian et al., 2005; Siller-Jackson et al., 2008). Our recent *in vivo* study reveals that osteocytic Cx43 HCs play a key role in endosteal anabolic

responses to mechanical stimulation (Zhao et al., 2022). Interestingly, Cx43 deletion in osteoblasts/osteocytes driven by the Bglap2 promoter, or in osteocytes driven by the 8 kb DMP1 promoter, shows an enhanced periosteal response to mechanical loading (Zhang et al., 2011; Grimston et al., 2012; Bivi et al., 2013). Mechanically stimulated osteocytes release factors that increase ALP activity and calcium deposition in osteoblasts while decreasing large-sized TRAP-positive osteoclasts (Xu et al., 2019). The outcome and cell model developed in this study will help our understanding of the underlying mechanism of important biological function of osteocytes and unveil therapeutic implications for future investigations.

DATA AVAILABILITY STATEMENT

The data sets presented in this article are not readily available. Requests to access the data sets should be directed to jiangj@uthscsa.edu.

AUTHOR CONTRIBUTIONS

Study design: RH, SG, and JJ. Data collection and analysis: RH. Data interpretation: RH, SG, and JJ. Drafting manuscript: RH and JJ. All authors contributed to the article and approved the submitted version.

FUNDING

This work was supported by the National Institutes of Health (NIH), grant no. 5RO1 AR072020 to JJ, and Welch Foundation, grant no. AQ-1507 to JJ.

ACKNOWLEDGMENTS

We thank Lynda Bonewald of Indiana University for generously providing IDG-SW3 cells and Paola Divieti Pajevic of Boston University for generously providing OCY454 cells.

REFERENCES

Bäck, S., Necarsulmer, J., Whitaker, L. R., Coke, L. M., Koivula, P., Heathward, E. J., et al. (2019). Neuron-Specific Genome Modification in the Adult Rat Brain Using Crispr-Cas9 Transgenic Rats. *Neuron* 102 (1), 105–119. doi:10.1016/j.neuron.2019.01.035

Bao, B., Jiang, J., Yanase, T., Nishi, Y., and Morgan, J. R. (2011). Connexon-Mediated Cell Adhesion Drives Microtissue Self-assembly. *FASEB J.* 25 (1), 255–264. doi:10.1096/fj.10-155291

Batra, N., Kar, R., and Jiang, J. X. (2012). Gap Junctions and Hemichannels in Signal Transmission, Function and Development of Bone. *Biochim. Biophys. Acta (Bba) - Biomembranes* 1818 (8), 1909–1918. doi:10.1016/j.bbamem.2011.09.018

Bivi, N., Condon, K. W., Allen, M. R., Farlow, N., Passeri, G., Brun, L. R., et al. (2012). Cell Autonomous Requirement of Connexin 43 for Osteocyte Survival: Consequences for Endocortical Resorption and Periosteal Bone Formation. *J. Bone Miner Res.* 27 (2), 374–389. doi:10.1002/jbmr.548

Bivi, N., Lezcano, V., Romanello, M., Bellido, T., and Plotkin, L. I. (2011). Connexin43 Interacts with βarrestin: A Pre-requisite for Osteoblast Survival Induced by Parathyroid Hormone. *J. Cel. Biochem.* 112 (10), 2920–2930. doi:10.1002/jcb.23208

Bivi, N., Pacheco-Costa, R., Brun, L. R., Murphy, T. R., Farlow, N. R., Robling, A. G., et al. (2013). Absence of Cx43 Selectively from Osteocytes Enhances Responsiveness to Mechanical Force in Mice. *J. Orthop. Res.* 31 (7), 1075–1081. doi:10.1002/jor.22341

Boyce, B. F., and Xing, L. (2008). Functions of Rankl/Rank/Opg in Bone Modeling and Remodeling. *Arch. Biochem. Biophys.* 473 (2), 139–146. doi:10.1016/j.abb.2008.03.018

Chaible, L. M., Sanches, D. S., Cogliati, B., Mennecier, G., and Dagli, M. L. Z. (2011). Delayed Osteoblastic Differentiation and Bone Development in Cx43 Knockout Mice. *Toxicol. Pathol.* 39 (7), 1046–1055. doi:10.1177/0192623311422075

Chande, S., and Bergwitz, C. (2018). Role of Phosphate Sensing in Bone and Mineral Metabolism. *Nat. Rev. Endocrinol.* 14 (11), 637–655. doi:10.1038/s41574-018-0076-3

Cheng, B., Zhao, S., Luo, J., Sprague, E., Bonewald, L. F., and Jiang, J. X. (2001). Expression of Functional Gap Junctions and Regulation by Fluid Flow in Osteocyte-Like Mlo-Y4 Cells. *J. Bone Miner Res.* 16 (2), 249–259. doi:10.1359/jbmr.2001.16.2.249

Cherian, P. P., Cheng, B., Gu, S., Sprague, E., Bonewald, L. F., and Jiang, J. X. (2003). Effects of Mechanical Strain on the Function of Gap Junctions in Osteocytes Are Mediated through the Prostaglandin Ep_2 Receptor. *J. Biol. Chem.* 278, 43146–43156. doi:10.1074/jbc.m302993200

Cherian, P. P., Siller-Jackson, A. J., Gu, S., Wang, X., Bonewald, L. F., Sprague, E., et al. (2005). Mechanical Strain Opens Connexin 43 Hemichannels in Osteocytes: A Novel Mechanism for the Release of Prostaglandin. *Mol. Biol. Cel* 16 (7), 3100–3106. doi:10.1091/mbc.e04-10-0912

Chu, V. T., Weber, T., Graf, R., Sommermann, T., Petsch, K., Sack, U., et al. (2016). Efficient Generation of Rosa26 Knock-In Mice Using Crispr/Cas9 in C57bl/6 Zygotes. *BMC Biotechnol.* 16, 4. doi:10.1186/s12896-016-0234-4

Chung, D. J., Castro, C. H. M., Watkins, M., Stains, J. P., Chung, M. Y., Szejnfeld, V. L., et al. (2006). Low Peak Bone Mass and Attenuated Anabolic Response to Parathyroid Hormone in Mice with an Osteoblast-Specific Deletion of Connexin43. *J. Cel Sci* 119 (Pt 20), 4187–4198. doi:10.1242/jcs.03162

Connors, B. W. (2012). Tales of a Dirty Drug: Carbenoxolone, Gap Junctions, and Seizures. *Epilepsy Curr.* 12 (2), 66–68. doi:10.5698/1535-7511-12.2.66

Creecy, A., Damrath, J. G., and Wallace, J. M. (2020). Control of Bone Matrix Properties by Osteocytes. *Front. Endocrinol.* 11, 578477. doi:10.3389/fendo.2020.578477

Dallas, S. L., and Bonewald, L. F. (2010). Dynamics of the Transition from Osteoblast to Osteocyte. *Ann. N. Y Acad. Sci.* 1192, 437–443. doi:10.1111/j.1749-6632.2009.05246.x

Dallas, S. L., Prideaux, M., and Bonewald, L. F. (2013). The Osteocyte: An Endocrine Cell ... and More. *Endocr. Rev.* 34 (5), 658–690. doi:10.1210/er.2012-1026

Davis, H. M., Pacheco-Costa, R., Atkinson, E. G., Brun, L. R., Gortazar, A. R., Harris, J., et al. (2017). Disruption of the Cx43/Mir21 Pathway Leads to Osteocyte Apoptosis and Increased Osteoclastogenesis with Aging. *Aging cell* 16 (3), 551–563. doi:10.1111/acel.12586

Donahue, H. J., Li, Z., Zhou, Z., and Yellowley, C. E. (2000). Differentiation of Human Fetal Osteoblastic Cells and Gap Junctional Intercellular Communication. *Am. J. Physiology-Cell Physiol.* 278 (2), C315–C322. doi:10.1152/ajpcell.2000.278.2.C315

el-Fouly, M. H., Trosko, J. E., and Chang, C.-C. (1987). Scrape-Loading and Dye Transfer. A Rapid and Simple Technique to Study Gap Junctional Intercellular Communication. *Exp. Cel Res.* 168 (2), 422–430. doi:10.1016/0014-4827(87)90014-0

Franz-Odendaal, T. A., Hall, B. K., and Witten, P. E. (2006). Buried Alive: How Osteoblasts Become Osteocytes. *Dev. Dyn.* 235 (1), 176–190. doi:10.1002/dvdy.20603

Goodenough, D. A., Goliger, J. A., and Paul, D. L. (1996). Connexins, Connexons, and Intercellular Communication. *Annu. Rev. Biochem.* 65, 475–502. doi:10.1146/annurev.bi.65.070196.002355

Gramsch, B., Gabriel, H.-D., Wiemann, M., Grümmer, R., Winterhager, E., Bingmann, D., et al. (2001). Enhancement of Connexin 43 Expression Increases Proliferation and Differentiation of an Osteoblast-Like Cell Line. *Exp. Cel Res.* 264 (2), 397–407. doi:10.1006/excr.2000.5145

Grimston, S. K., Brodt, M. D., Silva, M. J., and Civitelli, R. (2008). Attenuated Response to *In Vivo* Mechanical Loading in Mice with Conditional Osteoblast Ablation of the Connexin43 Gene (Gja1). *J. Bone Miner Res.* 23 (6), 879–886. doi:10.1359/jbmr.080222

Grimston, S. K., Watkins, M. P., Brodt, M. D., Silva, M. J., and Civitelli, R. (2012). Enhanced Periosteal and Endocortical Responses to Axial Tibial Compression Loading in Conditional Connexin43 Deficient Mice. *PLoS One* 7 (9), e44222. doi:10.1371/journal.pone.0044222

Hua, R., Zhang, J., Riquelme, M. A., and Jiang, J. X. (2021). Connexin Gap Junctions and Hemichannels Link Oxidative Stress to Skeletal Physiology and Pathology. *Curr. Osteoporos. Rep.* 19 (1), 66–74. doi:10.1007/s11914-020-00645-9

Irion, S., Luche, H., Gadue, P., Fehling, H. J., Kennedy, M., and Keller, G. (2007). Identification and Targeting of the Rosa26 Locus in Human Embryonic Stem Cells. *Nat. Biotechnol.* 25 (12), 1477–1482. doi:10.1038/nbt1362

Jat, P. S., Noble, M. D., Ataliotis, P., Tanaka, Y., Yannoutsos, N., Larsen, L., et al. (1991). Direct Derivation of Conditionally Immortal Cell Lines from an H-2kb-Tsa58 Transgenic Mouse. *Proc. Natl. Acad. Sci. U.S.A.* 88 (12), 5096–5100. doi:10.1073/pnas.88.12.5096

Jiang, J. X., Siller-Jackson, A. J., and Burra, S. (2007). Roles of Gap Junctions and Hemichannels in Bone Cell Functions and in Signal Transmission of Mechanical Stress. *Front. Biosci.* 12, 1450–1462. doi:10.2741/2159

Jiang, W., Hua, R., Wei, M., Li, C., Qiu, Z., Yang, X., et al. (2015). An Optimized Method for High-Titer Lentivirus Preparations without Ultracentrifugation. *Sci. Rep.* 5, 13875. doi:10.1038/srep13875

Kalajzic, I., Braut, A., Guo, D., Jiang, X., Kronenberg, M. S., Mina, M., et al. (2004). Dentin Matrix Protein 1 Expression during Osteoblastic Differentiation, Generation of an Osteocyte Gfp-Transgene. *Bone* 35 (1), 74–82. doi:10.1016/j.bone.2004.03.006

Kato, Y., Windle, J. J., Koop, B. A., Mundy, G. R., and Bonewald, L. F. (1997). Establishment of an Osteocyte-Like Cell Line, Mlo-Y4. *J. Bone Miner Res.* 12 (12), 2014–2023. doi:10.1359/jbmr.1997.12.12.2014

Kawatsura, R., Hara, Y., Akiyama, M., Tachikawa, N., and Nakahama, K.-i. (2022). Gap Junctional Intercellular Communication Attenuates Osteoclastogenesis Induced by Activated Osteoblasts. *Biochem. Biophysical Res. Commun.* 597, 71–76. doi:10.1016/j.bbrc.2022.01.118

Kitaura, H., Marahleh, A., Ohori, F., Noguchi, T., Shen, W.-R., Qi, J., et al. (2020). Osteocyte-Related Cytokines Regulate Osteoclast Formation and Bone Resorption. *Int. J. Mol. Sci.* 21 (14), 5169. doi:10.3390/ijms21145169

Lecanda, F., Towler, D. A., Ziambaras, K., Cheng, S.-L., Koval, M., Steinberg, T. H., et al. (1998). Gap Junctional Communication Modulates Gene Expression in Osteoblastic Cells. *Mol. Biol. Cel* 9 (8), 2249–2258. doi:10.1091/mbc.9.8.2249

Lecanda, F., Warlow, P. M., Sheikh, S., Furlan, F., Steinberg, T. H., and Civitelli, R. (2000). Connexin43 Deficiency Causes Delayed Ossification, Craniofacial Abnormalities, and Osteoblast Dysfunction. *J. Cel Biol* 151 (4), 931–944. doi:10.1083/jcb.151.4.931

Li, Z., Zhou, Z., Yellowley, C. E., and Donahue, H. J. (1999). Inhibiting Gap Junctional Intercellular Communication Alters Expression of Differentiation Markers in Osteoblastic Cells. *Bone* 25 (6), 661–666. doi:10.1016/s8756-3282(99)00227-6

Lima, F., Niger, C., Hebert, C., and Stains, J. P. (2009). Connexin43 Potentiates Osteoblast Responsiveness to Fibroblast Growth Factor 2 via a Protein Kinase C-Delta/Runx2-Dependent Mechanism. *Mol. Biol. Cel* 20 (11), 2697–2708. doi:10.1091/mbc.E08-10-1079

Ma, J., Köster, J., Qin, Q., Hu, S., Li, W., Chen, C., et al. (2016). Crispr-Do for Genome-Wide Crispr Design and Optimization. *Bioinformatics* 32 (21), 3336–3338. doi:10.1093/bioinformatics/btw476

Ma, L., Hua, R., Tian, Y., Cheng, H., Fajardo, R. J., Pearson, J. J., et al. (2019). Connexin 43 Hemichannels Protect Bone Loss during Estrogen Deficiency. *Bone Res.* 7, 11. doi:10.1038/s41413-019-0050-2

Musil, L. S., and Goodenough, D. A. (1991). Biochemical Analysis of Connexin43 Intracellular Transport, Phosphorylation, and Assembly into Gap Junctional Plaques. *J. Cel Biol* 115 (5), 1357–1374. doi:10.1083/jcb.115.5.1357

Orellana, J. A., Sáez, P. J., Cortés-campos, C., Elizondo, R. J., Shoji, K. F., Contreras-Duarte, S., et al. (2012). Glucose Increases Intracellular Free Ca(2+) in Tanycytes via Atp Released through Connexin 43 Hemichannels. *Glia* 60 (1), 53–68. doi:10.1002/glia.21246

Pfeifer, I., Anderson, C., Werner, R., and Oltra, E. (2004). Redefining the Structure of the Mouse Connexin43 Gene: Selective Promoter Usage and Alternative Splicing Mechanisms Yield Transcripts with Different Translational Efficiencies. *Nucleic Acids Res.* 32 (15), 4550–4562. doi:10.1093/nar/gkh792

Plotkin, L. I., Lezcano, V., Thostenson, J., Weinstein, R. S., Manolagas, S. C., and Bellido, T. (2008). Connexin 43 Is Required for the Anti-Apoptotic Effect of Bisphosphonates on Osteocytes and Osteoblasts *In Vivo*. *J. Bone Mineral Res.* 23 (11), 1712–1721. doi:10.1359/jbmr.080617

Plotkin, L. I., Manolagas, S. C., and Bellido, T. (2002). Transduction of Cell Survival Signals by Connexin-43 Hemichannels. *J. Biol. Chem.* 277 (10), 8648–8657. doi:10.1074/jbc.M108625200

Qin, L., Liu, W., Cao, H., and Xiao, G. (2020). Molecular Mechanosensors in Osteocytes. *Bone Res.* 8, 23. doi:10.1038/s41413-020-0099-y

Reaume, A. G., de Sousa, P. A., Kulkarni, S., Langille, B. L., Zhu, D., Davies, T. C., et al. (1995). Cardiac Malformation in Neonatal Mice Lacking Connexin43. *Science* 267 (5205), 1831–1834. doi:10.1126/science.7892609

Riggan, L., Hildreth, A. D., Rolot, M., Wong, Y.-Y., Satyadi, W., Sun, R., et al. (2020). Crispr-Cas9 Ribonucleoprotein-Mediated Genomic Editing in Mature Primary Innate Immune Cells. *Cel Rep.* 31 (7), 107651. doi:10.1016/j.celrep.2020.107651

Riquelme, M. A., Burra, S., Kar, R., Lampe, P. D., and Jiang, J. X. (2015). Mitogen-Activated Protein Kinase (Mapk) Activated by Prostaglandin E2 Phosphorylates Connexin 43 and Closes Osteocytic Hemichannels in Response to Continuous Flow Shear Stress. *J. Biol. Chem.* 290 (47), 28321–28328. doi:10.1074/jbc.M115.683417

Riquelme, M. A., Kar, R., Gu, S., and Jiang, J. X. (2013). Antibodies Targeting Extracellular Domain of Connexins for Studies of Hemichannels. *Neuropharmacology* 75, 525–532. doi:10.1016/j.neuropharm.2013.02.021

Robling, A. G., and Bonewald, L. F. (2020). The Osteocyte: New Insights. *Annu. Rev. Physiol.* 82, 485–506. doi:10.1146/annurev-physiol-021119-034332

Sanjana, N. E., Shalem, O., and Zhang, F. (2014). Improved Vectors and Genome-Wide Libraries for Crispr Screening. *Nat. Methods* 11 (8), 783–784. doi:10.1038/nmeth.3047

Schaffler, M. B., Cheung, W.-Y., Majeska, R., and Kennedy, O. (2014). Osteocytes: Master Orchestrators of Bone. *Calcif Tissue Int.* 94 (1), 5–24. doi:10.1007/s00223-013-9790-y

Schiller, P. C., D'Ippolito, G., Balkan, W., Roos, B. A., and Howard, G. A. (2001). Gap-Junctional Communication Is Required for the Maturation Process of Osteoblastic Cells in Culture. *Bone* 28 (4), 362–369. doi:10.1016/s8756-3282(00)00458-0

Shalem, O., Sanjana, N. E., Hartenian, E., Shi, X., Scott, D. A., Mikkelsen, T. S., et al. (2014). Genome-Scale Crispr-Cas9 Knockout Screening in Human Cells. *Science* 343 (6166), 84–87. doi:10.1126/science.1247005

Siller-Jackson, A. J., Burra, S., Gu, S., Xia, X., Bonewald, L. F., Sprague, E., et al. (2008). Adaptation of Connexin 43-Hemichannel Prostaglandin Release to Mechanical Loading. *J. Biol. Chem.* 283 (39), 26374–26382. doi:10.1074/jbc.M803136200

Spatz, J. M., Wein, M. N., Gooi, J. H., Qu, Y., Garr, J. L., Liu, S., et al. (2015). The Wnt Inhibitor Sclerostin Is Up-Regulated by Mechanical Unloading in Osteocytes *In Vitro*. *J. Biol. Chem.* 290 (27), 16744–16758. doi:10.1074/jbc.M114.628313

Stains, J. P., and Civitelli, R. (2016). Connexins in the Skeleton. *Semin. Cel Dev Biol* 50, 31–39. doi:10.1016/j.semcdb.2015.12.017

Tarzemany, R., Jiang, G., Jiang, J. X., Larjava, H., and Häkkinen, L. (2017). Connexin 43 Hemichannels Regulate the Expression of Wound Healing-Associated Genes in Human Gingival Fibroblasts. *Sci. Rep.* 7 (1), 14157. doi:10.1038/s41598-017-12672-1

Upham, B. L., Suzuki, J., Chen, G., Wang, Y., McCabe, L. R., Chang, C.-C., et al. (2003). Reduced Gap Junctional Intercellular Communication and Altered Biological Effects in Mouse Osteoblast and Rat Liver Oval Cell Lines Transfected with Dominant-Negative Connexin 43. *Mol. Carcinog.* 37 (4), 192–201. doi:10.1002/mc.10137

Wang, F., Guo, T., Jiang, H., Li, R., Wang, T., Zeng, N., et al. (2018). A Comparison of Crispr/Cas9 and Sirna-Mediated Aldh2 Gene Silencing in Human Cell Lines. *Mol. Genet. Genomics* 293 (3), 769–783. doi:10.1007/s00438-018-1420-y

Wang, K., Le, L., Chun, B. M., Tiede-Lewis, L. M., Shiflett, L. A., Prideaux, M., et al. (2019). A Novel Osteogenic Cell Line that Differentiates into GFP-Tagged Osteocytes and Forms Mineral With a Bone-Like Lacunocanalicular Structure. *J. Bone Miner Res.* 34 (6), 979–995. doi:10.1002/jbmr.3720

Wang, T., Lander, E. S., and Sabatini, D. M. (2016). Viral Packaging and Cell Culture for Crispr-Based Screens. *Cold Spring Harb Protoc.* 2016 (3), pdb.prot090811. doi:10.1101/pdb.prot090811

Watkins, M., Grimston, S. K., Norris, J. Y., Guillotin, B., Shaw, A., Beniash, E., et al. (2011). Osteoblast Connexin43 Modulates Skeletal Architecture by Regulating Both Arms of Bone Remodeling. *Mol. Biol. Cel* 22 (8), 1240–1251. doi:10.1091/mbc.E10-07-0571

Woo, S. M., Rosser, J., Dusevich, V., Kalajzic, I., and Bonewald, L. F. (2011). Cell Line Idg-Sw3 Replicates Osteoblast-To-Late-Osteocyte Differentiation *In Vitro* and Accelerates Bone Formation *In Vivo*. *J. Bone Miner Res.* 26 (11), 2634–2646. doi:10.1002/jbmr.465

Xu, H., Gu, S., Riquelme, M. A., Burra, S., Callaway, D., Cheng, H., et al. (2015). Connexin 43 Channels Are Essential for Normal Bone Structure and Osteocyte Viability. *J. Bone Miner Res.* 30 (3), 436–448. doi:10.1002/jbmr.2374

Xu, L. H., Shao, H., Ma, Y. H. V., and You, L. (2019). Ocy454 Osteocytes as an *In Vitro* Cell Model for Bone Remodeling under Mechanical Loading. *J. Orthop. Res.* 37 (8), 1681–1689. doi:10.1002/jor.24302

Ya, J., Erdtsieck-Ernste, E. B. H. W., de Boer, P. A. J., van Kempen, M. J. A., Jongsma, H., Gros, D., et al. (1998). Heart Defects in Connexin43-Deficient Mice. *Circ. Res.* 82 (3), 360–366. doi:10.1161/01.res.82.3.360

Yang, W., Harris, M. A., Heinrich, J. G., Guo, D., Bonewald, L. F., and Harris, S. E. (2009). Gene Expression Signatures of a Fibroblastoid Preosteoblast and Cuboidal Osteoblast Cell Model Compared to the Mlo-Y4 Osteocyte Cell Model. *Bone* 44 (1), 32–45. doi:10.1016/j.bone.2008.08.133

Yang, Y., Liu, W., Wei, J., Cui, Y., Zhang, D., and Xie, J. (2021). Transforming Growth Factor-B1-Induced N-Cadherin Drives Cell-Cell Communication through Connexin43 in Osteoblast Lineage. *Int. J. Oral Sci.* 13 (1), 15. doi:10.1038/s41368-021-00119-3

Zhang, Y., Paul, E. M., Sathyendra, V., Davison, A., Sharkey, N., Bronson, S., et al. (2011). Enhanced Osteoclastic Resorption and Responsiveness to Mechanical Load in Gap Junction Deficient Bone. *PLoS One* 6 (8), e23516. doi:10.1371/journal.pone.0023516

Zhao, D., Riquelme, M. A., Guda, T., Tu, C., Xu, H., Gu, S., et al. (2022). Connexin Hemichannels with Prostaglandin Release in Anabolic Function of Bone to Mechanical Loading. *Elife* 11, e74365. doi:10.7554/eLife.74365

Conflict of Interest: The authors declare that the research was conducted in the absence of any commercial or financial relationships that could be construed as a potential conflict of interest.

Publisher's Note: All claims expressed in this article are solely those of the authors and do not necessarily represent those of their affiliated organizations, or those of the publisher, the editors, and the reviewers. Any product that may be evaluated in this article, or claim that may be made by its manufacturer, is not guaranteed or endorsed by the publisher.

Frontiers in
Cell and Developmental Biology

Explores the fundamental biological processes of life, covering intracellular and extracellular dynamics.

The world's most cited developmental biology journal, advancing our understanding of the fundamental processes of life. It explores a wide spectrum of cell and developmental biology, covering intracellular and extracellular dynamics.

Discover the latest Research Topics

See more →

Frontiers

Avenue du Tribunal-Fédéral 34
1005 Lausanne, Switzerland
frontiersin.org

Contact us

+41 (0)21 510 17 00
frontiersin.org/about/contact